

**ECOLOGICAL MODELING OF THE LOWER TROPHIC LEVELS
OF LAKE ERIE**

DISSERTATION

Presented in Partial Fulfillment of the Requirements for
the Degree of Doctor of Philosophy in the Graduate
School of The Ohio State University

By

Hongyan Zhang

The Ohio State University

2006

Dissertation Committee:

Professor David A. Culver, Adviser

Professor Elizabeth A. Marschall

Professor Robert M. Sykes

Approved by

Adviser

Evolution, Ecology and Organismal Biology
Graduate Program

ABSTRACT

Lake Erie has been a very dynamic ecosystem for decades. It underwent eutrophication as its human population increased from the 1950s. Water quality has improved since we reduced the external phosphorus loading to Lake Erie. Then, invasive species, zebra mussels (*Dreissena polymorpha*) and quagga mussels (*Dreissena bugensis*), built large populations in Lake Erie and changed the functions and structures of the ecosystem. All these changes have been studied and recorded by laboratory experiments and field monitoring. However, questions regarding the effects of the phosphorus loading reduction program on the Lake Erie ecosystem, the relative importance of internal and external phosphorus loading, and the impacts of dreissenid mussels on the Lake Erie ecosystem are still unanswered, because studies of the isolated components of an ecosystem will never be sufficient to reveal the functional patterns of its interactions and system properties. Holistic approaches, e.g., ecological modelling, are urgently needed to study the system as a whole. The extensive ecological knowledge and data that have been accumulated, together with the developments in computer technology, set a strong base for ecological models.

This study uses field data to construct such an ecological model of Lake Erie, EcoLE, and then uses it to investigate the impacts of hydrodynamics (Chapter 2), internal and external phosphorus loading (Chapter 3), and dreissenid mussels on the lower trophic levels of the ecosystem (Chapter 4).

EcoLE is a two-dimensional (longitudinal-vertical) model, including physical, chemical and biological components, based on a hydrodynamic and water quality model, CE-QUAL-W2, which was developed by the US Army Corps of Engineers and adapted for hydrodynamic simulation of Lake Erie by Boegman *et al.* (2001). The EcoLE model uses meteorological data that have recorded every 3 hr along the southern shoreline of Lake Erie to simulate the hydrodynamics of the lake. EcoLE is an open system. Besides the interactions at water-air and water-sediment interfaces, it has 9 tributaries and two outflows. There are more than 20 biochemical state variables in the model, among which phosphorus, algae, and zooplankton are focuses of this study. Data from year 1997 are used for calibration, while data from 1998 and 1999 are used for verification.

EcoLE's water thermal stratification predictions agree well with the results of other studies. The simulated surface and bottom water temperatures also show a good agreement with field observations. The simulated values of biological and nutrient state variables had reasonable agreement with field measurements. Although the model's performance for verification years (1998, 1999) are as good as those of the calibration year (1997), the wide standard deviations of field biological measurements and model simulations as well as the complexity of an ecosystem make us consider our model more as a valid analytical tool rather than a predictive one at this moment.

By turning on and off mixing terms in the constituent transport equation in the model, the impacts of hydrodynamics on the energy flows are investigated (Chapter 2). With mixing processes turned off in the model, total dissolved phosphorus concentrates in the lower water strata. Restoring mixing processes brings more dissolved phosphorus

into the upper water strata and supports more abundant non-diatom edible algae (NDEA), resulting in less total dissolved phosphorus accumulated in the whole water column. Hydrodynamics also plays an important role in diatom development in the water column. Without mixing processes, diatom biomass decreases dramatically during stratification. With the ability to grow under low light levels, non-diatom inedible algae (NDIA) develop a large amount of biomass in the lower water strata, depending on the amount of available phosphorus in the whole water column and are less affected by hydrodynamics. In the western basin, dreissenid grazing impacts on NDEA without mixing processes decreases 80% from that with mixing processes.

The relative importance of external and internal phosphorus loading is evaluated by comparing their spatial distributions and total amounts as phosphorus (Chapter 3). Analysis of lake-wide longitudinal distributions of total phosphorus loaded from external sources shows that the external loads are mainly concentrated in the western basin and the west central basin, and have minor direct effects on the east central and the eastern basins during the growing season. The external phosphorus loading is of the same magnitude as the internal phosphorus loading in the western basin, while the internal loading is much more important than the external in the central and the eastern basins. Phosphorus is distributed homogeneously in the water column in the western basin. In the stratified central and eastern basins, however, phosphorus released by organic matter decomposition and pelagic communities (algae and crustaceans) is concentrated in the epilimnion, supporting approximate by 60% of the daily algal P-demands, while phosphorus excreted by dreissenids and that released by anoxic sediments is concentrated

in the hypolimnion. Different algal groups, NDEA, NDIA, and diatoms have different responses to the changes in the external phosphorus loading among years. Caution should be used if managers seek to change the current phosphorus loading reduction program.

The impacts of dreissenid mussels on nutrients, algae, and crustacean zooplankton are investigated in Chapter 4. Compared with zooplankton, dreissenids' grazing impact on NDEA varied among years in the western basin. In the dry year (1999), their impacts on NDEA exceeded those of crustacean zooplankton, while in the other two years they were less than those of the crustaceans. Dreissenids have equal grazing impacts on diatoms as do the crustacean zooplankton in the western basin. Nevertheless, mussel daily grazing impact is less than 10% of the NDEA and diatom biomass. Although the mussels filter 20% of the water column volume daily, their low daily grazing impacts on the algae indicate the limited availability of algae to the bottom-dwelling dreissenids. Dreissenids graze only 1-2% of the NDEA and diatoms in the central and eastern basins. When we artificially increase the mussels' population density or body size in the model, their grazing impacts on NDEA in the western basin decrease, while grazing on diatoms continues to increase. Dreissenid mussels increase non-diatom inedible algae (NDIA) rapidly with increasing mussel population size, because the dreissenid population excretes a large amount of ammonia and phosphorus. These amounts increase rapidly with increasing mussel population size. Nitrification of ammonia might speed oxygen depletion in the hypolimnion of the central basin. Dreissenid mussels affect crustacean zooplankton mainly through their impacts on NDEA. Our results indicate that dreissenid

mussels had weak direct grazing impacts on algal biomass, while indirect effects of their nutrient excretion have a lot more impact on the system.

To my parents, my husband and my son

ACKNOWLEDGMENTS

I would like to express my sincere thanks to my advisor Dr. Culver for his consistent support, kind encouragement, tireless guidance and personal concern. I am especially grateful for his saying “that is why I am here” whenever I felt frustrated and turned to him. I would not have been able to get so far without his advice, patience and great help.

I also want to thank Dr. Marschall and Dr. Sykes for serving on both my candidacy and dissertation committees. Every meeting with Dr. Marschall has been informative, pleasant and encouraging. Each time after I talked with Dr. Marschall, I could not help pushing myself to work harder and faster. I am very appreciative of Dr. Sykes for his valuable advice and insightful questions that inspired my research, broadened my view and sharpened my thoughts. I also want to thank him for his kind suggestions on my future career. I also want to thank Dr. Aday for his encouragement and his kindly serving on my candidacy committee.

I am sincerely grateful to Dr. Leon Boegman for his quick responses to my many questions about his application of the CE-QUAL-W2 model to Lake Erie and his generosity in sharing information.

I also want to thank my lab fellows, Dr. Kwee Tew, Dr. William Edwards, Dr. Doug Kane, Cathy Doyle, Joe Conroy, Nate Gargas, Erin Hass, and Artie McCollum for their support and friendship. The Limnology Lab has been a great place to study and

work for me. I want to particularly thank Annie Jacob for her friendship and for kindly letting me stay at her home whenever needed after my family moved to Michigan.

I am very appreciative of the department of Evolution, Ecology and Organismal Biology and The Ohio State University for their support of my education over the years. This has been a happy and accomplishing period of time of my life which I will remember forever.

This research was sponsored by the Ohio Lake Erie Office – Lake Erie Protection Fund Project # LEPF 98-17, and the Ohio Department of Natural Resources as part of the Federal Aid in Sport Fish Restoration Program (F-69-P, Fish Management in Ohio) administered jointly by the U.S. Fish and Wildlife Service and the Ohio Division of Wildlife and the United States Environmental Protection Agency (GL-97590101).

Finally, I must take this opportunity to express my deep gratitude to my husband, Shugang Jiang, and my son, Chaoran, for their love and support. My husband has been a great mentor to me. My deep gratitude is also extended to my parents, my sister and my brother for their help and encouragement and for keeping faith in me.

VITA

- July 27, 1972 Born Shandong, China
- 1997 M.S. Fisheries, Ocean University of China,
Qingdao, Shandong, China
- 1997-1999 Research Assistant, Institute of Oceanography,
Chinese Academy of Sciences, Qingdao,
Shandong, China
- 1999-present Graduate Teaching and Research Associate,
The Ohio State University, Columbus, OH

PUBLICATIONS

1. Conroy, J.D., Edwards, W.J., Pontius, R.A., Kane, D.D., Zhang, H., Shea, J.F., Richey, J.N., and Culver, D.A. 2005. Soluble nitrogen and phosphorus excretion of exotic freshwater mussels (*Dreissena* spp.): potential impacts for nutrient remineralization in western Lake Erie. *Freshwater Biology*, 50: 1146-1162.
2. Wang, R., Zhang, H., Wang, K., and Zuo, T. 2002. Distribution and population dynamics of *Paracalanus parvus*, *Paracalanus crassirostris*, and *Acartia bifilosa* (Copepoda, Calanoida) in the Bohai Sea. *Chinese Journal of Oceanology and Limnology*. 20(4):348-357.
3. Wang, R., Zhang, H., Wang, K., and Zuo, T. 2002. Function performed by small copepods in marine ecosystem. *Oceanologia Et Limnologia Sinica*, 33(5): 453-460.

FIELDS OF STUDY

Major Field: Evolution, Ecology and Organismal Biology

TABLE OF CONTENTS

	Page
Abstract.....	ii
Dedication.....	vii
Acknowledgments.....	viii
Vita.....	x
List of Tables.....	xii
List of Figures.....	xv
Chapters:	
1. Introduction.....	1
2. Construction and application of a two-dimensional ecological model of Lake Erie	
Abstract.....	14
Introduction.....	15
Model Description.....	17
Simulation and Results.....	27
Discussion.....	36
3. Application of a two-dimensional ecological model to evaluate the effects of external phosphorus loading on Lake Erie’s lower trophic levels.	
Abstract.....	98
Introduction.....	99
Model Description.....	103
Simulation and Results.....	110
Discussion.....	117
4. Application of a two-dimensional ecological model to evaluate the impacts of exotic mussels on the Lake Erie ecosystem.	
Abstract.....	154
Introduction.....	155
Methods.....	159
Simulation and Results.....	161
Discussion.....	172
5. Conclusions and Discussion.....	203
Bibliography.....	211

LIST OF TABLES

<u>Table</u>	<u>Page</u>
2.1 A list of equations used in the model. a, equations from Cole and Buchak (1995); b, modified from Cole and Buchak (1995); c, modified from Scavia <i>et al.</i> (1988); d, from Fennel and Neumann (2003); e, this study; f, from Conroy <i>et al.</i> (2005b).....	43
2.2 Phytoplankton taxa in Lake Erie (from LEPAS database, OSU,OH, USA). Note the ‘diatom’ notations in first column and ‘edible/inedible’ of the last column, which are the bases of our algal grouping in EcoLE.	51
2.3 Kinetic rates used in the model (modified from Boegman 1999). Superscript numbers indicate different references other than Cole and Buchak (1995).....	53
2.4 Kinetic rates of dreissenid mussels used in the EcoLE model.....	57
2.5 Input data needed to run EcoLE and their sources.	58
2.6 Results of paired t-test ($p < 0.05$) of the mean difference between modeled and observed values of six state variables for three years. “-” indicates significant difference. “+” indicates no significant difference.	59
2.7 Comparisons of simulated daily grazing rates of dreissenid mussels on algae ($mt\ C\ d^{-1}$) between “with” and “without” physical mixing processes in each of the three basins over each of the three years. The values are mean daily grazing rates on both NDEA and diatoms over simulation periods. “%” columns contain the percentages of decrease of grazing rates under no mixing from those under mixing.	60
2.8 Statistical results of the uncertainties due to changing the simulated dreissenid population densities. Significant differences between density factor 1 and 0.1 or 1 and 10 are indicated by different letters in the last column.....	61
3.1 P loads (metric tons per season) from tributaries and WasteWater Treatment Plants (WWTP) in 1997, 1998, 1999. The sources are listed by location around the lake basin from the west to the east.	129

3.2	Comparisons of mussel biomass (g DW m ⁻²) between Jarvis <i>et al.</i> 's population with various sizes and EcoLE's 10-mm population.	130
3.3	Comparison of the 1997 basin-wide plankton biomass and productivity with or without the external phosphorus loading, averaged over the entire simulation period from May 10 to September 30.	131
3.4	As Table 3.3, but for June 10 through October 30, 1998.....	132
3.5	As Table 3.3, but for May 20 through September 29, 1999.	133
3.6	Basin-wide P cycling of 1997, shown as concentrations in major pools, rates of transfer between pools, and the fraction (%) of those located in the top 12 m of the water column. DP: SRP and P in dissolved organic matter; PP: P in phytoplankton and detritus; CP: P in crustaceans; PP→DP: phosphorus excretion by phytoplankton and release due to decomposition of detritus; CP→DP: phosphorus excretion by crustaceans; MP→DP: phosphorus excretion by dreissenids; SED→DP: phosphorus release by sediments under anoxic conditions; PP→SED: phosphorus loss to sediment due to sedimentation of PP; External loading: DP loading from tributaries of Lake Erie; Withdrawals: total phosphorus (DP+PP) loss through the Welland Canal and the Niagara River; Exchange between basins: net total phosphorus transported by horizontal currents between basins. All values are an average over the simulation period from May 10 to September 30, 1997.....	134
3.7	As Table 3.6, but for June 10 through October 30, 1998.....	136
3.8	As Table 3.6, but for May 20 through September 29, 1999	137
3.9	Results of paired t-test (p<0.05) of the mean difference between modeled and observed values of six state variables for three years with modified external phosphorus loading. “-” indicates significant difference. “+” indicates no significant difference. Differences between with and without modification of external phosphorus loading are indicated by the parentheses, which hold the t-test results of Table 2.6.	138
3.10	The effects of phosphorus loading from unmonitored non-point sources on basin-wide phytoplankton biomass, under the conditions of 1997.....	139
3.11	Comparisons of the net sedimentation rates of phosphorus in the three Lake Erie basins from Burn's (1976) study (their table 8) and ours.	140
4.1	Basin-wide impacts of dreissenids on NDEA (non-diatom edible algae) and diatoms, compared with those of crustacean zooplankton.....	181

4.2	The relative importance of nutrients excreted by dreissenid mussels to the basin-wide nutrient mass.....	182
4.3	Comparisons of effects of different treatments on SRP (metric tons) in the upper water. Means are the averages of daily model outputs of basin-wide SRP over the simulation periods. Fractions are the means of treatments to that of the full model.....	183

LIST OF FIGURES

<u>Figure</u>	<u>Page</u>
2.1 Flowchart of the model EcoLE (from Boegman 1999). Major differences between model EcoLE and model CE-QUAL-W2 are in the block ‘Constituents’	62
2.2 Flowchart of constituents in the model EcoLE. Construction of model EcoLE focuses on subroutine constructions of constituent calculations that are embedded in model CE-QUAL-W2.	63
2.3 EcoLE’s longitudinal-vertical resolution plane (longitudinal cross-section), showing width contours of 20 km intervals (from Boegman 1999).	64
2.4 Model structure of the chemical and biological components of EcoLE.	65
2.5 Reshaping the western basin from staircase (a) to rectangular box (b) by keeping surface area B_1 constant and adjusted depth H_i so that $B_1 \sum_{i=1}^m H_i \approx \sum_{i=1}^n B_i H_i$, where $m \leq n$ (after Boegman <i>et al.</i> 2006). The adjustment allows estimation of the effects of dreissenids, which are distributed only in the bottom cell of the rectangular box. The gray dots indicate the location of dreissenid mussels, while dreissenid population in a model cell is determined by the sedimental area and mussel density.	66
2.6 Water levels of Lake Erie, 1965-1999 (data from Tim Hunter, USGS). Open squares are averages from January to December and solid squares are averages from May to October. The arrow points to year 1997 followed by 1998 and 1999.	67
2.7 Lake Erie sampling sites yielding monitoring data used in the simulations.	68
2.8 The 1997 simulation of vertical distributions of temperature outputs of EcoLE from representative segments in the western basin (segment 30, 9m, a), central basin (segment 95, 26m, b) and eastern basin (segment 175, 64m, c) over the simulation period. Simulated dates were May 10 to Sep. 30. Note the different scales on the y-axis.	69
2.9 As Figure 2.8, but for June 10 through October 30, 1998.	70
2.10 As Figure 2.8, but for May 30 through September 29, 1999.	71

2.11	1997's comparisons between the modeled and the observed surface temperatures (a) and bottom temperatures (b). The light bars are means of temperatures measured in the month and the basin. The dark bars are means of temperatures sampled in the model output corresponding to dates and locations (segments) of the field measurements. Error bar represents one standard deviation of the mean.	72
2.12	As Figure 2.11, but for 1998.....	73
2.13	As Figure 2.11, but for 1999.....	74
2.14	Model calibration (year 1997) for non-diatom edible algae, diatoms, copepods, cladocerans, TP-F and NH ₄ . Plotted values represent seasonal averages for field observations (black circles) and model predictions (open circles) of field sampling segments from west (0) to east (220). The western basin ends at segment 49, and the central basin ends at segment 156.	75
2.15	Model verification of 1998 for non-diatom edible algae, diatoms, copepods, cladocerans, TP-F and NH ₄	76
2.16	Model verification of 1999 for non-diatom edible algae, diatoms, copepods, cladocerans, TP-F and NH ₄	77
2.17	Comparisons of NDIA biomass between observations and predictions for 1997, 1998 and 1999. Biomass values are averages of August and September. Note the different scales on the y-axis of 1998.	78
2.18	Relative error vs. sample percentile for NDEA, Diatoms, Cladocerans, Copepods, TP-F and NH ₄ of three years. The vertical dash line indicates the median relative errors of state variables.	79
2.19	The 1997 simulation results of water column concentrations (g P m ⁻²) (a) and concentration (mg P l ⁻¹) distributions (b) of TP-F with (upper panel) and without (lower panel) mixing processes on August 30.....	80
2.20	The 1998 simulation results of water column concentrations (g P m ⁻²) (a) and concentration (mg P l ⁻¹) distributions (b) of TP-F with (upper panel) and without (lower panel) mixing processes on August 30.....	81
2.21	The 1999 simulation results of water column concentrations (g P m ⁻²) (a) and concentration (mg P l ⁻¹) distributions (b) of TP-F with (upper panel) and without (lower panel) mixing processes on August 30.....	82
2.22	The 1997 simulation results of water column concentrations (g DW m ⁻²) (a) and concentration (g DW m ⁻³) distributions (b) of non-diatom edible algae	

with (upper panel) and without (lower panel) mixing processes on August 30.....	83
2.23 As Figure 2.22, but for non-diatom edible algae on August 30, 1998.....	84
2.24 As Figure 2.22, but for non-diatom edible algae on August 30, 1999.	85
2.25 As Figure 2.22, but for non-diatom inedible algae on August 30, 1997.....	86
2.26 As Figure 2.22, but for non-diatom inedible algae on August 30, 1998.....	87
2.27 As Figure 2.22, but for non-diatom inedible algae on August 30, 1999.....	88
2.28 As Figure 2.22, but for diatoms on August 30, 1997.	89
2.29 As Figure 2.22, but for diatoms on August 30, 1998.....	90
2.30 As Figure 2.22, but for diatoms on August 30, 1999.....	91
2.31 Carbon pools (in boxes) and carbon flows (arrows) in the model. CZ: crustacean zooplankton; NDEA: non-diatom edible algae; NDIA: non-diatom inedible algae; OM: organic matter; Mussels: zebra and quagga mussels.....	92
2.32 Relative sizes of the carbon pools (10^3 mt C) in the model. Values are the averages of daily outputs over simulation period of each year. Dark bars are basin-wide carbon mass. Light bars are carbon mass in the top 12m water column or non-bottom layer water column if water is less than 12m deep. Numbers on the bars indicate the percentage of light bar values to the corresponding dark bar values. NDEA stands for non-diatom edible algae; NDIA stands for non-diatom inedible algae; OM stands for organic matter; and CZ stands for crustacean zooplankton.	93
2.33 The 1997 simulation's averaged carbon flows (mt C d^{-1}) over simulation period. Note the flows were calculated every 30 minutes and the averaged values have been converted from g C s^{-1} to mt C d^{-1} . Dark bars are basin-wide carbon flows; light bars are carbon flows in the water column above 12m. Negative numbers refer to losses from the basin.....	94
2.34 As Figure 2.33, but for 1998.	96
2.35 As Figure 2.33, but for 1999.	97
3.1 Locations of tributaries around Lake Erie. 1. the Maumee River (segment 2); 2.the Toledo WWTP (segment 2); 3. the Detroit River (segments 12-14); 4. the Sandusky River (segment 50); 5. the Cleveland westerly WWTP (segment 82); 6. the Cuyahoga River (segment 83); 7. the Cleveland	

	easterly WWTP (segment 89); 8. the Erie WWTP (segment 158). The line WC is the border between the western basin and the central basin, and the line CE is the border between the central basin and the eastern basin	141
3.2	P pools and cycling pathways that considered in EcoLE. DP: SRP and P in dissolved organic matter; PP: P in phytoplankton and detritus; CP: crustacean phosphorus content; PP→DP: phosphorus excretion by phytoplankton and release due to decomposition of detritus; CP→DP: phosphorus excretion by crustaceans; MP→DP: phosphorus excretion by dreissenids; SED→DP: phosphorus release by sediments under anoxic conditions; PP→SED: phosphorus loss to sediment due to sedimentation of PP; External loading: TP loading from tributaries of Lake Erie; Withdrawals: total phosphorus (DP+PP) loss through the Welland Cannel and the Niagara River; Exchange between basins: net total phosphorus transported by horizontal currents between basins.	142
3.3	Monthly phosphorus inputs into Lake Erie from the Maumee River. a) total phosphorus and b) soluble reactive phosphorus. Solid lines for 1997, dash lines for 1998 and dot lines for 1999. There are four loading peaks: March and June of 1997 and the spring and autumn of 1998. Data are from Richards, R.P., Water Quality Laboratory, Heidelberg College, Ohio.....	143
3.4	The horizontal distribution of the external TP loading in Lake Erie at the end of simulations (September 30, 1997; October 30, 1998; and September 29, 1999). These distributions were the results of physical mixing processes, while the chemical and biological processes were inactivated. The phosphorus peaks at the west central basin (segment 50 - 80) were more likely an accumulation of loading in the western basin, rather than the direct external loading into the central basin. The peak was centered at segment 70 in the highest external loading year (1997), at segment 55 in the lowest external loading year (1999). In 1998, the peak was a median one in terms of magnitude and location.	144
3.5	The spatial distribution of the external TP loading in Lake Erie at the end of simulation periods (September 30, 1997; October 30, 1998; and September 29, 1999). The distributions were the results of physical mixing processes, while the chemical and biological processes were inactivated.....	145
3.6	The concentrations of the TP (solid lines) and SRP (dot lines) loaded in Lake Erie accumulated over simulation periods (May 10-September 30, 1997; June 10 – October 30, 1998; May 20 – September 29, 1999). These concentrations are averages over the upper water above 12m of each segment. There was a much higher cumulative peak of TP and SRP input in the west western basin in 1998 than in 1997 and 1999.....	146

3.7	SRP excreted by crustaceans over the simulation period of 1997: the spatial distributions of SRP (upper panels), the water column concentrations of SRP of each segment (middle panels) and the average SRP concentrations of the non-bottom top 12 m water of each segment (lower panels).....	147
3.8	As Figure 3.7, but for SRP released by organic mater decay	148
3.9	As Figure 3.7, but for SRP excreted by dreissenid mussels	149
3.10	As Figure 3.7, but for SRP released by anoxic sediment.....	150
3.11	1997's comparisons between the simulations and field observations of state variables with bioavailable phosphorus from external sources being adjusted according to De Pinto <i>et al.</i> (1981) and Young <i>et al.</i> (1982).....	151
3.12	As Figure 3.11, but for 1998.....	152
3.13	As Figure 3.11, but for 1999.....	153
4.1	Comparisons of seasonal means of basin-wide NDEA biomass of seven model treatments. The error bar represents one standard deviation of the mean. Note the different scales on the y-axis	184
4.2	As Figure 4.1, but for basin-wide diatom biomass	185
4.3	As Figure 4.1, but for basin-wide NDIA biomass	186
4.4	Comparisons of seasonal means of basin-wide zooplankton biomass of different model treatments of mussels. The error bar represents one standard deviation of the mean. Note the different scales on the y-axis.....	187
4.5	As Figure 4.4, but on crustacean zooplankton production.....	188
4.6	As Figure 4.4, but on grazing rates of crustacean zooplankton	189
4.7	Uncertainty analysis of different combinations of density and body size of dreissenid mussel populations on basin-wide NDEA biomass. The values are averaged over the simulation period. Note the different scales on the y-axis	190
4.8	Uncertainty analysis of different combinations of density and body size of dreissenid mussel populations on basin-wide NDEA net productivity. The values are averaged over the simulation period. Note the different scales on the y-axis.....	191
4.9	Uncertainty analysis of different combinations of density and body size of dreissenid mussel populations on basin-wide mussels' grazing impacts on	

NDEA. The values are averaged over the simulation period. Note the different scales on the y-axis.....	192
4.10 As Figure 4.7, but on basin-wide diatom biomass.....	193
4.11 As Figure 4.8, but on diatom net productivity. The negative values indicate that the respiration loss is greater than the photosynthesis in the whole basin.	194
4.12 As Figure 4.9, but on mussels' grazing impacts on diatoms	195
4.13 As Figure 4.7, but on basin-wide NDIA biomass.....	196
4.14 As Figure 4.8, but on NDIA net productivity. The negative values indicate that the respiration loss is greater than the photosynthesis in the whole basin	197
4.15 Uncertainty analysis of different combinations of density and body size of dreissenid mussel populations on basin-wide P excretion rates of dreissenid mussel populations. The values are averaged over the simulation period. Note the different scales on the y-axis.....	198
4.16 As Figure 4.15, but on ammonia excretion rates of dreissenid mussel populations.....	199
4.17 Uncertainty analysis of different combinations of density and body size of dreissenid mussel populations on basin-wide crustacean zooplankton biomass. The values are averaged over the simulation period. Note the different scales on the y-axis.....	200
4.18 Uncertainty analysis of different combinations of density and body size of dreissenid mussel populations on basin-wide crustacean zooplankton grazing on NDEA and diatoms. The values are averaged over the simulation period. Note the different scales on the y-axis.....	201
4.19 As Figure 4.17, but on basin-wide crustacean production.....	202

CHAPTER 1

INTRODUCTION

Lake Erie, the smallest of the Laurentian Great Lakes, has been the subject of human activities (waste discharge and control, wetland destruction, species introductions, etc.), and the effects of these activities (changes in water quality, fish population dynamics, exotic species, erosion of the shoreline, etc.) have been well tracked (Johannsson *et al.* 2000, McGucken 2000). In the 1970s, with the increase of human population in its watershed, Lake Erie suffered from water quality problems. Gilbertson *et al.* (1972) noted that as the human population around the Lake Erie basin doubled from 1931 to 1966, the contribution of municipal phosphorus to the lake increased from 3,400 metric tons yr⁻¹ to 17,800 metric tons yr⁻¹. In 1967, 27,300 metric tons of phosphorus entered the lake, 60% of which was from municipal discharge. Thus, as Lake Erie eutrophicated rapidly (Davis 1964), nutrient inputs led to excessive phytoplankton in the lake, increasing at a rate of 122.0 cells ml⁻¹ yr⁻¹ between 1956 and 1964 (Braidech *et al.* 1972). Consequently, abundant senescent and dead algae settled down to the bottom. A settling rate of 21,700 cells cm⁻² day⁻¹ was recorded in 1970 by Braidech *et al.* This algal “rain” down to the bottom resulted in a high oxygen depletion rate. For example, Burns and Ross (1971, but see in Wetzel 2001) estimated that bacterial decomposition of algal sedimentation contributed 88% of the hypolimnion oxygen consumption in the central

basin of Lake Erie. Dobson and Gilbertson (1972) found that the oxygen depletion rate in the hypolimnion of the Central Basin was $3.6 \text{ mg l}^{-1} \text{ month}^{-1}$ in 1970, which was more than double the rate of 1929. This depletion rate exceeded the critical depletion rate ($3.0 \text{ mg l}^{-1} \text{ month}^{-1}$) and predicted that much of the basin would become deoxygenated before the autumn overturn. In turn, oxygen depletion killed fish and many other favored organisms and replaced them with undesirable species. The lake water became odorous and less suitable as a municipal water source. Even worse, it could trigger an undesirable cyclic process in the ecosystem, i.e., anoxic conditions cause a release of phosphorus from the sediments, while anoxic conditions are the result of high productivity resulting from excessive nutrient supply (Burns and Ross 1972).

The results of “Project Hypo” (1972) confirmed the recommendations from the International Joint Commission (1969) to remove phosphate from detergents, reduce phosphorus from municipal and industrial effluents, and control phosphorus from agricultural activities, and led to the Canada/US Water Quality Agreement that aimed to reduce the external loading of phosphorus to Lake Erie. The external phosphorus input to Lake Erie decreased from $27,000 \text{ t yr}^{-1}$ in 1970 to $12,000 \text{ t yr}^{-1}$ in 1983, where it stabilized below $13,000 \text{ t yr}^{-1}$ with an exception of $17,000 \text{ t yr}^{-1}$ in 1997 (Dolan 1993 and personal communication). However, the point-source nitrogen loading to the western basin of Lake Erie increased significantly (10 to $140 \text{ } \mu\text{g N L}^{-1}$) from 1975 to 1990 and resulted in a high N:P ratio (Richards and Baker 1993). Decline in the external phosphorus loading led to a reduction of 40% in total phytoplankton biomass by the late 1970s, 65% by the mid 1980s in the western basin, and a reduction of 80% in blue-greens and filamentous greens by the mid-1980s (Makarewicz and Bertram 1991, Gopalan *et al.* 1998). Since

1970, the oxygen depletion in the hypolimnion of the central basin has shown a slight downward trend (Bertram 1993).

The ecological processes affected by the P reduction were not simple. Before we could obtain a clear evaluation of how successful this water quality management approach was, dreissenid mussels (*Dreissena polymorpha* and *D. bugensis*) invaded Lake Erie and established a high-density population in the late 1980s (Hebert *et al.* 1989, Griffiths *et al.* 1991, May and Marsden 1992). The mussels increased water clarity, which enhanced the effects of P loading reduction, but mussels also counter the effects of P loading reduction by increasing the soluble reactive phosphorus and ammonia concentrations by excretion, and selectively favor the proliferation of blue-green algae (Vanderploeg *et al.* 2001, Bierman *et al.* 2005). Numerous studies and monitoring programs have been carried out in order to understand these ecological processes in Lake Erie and provide information for lake management. However, our understanding about the effects of the P loading reduction on the ecosystem shifted from being unclear to being controversial. On one hand, the increases of water clarity raised concerns among some fisheries managers that the system productivity may become too low to support desired rates of sport fish production (Anderson *et al.* 2001, Schloesser and Nalepa 2001, Wilhelm *et al.* 2003). On the other hand, increases in frequency and magnitude of *Microcystis* blooms in recent years suggest that there is still a lot more P available than desired (Vanderploeg *et al.* 2001, Vincent *et al.* 2004, Bierman *et al.* 2005, Conroy and Culver 2005, Conroy *et al.* 2005a, Rinta-Kanto *et al.* 2005).

Field measurements about changes in organismal densities or nutrient concentrations before and after an event cannot clearly define the event's effects when it

is confounded with other events. Thus, ecological modelling is increasingly adopted as a crucial approach to studying functional patterns of interactions and properties of an ecosystem as a whole (Jorgensen and Muller 2000). Furthermore, the accumulation of ecological knowledge and field monitoring of Lake Erie makes it possible to construct viable ecological models of the lake.

In this study, a two-dimensional ecological model of Lake Erie, EcoLE, which includes physical, chemical and biological processes, is built. After the model is calibrated using monitoring data from 1997 and verified using data from 1998 and 1999, it is used to separate and investigate the impacts of hydrodynamics on Lake Erie's lower trophic levels, as well as the impacts of external phosphorus loading and the activities of the exotic mussels (*Dreissena* spp.).

Meteorological and climatological effects

Weather conditions over Lake Erie cannot be ignored in order to understand and model the Lake Erie ecosystem. Lake Erie is centered at 42°15' north latitudes and 81°15' west longitudes, with its long axis oriented at about N70°E. The lake is approximately 386 kilometers (240 miles) long and more than 80 kilometers (50 miles) wide near the midpoint of its long axis, so wind stress has an ample opportunity to affect the distribution of solutes, and suspended matter, especially to affect seasonal thermal stratification in the lake.

Each of the three Lake Erie basins has unique physical features. The shallow western basin of Lake Erie exhibits no major seasonal thermal stratification. However,

solar heating during the day and intrusions of cold central basin water cause stable stratification of the water column 60% of the time (Ackerman *et al.* 2001). The relatively flat-bottomed Central Basin and the deep eastern basin experience a typical seasonal pattern for a temperate lake, which has a quiescent winter period with the maximum density water (4°C) sinking to the lake bottom, water turnovers in Spring and Autumn bringing the nutrients into the water column and resulting in algal blooms, and a stratified summer period (Wetzel, 1983). Stratification, which effectively cuts the hypolimnion off from the euphotic zone, is usually firmly established in the central and eastern basins by the middle of July (Schertzer *et al.*, 1987).

Air temperature and wind conditions are the main factors in late spring and early summer that determine when the summer stratification in Lake Erie establishes and where in the water column the metalimnion is located. Thus, they control the hypolimnion thickness and water temperature in Lake Erie, while the volume of the hypolimnion and water temperature are two important factors regarding dissolved oxygen depletion rates in the hypolimnion of the Central Basin and the Eastern Basin (Bertram 1993). For example, high temperature and high wind speed in spring tend to establish an early stratification and a deep metalimnion, which results in a small volume of warm hypolimnion with low oxygen for a long stratification period with a high oxygen depletion rate. Lam *et al.* (1983) found that weather factors play a dominant role in the seasonal variations of dissolved oxygen concentration in the hypolimnion, masking the effects of the phosphorus removal program.

The spring melt-related tributary loads are also greatly affected by climate conditions and need a greater monitoring system. Wet weather could result in an increase

in phosphorus loading. Tributary loads to lakes can vary significantly from one year to another, depending on meteorological (and runoff) conditions. Natural meteorological fluctuations result in large temporal variations in tributary loads to the lakes. For example, tributary flows varied as high as $\pm 45\%$ relative to the mean flow to Lake Erie between 1962 and 1976, which might lead to a large range of total non-point TP loads of as much as 8600 ± 4100 metric tons yr^{-1} for Lake Erie (Gregor and Johnson 1976). Obviously, effective management designs and assessment of the effects of management strategies require consideration of natural tributary load variability.

Effects of dreissenids

Since 1990, the establishment of the zebra mussel (*Dreissena polymorpha*) has attracted a lot of attention, and, later, another exotic species, the quagga mussel (*Dreissena bugensis*), invaded Lake Erie in 1991 and is replacing the zebra mussel and has become dominant in the central and eastern basins (May and Marsden 1992, Mills *et al.* 1999, Jarvis *et al.* 2000). Impacts of mussels on Lake Erie interact with the effects of reduction in external phosphorus loading, interrupting a final evaluation of the effects of human activities to reduce external P loading.

Dreissena spp. cause rapid nutrient regeneration (Gardner *et al.* 1995, Heath *et al.* 1995, Holland *et al.* 1995, Arnott and Vanni 1996, James *et al.* 1997, Conroy *et al.* 2005b). According to Mellina *et al.* (1995) dreissenids accumulate P into growth at rates as high as $1 \text{ mg P m}^{-2} \text{ day}^{-1}$. Compared with the external TP input on an areal basis ($3.64 \text{ mg m}^{-2} \text{ day}^{-1}$ in the western basin), the P in the zebra mussel tissues represents a significant phosphorus pool. Mussels have also altered nutrient cycling through

rem mineralization. For example, James *et al.* (1997) found the range of soluble reactive phosphorus excretion rates to be 0.3-2.5 mg P m⁻² day⁻¹ at zebra mussel densities of 170-1300 ind. m⁻², while soluble nitrogen excretion rates were 5.3-34.2 mg N m⁻² day⁻¹ at similar densities. Mellina *et al.* (1995) showed that the phosphorus excretion rate of the zebra mussel population in western Lake Erie was 6.1 mg P m⁻² day⁻¹, or 29% of total P filtered daily, while 53% of the total P filtered daily was lost due to mortality. Arnott and Vanni (1996) found that the excretion rates changed seasonally with higher rates in July or August when the soft tissue biomass decreased. They estimated that in a rough comparison with other P resources (including the external P loading), zebra mussel P recycling rates were a major factor in the recycling and flow of P in the western basin, Lake Erie. In contrast, few studies on the quagga mussel excretion have been published. Conroy *et al.* (2005b) compared the nitrogen and phosphorus remineralization rate of zebra mussels and littoral quagga mussels, and found that zebra mussels excrete more phosphorus than littoral quagga mussels, but found no difference in nitrogen excretion rates. Overall, phosphorus excretion of dreissenid mussels has weakened the impact of the external phosphorus reduction program. For instance, Makarewicz *et al.* (2000) found that in western Lake Erie the soluble reactive phosphorus (SRP) increased by 180% from the pre-*Dreissena* period to the post-*Dreissena* period.

Besides recycling nutrients, *Dreissena* spp. decrease algal concentrations and increase water clarity due to their high density and filtration activity, which enhance the effect of the reduction of external P loading. However, this also raises an ambiguity about the cause of water clarity. It is still unclear which factor, the decrease in external P

loading or the invasion of dreissenids plays the main role in water clarity (Nicholls 1997, Barbiero and Tuchman 2004).

The zebra mussel grazing impacts on phytoplankton have been intensively studied. Zebra mussels can theoretically filter a volume equivalent to that of the entire Lake Erie within 1-3 days (Bunt *et al.* 1993, Leach 1993). Holland (1995) reported a decrease of over 80% of diatoms since the invasion of zebra mussels. There are fewer studies on grazing pressure on phytoplankton by quagga mussels. However, comparison studies showed that there was no difference in the clearance rate per mussel between zebra mussels and quagga mussels (Baldwin *et al.* 2002). However, grazing rates of zebra mussels measured in the laboratory cannot be applied directly into the field. Pontius (2000) measured the effect of zebra mussels' aggregation in clumps on their clearance rates in cages in Lake Erie. She found that the mean grazing impact of mussels in clumps of 20-60 mussels was only 30% (range 21 to 47%) of that if the same-sized mussels had been detached from each other and were free to move about the cage. She suggested that this percentage (30%) would be even smaller in nature, where densities of 20,000 ind.m⁻² resulted in much larger clumps than those in her grazing experiments. Furthermore, Mellina *et al.* (1995) implied an algal density threshold to filtering by mussels, below which filtration rates of zebra mussels diminished or became highly variable, and even in a 40-L tank, zebra mussels could not deplete the algae. The fluid mechanics associated with turbulent mixing over the mussel bed are also very important in terms of algae availability to mussels. Ackerman *et al.* (2001) investigated the benthic-pelagic coupling over an isolated offshore zebra mussel reef (in 7-11 m of water) in western Lake Erie and found a concentration boundary layer of chlorophyll *a* and

seston extending 2 m above the mussel reef. The ability of mussels to consume algae depends highly on the processes affecting the delivery of algae from the euphotic zone down to the concentration boundary layer where the mussels live.

It is also still a question whether mussels direct the changes of phytoplankton community structure. Fanslow *et al.* (1995) found that filtration rates were not related to seston composition. Similarly, Horgan and Mills (1997) found that clearance rates of zebra mussels did not differ among particles up to 150 μm . They also observed that zebra mussel collected particles as large as 1.2mm. Ten Winkel and Davids (1982) showed that zebra mussels collected phytoplankton up to 750 μm and then selected particles of 15-40 μm for digestion once these are inside the mantle cavity, while the egested particles, which may be still alive in the pseudofeces, could be resuspended into water column by turbulence. Thus, zebra mussels can promote *Microcystis aeruginosa* blooms through selective rejection of these algae (Vanderploeg *et al.* 2001, Bierman *et al.* 2005).

Roles of zooplankton

Another inseparable component in this puzzle is zooplankton. This group has similar ecological functions as mussels, but consists of much smaller individuals distributed all over the water column. Phytoplankton is thus more available to zooplankton than to benthic mussels, while the phosphorus excreted by zooplankton is more available to phytoplankton than that excreted by benthic mussels. Moreover, zooplankton is a good food source for fish juveniles and is critical for recruitment of the fish population (Wu and Culver 1994, Gopalan *et al.* 1998, Romare *et al.* 1999).

Zooplankton can also excrete a large amount of phosphorus (Hantke *et al.* 1996; Gulati *et*

al. 1995; Goma *et al.* 1996). For example, zooplankton in Lake Vechten provided 22-239% of the phosphorus demand by phytoplankton populations depending on season (Gulati *et al.* 1995). Moegenberg and Vanni (1991) showed that zooplankton nutrient excretion reduced the intensity of phosphorus and nitrogen limitation for phytoplankton. Goma *et al.* (1996) found that peaks in urea concentration in the nutrient pool coincided with peaks in zooplankton biomass. Furthermore, from rough data, Arnott and Vanni (1996) estimated that the P release by *Daphnia* spp. and the zooplankton community in Lake Erie was greater than the external P loading.

It is well known that the zooplankton is largely responsible for the midsummer clear-water phase in many lakes. A long-term (20 years) study showed a principal minimum in chlorophyll was ascribable to grazing by *Daphnia* (Talling 2003). Deneke and Nixdorf (1999) found that a high biomass of large *Daphnia* led to a clear-water phase in two lakes where edible algae dominated. Wu and Culver (1991) calculated the peak of *Daphnia* clearance rates in Lake Erie to be greater than $200 \text{ ml L}^{-1} \text{ d}^{-1}$. In Lathrop *et al.*'s (1999) linear model for predicting mean Secchi disk depth, the Secchi depths were positively related to midsummer *Daphnia* biomasses.

Mathematical modeling of Lake Erie water quality

Because of the complexity of the interaction among biological, chemical, and physical components of the lake it is not easy to answer questions at an ecosystem level, such as how radiant energy fixed by photosynthesis in Lake Erie is dissipated throughout the food web and how we could control the energy and direct it into the economical trophic components (e.g., sport fish). More specifically, it is not easy to separate the

effects of the recent changes in P loading from the effects of dreissenid mussels or fish recruitment, causing great frustration for lake managers. Lake managers and the public they serve, therefore, need an ecosystem-based method to interpret current changes in the lake and likely future outcomes of various management strategies. Mathematical models, with their potential to help us diagnose and predict changes in how Lake Erie functions best serve this need.

The models constructed in the 1970's and the early 1980's focused on simulation of water quality under varying conditions of external nutrient loading (Di Toro *et al.* 1973; Di Toro and Connolly 1980, Rodgers and Salisbury 1981, Bierman *et al.* 1984). These models assumed no circulation or only a steady-state circulation pattern in the lake. They contained no or few functional phytoplankton and zooplankton classes and do not account for interactions within or among trophic levels. The phosphorus load was instantaneously and completely mixed throughout the lake water. Moreover, zebra mussels and quagga mussels were introduced after these comprehensive models were written. So the dynamic Lake Erie keeps us refining, enriching and enhancing models we have, and even developing new models for the ecosystem. For example, many conceptual models were proposed at the Great Lakes Modeling Summit: Focus on Lake Erie hosted by the Council of Great Lakes Research Managers on May 27-28, 1999. These modern models are more complex than the previous ones. They tend to integrate 'specific' models of nutrients, phytoplankton, zooplankton, fish, zebra mussels, and hydrodynamics, etc. into a comprehensive model with more detailed food web structure and a dynamic physical environment. Progress in theoretical understanding and quantitative description of Lake Erie ecosystem and its responses to changes in physical

forcing or nutrient input can be achieved by coupling circulation models and chemical-biological models (Sprules *et al.* 2000, DePinto *et al.* 2000, and Culver 2000).

Goals

Goal I: To modify and apply a two-dimensional hydrodynamic model to Lake Erie. We also used our extensive temporal and spatial information on plankton and nutrients to construct a food web model that includes nutrients, phytoplankton, zooplankton, zebra mussels, and quagga mussels on fine temporal and spatial scales. We then coupled these two models to produce a comprehensive ecological model that includes physical, chemical and biological components.

Goal II: To calibrate the model of the interactions among nutrients and the lower trophic levels of Lake Erie using data from 1997, and to verify the model using data from 1998 and 1999.

Goal III: To use the model to analyze the impacts of recent ecosystem changes in Lake Erie. The following 4 hypotheses were tested.

Hypothesis 1 Hydrodynamics strongly affect the availability of nutrients to phytoplankton and the availability of phytoplankton to dreissenids.

Hypothesis 2 Internal phosphorus loading is more important to phytoplankton growth than external loading, in terms of availability and quantity.

Hypothesis 3 Dreissenids can depress the phytoplankton community in Lake Erie and mask the influence of zooplankton grazing.

Hypothesis 4 Dreissenids affect the anoxia in the hypolimnion of the central basin of Lake Erie.

In chapter 2, model development (Goals I, II and Hypothesis 1) is described in detail. Impacts of physical mixing processes on the lower trophic levels are demonstrated by turning on/off the mixing processes when running the model. Finally a carbon flow diagram is constructed to investigate the fate of energy in the ecosystem.

In chapter 3, the model is used to evaluate the influences of external and internal phosphorus sources on the lower trophic levels (Hypothesis 2). Each source is singled out with its total amount and distribution over the lake. By setting external phosphorus loading to zero, the ultimate effects of the point-source phosphorus loading reduction are investigated. Similar to constructing a carbon flow diagram in chapter 2, a phosphorus flow diagram is constructed to show the fate of phosphorus in the lake.

In chapter 4, the impacts of dreissenid mussels (Hypotheses 1,3,4) are estimated by comparing mussels' grazing impact with the phytoplankton biomass and mussels' nutrient excretion with the basin-wide nutrient contents. Food competition between dreissenid mussels and cladocerans is investigated. Dreissenid population densities and body size are varied to examine the ramifications of our imprecise (and inaccurate) dreissenid population estimates with respect to the impacts of dreissenids on nutrients, phytoplankton, cladocerans and oxygen in the hypolimnion.

In chapter 5, Results from the previous chapters are summarized and some interesting topics for future study are discussed.

CHAPTER 2

CONSTRUCTION AND APPLICATION OF A TWO-DIMENSIONAL ECOLOGICAL MODEL OF LAKE ERIE

ABSTRACT

In this study, a complex ecological model, EcoLE, has been constructed based on a two-dimensional hydrodynamic and water quality model of Lake Erie. Data from 1997 are used to calibrate the model, while data from 1998 and 1999 are used to verify the model. EcoLE's predictions of water thermal stratification agree well with results of other studies. The simulated surface and bottom water temperatures show good agreement with field observations. In spite of limitations of the model, such as no discrimination of nearshore and offshore conditions, no external algal loading, no recruitment processes from diapause eggs of zooplankton, etc., the simulated values of biological and nutrient state variables matched well with field measurements. Although EcoLE's performance for the verification years is as good as that of the calibration year, the wide standard deviations of field measurements and model simulations as well as the complexity of an ecosystem of this size make us consider our model more as a valid analytical tool rather than a predictive one at this moment. By turning on/off physical mixing processes, the impacts of hydrodynamics on lower trophic levels of Lake Erie were investigated. Without mixing, total dissolved phosphorus (TP-F) concentrates in

the lower water column. Mixing processes bring more dissolved phosphorus into the upper water and support more abundant non-diatom edible algae (NDEA) there, resulting in less dissolved phosphorus accumulated in the water column. Hydrodynamics also played an important role in diatom development in the water column. Without mixing processes diatom biomass decreased dramatically during stratification. With their low light requirement, non-diatom inedible algae (NDIA) developed a large amount of biomass in the lower water column. Organic matter was the largest carbon pool, while crustacean zooplankton played an active role in the carbon flows of pelagic food web. The balance between organic matter sedimentation and decomposition tends to occur on the basin surficial sediments, especially in the central basin.

INTRODUCTION

Lake Erie is the southernmost of the Great Lakes. Its relatively warm weather and high productivity attracted more people than the other Great Lakes, but has made it become increasingly a repository of municipal and industrial wastes before the 1970s. Fortunately, its water quality has been improved extensively since the phosphorus reduction program was implemented (Rosa and Burns 1987, Makarewicz and Bertram 1991; Bertram 1993, Holland 1993, Leach 1993, Krieger *et al.* 1996, Gopalan *et al.* 1998). The external phosphorus loading target of 11,000 mt yr⁻¹ was set up according to results of several phosphorus models (Chapra 1979, Vollenweider *et al.* 1979, Di Toro and Connolly 1980) that predicted that by meeting this target, anoxia in the hypolimnion in the central basin in Lake Erie would be gradually eliminated. Chapra's (1979) and Vollenweider *et al.*'s (1979) models assumed that each basin was a completely mixed

reactor. Di Toro and Connolly's (1980) model further divided the central and eastern basins into two layers, epilimnion and hypolimnion. None of them took real-time meteorological conditions into consideration, nor were physical mixing processes included. The interactions between segments were set as constants. These models are too simple to make further analysis of the present water quality situation in Lake Erie.

As we understand the ecosystem more, a new ecological model with finer resolution is needed to reveal the major spatial variations. For example, the thickness of metalimnion changes over stratification seasons (Lam *et al.* 1983, McCune 1998). For another example, nutrients loaded from tributaries should not be considered well mixed into basins immediately (Lam *et al.* 1983).

Another drawback of the former models is that they did not have a mussel component. As bottom dwellers, dreissenid mussels only can access algae above the mussel bed and generate a concentration boundary layer of 2 m at lake bottom (MacIsaac *et al.* 1999, Pontius 2000, Ackerman *et al.* 2001, Edwards *et al.* 2005). Thus, dreissenids' impacts on phytoplankton highly rely on physical mixing processes (MacIsaac *et al.* 1999, Edwards *et al.* 2005). Hydrodynamic simulation with daily meteorological data input is indispensable to investigate the impacts of dreissenid mussels on Lake Erie.

This study constructs a two-dimensional mathematical model, EcoLE, which includes physical, chemical and biological component. These two dimensions (longitude and vertical) catch the main spatial characteristics of Lake Erie that will affect water quality managements. For example, longitudinally, Lake Erie is eutrophic in the western basin and becomes less eutrophic eastwards. Vertically, Lake Erie has seasonal and diel thermostratification, and mussel populations create boundary layers at the bottom.

Adding another dimension, latitudinal, surely will catch additional phenomena, like gyres, or the Maumee and Sandusky river plumes traveling along the southern shore, or concentration gradients of nutrients and plankton between the nearshore and offshore zones. However, running three-dimensional models on a computer is very time consuming. For example, the three-dimensional GLCFS (Great Lakes Coastal Forecasting System) is run on a supercomputer, so one surely cannot finish a single run within two hours on a PC. Moreover, GLCFS is a purely physical model and today has no chemical or biological components at all.

After calibration and verification of EcoLE, it is used to demonstrate the effects of hydrodynamics on the distribution of algae and nutrients and estimate carbon flows among state variables. We hypothesize that hydrodynamics play an important role in the availability of nutrients to phytoplankton and the availability of phytoplankton to dreissenids. This study will assist research on zebra mussel impacts, fish habitats and recruitment, and water quality management.

MODEL DESCRIPTION

The physical model

CE-QUAL-W2 model (version 2.0), originally developed by US Army Corps of Engineers, is a two-dimensional, longitudinal/vertical, hydrodynamic and water quality model which was constructed to simulate relatively long and narrow waterbodies exhibiting longitudinal and vertical water quality gradients (Cole and Buchak 1995). It has been applied to more than 400 water bodies of various kinds (rivers, reservoirs, lakes and estuaries) all over the world. This model has six variables for hydrodynamic

simulation: free water surface elevation, pressure, horizontal velocity, vertical velocity, constituent concentration, and density. The relations among these variables are expressed by six equations: the horizontal momentum equation, the constituent transport equation, the free water surface elevation equation, the hydrostatic-pressure equation, the continuity equation, and the equation of state (Table 2.1). This model also includes 21 water quality variables: a conservative tracer (such as a dye), suspended solids, coliform, dissolved solids, labile dissolved organic matter (DOM), refractory DOM, algae, labile particulate organic matter (POM), phosphorus, ammonium, nitrate+nitrite, dissolved oxygen, sediment, inorganic carbon, alkalinity, pH, carbon dioxide, bicarbonate, carbonate, iron, and chemical/biological oxygen demand (CBOD). Figure 2.1 shows the flow chart of model CE-QUAL-W2, whereas Figure 2.2 emphasizes the model steps of the constituents.

Boegman *et al.* (2001) modified this model to simulate Lake Erie hydrodynamics for 1994. They divided Lake Erie into as many as 65 vertical layers at 1-m intervals and 222 longitudinal segments from west to east (Figure 2.3). The depths of segments were assigned relative to the Great Lakes Datum (GLD) of 1985. A unique width was specified for each cell. The vertical eddy viscosity (A_z) was adjusted such that optimal agreement with the temperature and current data was obtained. After the modification, the model did well in simulating water levels. Currents were also simulated well except in deep water (24-m depth, 1 m above the bed).

Our model, EcoLE, uses Boegman *et al.*'s modified CE-QUAL-W2 model to simulate the physical environment of Lake Erie with physical, chemical and biological input data from 1997, 1998, and 1999. No other changes in the program of the physical

component are made except those parts related to short-wave solar radiation and wind. Boegmen *et al.* used meteorological data measured from buoys on the lake in 1994 with solar radiation measured directly, while the meteorological data used in this paper are from measurements taken every 3 hours on land along the shoreline of Lake Erie (Toledo Express Airport, OH; Cleveland Hopkins International Airport, OH; Erie Terminal Building, PA; Greater Buffalo International Airport, NY) and no solar radiation data are available for 1997, 1998, or 1999. However, the original version of CE-QUAL-W2 (Cole and Buchak 1995) uses meteorological data measured on land and solar radiation is calculated from solar altitude and azimuth, and then adjusted by cloud cover. Thus we adopt Cole and Buchak's (1995) codes for calculating solar radiation and wind over the lake.

The chemical-biological model

EcoLE's chemical and biological components are based on those in model CE-QUAL-W2, but EcoLE has more new features. It divides the phytoplankton into three functional groups, and zooplankton submodels are also included. Dreissenid mussels are included as external grazing and excretion forces (but not as a state variable) (Figure 2.4 and Table 2.1). Reflecting the availability of field data, the growing season is simulated from May 10 to September 30 of 1997, from June 10 to October 30 of 1998, and from May 20 to September 29 of 1999.

Phytoplankton Phytoplankton is the primary producer and is the base of the food web in most freshwater systems. Phytoplankton is modeled as three groups, non-

diatom edible algae (NDEA), non-diatom inedible algae (NDIA), and diatoms. The algae edible and inedible by herbivorous zooplankton are defined as in the Lake Erie Plankton Abundance Study Database (LEPAS) at the Ohio State University (Table 2.2). NDIA are dominated by cyanobacteria (blue-green algae). Phytoplankton is simulated based on the conservation of mass. We assume that the only source of algae to the lake is photosynthesis in the model, as external loading data are not available. Algal growth is governed by temperature, light, and nutrients, as discussed in the next section.

Phytoplankton temperature adjustment functions (λ_T) An asymmetric temperature function is applied to simulate the influence of temperature on phytoplankton biological processes (Thornton and Lessem 1978, see in Bowie *et al.* 1985), which combines two logistic equations to describe the rising (γ_r) and falling (γ_f) limbs of the temperature optimum curve. Compared with most temperature functions with a single optimum temperature value, a no-growth low temperature (T_l) and a no-growth high temperature (T_h), the asymmetric temperature function allows an optimum temperature range (T_2 - T_3). Diatoms tend to have a lower optimum temperature range, while blue-green algae tend to have a higher optimum temperature range than greens (Hartley and Potos 1971).

$$\lambda_T = 0 \quad \text{where } T \leq T_l$$

$$\lambda_T = \frac{K_1 e^{\gamma_r(T-T_l)}}{1 + K_1 e^{\gamma_r(T-T_l)} - K_1} \cdot \frac{K_4 e^{\gamma_f(T_h-T)}}{1 + K_4 e^{\gamma_f(T_h-T)} - K_4} \quad \text{where } T_l < T < T_h$$

$$\lambda_T = 0 \quad \text{where } T \geq T_h$$

$$\text{where, } \gamma_r = \frac{1}{T_2 - T_1} \ln \frac{K_2(1 - K_1)}{K_1(1 - K_2)}$$

$$\gamma_f = \frac{1}{T_4 - T_3} \ln \frac{K_3(1 - K_4)}{K_4(1 - K_3)}$$

Light limitation (λ_l) Steele's (1965) formulation is used to simulate the light

limitation, which includes photoinhibition effects. $\lambda_l = \frac{I}{I_s} e^{(1 - \frac{I}{I_s})}$

where, I_s is the saturating light intensity

I is the available light intensity at depth z : $I = (1 - \beta)I_0 e^{-\eta z}$

I_0 is the light intensity at water surface;

β is the fraction of solar radiation absorbed at the water surface;

η is the light extinction coefficient, combination of the extinction effects of water, inorganic and organic suspended solids.

Nutrient limitation (λ_i) Nitrogen and phosphorus are the most commonly modeled limiting nutrients, plus silicon for diatoms. The most commonly used formulation for computing the nutrient limiting factor is based on the Michaelis-Menten or Monod relationship, which assumes that the nutrient compositions of the algal cells remain constant and the external nutrient concentrations Φ of available nutrients (i) affect the algal growth rates by a factor, λ .

$$\lambda_i = \frac{\Phi_i}{P_i + \Phi_i}$$

where, P_i is the half-saturation constant for the nutrient i .

Between nitrate and ammonia, algae prefer ammonia. This preference is expressed as a preference factor (P_{NH4}) (Cole and Wells 2003):

$$P_{NH4} = \Phi_{NH4} \frac{\Phi_{NO3}}{(K_{NH4} + \Phi_{NH4})(K_{NH4} + \Phi_{NO3})} + \Phi_{NH4} \frac{K_{NH4}}{(\Phi_{NH4} + \Phi_{NO3})(K_{NH4} + \Phi_{NO3})}$$

We output all the calculated results of limiting factors from the model for all three years and found no case that nitrogen is a limiting factor. So we will focus on phosphorus during this study.

It is assumed that zooplankton selectively graze on algae, which is modeled by assigning a weight to each algal group, i.e., 1.0 for NDEA, 0.5 for diatoms (Scavia *et al.* 1988) and 0 for NDIA. It is assumed that mussels graze on NDEA and diatoms indiscriminately (Fanslow *et al.* 1995, Horgan and Mills 1997). However, as blue-green algae are selectively rejected by dreissenid mussels (Vanderploeg *et al.* 2001), the net loss of blue-green algae due to mussel grazing is set to zero.

Zooplankton The energy fixed by phytoplankton moves up to zooplankton, which further affects fish recruitment. A clear water phase occurs in mid summer in many waters as a result of zooplankton grazing (Deneke and Nixdorf, 1999; Wu and Culver 1991). Cladocerans and copepods are two dominant zooplankton groups in Lake Erie after May (Wu and Culver 1991). So this paper focuses on these two crustacean groups. Fennel and Neumann's (2003) stage-structured population model of copepods is modified and added to our model. This copepod population submodel contains 4 state variables: copepod eggs, copepod nauplii, copepod copepodites, and copepod adults. A general mass conservation model, modified from Scavia *et al.*'s (1988) model is used to simulate cladocerans. It is assumed that crustaceans consume edible algae (NDEA and

edible diatoms) as well as non-living organic particles (Talling 2003). All model parameters and their values used are listed in Table 2.3.

Mussels Two processes of dreissenid mussels are included in the EcoLE model, i.e., grazing on phytoplankton and excreting nutrients. Dreissenid mussel densities estimated by Jarvis *et al.* (2000), which varied with water depth, are used in this study. Thus, sedimental area and water depth are two determinant factors of mussel population size. EcoLE is a two-dimensional model without discrimination of nearshore and offshore conditions, so algae at the nearshore and the offshore have equal accessibility to the mussels in the same model cell. A systematic error arises since mussels are only located on the nearshore rocks or sediment which is a much smaller area compared to the whole cell. To minimize this system error, we reshape each modeling segment (water column) in the shallow and flat western basin from a staircase box to a rectangular box. The deep central and eastern basins are not reshaped. To reshape the western basin, we set the surface area of the segment constant and adjust the depth (1 m resolution) so that the volume of the rectangular box (segment) is the closest to the real volume of the segment measured from the bathymetry (Figure 2.5). After the adjustment, all cells in a segment have the same size. Mussels are located only in the bottom cell, which has a sedimental area equal to the surface area of the segment. In the central and eastern basins, however, mussels are located in each cell (Figure 2.5a).

For simplicity, it is assumed that mussels in the western basin are all zebra mussels, whereas in the central and eastern basins they are all quagga mussels (Jarvis *et al.* 2000). It is also assumed that the mussels are uniform in size when not specifically

simulated otherwise. In chapter 4, sizes of the mussels are varied to better evaluate their impact on the ecosystem. Dreissenid filtering rates, nutrient excretion rates, and respiration rates used in the model are listed in Table 2.4.

Nutrients We modified Cole and Buchak's (1995) nutrient submodels by adding recycling components by crustaceans and dreissenids, such as respiration, excretion, ingestion, egestion, in the corresponding nutrient pools or pathways (Table 2.1).

Instead of using a constant, the sediment oxygen demand (SOD) is expressed as a function of oxygen concentration and temperature (Lucas and Thomas 1972, Lam *et al.* 1987).

$$S_{od} = S_{od\max} \frac{\Phi_{DO}}{\Phi_{DO} + O_h} \theta^{(T-20)}$$

$S_{od\max}$: maximum sediment oxygen demand at 20°C, g O₂ m⁻² d⁻¹,

O_h : oxygen concentration half-saturation constant, 1.4 g O₂ m⁻³.

Fish and benthos For a complete food web model, fish and benthos should be included as well. However, due to time and labor limitation of a doctoral research, we do not include those components in the model explicitly. Nevertheless, we implicitly include major connections of these components to water quality and plankton. For example, we have a predation loss term in the zooplankton submodel to include fish predation implicitly. For another example, oxygen demand of benthos is considered as part of the sediment oxygen demand. We assume that phosphorus excretion of benthos is refined within the sediment-water interface due to oxic conditions. Under anoxic

conditions, the accumulated phosphorus excreta are released to the water column as part of the anoxic sediment release. Fish phosphorus excretion is not considered in EcoLE. Fish play an important role in transporting nutrients from the hypolimnion to the epilimnion during stratification periods and adding “new” phosphorus to the epilimnion (Brabrand *et al.* 1990, Schaus *et al.* 1997, Vanni 2002, Bunnell *et al.* 2005, Vanni *et al.* 2006). However, this portion of phosphorus loading is much lower than planktonic community excretion in large lakes (Hudson *et al.* 1999), although it could supply a substantial amount of algal phosphorus-demand in some reservoirs (Vanni *et al.* 2006).

Data and data sources

It is challenging to collect all the data needed for such a complex ecosystem model. All help from the data source agencies (Table 2.5) is greatly appreciated. This model takes into consideration 7 tributaries of Lake Erie, including rivers and wastewater treatment plants (WWTP). They are the Detroit, Maumee, Sandusky Rivers and the Toledo WWTP OH, Cleveland Westerly WWTP OH, Cleveland Easterly WWTP OH, and Erie WWTP PA. For each tributary, flows, nutrient concentrations, and water temperatures are needed. Outflows are needed for two withdrawals, the Niagara River and the Welland Canal. Climate data include wind speed, wind direction, cloud cover, precipitation and air temperatures.

Physical, chemical and biological data needed to initialize the water quality state variables, and calibrate and verify the model are from the LEPAS Database. Data from 1997 are used for calibration, while data from 1998 and 1999 are used for verification. These three data sets have different external phosphorus loading scenarios. Year 1997

was a wet year with the highest TP loading; however it had similar SRP loading as did year 1998 (Table 3.1 and Figure 2.6). 1999 was a dry year with both the lowest TP and SRP loading of the three years. Thus, if the results of calibration and verification are good, it indicates that EcoLE can realistically reflect the impacts of various external phosphorus loads on the Lake Erie ecosystem. We will be more confident to use it as a water quality management analysis tool.

The sampling sites of 1997, 1998 and 1999 are consistent among years (Figure 2.7). Note that in the west central basin, the sampling sites are all nearshore stations and close to the mouth of Sandusky Bay.

Error analysis

Paired t-test (MINITAB 14) is used to test the significant difference ($p < 0.05$) between the means of model predictions and field measurements.

Mean relative error (Lam *et al.* 1983) is also used to assess the adequacy of the model, which is defined as $E = \frac{1}{N} \sum | \hat{c}_i - c_i | / \hat{c}_i$

Where, \hat{c}_i and c_i are the observed and the modeled values, and N is the number of pairs of the observed and modeled values. The median relative error refers to the mean relative error of the first 50% of the relative error samples which have been arranged in increasing order. The median relative error is regarded as a useful error statistic (Di Toro 1983; Lam *et al.* 1983).

SIMULATION AND RESULTS

Meteorological conditions and physical simulation

May to September is a relatively calm period. There was seldom any storm, and only two strong gales were recorded, in May and July, 1999. Most of the time wind speed was less than 14 m s^{-1} . 72% of the records in 1997 showed wind speed was less than 5.5 m s^{-1} . This number was 79% and 75% for 1998 and 1999 respectively. 1999 was a drier year than the other two years (Figure 2.6), which is also reflected in the mean modeled volume of Lake Erie, 501, 500 and 490 km^3 for 1997, 1998, and 1999, respectively.

The temperature in the western basin was relatively homogeneous across depth most of the time. Weak stratifications in the western basin (Figure 2.8a-2.10a) were partially due to the biased temperature sampling from the model, which occurred at noon each day. In the central and eastern basins, however, the model showed a strong thermal stratification with durations of over 2 months (Figures 2.8b, c-2.10b, c). The depth of the metalimnion bottom in the central basin was 12 m at the western end and increased to 16 m in the eastern end, thus the metalimnion was a tilted stratum that moved with frequent internal seiches.

The surface and bottom water temperature measurements taken with the plankton collections are used to evaluate the success of the physical simulation (Figures 2.11-2.13). Comparisons of the monthly means between the simulations and field measurements show that simulated temperatures agree with field measurements well for all three basins of 1997 (Figure 2.11). The differences between simulated and measured monthly means are all less than 1.2°C for bottom temperatures. The differences are higher for the 1997

surface temperatures, but most of them are less than 2.0 °C, except that of the eastern basin of June. For 1998, there is good agreement between modeled surface temperatures and measured ones. Most of the differences are less than 2.0 °C, except central and eastern basins in October (Figure 2.12a). The simulated 1998 bottom temperatures have fair agreement with the field measurements. There are 5 out of 14 cases have higher differences than 2.0 °C . The largest difference occurs in the central basin of October, when there are only two field observations available (Figure 2.12b). For 1999, a decent agreement between the model simulations and field measurements resulted for both surface and the bottom temperatures. Most of differences between model simulations and field measurements are less than 2.0 °C, except for that of surface temperatures of the western and central basins of June (Figure 2.13). From this, we conclude that using Cole and Buchak's (1995) algorithm and cloud cover data from NOAA adequately reflects the radiant input to the lake.

Chemical-biological simulations

Figures 2.14-2.16 show the simulation results of six state variables: NDEA, diatoms, copepods, cladocerans, total dissolved phosphorus (TP-F), and ammonia (NH₄). The simulations of NDIA are not calibrated and verified because of a paucity of frequent initial data. In late May or early June there were few *Microcystis* colonies observed in the water column, which means most of the model cells have no NDIA at the beginning of the simulations. Cynobacterial populations in the lake begin from resting cells in the surficial sediments and/or from riverine inputs. However, simulation results related to

NDIA were also investigated to obtain insights of NDIA dynamics using low artificial initial values replacing the zeros.

1997 was taken as the calibration year, while 1998 and 1999 are verification years. During verification, all calibrated parameters are kept intact, while the meteorological data, external loading, and initial values of state variables of the verification years are used in the simulations. In 1997, the model simulations matched with the field observations well for diatoms, TP-F, and NH_4 . However, model predicted lower values of NDEA, copepods and cladocerans in the west central basin (segments 50-80) than we found in field measurements. Similar simulation results occurred in verification years, 1998 and 1999, except that simulated biomass of copepods had a good match with high values in the west central basin. Even when the maximum growth rate of NDEA was increased, the model-predicted values were still lower than the field observations. Calibrating the model with these unnaturally high maximum growth rates would deplete the nutrients and slow algal growth. In the west central basin, the high observed values of NDEA are likely due to inputs from other sources, such as loading from tributaries, or resuspension of algae from the bottom. The low predicted values of cladoceran biomass in the west central basin are a consequence of the low predicted values of NDEA. Compared with the good match between simulations and observations of copepods in 1998 and 1999, the lower prediction in 1997 may indicate that the start date of simulation is important. Simulation in 1997 started on May 10, which is 10 days earlier than 1999 and 20 days earlier than 1998. The recruitment from diapausing eggs might still play an important role in copepod population dynamics during this time of 1997, however, this process is not considered in the model.

To examine the agreement the model's estimate of NDIA relative to field measurements, we average NDIA biomass for August and September for both field measurements and corresponding model predictions for all three years (Figure 2.17). We chose August and September because during these two months blue-green algal blooms are obvious (if they occur) and NDIA biomass is less affected by processes mentioned above (e.g., riverine loading). The model results show that the predictions of NDIA biomass are at the same range of field measurements for 1997 and 1999, while they are 90% lower than field measurements for 1998 when there were blue-green algal blooms. As the many NDIA loading sources are not considered in the model, our model does not predict a high NDIA abundance in the western basin as observed in 1998. However, our model does predict higher abundance of NDIA in the western basin that year.

Error analysis

Paired t- test (Table 2.6) shows that the mean differences are not significant for most of the cases. It is not surprising that there are several cases that are significant different given the complexity of the ecosystem and missing processes (for examples, algal loading from rivers, P loading from unmonitored non-point sources, etc.). However, as we are going to use this model to investigate the impacts of the external phosphorus loading program on the Lake Erie ecosystem, we certainly want to make sure that the phosphorus simulation is realistic. There are four cases that the means are significantly different. However, taking the 95% confident intervals into account, they are all small and below the measurement precision, which is 0.01 mg l^{-1} .

Median relative errors (Figure 2.18) are all below 50% for all six state variables and all three years. For 1997, TP-F has the lowest median relative error, 12%, while Copepods has the highest, 47%. For 1998, NDEA has the lowest, 17%, while Diatoms has the highest, 32%. For 1999, NH₄ has the lowest, 16%, while Diatoms has the highest, 41%. In general NDEA, TP-F and NH₄ have lower median relative errors and Diatoms and Copepods have higher median relative errors. The median relative errors of TP-F are all below 20% for three years.

Nutrient and algal distributions with/without physical mixing processes

Physical mixing processes are turned on and off to investigate their impacts on phytoplankters and nutrients in terms of concentrations and distributions. By turning off physical mixing processes we mean setting the two advection and two diffusion terms in the constituent transport equation (Table 2.1) to zero. The simulations of water movements and heat distribution in the lake are still on. The simulated concentrations and distributions of total dissolved phosphorus (TP-F), NDEA, NDIA and diatoms on August 30 of each year were investigated when the seasonal thermal stratifications firmly established.

The results show that the water column concentrations of total dissolved phosphorus with mixing processes were lower than those without for all three years (Figures 2.19a, 20a, 21a). There were extremely high concentration-peaks in the water column without mixing processes, while no such obvious peaks occurred in water column with mixing processes. Although there was less total dissolved phosphorus in the whole water column without mixing than with mixing processes, the total dissolved phosphorus

concentrations in the upper water with mixing processes were higher than those without (Figures 2.19b, 2.20b, 2.21b).

For 1997, NDEA water column concentrations were higher with mixing processes than those without mixing for most of the segments, except for some of the segments that directly received external phosphorus loading (Figure 2.22a). Similar results occurred for 1998 and 1999, except in the eastern basin simulations the differences between with and without mixing became less obvious (Figures 2.23a, 2.24a). NDEA distributed evenly in the epilimnion with mixing processes, while the distributions of NDEA show strong patchiness without mixing (Figures 2.22b, 2.23b, 2.24b).

The water column concentrations of NDIA had similar magnitude between with and without mixing simulations (Figures 2.25a, 2.26a, 2.27a), while the vertical distributions showed clearly different patterns. NDIA moved to upper water with mixing processes while NDIA concentrated at the bottom of the western basin or metalimnion of the central and eastern basins without mixing processes (Figures 2.25b, 2.26b, 2.27b).

Mixing processes also showed strong impacts on diatoms. With mixing processes, diatoms had much higher concentrations in the water column than those without mixing processes (Figures 2.28, 2.29, 2.30). In fact, without mixing processes diatoms tended to sink out of the euphotic zone due to their heavy silica frustules.

The mixing processes result in more algae available to the bottom water and increased the daily grazing rates of dreissenid mussels consistently in three basins during three simulation years (Table 2.7). The grazing rates of dreissenids without mixing were only 20% of those with mixing in the western basin, 40-50% in the central basin and 60-70% in the eastern basin.

Carbon pools

One use of an ecological model is to provide a holistic picture of the ecosystem which hardly can be fulfilled by field observations. For example, I have constructed carbon flow diagrams for each model year (Figures 2.31-2.35).

The seasonal averages of carbon pools are basin-wide carbon content of state variables, NDEA, NDIA, Diatoms, OM (organic matter), and CZ (crustacean zooplankton, i.e., cladocerans+copepods), which are calculated by

$$\frac{\sum^t \sum^j \sum^i C_{ijt} V_{ijt}}{N},$$

where C_{ijt} is the concentration of a state variable in the i^{th} model layer, the j^{th} segment and at time t (g m^{-3}). V is the water volume of the corresponding model cell (m^3). N is the total numbers of outputs of a carbon pool during a simulation period.

The results of carbon pool analysis (Figure 2.32) show that OM is the largest basin-wide carbon pool, while CZ was the smallest one for all three basins and all three model years in Lake Erie. The relative sizes of different algal-carbon pools varied among basins and years. For example, in the western basin NDEA was the largest algal-carbon pool and Diatoms was the smallest in 1997, while NDIA was the largest and Diatoms was the smallest in 1998, NDEA was the largest and NDIA was the smallest in 1999.

More than 90% of the NDEA and diatoms were in the upper water (above 12m excluding the bottom layer) column in the western basin. This number decreases to 85% in the central basin and 80% (60% for 1999) in the eastern basin as the thickness of epilimnion increases from west to east. NDIA was mainly distributed in the lower waters (refers to bottom layers and water deeper than 12m). Only about 50% of the NDIA was

in the upper water in the western basin, except during the blue-green algal bloom year, 1998, when about 70% of NDIA was in the upper water. As low as 30% of NDIA was in the upper water of the central basin and as low as 10% was in the upper water of the eastern basin. 85% of the OM was in the upper water of the western basin, 70% for the central basin, while it was only about 40% for the eastern basin. 90% of the CZ was in the upper water of the western basin, 80% for the central basin and 60% (80% in 1998) for the eastern basin.

Carbon flows

Daily basin-wide carbon flows (F , calculated as g C s^{-1} and converted into mt C d^{-1}) among state variables and mussels and sediment are calculated by:

$$F = \frac{\sum_t \sum_j \sum_i Q_{ijt} V_{ijt}}{N},$$

where, Q_{ijt} is the carbon flow (or bio-chemical process rate) from one state variable to another within a model cell (i, j) at time t ($\text{g C m}^{-3} \text{s}^{-1}$). For example, Q_{ijt} for carbon flow from NDEA to CZ is the total NDEA carbon per m^3 that grazed by CZ at model cell (i, j) at time t .

The net daily carbon exchanges between connected basins are seasonal averages of the summation of the net exchange of carbon mass of NDEA, NDIA, diatoms, copepods, cladocerans, DOM and POM at the transections. The carbon exchanges at the intersection between segment 49 and 50 are considered the exchanges between the western and the central basins, while the carbon exchanges at the intersection between segment 156 and segment 157 are considered the exchanges between the central and the western basins. Both horizontal advection and dispersion are included.

There are two main OM sources, dead algae and sloppy grazing of crustacean zooplankton (Figures 2.33-2.35). The carbon flows related to CZ are high and mainly occur in the upper water, which indicates CZ is an active component of the upper water food web. Carbon flows from algae to dreissenids are smaller than those from algae to CZ, although exceptions occur in the dry year, 1999. In the central and the eastern basins, dreissenids access all algae equally well in a model cell (due to the lateral averaging limitation of the model), so the carbon flows from algae to dreissenid mussels were over-estimated. Algal sedimentation rates were low. One of the reasons is that the dead or broken algae are considered as organic matter not algae. Thus, algae become organic matter during sinking before they reach the sediment. This also explains the high settlement rates of OM in our model. More than 80% of the net NDEA and diatom production occurs in the upper water in the western basin, while more than 100% occurs in the upper water in the central and eastern basins. The results of more algal production in the upper water than in the whole basin indicated that there was negative net production in the lower water in the central and eastern basin. NDIA had low basin-wide production and very low upper-water production. The negative production of NDIA in the upper water indicated NDIA were not strong nutrient competitors with NDEA and diatoms. Sedimental decompositions had the same magnitude of organic matter sedimentations. The central basin retained less carbon transported from the western basin than that transported to the eastern basin. A negligible accumulation occurred in the central basin for 1997, and 112 and 40 mt C for 1998 and 1999, respectively, while these numbers were 260, 216, and 172 mt C for the eastern basin of 1997, 1998 and 1999, respectively.

DISCUSSION

Physical simulations

The seasonal temperature distributions showed that there was no strong seasonal thermal stratification in the western basin. However, it was not always thermally homogeneous either. This weak stratification was observed by some studies and thought to be crucial for understanding the impact of dreissenid mussels on Lake Erie (Ackerman *et al.* 2000, Edwards *et al.* 2005). The duration of simulated seasonal stratifications in the central basin and the eastern basin agrees well with that reported by Schertzer *et al.* (1987). The water started to stratify in early June and became firmly stratified in early July. Fall turnover was about to occur by the end of September and stratification disappeared by the end of October (Figures 2.8b-10b). Results of this study also showed that there were relatively homogeneous temperatures within the epilimnion and hypolimnion, while the metalimnion became thinner with time. McCune (1998) and Edwards (2002) studied the mixing processes in the central basin and found a pattern similar to the results of this study. Modeled temperatures of the surface and bottom water of Lake Erie showed good agreement with the field observations. With these results we consider that EcoLE catches the major characteristics of the physical processes that can affect the chemical and biological processes.

The agreement of our simulation hydrodynamic results and those reported in Boegman *et al.* (2001) indicates that meteorological data measured either on land or on the lake can result in good simulations, and whether the solar radiation is measured directly on the lake or not. However, using meteorological data measured on land is

more convenient for modelers because on-land measurements have a much longer history and are easier to access.

Chemical and biological simulations

The EcoLE model predictions showed good agreement with observations. However, we also saw large standard deviations among the field observations as well as the simulations. This is a complex model and has numerous parameters and equations. The intensive monitoring program (sampled monthly, with some stations of some years sampled weekly) provides hundreds of observational data for calibration and verification. However, these data are still sparse for a model with high temporal and spatial resolution. For example, spatial interpolation has to be used to initialize the state variables for most of the segments, which may misrepresent the patchiness of phytoplankton and zooplankton. Another source of error could be the inherent limitation of a laterally averaged two-dimensional model. The model cannot predict the difference between the nearshore and offshore observations. However, we could not arbitrarily discard the nearshore or offshore field-collected data, since this would make the already sparse field data even less abundant. Plankton abundance is not always significantly different between nearshore and offshore sites (Wu and Culver 1994). Thus, data of each segment are averaged and investigated together with their standard deviations. Uncertainties also arise due to the simplified dreissenid population distribution used in the model. It is quite possible that the population densities are, in fact, ten times higher or lower than the ones we used in the model. Our uncertainty analysis showed that 10-fold differences in the dreissenid population density resulted in significant differences in the lake-wide means of

mass of state variables (Table 2.8). Given the above conditions, our model still holds the main characteristics of bio-chemical processes in Lake Erie. Thus, we are confident to use this model qualifiedly to analysis ecological processes. However, it should be used for quantitative prediction with caution.

Effects of physical mixing on lower trophic levels

Simulated results of with/without physical mixing processes clearly demonstrate the importance of physical mixing in bringing nutrients to algae in the upper water. Without mixing there was more total dissolved phosphorus (TP-F) accumulated in the whole water column, while there was less TP-F in the upper water than that with mixing. The result of more abundant algae in the upper water with mixing than that without further confirmed that mixing processes brought more dissolved phosphorus to the upper water and resulted in less dissolved phosphorus accumulated in the water column. Simulated results also showed that mixing processes bring more algae to benthic mussels. We accept our hypothesis that hydrodynamics plays an important role in the availability of nutrients to phytoplankton and the availability of phytoplankton to dreissenids.

These results have two implications. One is that increasing mixing processes under windy weather will enhance the energy flows through food webs, while weak mixing processes under calm and hot weather when stratification becomes strong will result in patchy distributions and slow down energy flows through the food web. Thus, not only does weather determine how much nutrient runoff into Lake Erie, it also plays a role in how much nutrients accumulated.

The other implication is the importance of hydrodynamics in evaluating the impacts of dreissenid mussels on basins or the whole lake. In the shallow and well mixed spots, mussels show their tremendous grazing influences (MacIsaac *et al.* 1992, Bunt *et al.* 1993). However, in the less well mixed areas or the whole basins, mussel impacts are restricted to the bottom boundary layers and consume far less than the expectations from extrapolating laboratory results or several-station measurements (Ackerman *et al.* 2001, Edwards *et al.* 2005).

Mixing processes showed strong influences on algal succession. The loss of diatoms without mixing mainly was due to sinking and silica limitation. The sinking rate in our model is 0.1 m d^{-1} , which is far less than 0.8 m d^{-1} used by Scavia *et al.* (1988) in their model. Silica limitation might play an even more important role, as diatom-derived organic matter sinks fast at 0.8 m d^{-1} and no resuspension occurs without mixing. Thus, the only source of silica is tributary loading, which is concentrated at the entrance model cells without mixing. No mixing is an extreme condition that would not happen in the field. However, low mixing conditions do exist in the field, such as during stratification seasons, when diatoms usually are very low.

Interestingly, basin-wide NDIA biomass did not change much between with and without mixing processes, although vertical distributions showed big differences. As NDIA are dominated by *Microcystis*, we discuss *Microcystis* below instead of NDIA.

Microcystis may be planktonic or benthic depending on environmental conditions such as light and nutrient levels (Paerl 1988). In our model, NDIA developed a high density at the bottom layer of the western basin and at the metalimnion of central and

eastern basins due to the tradeoff between light intensity and nutrient availability. Usually, blue-green algae have lower maximum growth rates and higher half-saturation phosphorus constants than other algae (Bowie *et al.* 1985, Scavia *et al.* 1988). Thus, a low light requirement is a critical parameter for *Microcystis* to successfully develop a bloom. Watanabe *et al.* (1985) reported that the growth rate increases with an increase in light and temperature. However, *Microcystis* grows well under low light conditions, 20-40 $\mu\text{E m}^{-2} \text{s}^{-1}$ (Watanabe *et al.* 1996, Hesse and Kohl 2001). Brookes *et al.* (1998, see in Brookes and Ganf 2001) reported *Microcystis* formed benthic mats that float to the surface as the population ages. Edwards *et al.* (2005) observed a high density *Microcystis* algal biomass above the mussel bed in August, 1995. Since *Microcystis* can migrate through the water column by regulating its buoyancy (Bonnet and Poulin 2002, Brookes and Ganf 2001) or by mixing currents (Howard 2001), vertical distribution of nutrients in Lake Erie should have no significant effects on *Microcystis* biomass in the water column. Babcock-Jackson (2000) also found that no significant relationship between spatial distribution of nutrients and *Microcystis* blooms. Therefore, calm and warm weather benefits *Microcystis* more than it does to other algal groups.

Carbon flows

It would be ideal to compare the computed carbon flows with the observed ones, if the latter were available. In the case of Lake Erie, however, carbon flows are rarely measured, since it is difficult to isolate one particular process from others that are strongly linked with it. Even if such process rates were measured in the field, the wide range of the estimates make the work less valuable to calibrate and verify a model. For

example, Hwang (1995, but see in Hwang and Heath, 1999) reported a range of algal primary productivity at a Lake Erie nearshore site to be 0.002-19.68 $\mu\text{g C l}^{-1} \text{hr}^{-1}$ and 0.002-0.924 $\mu\text{g C l}^{-1} \text{hr}^{-1}$ for an offshore site. Our average modeled algal primary productivity at the corresponding segment was 0.01 $\mu\text{g C l}^{-1} \text{hr}^{-1}$ with a maximum of 4.90 $\mu\text{g C l}^{-1} \text{hr}^{-1}$ at the surface and a minimum of -0.047 $\mu\text{g C l}^{-1} \text{hr}^{-1}$ at 1 m above the bottom.

Our simulated sedimentation rates were much smaller than those in Braidech *et al.*'s (1972) study. They reported sedimentation of organic matter (volatile solids) in the central basin from June to August of 1970 at a rate of 610-1,770 $\text{mg m}^{-2} \text{d}^{-1}$, while ours were 51-94 $\text{mg m}^{-2} \text{d}^{-1}$ among three simulation years. However, our data are basin-wide averages, while theirs were from two offshore stations. Kemp *et al.* (1976) measured sedimentation rates at 10 sample locations distributed in three basins of 1970. Their sedimentation rates (their Table 1) were of total sediments, of which only 10% was organic carbon. If we use a ratio of 0.45 for organic carbon to organic matter, their sedimentation rates of organic matter were 516-2178 $\text{mg m}^{-2} \text{d}^{-1}$, 240-724 $\text{mg m}^{-2} \text{d}^{-1}$ and 1311-3066 $\text{mg m}^{-2} \text{d}^{-1}$ for the western, central and eastern basins, respectively. Ours were 150-331 $\text{mg m}^{-2} \text{d}^{-1}$, 51-94 $\text{mg m}^{-2} \text{d}^{-1}$, and 45-99 $\text{mg m}^{-2} \text{d}^{-1}$ for the western, central and eastern basins, respectively. There were substantial decreases in the central and eastern basins. The high value of ours in the western basin is attributed to blue-green algal blooms and high tributary loading in 1998. However, to be cautious, we are hesitant to claim the decreasing trend between the sedimentation rates of these two studies in the western basin due to uncertainties of the model. Thus, it is still necessary to keep this philosophy in mind to deal with uncertainty - prepare for the 'worst'.

In summary, our ecological model predictions showed a good agreement with the observations with reasonable process rates indicated by carbon flows. However, this model should not be taken as final. It should be used as an analytical tool rather than a predictive one. The physical mixing processes showed their importance in the spatial distributions of algae and nutrients as well as algal succession. Crustacean zooplankton played an active role in the pelagic food web. Organic matter sedimentation decreased compared with that of the 1970s. Balance between organic matter sedimentation and decomposition tended to occur on the basin sediments, especially in the central basin.

Hydrodynamic equations^a:

Horizontal momentum

$$\frac{\partial UB}{\partial t} + \frac{\partial UUB}{\partial x} + \frac{\partial WUB}{\partial z} = \frac{1}{\rho} \frac{\partial BP}{\partial X} + \frac{\partial \left(BA_x \frac{\partial U}{\partial x} \right)}{\partial x} + \frac{\partial B\tau_x}{\partial z},$$
$$\tau_x = -A_z \frac{\partial U}{\partial z} + \tau_{wx} e^{-2kz}$$

Constituent Transport

$$\frac{\partial B\Phi}{\partial t} + \underbrace{\frac{\partial UB\Phi}{\partial x} + \frac{\partial WB\Phi}{\partial z}}_{\text{advection}(x,z)} - \underbrace{\frac{\partial \left(BD_x \frac{\partial \Phi}{\partial x} \right)}{\partial x} - \frac{\partial \left(BD_z \frac{\partial \Phi}{\partial z} \right)}{\partial z}}_{\text{diffusion}(x,z)} = q_\Phi B - S_\Phi B$$

Free Water Surface Elevation

$$\frac{\partial B_\eta \eta}{\partial t} = \frac{\partial}{\partial x} \int_\eta^h UB dz - \int_\eta^h qB dz$$

Hydrostatic Pressure

$$\frac{\partial P}{\partial z} = \rho g$$

Continuity

$$\frac{\partial UB}{\partial x} + \frac{\partial WB}{\partial z} = qB$$

Equation of State

$$\rho = f(T_w, \Phi_{TDS}, \Phi_{SS})$$

Heat budget equation:

$$H_n = H_s + H_a + H_e + H_c - (H_{sr} + H_{ar} + H_{br})$$

Continued

Table 2.1. A list of equations used in the EcoLE model developed in this study. a, equations from Cole and Buchak (1995); b, modified from Cole and Buchak (1995); c, modified from Scavia *et al.* (1988); d, from Fennel and Neumann (2003); e, this study; f, from Conroy *et al.* (2005b).

Table 2.1. continued

where,

-
- U : longitudinal, laterally averaged velocity, m sec^{-1}
 - B : waterbody width, m
 - t : time, sec
 - x : longitudinal Cartesian coordinate: x is along the lake centerline at the water surface, positive to the right.
 - z : vertical Cartesian coordinate: z is positive downward
 - W : vertical, laterally averaged velocity, m sec^{-1}
 - ρ : density, kg m^{-3}
 - P : pressure, N m^{-2}
 - A_x : longitudinal momentum dispersion coefficient
 - τ_x : shear stress per unit mass resulting from the vertical gradient of the horizontal velocity.
 - τ_{wx} : surface shear due to wind along the x-axis of the model
 - A_z : the vertical eddy viscosity.
 - Φ : laterally averaged constituent concentration
 - D_x : longitudinal temperature and constituent dispersion coefficient
 - D_z : vertical temperature and constituent dispersion coefficient
 - q_Φ : lateral inflow or outflow mass flow rate of constituent per unit volume
 - S_Φ : kinetics source/sink term for constituent concentrations
 - B_η : time and spatially varying surface width, m
 - η : free water surface location
 - h : total depth
 - q : lateral boundary inflow or outflow, $\text{m}^3 \text{sec}^{-1}$
 - g : acceleration due to gravity, m sec^{-2}
 - $f(T, \Phi_{TDS}, \Phi_{ss})$: density function dependent upon temperature, total dissolved solids or salinity, and suspended solids
 - H_n : net rate of heat exchange across the water surface
 - H_s : incident short wave solar radiation
 - H_a : incident long wave radiation
 - H_e : evaporative heat loss
 - H_c : heat conduction
 - H_{sr} : reflected short wave radiation
 - H_{ar} : reflected long wave radiation
 - H_{br} : back radiation from the water surface
 - T_s : water surface temperature
 - T_a : air temperature
-

Continued

Table 2.1. continued

Equations of non-living constituents^b

Inorganic suspended solids (Φ_{ss})

$$\frac{\partial \Phi_{ss}}{\partial t} = -\frac{\omega_{ss}}{\Delta z} \Phi_{ss}$$

Labile DOM (Φ_{ldom})

$$\frac{\partial \Phi_{ldom}}{\partial t} = \sum_j (K_{je} \Phi_j + (1 - P_m) K_{jm} \Phi_j) - \gamma_{om} K_{ldom} \Phi_{ldom}$$

j: refers to non-diatom edible algae, non-diatom inedible algae and diatoms

Detritus (Φ_{lpom})

$$\frac{\partial \Phi_{lpom}}{\partial t} = \sum_j P_m K_{jm} \Phi_j - K_{lpom} \gamma_{om} \Phi_{lpom} - \frac{\omega_{lpom}}{\Delta z} \Phi_{lpom} + f_{Clpom}$$

Diatom detritus (Φ_{Dpom})

$$\frac{\partial \Phi_{Dpom}}{\partial t} = P_m K_{Dm} \Phi_D - K_{Dpom} \gamma_{om} \Phi_{Dpom} - \frac{\omega_{Dpom}}{\Delta z} \Phi_{Dpom} + f_{CDpom}$$

D: diatoms

Phosphorus (Φ_P)

$$\begin{aligned} \frac{\partial \Phi_P}{\partial t} = & \sum_j (K_{jr} - K_{jg}) \delta_P \Phi_j + K_{ldom} \delta_P \gamma_{om} \Phi_{ldom} + K_{lpom} \delta_P \gamma_{om} \Phi_{lpom} \\ & + K_{Dpom} \delta_P \gamma_{om} \Phi_{Dpom} + \frac{S_P A_s}{\Delta V} + f_{mP} + f_{CP} \end{aligned}$$

Ammonium-Nitrogen (Φ_{NH_4})

$$\begin{aligned} \frac{\partial \Phi_{NH_4}}{\partial t} = & \sum_j (K_{jr} \Phi_j \delta_N - K_{jg} \Phi_j \delta_N P_{NH_4}) + K_{ldom} \delta_N \gamma_{om} \Phi_{ldom} + K_{lpom} \delta_N \gamma_{om} \Phi_{lpom} \\ & + K_{Dpom} \delta_N \gamma_{om} \Phi_{Dpom} + \frac{(S_{od} \delta_N / \delta_{om} + S_{NH_4}) A_s}{\Delta V} + K_{NO_3} \gamma_{NO_3} \Phi_{NO_3} - K_{NH_4} \gamma_{NH_4} \Phi_{NH_4} + f_{mNH_4} + f_{CNH_4} \end{aligned}$$

Continued

Table 2.1. continued

Nitrate-Nitrogen (Φ_{NO_3})

$$\frac{\partial \Phi_{NO_3}}{\partial t} = K_{NH_4} \gamma_{NH_4} \Phi_{NH_4} - K_{NO_3} \gamma_{NO_3} \Phi_{NO_3} - \sum_i (K_{ig} \Phi_i \delta_N (1 - P_{NH_4}))$$

Silicon (Φ_{Si})

$$\frac{\partial \Phi_{Si}}{\partial t} = K_{Dpom} \gamma_{om} \delta_{Si} \Phi_{Dpom} + \frac{(S_{od} \delta_{Si} / \delta_{om} + S_{Si}) A_s}{\Delta V} - K_{Dg} \delta_{Si} \Phi_D$$

Dissolved Oxygen (Φ_{DO})

$$\begin{aligned} \frac{\partial \Phi_{DO}}{\partial t} = & \sum_j (K_{jg} - K_{jr}) \delta_{om} \Phi_j - K_{NH_4} \delta_{NH_4} \gamma_{NH_4} \Phi_{NH_4} - K_{lpom} \delta_{om} \gamma_{om} \Phi_{lpom} \\ & - K_{Dpom} \delta_{om} \gamma_{om} \Phi_{Dpom} - \frac{S_{od} / \delta_{om} A_s}{\Delta V} - K_{ldom} \gamma_{om} \delta_{om} \Phi_{ldom} - A_{kt} E_o (\Phi'_{DO} - \Phi_{DO}) - f_{mO} - f_{CO} \end{aligned}$$

where, Φ_i = concentration of variable i, g m⁻³

Δz = model cell thickness, m

P_m = proportional of dead algae contributed to particulate organic matter.

K_i = kinetic rates, sec⁻¹

γ_i = temperature rate multipliers

δ_i = stoichiometric coefficients

A_s = sediment area, m²

ω_i = sinking rates, m sec⁻¹

ΔV = model cell volume, m³

S_i = sediment release rates, g m⁻² sec⁻¹

f_{Ci} = impact of crustacean activities on variable i, g m⁻³ sec⁻¹

f_{mi} = impact of mussels activities on variable i, g m⁻³ sec⁻¹

P_{NH_4} = ammonium preference factor

$$S_{od} = S_{od \max} \frac{\Phi_{DO}}{\Phi_{DO} + O_h} \theta^{(T-20)}$$

$S_{od \max}$: maximum sediment oxygen demand at 20°C, g O₂ m⁻² d⁻¹,

O_h : oxygen concentration half-saturation constant, g O₂ m⁻³.

Equations of phytoplankton^b

Diatoms (Φ_D):

$$\frac{\partial \Phi_D}{\partial t} = K_{Dg} \Phi_D - K_{Dr} \Phi_D - K_{De} \Phi_D - K_{Dm} \Phi_D - \frac{\omega_D}{\Delta z} \Phi_D - f_{mD} - f_{CD}$$

Continued

Table 2.1. continued.

Non-diatom edible algae (Φ_{NDEA}):

$$\frac{\partial \Phi_{NDEA}}{\partial t} = K_{NDEAg} \Phi_{NDEA} - K_{NDEAr} \Phi_{NDEA} - K_{NDEAe} \Phi_{NDEA} - K_{NDEAm} \Phi_{NDEA} - \frac{\omega_{NDEA}}{\Delta z} \Phi_{NDEA} - f_{mNDEA} - f_{CNDEA}$$

Non-diatom inedible algae (Φ_{NDIA}):

$$\frac{\partial \Phi_{NDIA}}{\partial t} = K_{NDIAg} \Phi_{NDIA} - K_{NDIAr} \Phi_{NDIA} - K_{NDIAe} \Phi_{NDIA} - K_{NDIAM} \Phi_{NDIAM} - \frac{\omega_{NDIA}}{\Delta z} \Phi_{NDIA}$$

Auxiliary functions:

Growth rates:

$$K_{ig} = \gamma_{ir} \gamma_{if} \lambda_{i \min} K_{ig \max}$$

Dark respiration rates:

$$K_{ir} = \gamma_{ir} K_{ir \max}$$

Photorespiration rates:

$$K_{ie} = \gamma_{ir} \gamma_{if} \lambda_{i1} K_{ie \max}$$

Mortality rates:

$$K_{im} = \gamma_{ir} \gamma_{if} K_{im \max}$$

Limiting factor (light):

$$\lambda_{i1} = \frac{I}{I_s} e^{\left(\frac{-I}{I_s} + 1\right)}$$

Limiting factor (phosphorus or nitrogen):

$$\lambda_{ij} = \frac{\Phi_j}{P_{ij} + \Phi_j}$$

Ammonium preference factor:

$$P_{NH4} = \Phi_{NH4} \frac{\Phi_{NOx}}{(K_{NH4} + \Phi_{NH4})(K_{NH4} + \Phi_{NOx})} + \Phi_{NH4} \frac{K_{NH4}}{(\Phi_{NH4} + \Phi_{NOx})(K_{NH4} + \Phi_{NOx})}$$

where i = diatoms, non-diatom edible algae or non-diatom inedible algae

γ_r = temperature rate multiplier for rising limb of curve

γ_f = temperature rate multiplier for falling limb of curve

λ_{\min} = multiplier for limiting growth factor (minimum of light, phosphorus and nitrogen)

I_s = saturating light intensity at maximum photosynthetic rate, $W m^{-2}$

Continued

Table 2.1. continued.

$K_{g\max}$	= maximum algal growth rate, s^{-1}
$K_{r\max}$	= maximum dark respiration rate, sec^{-1}
$K_{e\max}$	= maximum excretion rate constant, sec^{-1}
$K_{m\max}$	= maximum mortality rate, sec^{-1}
I	= available light, $W\ m^{-2}$
Φ_j	= phosphorus or nitrate+ammonium concentration or silicon, $g\ m^{-3}$
P_j	= half-saturation coefficients for phosphorus or nitrate+ammonium, or silicon, $g\ m^{-3}$
K_{NH_4}	= ammonia preference half-saturation coefficient, $g\ m^{-3}$, 0.01

Equations of Cladocerans^e

$$\frac{dZ}{dt} = (Ag - r - s)Z - P$$

where, A is assimilation rate
g is ingestion rate

$$g = g_{\max} \frac{F}{K + F}$$

g_{\max} is the maximal weight-specific ingestion rate.

K is the half-saturation constant.

F is the weighted combination of algae and detritus.

r is respiration loss, which consists of a basic value and a portion that

proportional to the food function. i.e. $r = (r_1 + r_2 \frac{F}{K + F})\theta^{(T-20)}$

s is the loss of starvation, $s = s_0 \min(1, 1 - \frac{g}{g_s})$,

P is the predation loss. $P = p_0 (\frac{Z}{Z_h + Z})Z$

Equations of Copepods^d

Populations:

$$\frac{dZ_e}{dt} = T_{ae}Z_a - T_{en}Z_e - \mu_e Z_e$$

$$\frac{dZ_n}{dt} = T_{en}Z_e + (g_n - l_n - \mu_n)Z_n - T_{nc}Z_n$$

Continued

Table 2.1. continued.

$$\frac{dZ_c}{dt} = T_{nc}Z_n + (g_c - l_c - \mu_c)Z_c - T_{ca}Z_c$$

$$\frac{dZ_a}{dt} = T_{ca}Z_c + (g_a - l_a - \mu_a)Z_a - T_{ae}Z_a$$

Auxiliary functions:

Ingestion rate:

$$g_i = \beta_0 e^{(aT)} (1 - e^{(-I_i^2 F^2)}) f(m_i, X_i)$$

Reproduction:

$$T_{ae} = \left(\frac{1}{2}\right) 0.3 g_a$$

Hatching rate:

$$T_{en} = h \theta (T - T_0) \exp(a(T - T_0))$$

Transfer rates to the next stage:

$$T_{i,i+1} = g_i f(< m_i >, m_i)$$

Food function:

$$F = \Phi_G + 0.5 * \Phi_D + 0.2 * \Phi_{dt}$$

Fermi function:

$$f(x, y) = \frac{1}{1 + \exp\left(\frac{20}{y}(x - y)\right)}$$

where, Z_i = total biomass of stage i.

μ_i = mortality rate per day

l_i = egestion rates per day, a portion of ingestion,

m_i = individual weight of stage i

X_i = critical individual weight

$< m_i >$ = molting weight

Activity functions of mussels and crustacean zooplankters^e

Detritus:

$$f_{Cdt} = ((1 - A)g \frac{\Phi_{NDEA} + 0.5 * \Phi_D}{K + F} - Ag \frac{0.5 * \Phi_{lpom}}{K + F}) Z_{cladoceran} + \sum_i^{copepod} (l_i - g_i \frac{0.2 * \Phi_{lpom}}{K + F}) Z_i$$

Continued

Table 2.1. continued

Excretion of crustaceans:

$$f_{CP} = \delta_{P-clad} r m_{cladoceran} + \sum_i^{copepod} \delta_{P-cop} r m_i$$

$$f_{CNH_4} = \delta_N r Z_{cladoceran} + \sum_i^{copepod} \delta_N r m_i$$

Excretion of dreissenid mussels^f (ZMP, QMP, MNH₄):

$$\log_{10}(ZMP) = 0.505[\log_{10}(W_{zm})] - 1.172$$

$$\log_{10}(QMP) = 0.297[\log_{10}(W_{qm})] - 1.195$$

$$\log_{10}(MNH_4) = 0.379[\log_{10}(W_m)] + 0.021$$

$$f_{zmp} = W_{zm} N_{zm} ZMP$$

$$f_{qmp} = W_{qm} N_{qm} QMP$$

$$f_{mNH_4} = W_m N_m MNH_4$$

Oxygen consumption:

$$f_{CO} = \delta_{om} r Z_{cladoceran} + \sum_i^{copepod} \delta_{om} r m_i$$

$$f_{mO} = \varepsilon_O W_{mussel} N_{mussel}$$

where,

δ_i = stoichiometric equivalent between nutrient and dry weight biomass.

ε_O = oxygen consumption rate of mussels, $g\ g^{-1}\ s^{-1}$

W_{mussel} = individual dry weight of mussels, g.

N_{mussel} = density of mussels, $\#\ m^{-3}$, areal density divided by depth of the water

Phylum	Genus/Description	Edible/Inedible
Chlorophyta	<i>Actinastrum</i>	Edible
Chlorophyta	<i>Ankistrodesmus</i>	Edible
Chlorophyta	<i>Carteria</i>	Edible
Chlorophyta	<i>Characium</i>	Edible
Chlorophyta	<i>Chlamydomonas</i>	Edible
Chlorophyta	<i>Closteriopsis</i>	Edible
Chlorophyta	<i>Coelastrum</i>	Edible
Chlorophyta	Colonial chlorophyte	Edible
Chlorophyta	<i>Cosmarium</i>	Edible
Chlorophyta	<i>Crucigenia</i>	Edible
Chlorophyta	<i>Dictyosphaerium</i>	Edible
Chlorophyta	<i>Dimorphococcus</i>	Edible
Chlorophyta	<i>Eutetramorus</i>	Edible
Chlorophyta	<i>Franceia</i>	Edible
Chlorophyta	<i>Golenkinia</i>	Edible
Chlorophyta	<i>Gonium</i>	Edible
Chlorophyta	<i>Kirchneriella</i>	Edible
Chlorophyta	<i>Lagerheimia</i>	Edible
Chlorophyta	<i>Oocystis</i>	Edible
Chlorophyta	<i>Pandorina</i>	Edible
Chlorophyta	<i>Pediastrum</i>	Edible
Chlorophyta	<i>Scenedesmus</i>	Edible
Chlorophyta	<i>Schroederia</i>	Edible
Chlorophyta	Solitary Green	Edible
Chlorophyta	<i>Sphaerocystis</i>	Edible
Chlorophyta	<i>Spirogyra</i>	Edible
Chlorophyta	<i>Staurastrum</i>	Edible
Chlorophyta	<i>Synura</i>	Edible
Chlorophyta	<i>Tetraedron</i>	Edible
Chlorophyta	<i>Treubaria</i>	Edible
Chrysophyta (Chrysophyceae)	<i>Dinobryon</i>	Edible
Chrysophyta (Chrysophyceae)	<i>Mallomonas</i>	Edible

Continued

Table 2.2. Phytoplankton taxa in Lake Erie (from LEPAS database, OSU,OH, USA). Note the ‘diatom’ notations in first column and ‘edible/inedible’ of the last column, which are the bases of our algal grouping in EcoLE.

Table 2.2. continued

Chrysophyta (diatoms)	<i>Asterionella</i>	Edible
Chrysophyta (diatoms)	Centric Diatom	Edible
Chrysophyta (diatoms)	<i>Cocconeis</i>	Edible
Chrysophyta (diatoms)	<i>Coscinodiscus</i>	Edible
Chrysophyta (diatoms)	<i>Cyclotella</i>	Edible
Chrysophyta (diatoms)	<i>Cymbella</i>	Edible
Chrysophyta (diatoms)	<i>Fragilaria</i>	Edible
Chrysophyta (diatoms)	<i>Gomphonema</i>	Edible
Chrysophyta (diatoms)	<i>Gyrosigma</i>	Edible
Chrysophyta (diatoms)	<i>Navicula</i>	Edible
Chrysophyta (diatoms)	<i>Nitzschia</i>	Edible
Chrysophyta (diatoms)	<i>Opephora</i>	Edible
Chrysophyta (diatoms)	Pennate Diatom	Edible
Chrysophyta (diatoms)	<i>Rhizosolenia</i>	Edible
Chrysophyta (diatoms)	<i>Rhoicosphenia</i>	Edible
Chrysophyta (diatoms)	<i>Stephanodiscus</i>	Edible
Chrysophyta (diatoms)	<i>Surirella</i>	Edible
Chrysophyta (diatoms)	<i>Synedra</i>	Edible
Chrysophyta (diatoms)	<i>Tabellaria</i>	Edible
Cryptophyta	<i>Chroomonas</i>	Edible
Cryptophyta	<i>Cryptomonas</i>	Edible
Cryptophyta	<i>Rhodomonas</i>	Edible
Chlorophyta	Chlorophyte Filament	Inedible
Chlorophyta	<i>Closterium</i>	Inedible
Chlorophyta	<i>Micractinium</i>	Inedible
Chlorophyta	Spiny Green	Inedible
Chrysophyta (diatoms)	<i>Melosira</i>	Inedible
Cyanophyta	<i>Anabaena</i>	Inedible
Cyanophyta	<i>Aphanizomenon</i>	Inedible
Cyanophyta	<i>Aphanocapsa</i>	Inedible
Cyanophyta	<i>Aphanothece</i>	Inedible
Cyanophyta	<i>Chroococcus</i>	Inedible
Cyanophyta	<i>Lyngbya</i>	Inedible
Cyanophyta	<i>Merismopedia</i>	Inedible
Cyanophyta	<i>Microcystis</i>	Inedible
Cyanophyta	Narrow filament	Inedible
Cyanophyta	<i>Oscillatoria</i>	Inedible
Cyanophyta	<i>Spirulina</i>	Inedible
Pyrrophyta	<i>Ceratium</i>	Inedible
Pyrrophyta	<i>Gymnodinium</i>	Edible
Pyrrophyta	<i>Peridinium</i>	Edible

Kinetic Parameter	Suggested Range (Cole and Buchak 1995)	Value Used
Diatoms:		
growth rate, day ⁻¹ , K_{Dgmax}	1.1-2.0, 3.0 ¹	3.0
mortality rate, day ⁻¹ , K_{Dmmax}	0.01-0.1	0.07
excretion rate, day ⁻¹ , K_{Demax}	0.01-0.04	0.01
dark respiration rate, day ⁻¹ , K_{Dtmax}	0.02-0.04, 0.05 ²	0.05
settling rate, m/day, ω_D	0.1-0.14, 0.8 ³	0.20
Algal half-saturation constant for ammonium, g m ⁻³ , P_{DNH4}	0.014, 0.03 ¹	0.03
Algal half-saturation constant for phosphorus, g m ⁻³ , P_{DP}	0.003-0.009, 0.002 ¹	0.002
Algal half-saturation constant for silica, g m ⁻³ , P_{DSi}	0.03 ²	0.03
Saturation intensity at maximum photosynthetic rate, W m ⁻² , I_{Ds}	75-150	120
S _i content of DW biomass, g g DW ⁻¹ , δ_{S_i}	0.21 ⁴	0.21
(1) Lower temperature for growth, °C, T_{D1}	4 ⁴	4
(2) Lower temperature for maximum growth, °C, T_{D2}	12 ⁴	12
(3) Upper temperature for maximum growth, °C, T_{D3}	16 ⁴	16
(4) Upper temperature for growth, °C, T_{D4}	35 ²	35
Fraction of algal growth rate at (1), K_{D1}	0.10	0.10
Fraction of algal growth rate at (2), K_{D2}	0.99	0.99
Fraction of algal growth rate at (3), K_{D3}	0.99	0.99
Fraction of algal growth rate at (4), K_{D4}	0.10	0.10
NDEA		
growth rate, day ⁻¹ , $K_{NDEAgmax}$	1.1-2.0, 3.0 ¹	3.0
mortality rate, day ⁻¹ , $K_{NDEAmmax}$	0.01-0.1	0.07
excretion rate, day ⁻¹ , $K_{NDEAemax}$	0.01-0.04	0.01
dark respiration rate, day ⁻¹ , $K_{NDEArmax}$	0.02-0.04, 0.05 ²	0.05
settling rate, m/day, ω_{NDEA}	0.1-0.14, 0.05 ³	0.05
Algal half-saturation constant for ammonium, g m ⁻³ , $P_{NDEANH4}$	0.014, 0.03 ²	0.03

Continued

Table 2.3. Kinetic rates used in the model (modified from Boegman 1999).
Superscript numbers indicate different references other than Cole and Buchak (1995).

Table 2.3. continued

Algal half-saturation constant for phosphorus, g m^{-3} , P_{NDEAP}	0.003-0.009, 0.002 ¹	0.002
Saturation intensity at maximum photosynthetic rate, W m^{-2} , I_{NDEAs}	75-150	120
(5) Lower temperature for growth, $^{\circ}\text{C}$, T_{NDEA1}	4 ⁴	4
(6) Lower temperature for maximum growth, $^{\circ}\text{C}$, T_{NDEA2}	18 ⁴	18
(7) Upper temperature for maximum growth, $^{\circ}\text{C}$, T_{NDEA3}	25 ⁴	25
(8) Upper temperature for growth, $^{\circ}\text{C}$, T_{NDEA4}	35 ²	35
Fraction of algal growth rate at (5), K_{NDEA1}	0.10	0.10
Fraction of algal growth rate at (6), K_{NDEA2}	0.99	0.99
Fraction of algal growth rate at (7), K_{NDEA3}	0.99	0.99
Fraction of algal growth rate at (8), K_{NDEA4}	0.10	0.10
NDIA		
growth rate, day^{-1} , $K_{NDIAgmax}$	1.1-2.0	2.0
mortality rate, day^{-1} , $K_{NDIAmmax}$	0.01-0.1	0.03
excretion rate, day^{-1} , $K_{NDIAemax}$	0.01-0.04	0.04
dark respiration rate, day^{-1} , $K_{NDIAatmax}$	0.02-0.04, 0.05 ²	0.05
settling rate, m/day , ω_{NDIA}	0.1-0.14, 0.05 ³	0.05
Algal half-saturation constant for ammonium, g m^{-3} , $P_{NDIANH4}$	0.001 ⁴	0.001
Algal half-saturation constant for phosphorus, g m^{-3} , P_{NDIAP}	0.010 ²	0.010
Saturation intensity at maximum photosynthetic rate, W m^{-2} , I_{NDIAs}	50 ¹	50
(9) Lower temperature for growth, $^{\circ}\text{C}$, T_{NDIA1}	15 ⁴	15
(10) Lower temperature for maximum growth, $^{\circ}\text{C}$, T_{NDIA2}	22 ⁴	22
(11) Upper temperature for maximum growth, $^{\circ}\text{C}$, T_{NDIA3}	30 ²	30
(12) Upper temperature for growth, $^{\circ}\text{C}$, T_{NDIA4}	35 ²	35
Fraction of algal growth rate at (9), K_{NDIA1}	0.10	0.10
Fraction of algal growth rate at (10), K_{NDIA2}	0.99	0.99
Fraction of algal growth rate at (11), K_{NDIA3}	0.99	0.99
Fraction of algal growth rate at (12), K_{NDIA4}	0.10	0.10
Fraction of algal biomass lost by mortality to detritus, P_m	0.8	0.8
Labile dissolved organic material decay rate, day^{-1} , K_{ldom}	0.12	0.12
Detritus decay rate, day^{-1} , K_{lpom}	0.06-0.08	0.08
Detritus settling rate, m day^{-1} , ω_{lpom}	0.35-0.5	0.5
Diatom detritus decay rate, day^{-1} , K_{Dpom}	0.08 ⁴	0.08
Diatom detritus settling rate, m day^{-1} , ω_{Dpom}	0.8 ⁴	0.8

Continued

Table 2.3. continued

(13) lower temperature for organic matter decay, °C, T_{OM1}	4-5	5.0
(14) Lower temperature for maximum organic matter decay, °C, T_{OM2}	20-25	25
Fraction of organic matter decay rate at (13), K_{OM1}	0.10	0.10
Fraction of organic matter decay rate at (14), K_{OM2}	0.99	0.99
Maximum sediment oxygen demand, g O ₂ m ⁻² day ⁻¹ , S_{odmax}	0.1-0.27 ^{5,6,7} , 1.6-3.9 ⁸	0.22
Oxygen half-saturation constant for SOD, g O ₂ m ⁻³ , O_h	1.4 ⁷	1.4
Temperature coefficient, θ	1.047-1.0147	1.047
Anaerobic sediment release rate of phosphorus, g m ⁻² d ⁻¹ , S_P	0.015-0.3, 0.001-0.002 ¹	0.002
Anaerobic release rate of ammonium, g m ⁻² d ⁻¹ , S_{NH4}	0.05-0.4, 0.004- 0.01 ¹	0.005
Ammonium decay rate (oxidation to nitrate), day ⁻¹ , K_{NH4}	0.12	0.12
(15) Lower temperature for ammonium decay, °C, T_{NH41}	5	5.0
(16) Lower temperature for maximum ammonium decay, °C, T_{NH42}	20-25	25
Fraction of nitrification rate at (15), K_{NH41}	0.10	0.10
Fraction of nitrification rate at (16), K_{NH42}	0.99	0.99
Nitrate decay rate, day ⁻¹ , K_{NO3}	0.05-0.15	0.05
(17) Lower temperature for nitrate decay, °C, T_{NO31}	5	5.0
(18) Lower temperature for maximum nitrate decay, °C, T_{NO32}	20-25	25
Fraction of denitrification rate at (17), K_{NO31}	0.10	0.10
Fraction of denitrification rate at (18), K_{NO32}	0.99	0.99
Oxygen stoichiometric equivalent for ammonium decay, δ_{NH4}	4.57	4.57
Oxygen stoichiometric equivalent for organic matter decay, δ_{om}	1.4	1.4
Oxygen stoichiometric equivalent for algal growth, δ_{ag}	1.4	1.4
Stoichiometric equivalent between organic matter and phosphorus, δ_P	0.005-0.011	0.01
Stoichiometric equivalent between organic matter and nitrogen, δ_N	0.08	0.08
Stoichiometric equivalent between organic matter and carbon, δ_C	0.45	0.45
Dissolved oxygen concentration at which anaerobic processes begin, g m ⁻³	0.05-0.1	0.1

Continued

Table 2.3. continued

<u>Parameter definitions and estimates for cladoceran submodel</u>		
Maximum consumption rate, d^{-1} , g_{max}	0.8-1.6 ¹	0.8-1.0
Basic respiration rate, d^{-1} , r_1	0.1 ¹	0.1
Food dependent respiration rate, d^{-1} , r_2	0.25 ¹	0.25
Assimilation rate, A	0.5-0.7 ¹	0.6
Half-saturation food constant, $g\ C\ m^{-3}$, K	0.18 ¹	0.16
Maximum starvation loss rate, d^{-1} , s_0	0.3 ⁴	0.3
Minimum non-starving consumption rate, d^{-1} , g_s	0.05 ⁴	0.05
Maximum predation loss rate, d^{-1} , P_0	0.8 ⁴	0.8
Half-saturation predation constant, $g\ DW\ m^{-3}$, Z_h	0.5 ⁴	0.5
<u>Parameter definitions and estimates for copepod submodel²</u>		
Egg mass, $mg\ C$, m_e	0.0001	0.0001
Nauplius mean mass, $mg\ C$, m_n	0.00022	0.00022
Adult mean mass, $mg\ C$, m_a	0.0026	0.0026
Copepodite mean mass, $mg\ C$, m_c	0.0016	0.0016
Nauplius molting mass, $mg\ C$, $\langle m_n \rangle$	0.0003	0.0003
Copepodite molting mass, $mg\ C$, $\langle m_c \rangle$	0.002	0.002
Adult molting mass, $mg\ C$, $\langle m_a \rangle$	0.003	0.003
Ivlev constant for copepodites, I_c^2	0.007	0.007
Ivlev constant of adult, I_a^2	0.0101	0.0101
Nauplius grazing rate at 0 °C, d^{-1} , β_n	0.5	0.5
Copepodite grazing rate at 0 °C, d^{-1} , β_c	0.30	0.30
Adult grazing rate at 0 °C, d^{-1} , β_a	0.12	0.12
Egg mortality rate, d^{-1} , μ_e	0.2	0.2
Nauplius mortality rate, d^{-1} , μ_n	0.033	0.033
Copepodite mortality rate, d^{-1} , μ_c	0.05	0.05
Adult mortality rate, d^{-1} , μ_a	0.025	0.025

1 Bowie et al. (1985 and references therein); 2 Scavia (1980); 3 Scavia *et al.* (1988); 4 This study; 5 Di Toro and Connolly (1980); 6 Lam *et al.* (1984); 7 Lam *et al.* (1987); 8 Lucas and Thomas (1972); 9 Fennel and Neumann (2003).

	Western Basin	Central Basin	Eastern Basin
Length(mm)-mass(mg) regression	$DW=0.0057L^{2.732}$ (1)	$DW=0.0046L^{2.848}$ (1)	$DW=0.004L^{2.96}$ (2)
Filtering rates ($l\ h^{-1}$)	$FR=1.919DW(g)^{0.88}$ (3)	$CR=0.2221DW^{0.5419}$ (4)	$CR=0.2221DW^{0.5419}$
Filtering rates($m^3\ day^{-1}$)	$FR=0.046DW(g)^{0.88}$ (3)	$CR=0.005DW^{0.5419}$ (4)	$CR=0.005DW^{0.5419}$ (4)
N excretion rate, (mg N g DW ⁻¹ d ⁻¹)	$\log_{10}(NH_4)=0.379\log_{10}(DW)$ $+0.021^{(1)}$	$\log_{10}(NH_4)=0.379\log_{10}(DW)$ $+0.021^{(1)}$	$\log_{10}(NH_4)=0.379\log_{10}(DW)$ $+0.021^{(1)}$
P excretion rate, (mg P g DW ⁻¹ d ⁻¹)	$\log_{10}(PO_4)=0.505\log_{10}(DW)$ $-1.172^{(1)}$	$\log_{10}(PO_4)=0.297\log_{10}(DW)$ $-1.195^{(1)}$	$\log_{10}(PO_4)=0.297\log_{10}(DW)$ $-1.195^{(1)}$
O ₂ consumption rates, (mg O ₂ g DW ⁻¹ d ⁻¹)	1.0 (6)	6.0 (6)	6.0 (6)

(1) Conroy *et al.* (2005b); (2) Roe and MacIsaac (1997); (3) Pontius (2000); (4) Baldwin et al. (2002); (5) Arnott and Vanni (1996); (6) This study.

Table 2.4. Kinetic rates of dreissenid mussels used in the EcoLE model.

Location	Data	Data sources
The central basin	Meteorological data	http://www.ncdc.noaa.gov/pdfs/lcd/lcd.html
Cleveland Easterly WWTP	constituent concentrations, inflow and water temperature	Sandra Kemper, OHEPA
Cleveland Westerly WWTP	constituent concentrations, inflow and water temperature	Sandra Kemper, OHEPA
Detroit River	constituent concentrations, inflow and water temperature	Richard N. Lundgren, DEQ Surface Water Quality Division, Lansing, MI John Koschik ,Hydraulic Engineer, USACE, Detroit District, Great Lakes Hydraulics and Hydrology Office
over Lake Erie Erie WWTP	meteorological data constituent concentrations, inflow and water temperature	http://www.ncdc.noaa.gov/pdfs/lcd/lcd.html Nichole Maywah, OHEPA
Lake Erie	bathymetry file	Leon Boegman, University of Western Australia
Lake Erie	Initialization of state variables	LEPAS database in OSU
Maumee River	constituent concentrations, inflow and water temperature	Peter Richards at Heidelberg College Mary Ann Silagy, OHEPA
Niagara River at Buffalo, NY	flows	Tim Hunter, USGS
over Lake Erie	Precipitation	Tim Hunter, USGS
Sandusky River	constituent concentrations, inflow and water temperature	Peter Richards, Heidelberg College and Mary Ann Silagy, OHEPA, Douglas A. Keller, OHEPA, Division Of Drinking And Ground Waters
Toledo WWTP	constituent concentrations, inflow and water temperature	Sandra Kemper, OHEPA
Welland Canal	withdrawals	Tim Hunter, USGS

Table 2.5. Input data needed to run EcoLE and their sources.

	WB	CB	EB
1997			
NDEA	+	+	+
Diatoms	+	+	+
Cladocceans	+	+	+
Copepods	-	-	+
TP-F	-	-	+
NH4	-	+	+
1998			
NDEA	+	-	+
Diatoms	-	+	+
Cladocceans	+	+	-
Copepods	+	-	-
TP-F	+	+	+
NH4	-	-	+
1999			
NDEA	-	+	+
Diatoms	+	+	+
Cladocceans	+	-	+
Copepods	+	+	+
TP-F	-	-	+
NH4	+	+	+

Table 2.6. Results of paired t-test ($p < 0.05$) of the mean difference between modeled and observed values of six state variables for three years. “-” indicates significant difference. “+” indicates no significant difference.

	WB			CB			EB		
	Mixing	No mixing	%	Mixing	No mixing	%	Mixing	No mixing	%
1997	235	51	78	210	92	56	71	43	40
1998	283	63	78	338	161	52	143	87	39
1999	354	75	79	365	193	47	308	217	29

Table 2.7. Comparisons of simulated daily grazing rates of dreissenid mussels on algae (mt C d^{-1}) between “with” and “without” physical mixing processes in each of the three basins over each of the three years. The values are mean daily grazing rates on both NDEA and diatoms over simulation periods. “%” columns contain the percentages of decrease of grazing rates under no mixing from those under mixing.

State variables	Density factor of mussels	Means	Standard deviations	Paired t-test (p<0.05)
NDEA		mg DW l ⁻¹		
	1	0.178	0.199	a
	0.1	0.203	0.270	b
	10	0.174	0.150	a
NDIA	1	0.128	0.166	a
	0.1	0.134	0.173	b
	10	0.150	0.187	a
Diatoms	1	0.034	0.083	a
	0.1	0.018	0.030	b
	10	0.420	0.543	b
Copepods	1	0.037	0.029	a
	0.1	0.041	0.032	b
	10	0.040	0.037	a
Cladocerans	1	0.013	0.012	a
	0.1	0.016	0.014	b
	10	0.013	0.016	a
TP-F		mg P l ⁻¹		
	1	0.005	0.003	a
	0.1	0.005	0.002	b
	10	0.010	0.011	b
NH4		mg N l ⁻¹		
	1	0.017	0.009	a
	0.1	0.013	0.005	b
	10	0.070	0.098	b

Table 2.8. Statistical results of the uncertainties due to changing the simulated dreissenid population densities. Significant differences between density factor 1 and 0.1 or 1 and 10 are indicated by different letters in the last column.

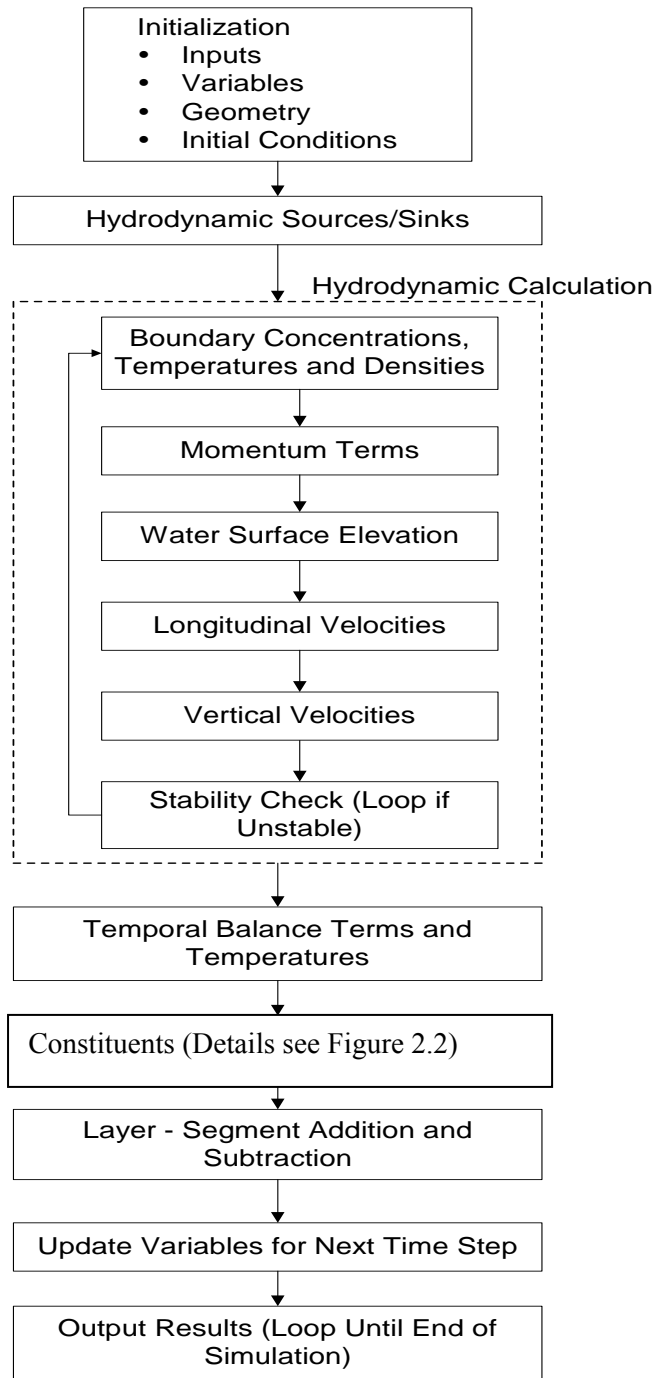


Figure 2.1. Flowchart of the model EcoLE (from Boegman 1999). Major differences between model EcoLE and model CE-QUAL-W2 are in the block ‘Constituents’.

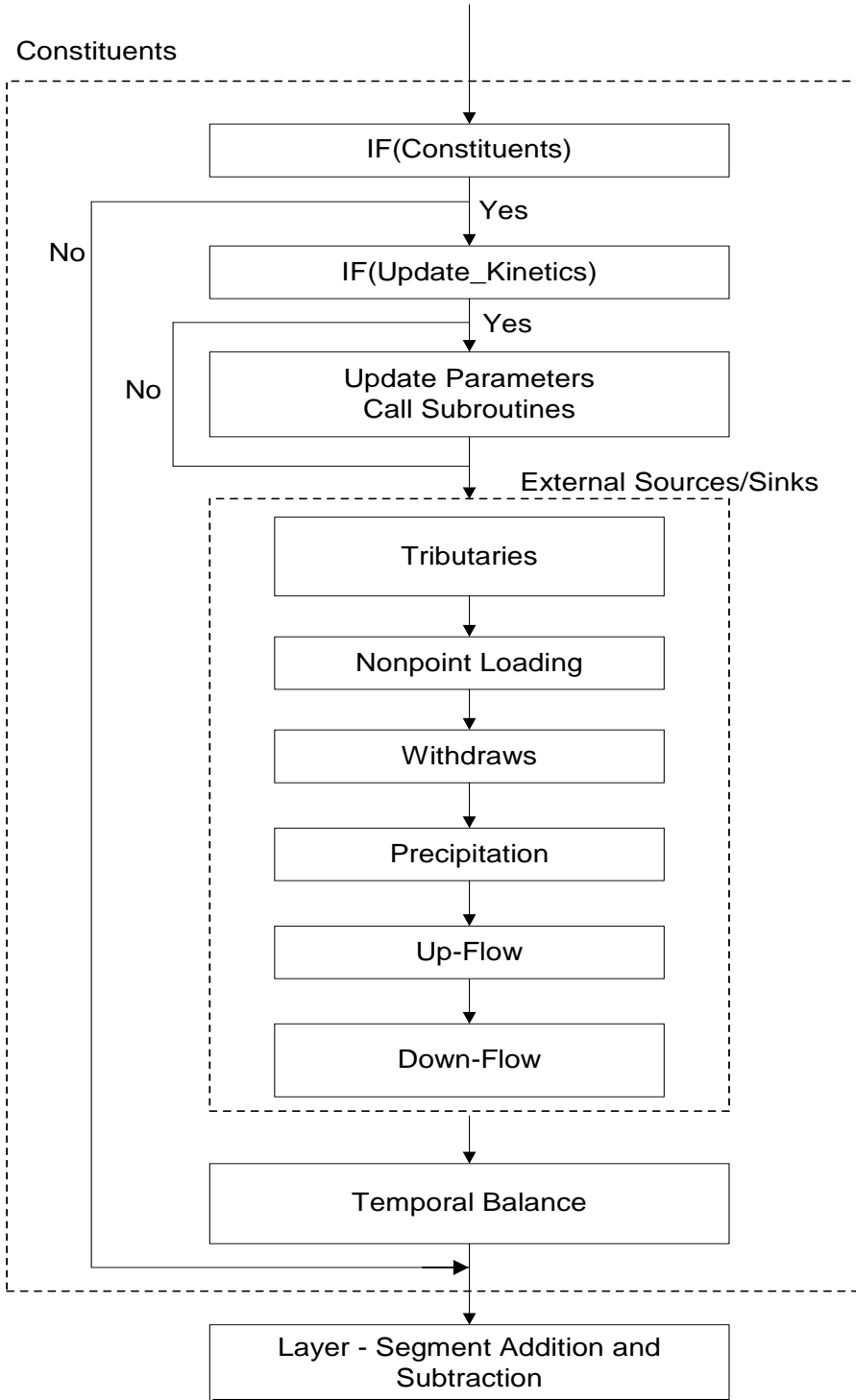


Figure 2.2. Flowchart of constituents in the model EcoLE. Construction of model EcoLE focuses on subroutine constructions of constituent calculations that are embedded in model CE-QUAL-W2.

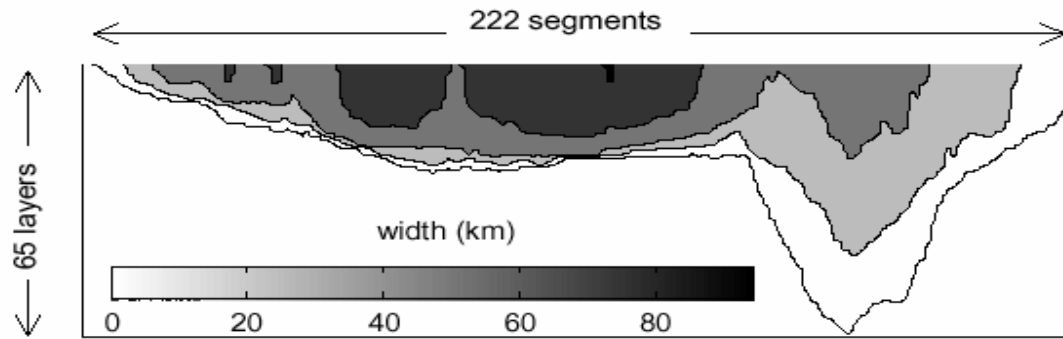


Figure 2.3. EcoLE's longitudinal-vertical resolution plane (longitudinal cross-section), showing width contours of 20 km intervals (from Boegman 1999).

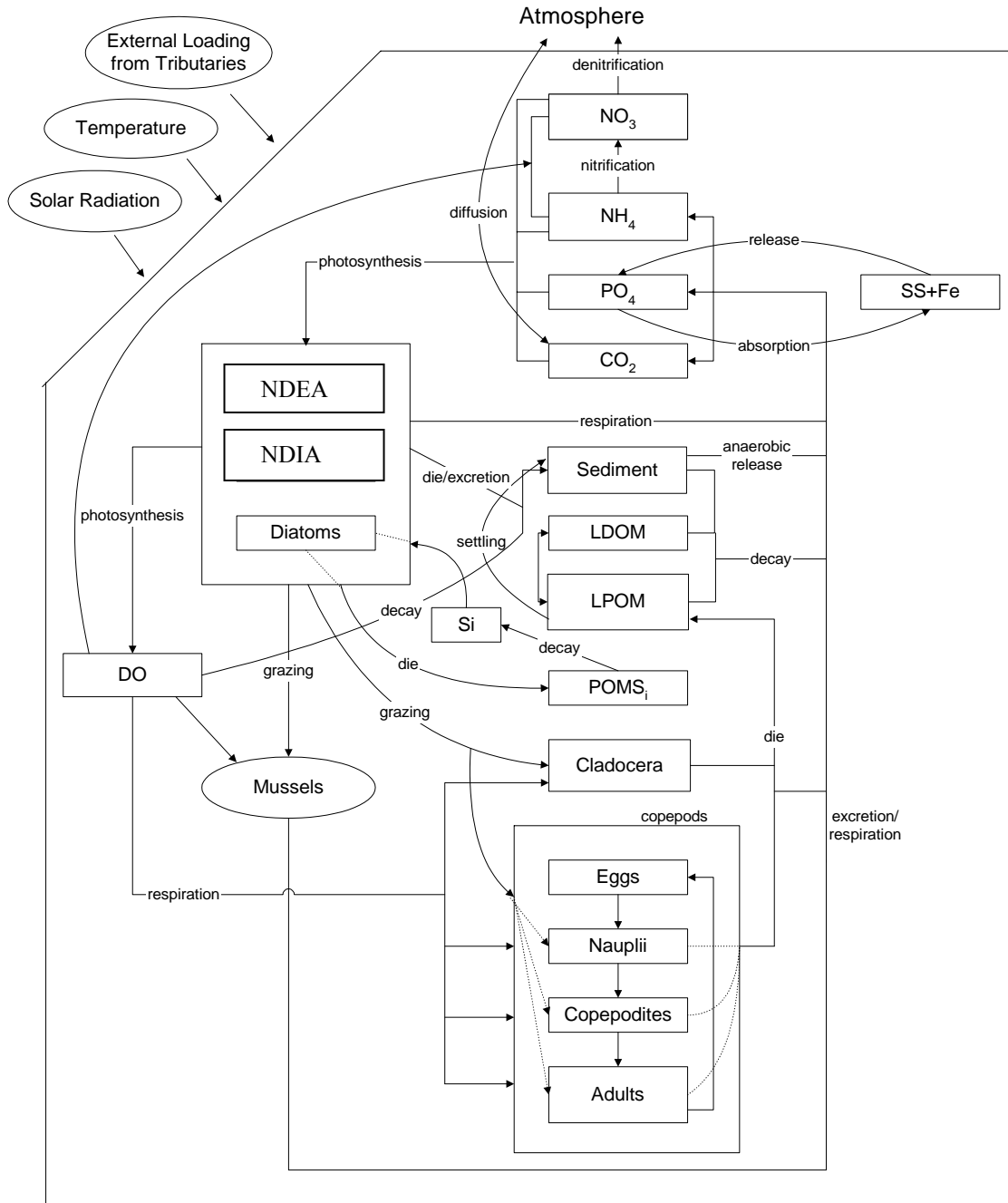
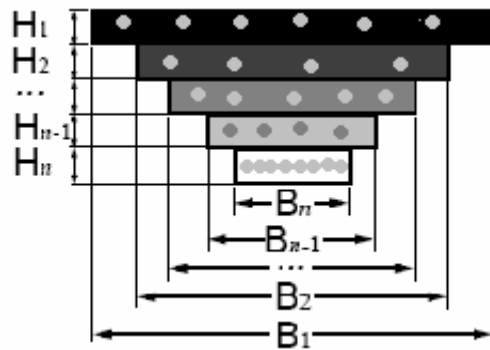


Figure 2.4. Model structure of the chemical and biological components of EcoLE.

a) Lateral staircase cross-sectional bathymetry



b) Lateral rectangular box bathymetry

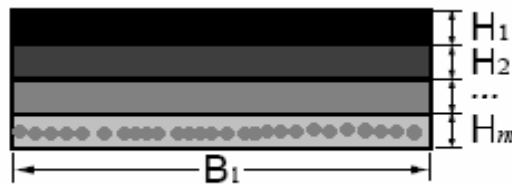


Figure 2.5. Reshaping the western basin from staircase (a) to rectangular box (b) by keeping surface area B_1 constant and adjusted depth H_i so that $B_1 \sum_{i=1}^m H_i \approx \sum_{i=1}^n B_i H_i$, where $m \leq n$ (after Boegman *et al.* 2006). The adjustment allows estimation of the effects of dreissenids, which are distributed only in the bottom cell of the rectangular box. The gray dots indicate the location of dreissenid mussels, while dreissenid population in a model cell is determined by the sedimental area and mussel density.

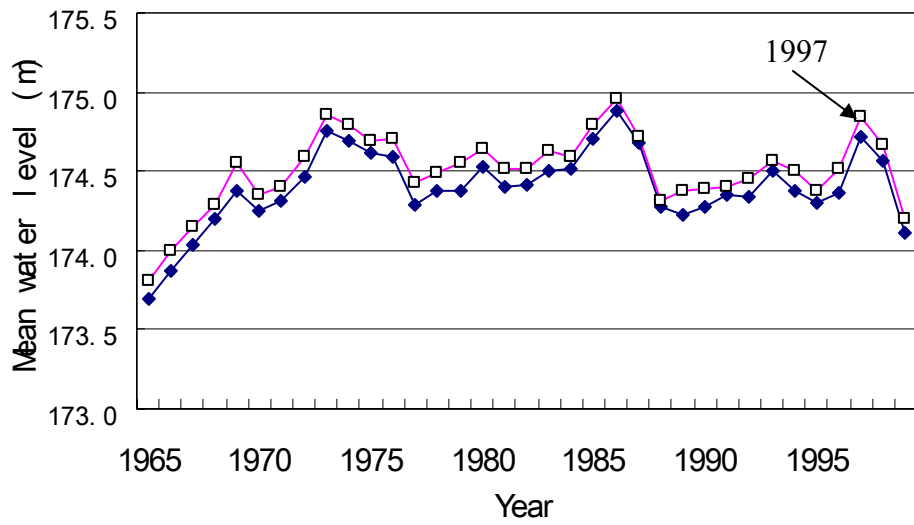
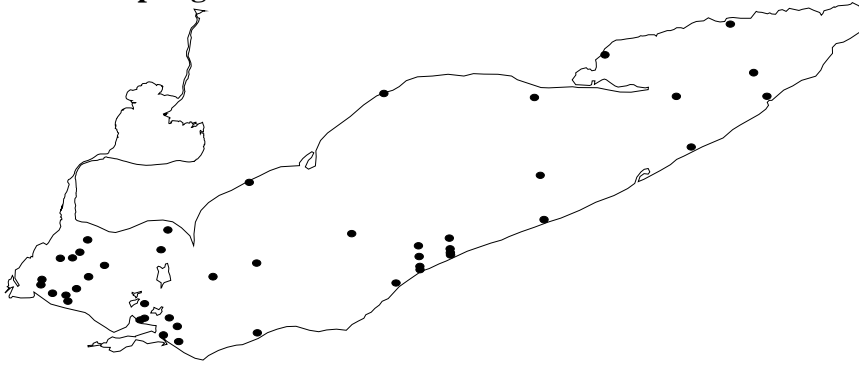
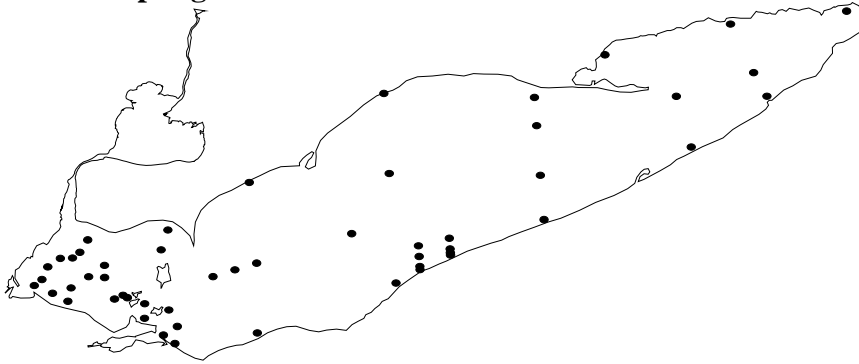


Figure 2.6. Water levels of Lake Erie, 1965-1999 (data from Tim Hunter, USGS). Open squares are averages from January to December and solid squares are averages from May to October. The arrow points to year 1997 followed by 1998 and 1999.

1997 Sampling Sites



1998 Sampling Sites



1999 Sampling Sites

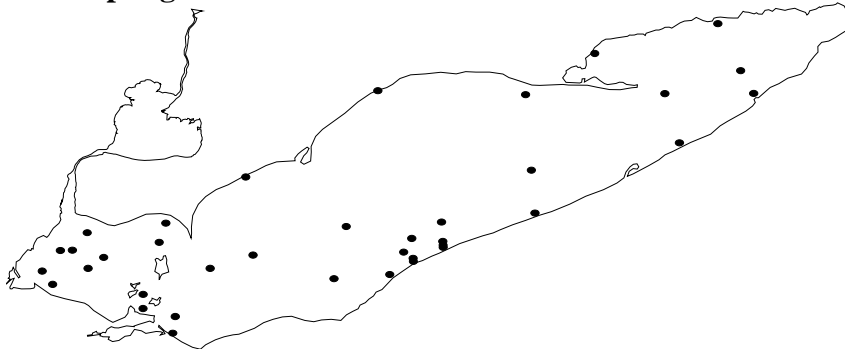
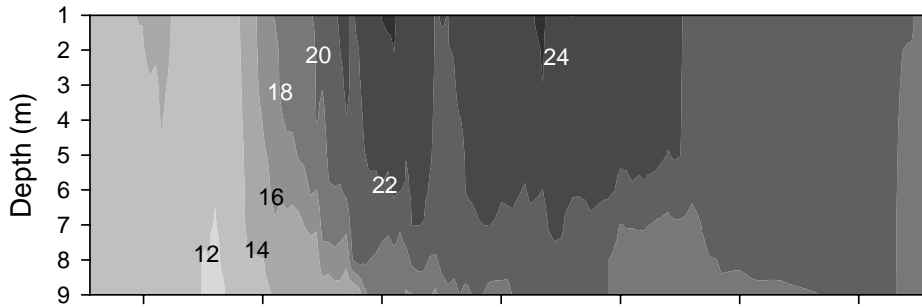
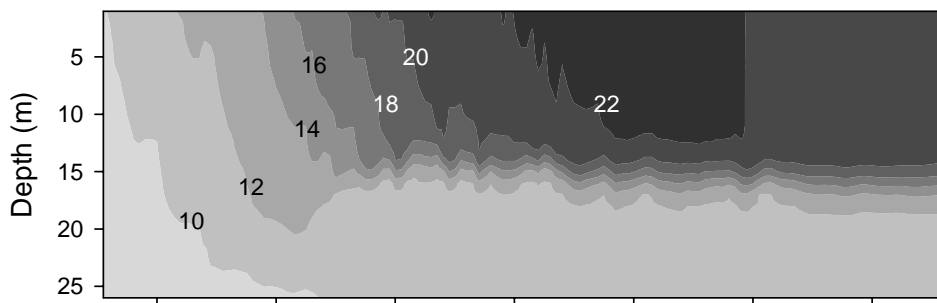


Figure 2.7. Lake Erie sampling sites yielding monitoring data used in the simulations.

a) Western Basin (segment 30), 1997



b) Central Basin (segment 95), 1997



c) Eastern Basin (segment 175), 1997

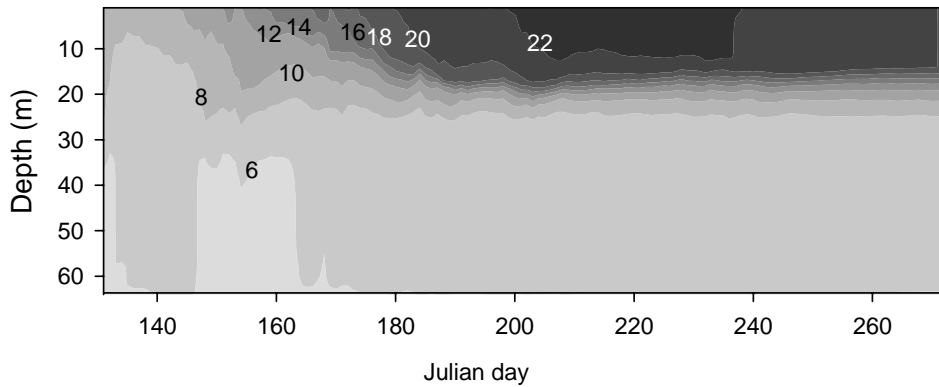
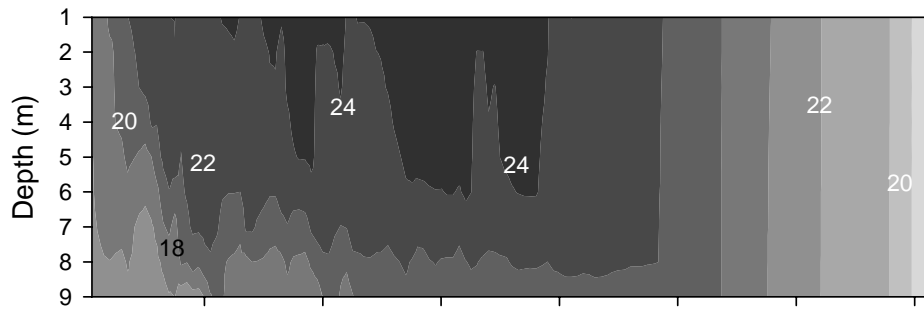
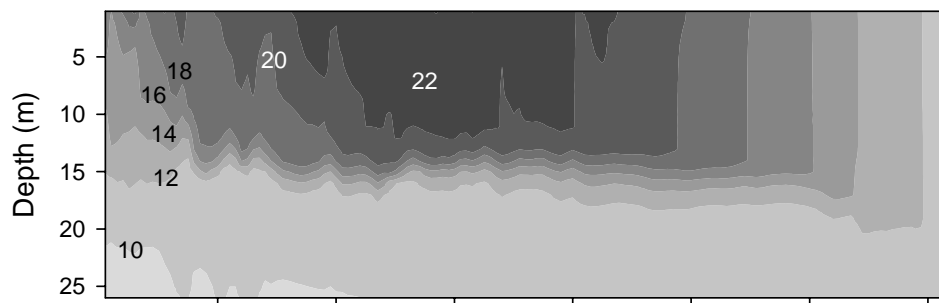


Figure 2.8. The 1997 simulation of vertical distributions of temperature outputs of EcoLE from representative segments in the western basin (segment 30, 9m, a), central basin (segment 95, 26m, b) and eastern basin (segment 175, 64m, c) over the simulation period. Simulated dates were May 10 to Sep. 30. Note the different scales on the y-axis.

a) Western Basin (segment 30), 1998



b) Central Basin (segment 95), 1998



c) Eastern Basin (segment 175), 1998

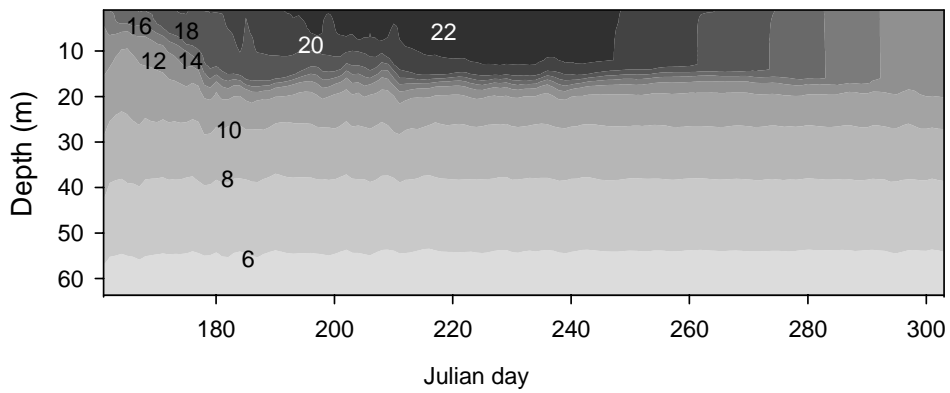
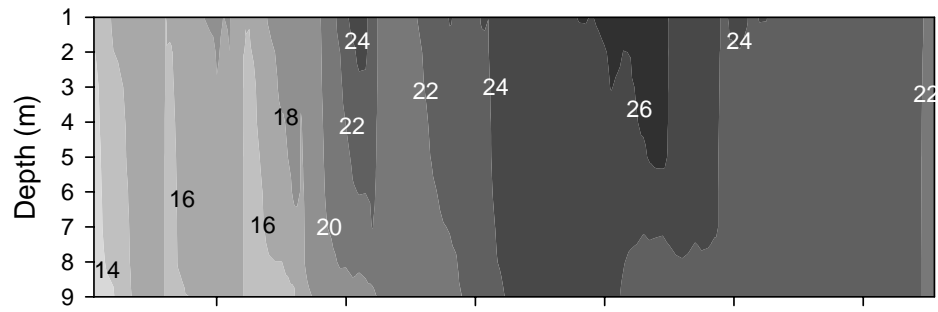
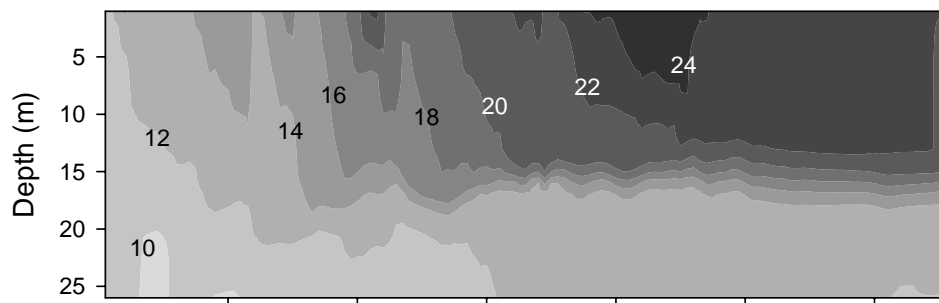


Figure 2.9. As Figure 2.8, but for June 10 through October 30, 1998.

a) Western Basin (segment 30), 1999



b) Central Basin (segment 95), 1999



c) Eastern Basin (segment 175), 1999

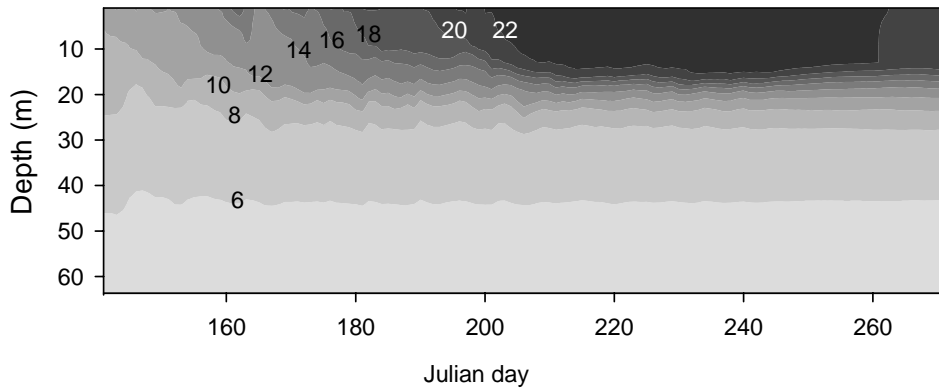
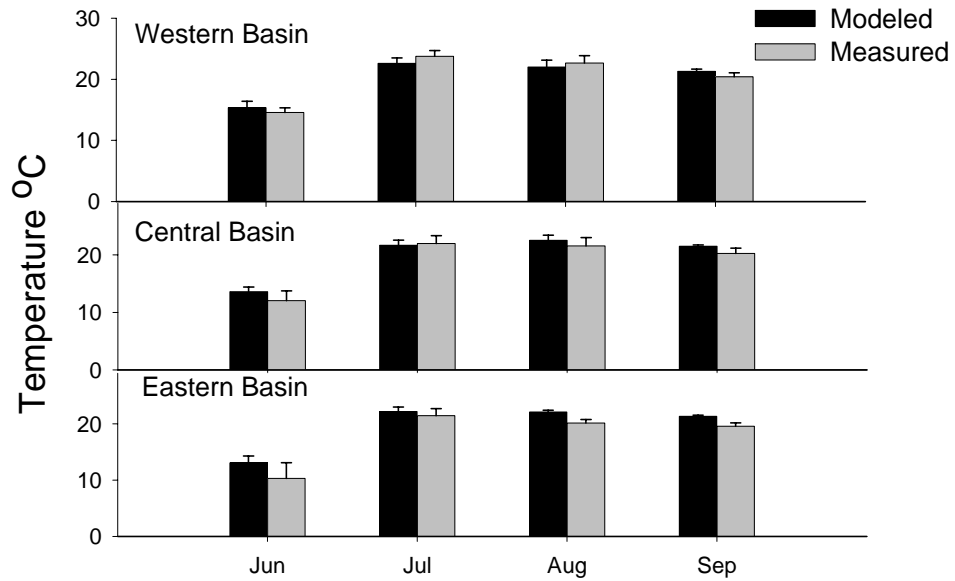


Figure 2.10. As Figure 2.8, but for May 30 through September 29, 1999.

a) Surface temperatures, 1997



b) Bottom temperatures, 1997

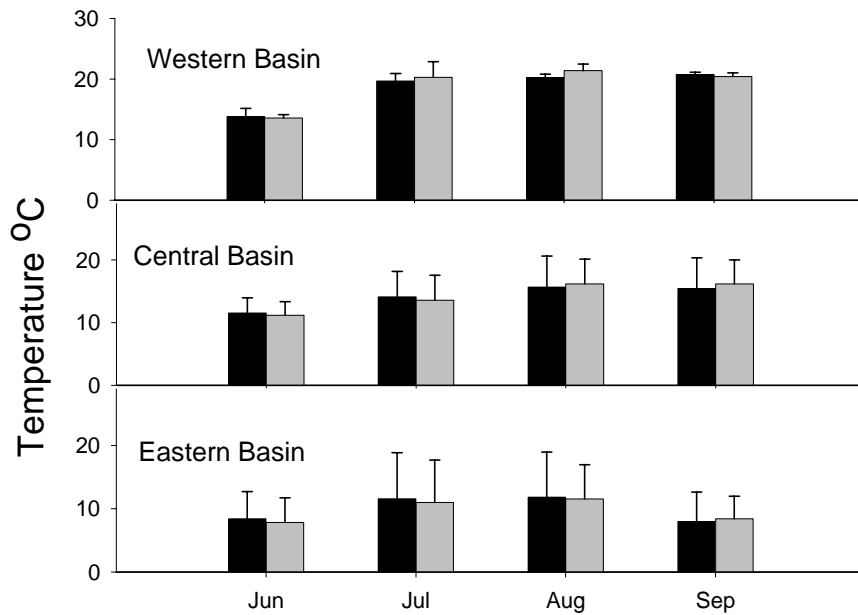


Figure 2.11. 1997's comparisons between the modeled and the observed surface temperatures (a) and bottom temperatures (b). The light bars are means of temperatures measured in the month and the basin. The dark bars are means of temperatures sampled in the model output corresponding to dates and locations (segments) of the field measurements. Error bar represents one standard deviation of the mean.

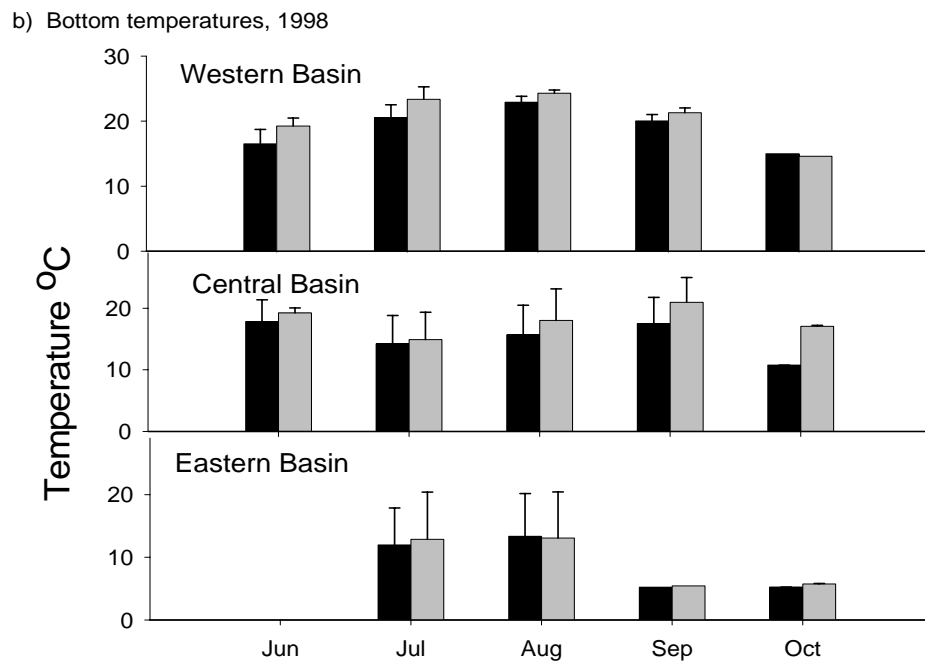
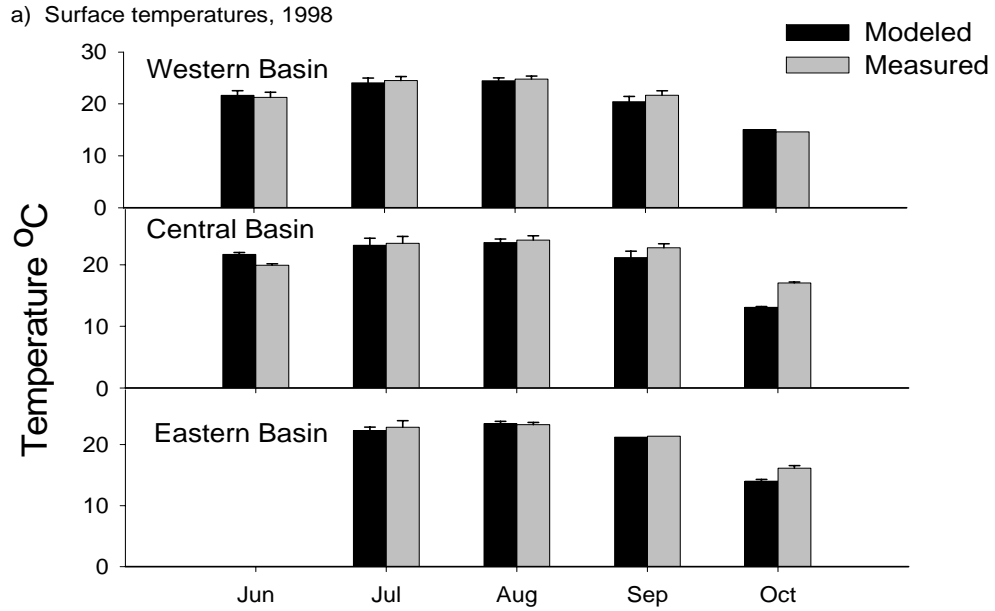


Figure 2.12. 1998's comparisons between the modeled and the observed surface temperatures (a) and bottom temperatures (b). The light bars are means of temperatures measured in the month and the basin. The dark bars are means of temperatures sampled in the model output corresponding to dates and locations (segments) of the field measurements. Error bar represents on standard deviation of the mean. Note there was no field measurement available in June in the eastern basin.

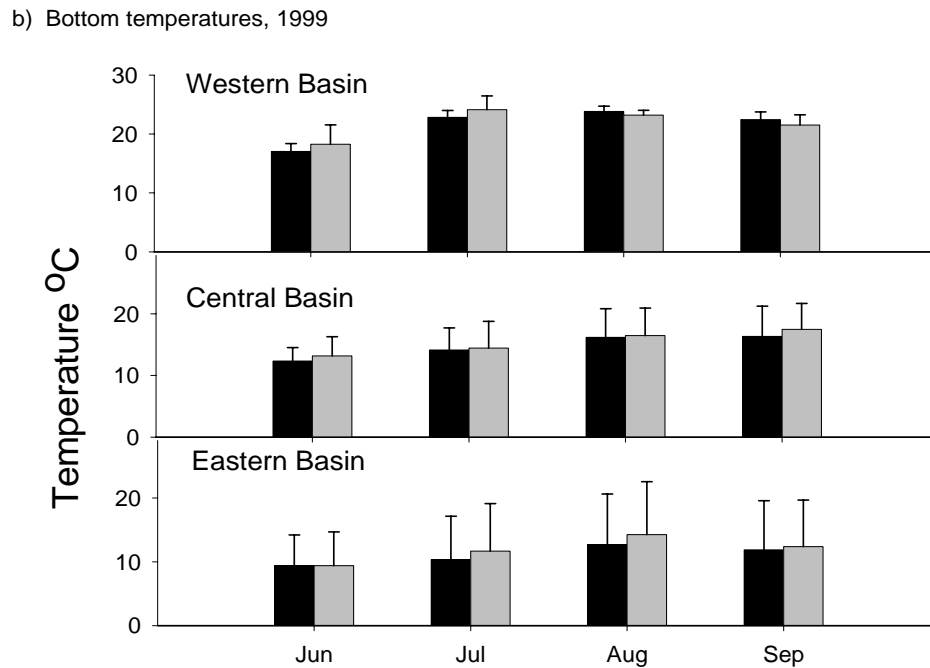
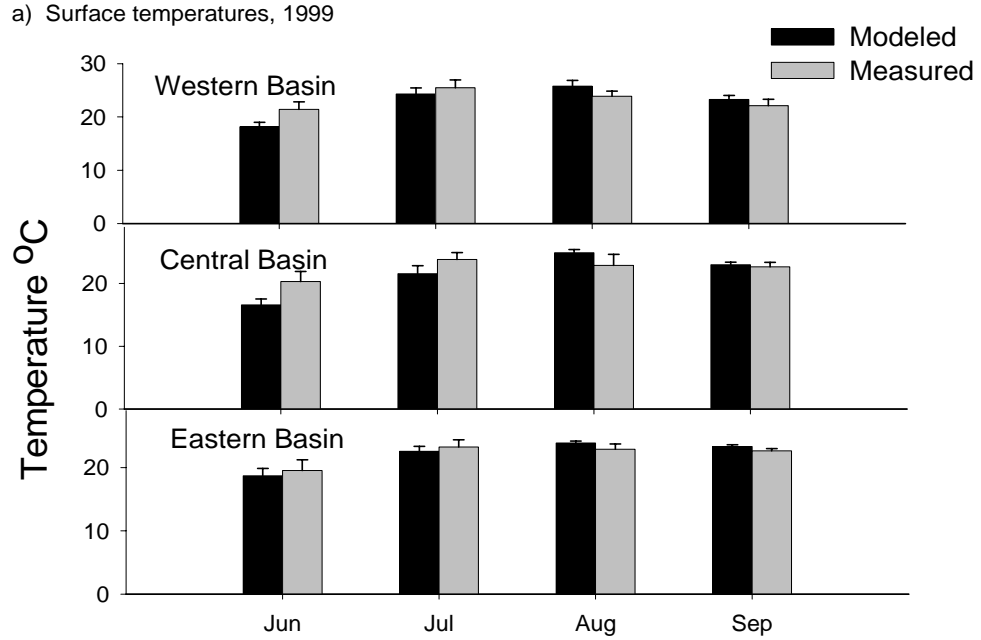


Figure 2.13. 1999's comparisons between the modeled and the observed surface temperatures (a) and bottom temperatures (b). The light bars are means of temperatures measured in the month and the basin. The dark bars are means of temperatures sampled in the model output corresponding to dates and locations (segments) of the field measurements. Error bar represents on standard deviation of the mean.

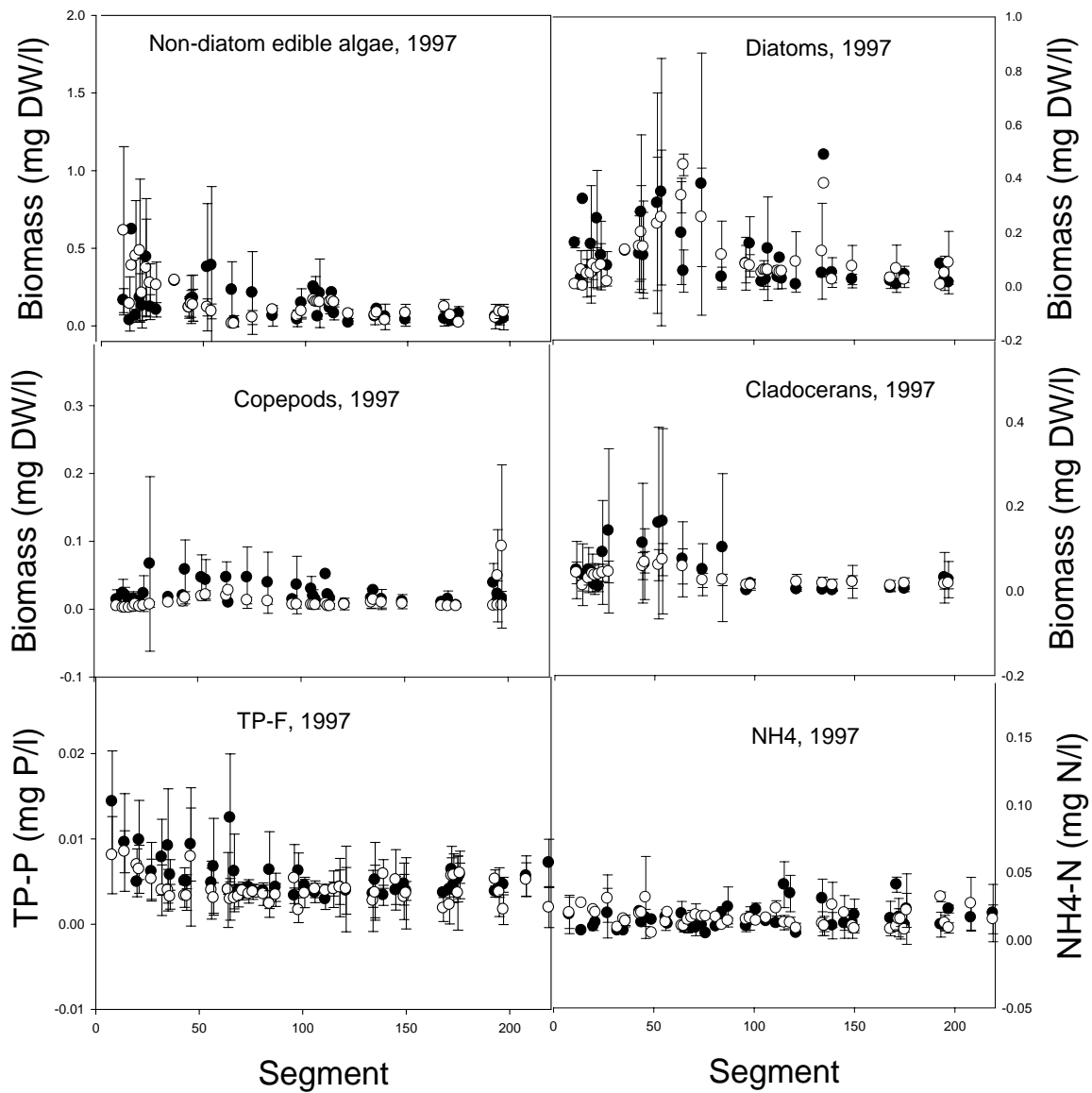


Figure 2.14. Model calibration (year 1997) for non-diatom edible algae, diatoms, copepods, cladocerans, TP-F and NH_4 . Plotted values represent seasonal averages for field observations (solid circles) and model predictions (open circles) of field sampling segments from west (1) to east (220). The western basin ends at segment 49, and the central basin ends at segment 156.

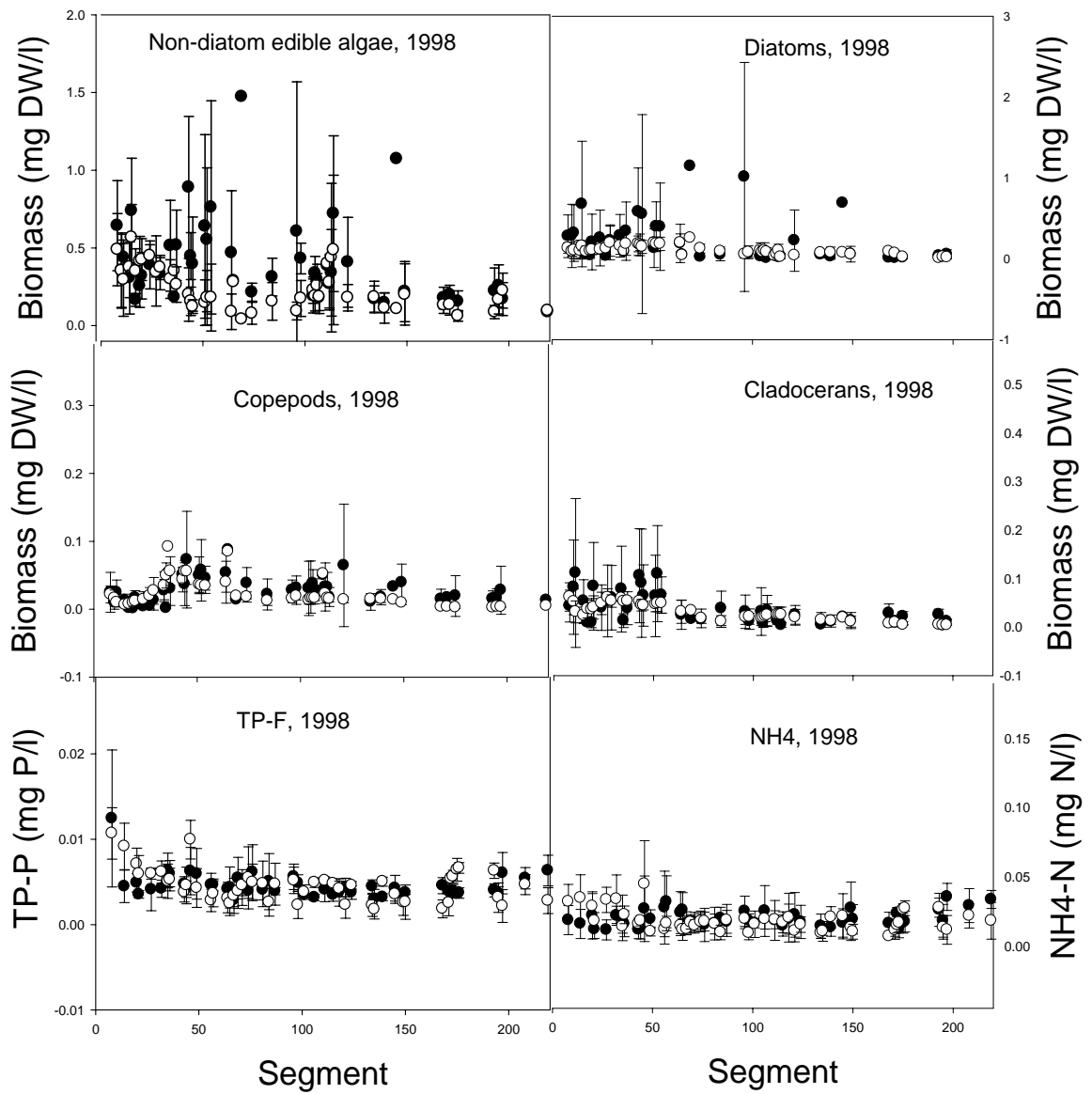


Figure 2.15. Model verification of 1998 for non-diatom edible algae, diatoms, copepods, cladocerans, TP-F and NH₄.

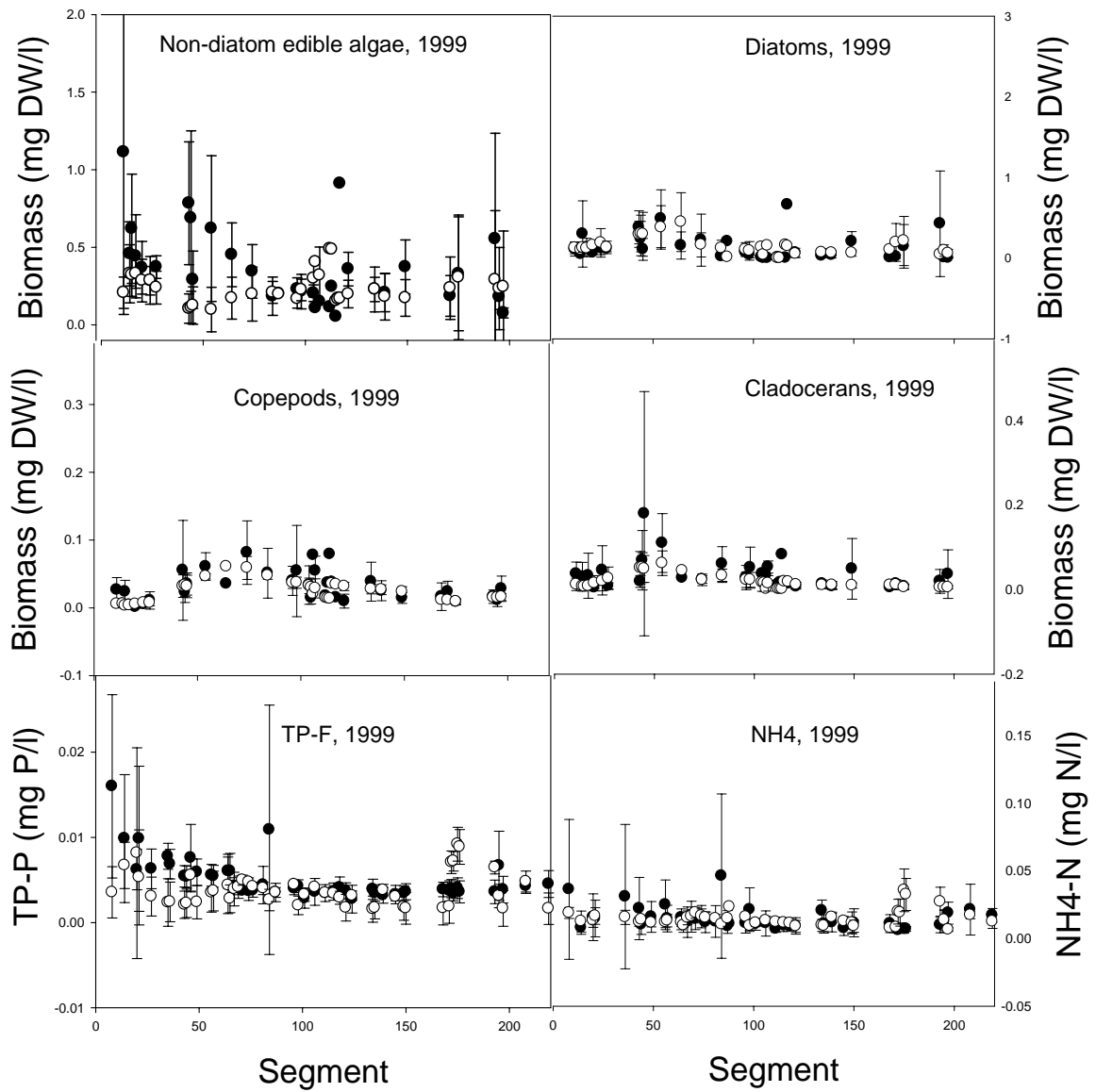


Figure 2.16. Model verification of 1999 for non-diatom edible algae, diatoms, copepods, cladocerans, TP-F and NH₄.

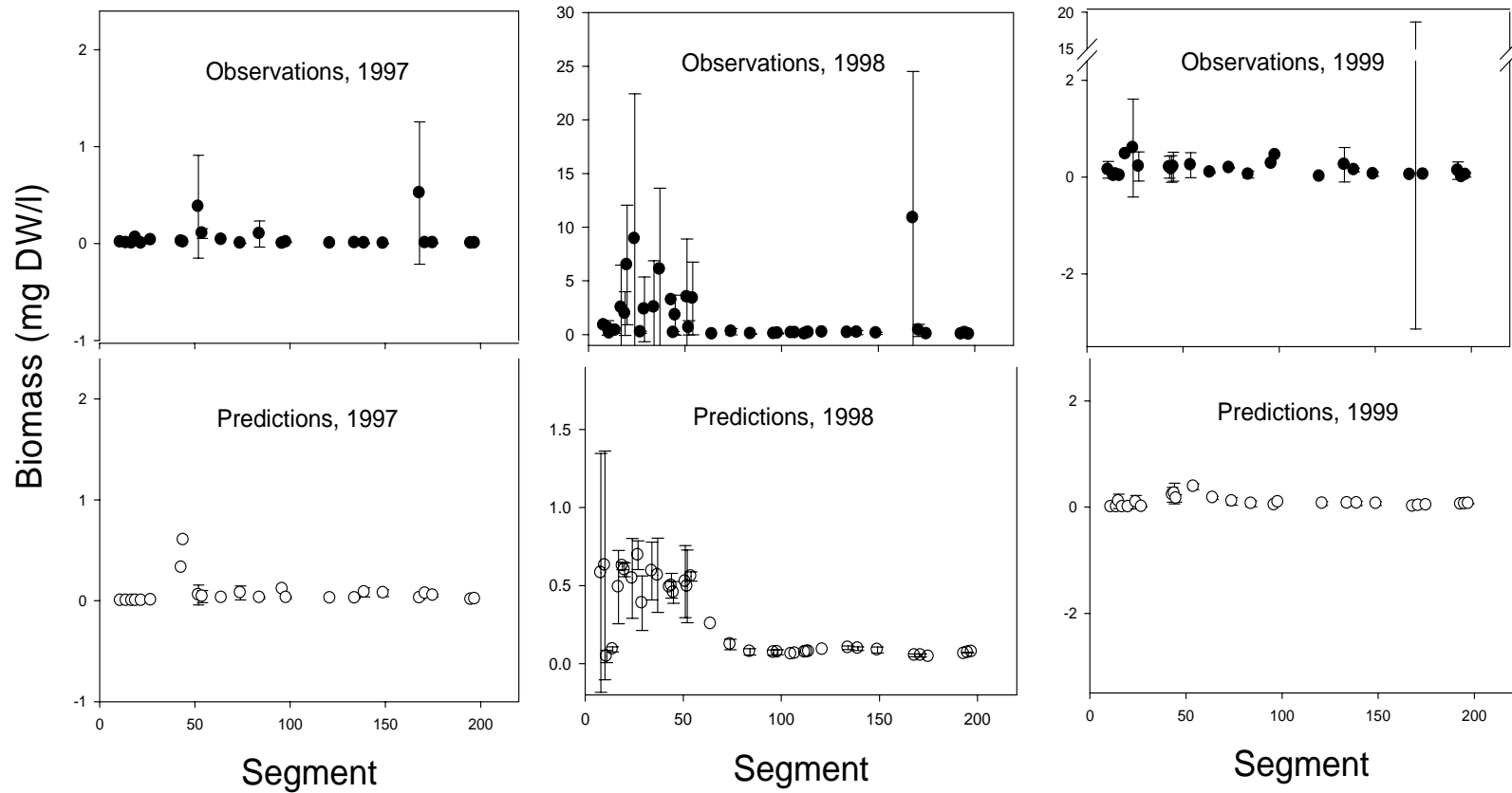


Figure 2.17. Comparisons of NDIA biomass between observations and predictions for 1997, 1998 and 1999. NDIA biomass are averages of August and September. Note the different scales on the y-axis of 1998.

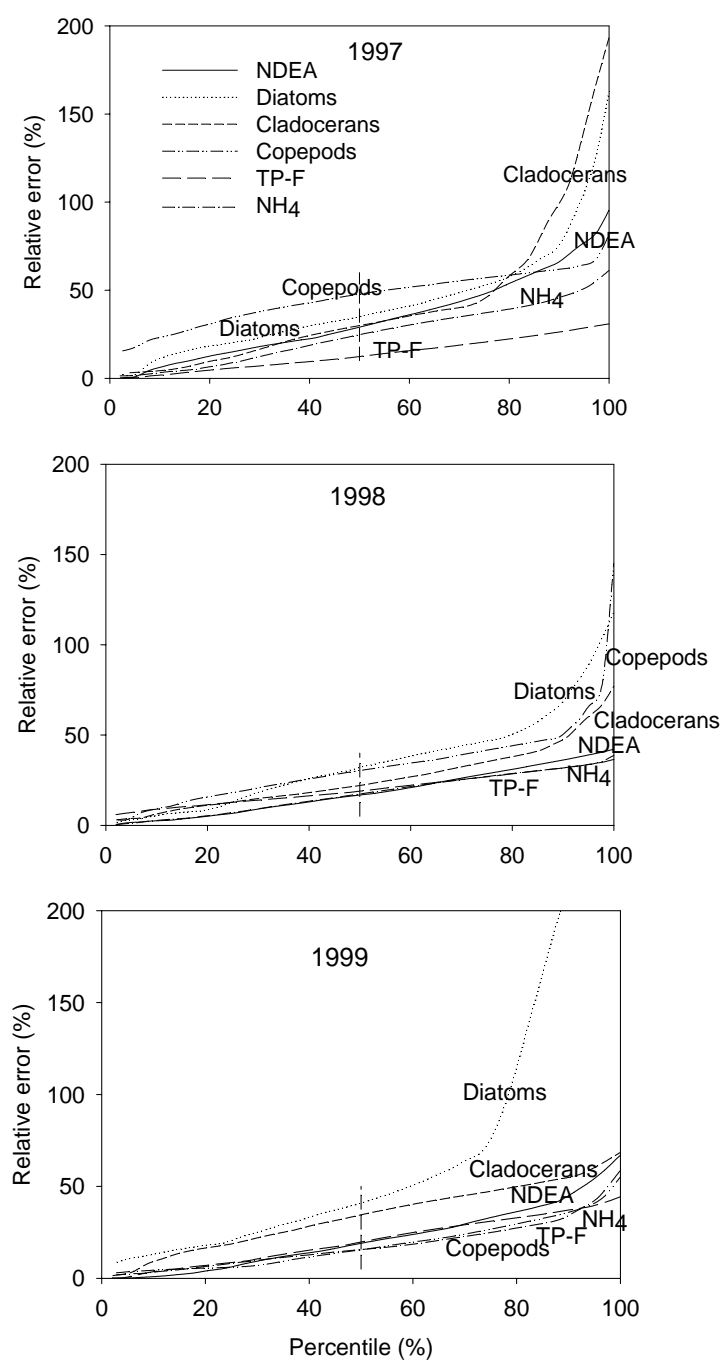
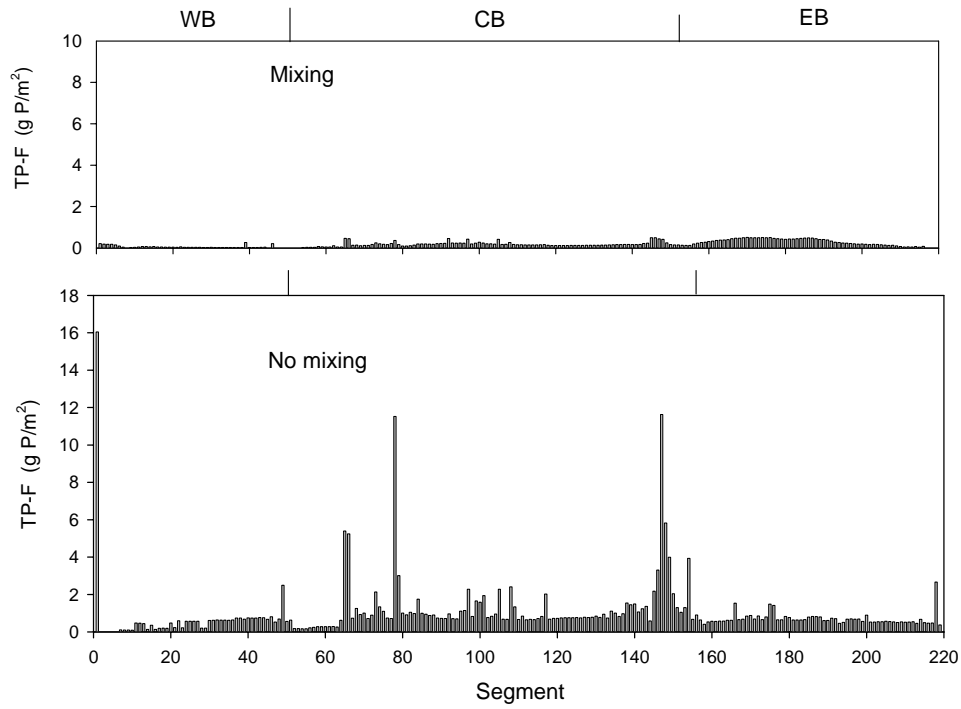


Figure 2.18 Relative error vs. sample percentile for NDEA, Diatoms, Cladocerans, Copepods, TP-F and NH₄ of three years. The vertical dash line indicates the median relative errors of state variables.

a) Water column concentrations of TP-F, 1997



b) Concentration distributions of TP-F, 1997

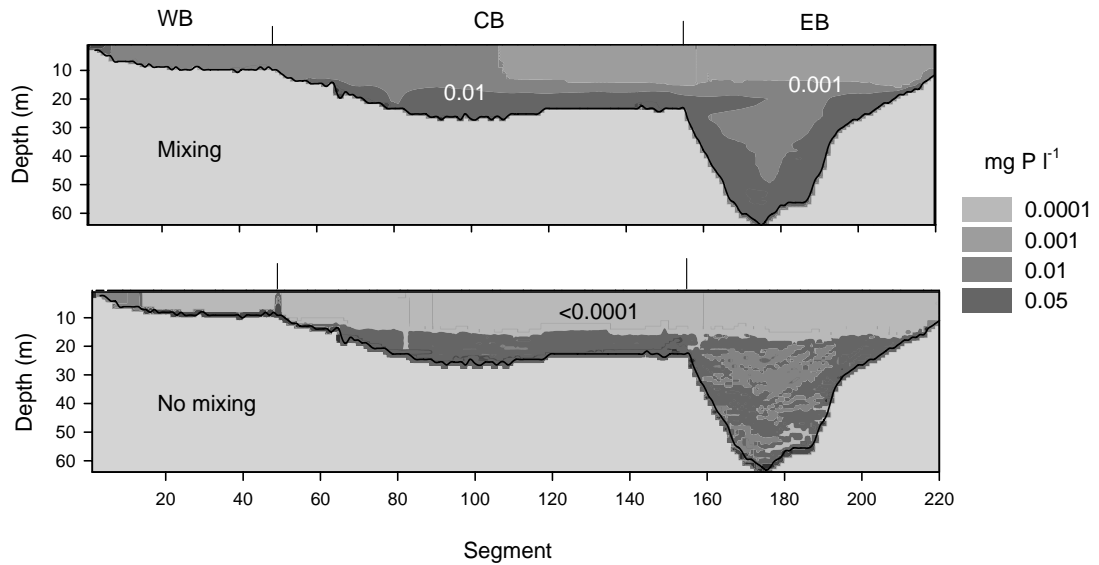
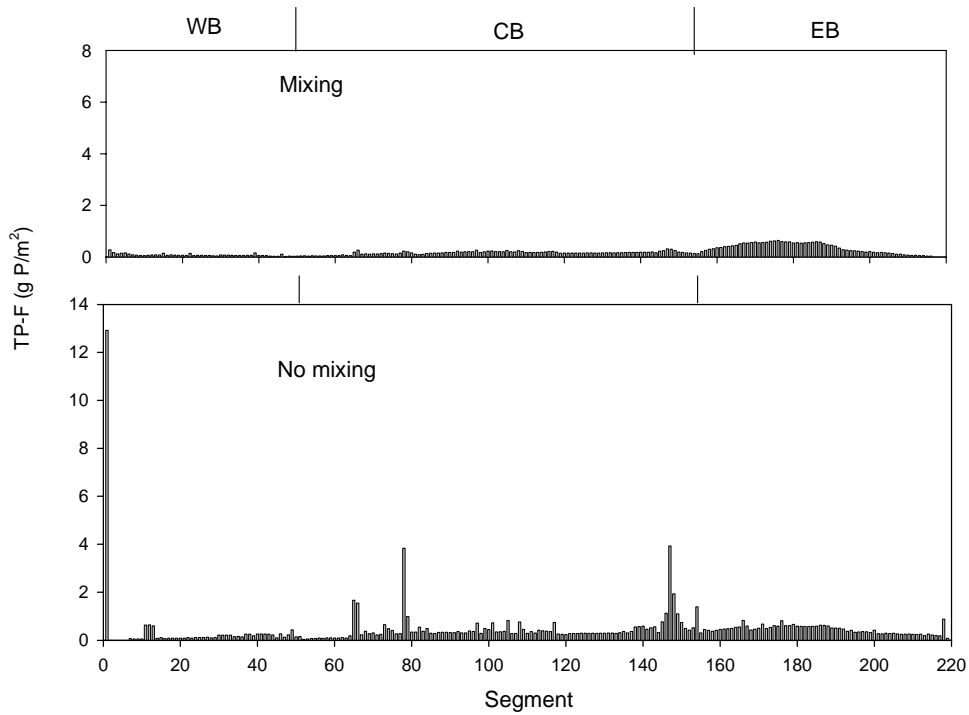


Figure 2.19. The 1997 simulation results of (a) water column concentrations (g P m^{-2}) and (b) concentration (mg P l^{-1}) distributions of total dissolved phosphorus (TP-F) with (upper panel) and without (lower panel) mixing processes on August 30.

a) Water column concentrations of TP-F, 1998



b) Concentration distributions of TP-F, 1998

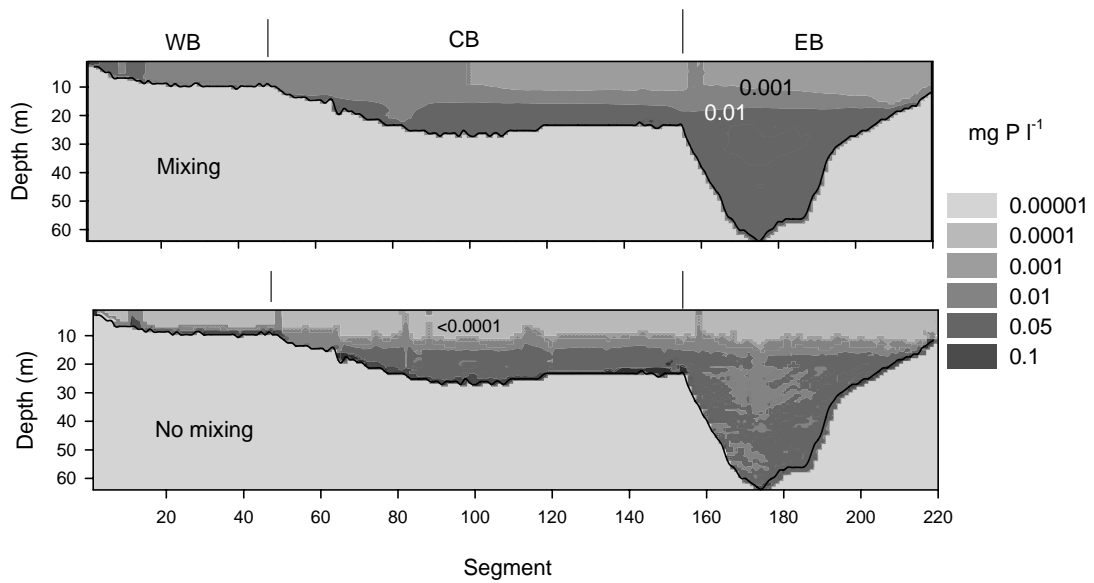
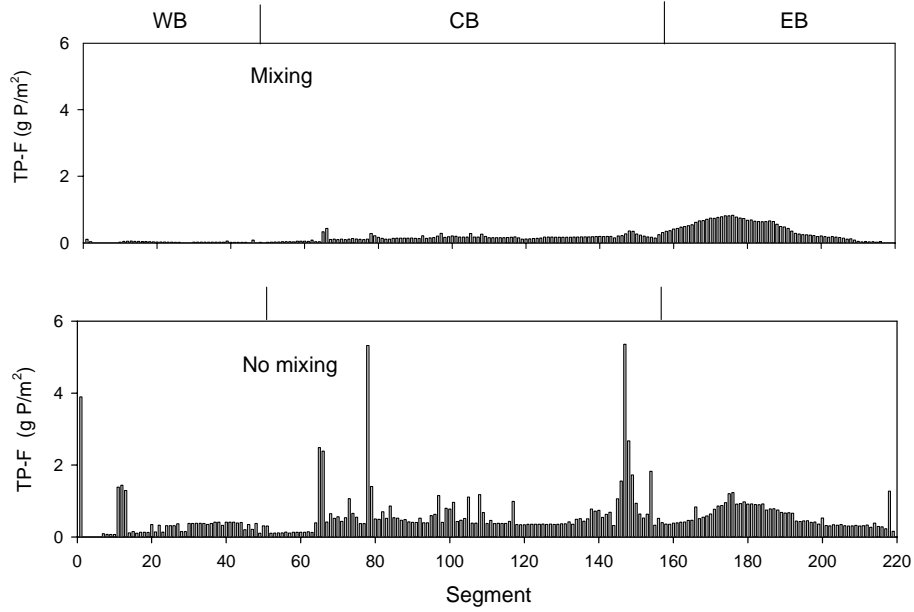


Figure 2.20. The 1998 simulation results of (a) water column concentrations (g P m^{-2}) and (b) concentration (mg P l^{-1}) distributions of total dissolved phosphorus (TP-F) with (upper panel) and without (lower panel) mixing processes on August 30.

a) Water column concentrations of TP-F, 1999



b) Concentration distributions of TP-F, 1999

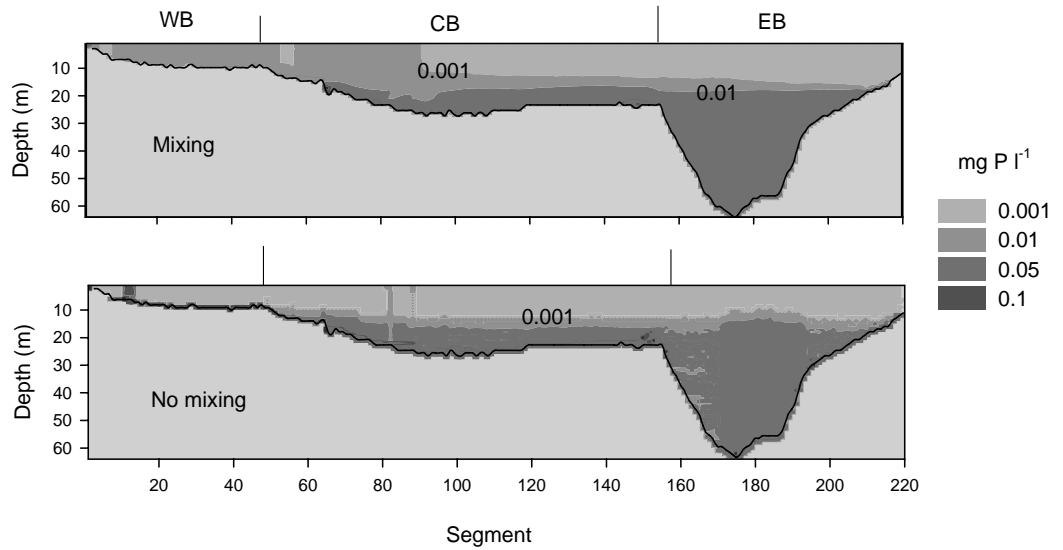
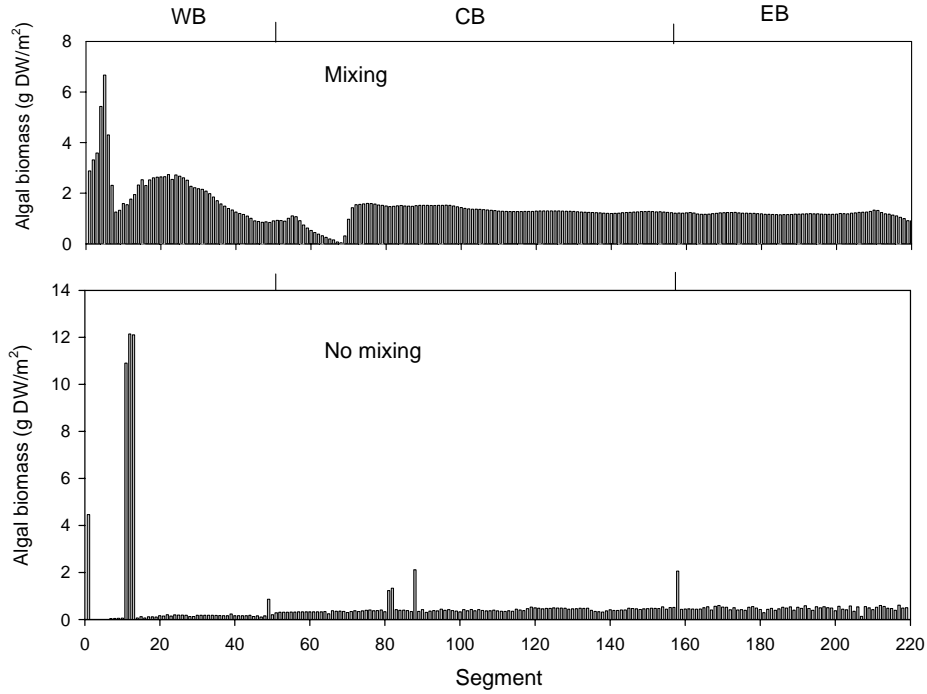


Figure 2.21. The 1999 simulation results of (a) water column concentrations (g P m^{-2}) and (b) concentration (mg P l^{-1}) distributions of total dissolved phosphorus (TP-F) with (upper panel) and without (lower panel) mixing processes on August 30.

a) Water column concentrations of non-diatom edible algae, 1997



b) Concentration distributions of non-diatom edible algae, 1997

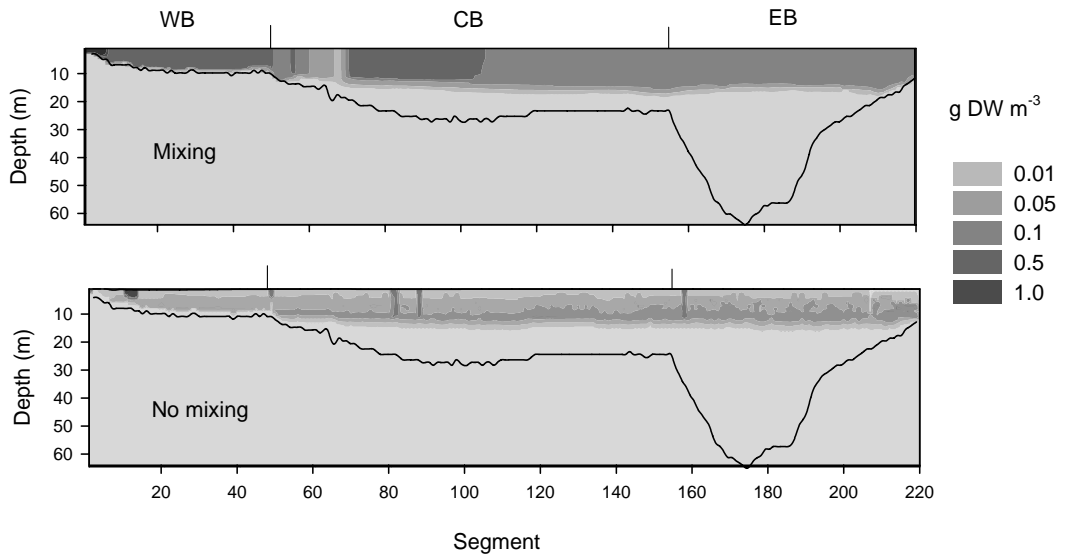
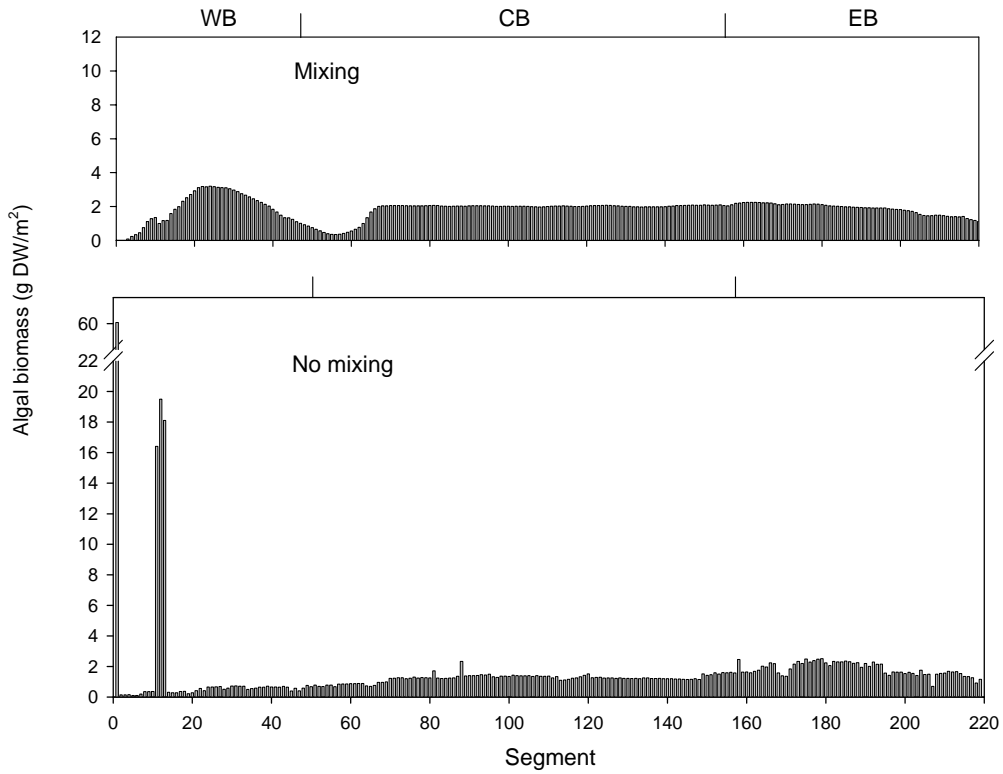


Figure 2.22. The 1997 simulation results of (a) water column concentrations of NDEA (g DW m^{-2}) and (b) concentration (g DW m^{-3}) distributions with (upper panel) and without (lower panel) mixing processes on August 30.

a) Water column concentrations of non-diatom edible algae, 1998



b) Concentration distributions of non-diatom edible algae, 1998

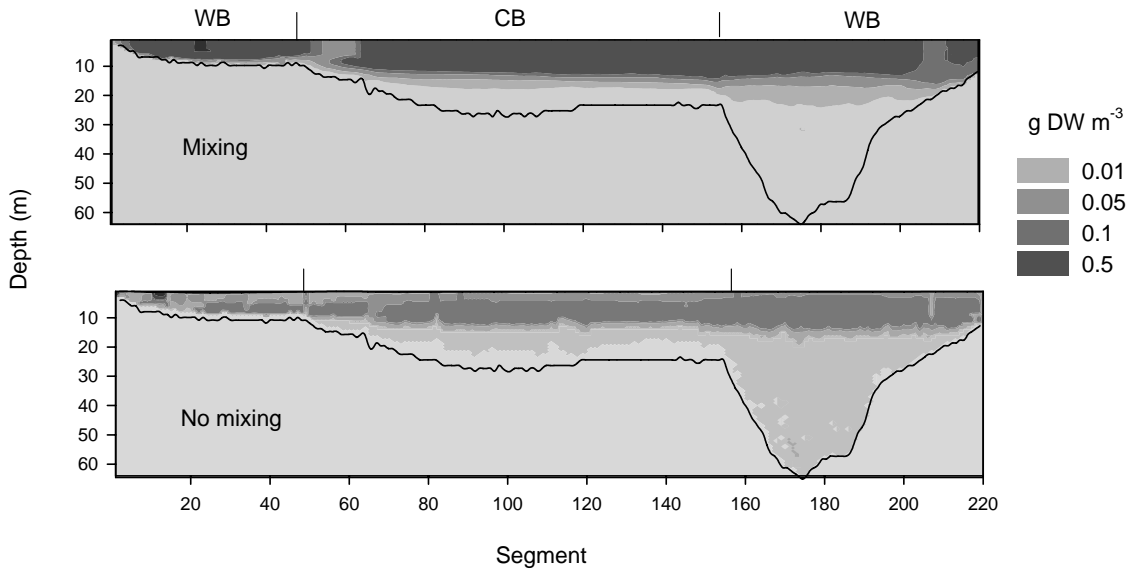
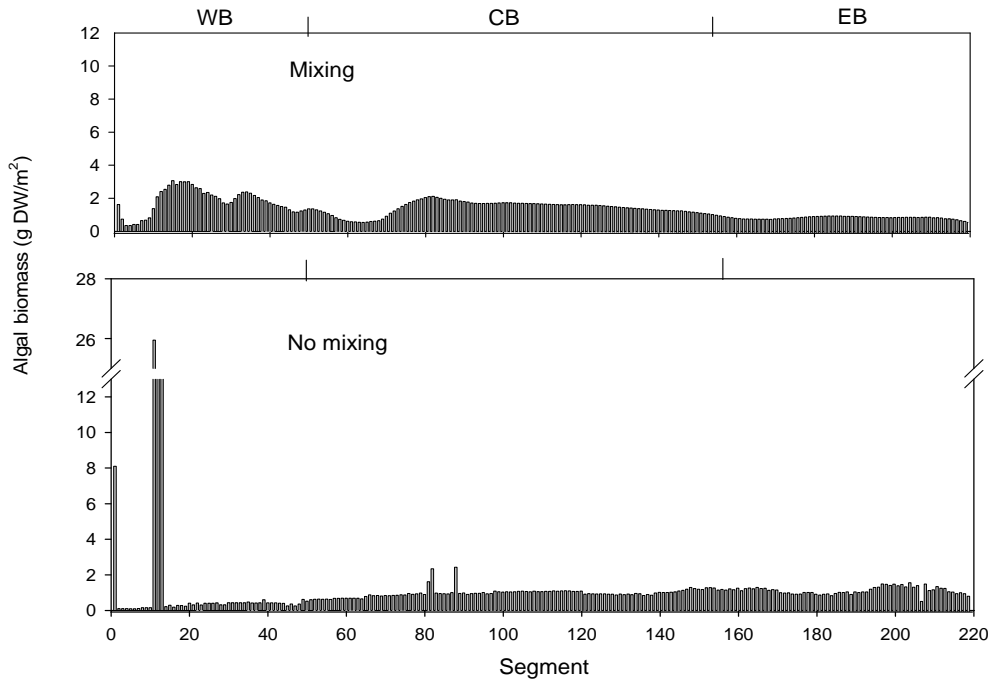


Figure 2.23. As Figure 2.22, but for non-diatom edible algae on August 30, 1998.

a) Water column concentrations of non-diatom edible algae, 1999



b) Concentration distributions of non-diatom edible algae, 1999

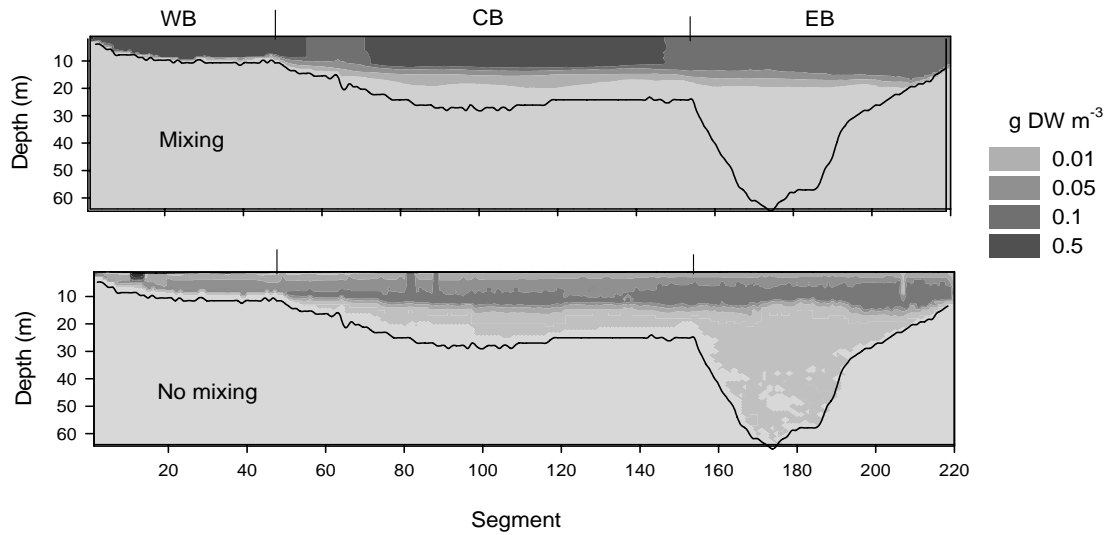
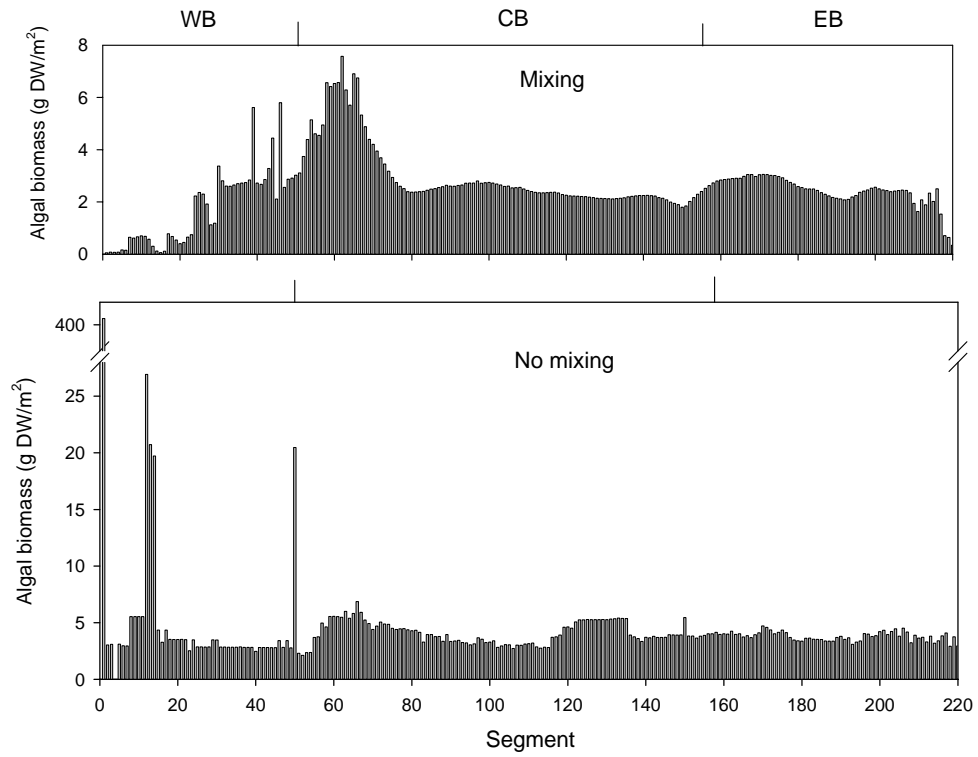


Figure 2.24. As Figure 2.22, but for non-diatom edible algae on August 30, 1999.

a) Water column concentrations of non-diatom inedible algae, 1997



b) Concentration distributions of non-diatom inedible algae, 1997

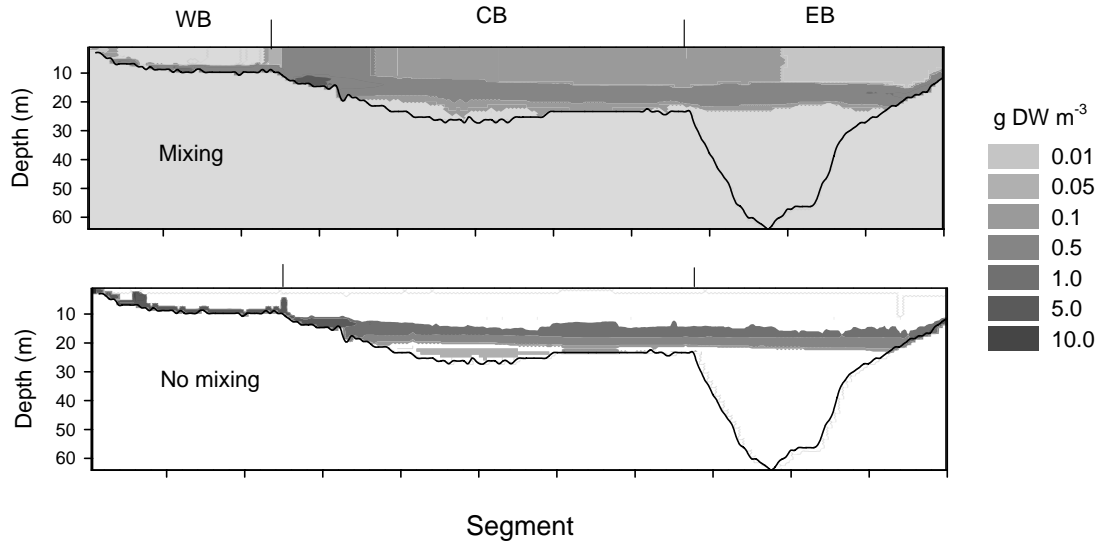
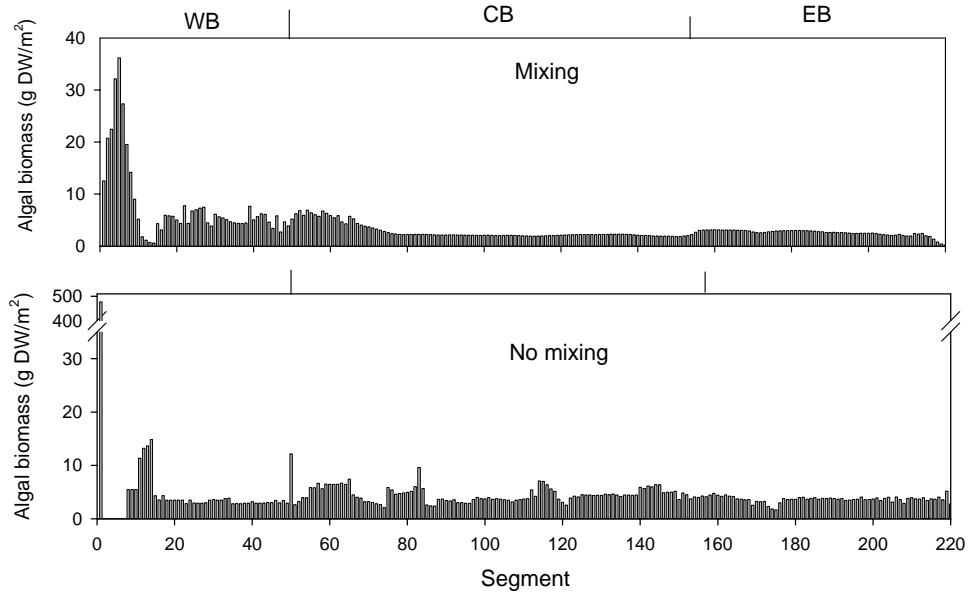


Figure 2.25. As Figure 2.22, but for non-diatom inedible algae on August 30, 1997.

a) Water column concentrations of non-diatom inedible algae, 1998



b) Concentration distributions of non-diatom inedible algae, 1998

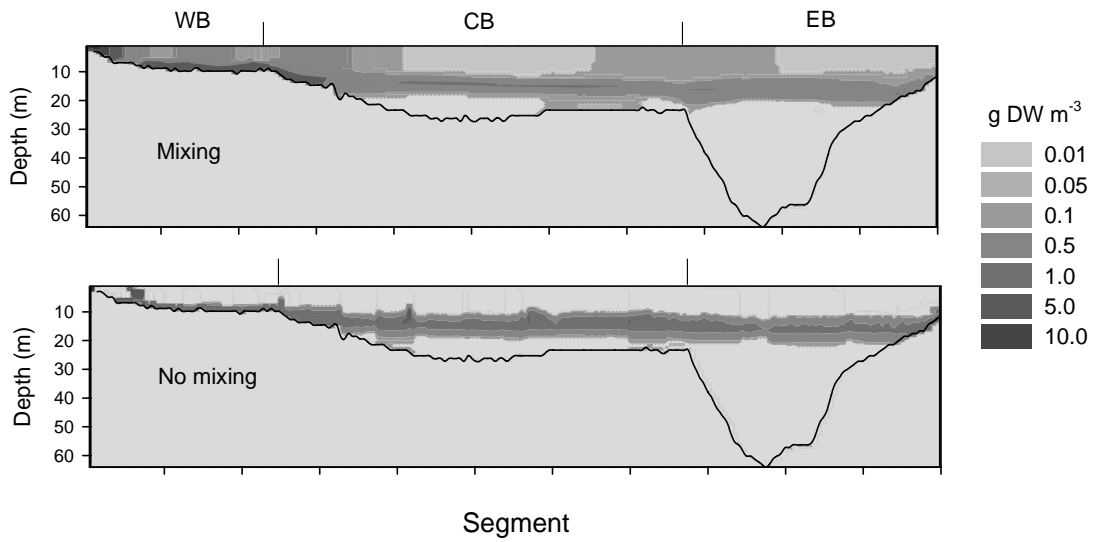
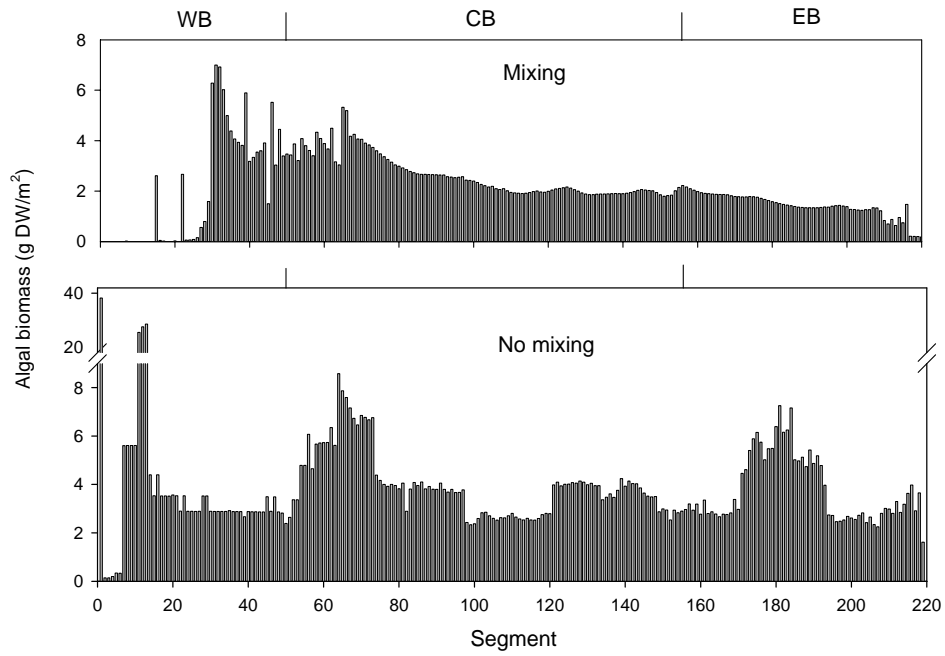


Figure 2.26. As Figure 2.22, but for non-diatom inedible algae on August 30, 1998.

a) Water column concentrations of non-diatom inedible algae, 1999



b) Concentration distributions of non-diatom inedible algae, 1999

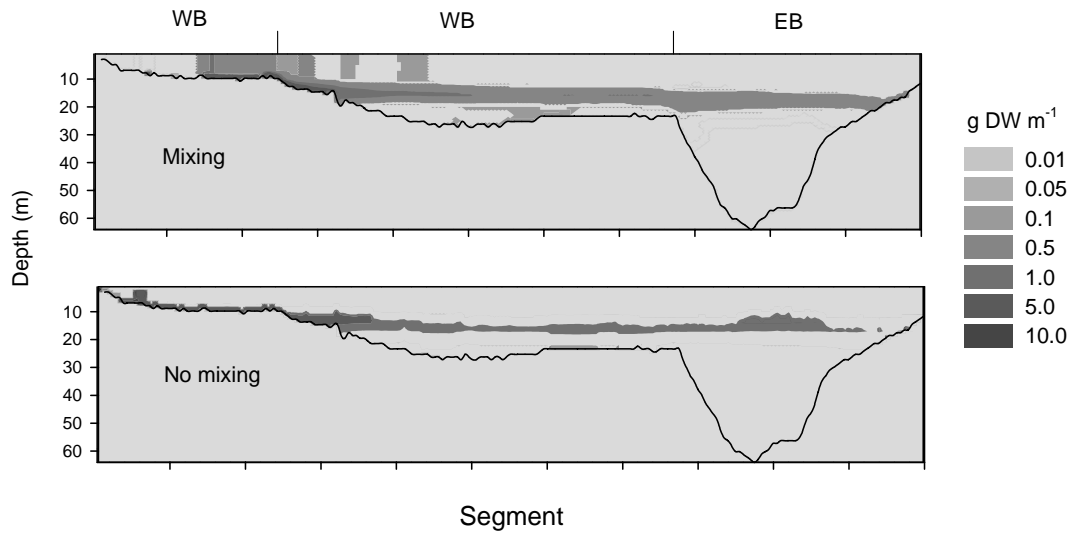
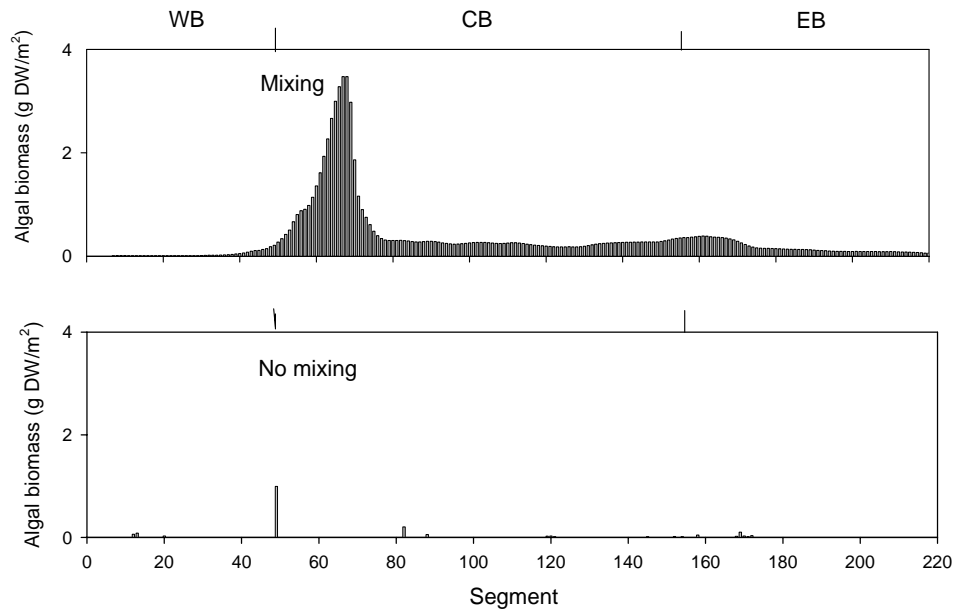


Figure 2.27. As Figure 2.22, but for non-diatom inedible algae on august 30, 1999.

a) Water column concentrations of diatoms, 1997



b) Concentration distributions of diatoms, 1997

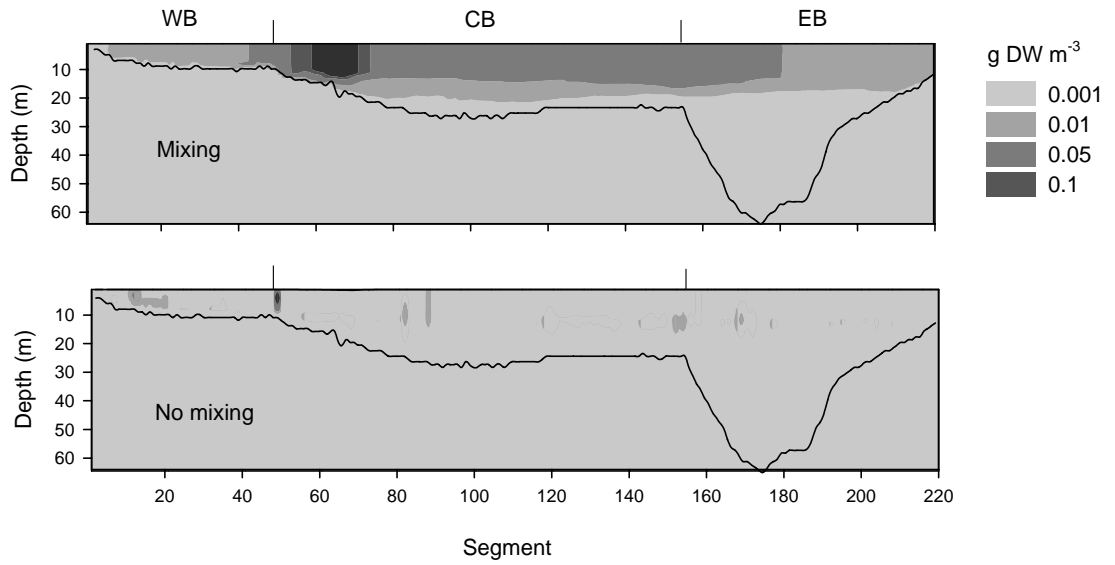
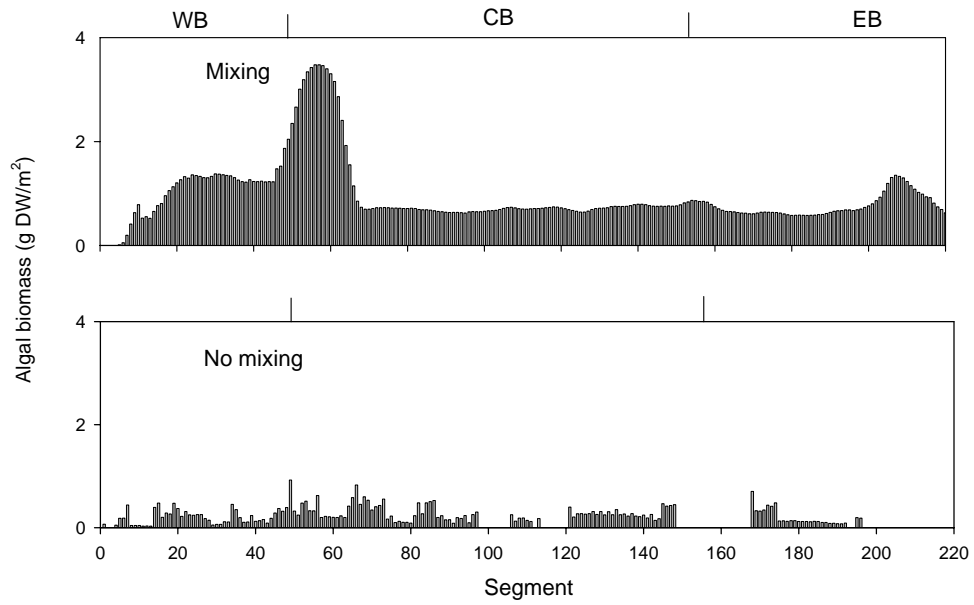


Figure 2.28. As Figure 2.22, but for diatoms on August 30, 1997.

a) Water column concentrations of diatoms, 1998



b) Concentration distributions of diatoms, 1998

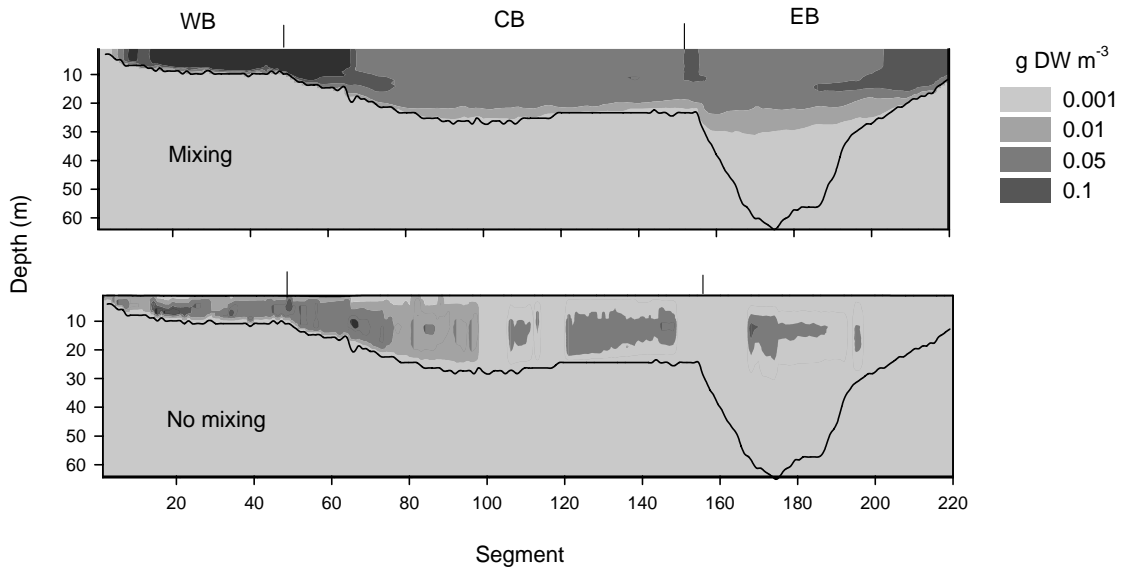
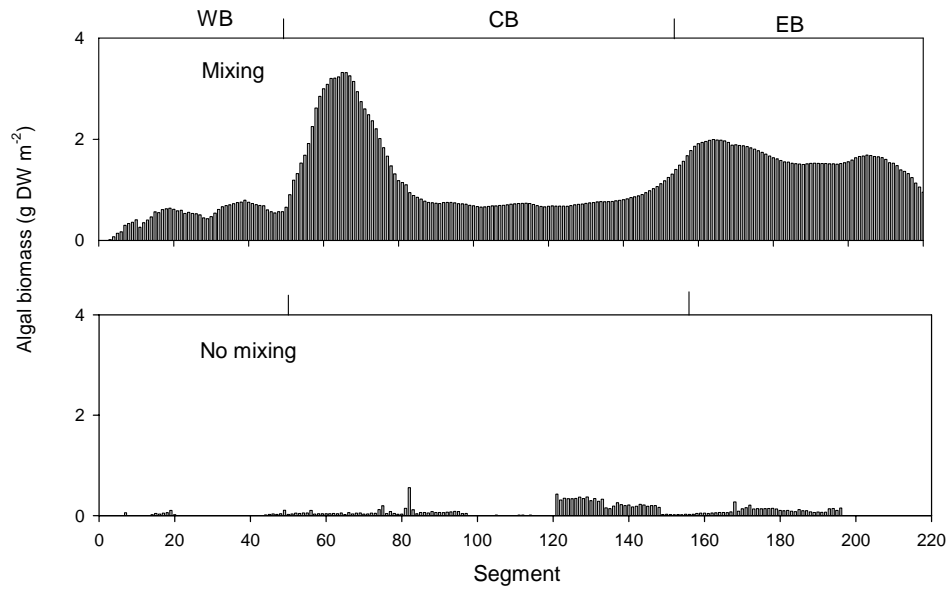


Figure 2.29. As Figure 2.22, but for diatoms on August 30, 1998.

a) Water column concentrations of diatoms, 1999



b) Concentration distributions of diatoms, 1999

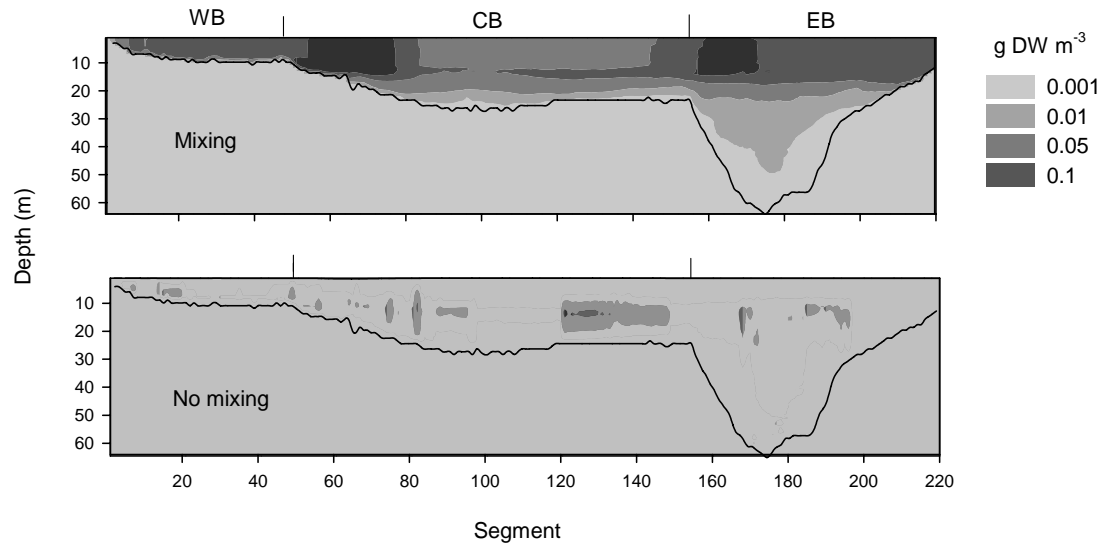


Figure 2.30. As Figure 2.22, but for diatoms on August 30, 1999.

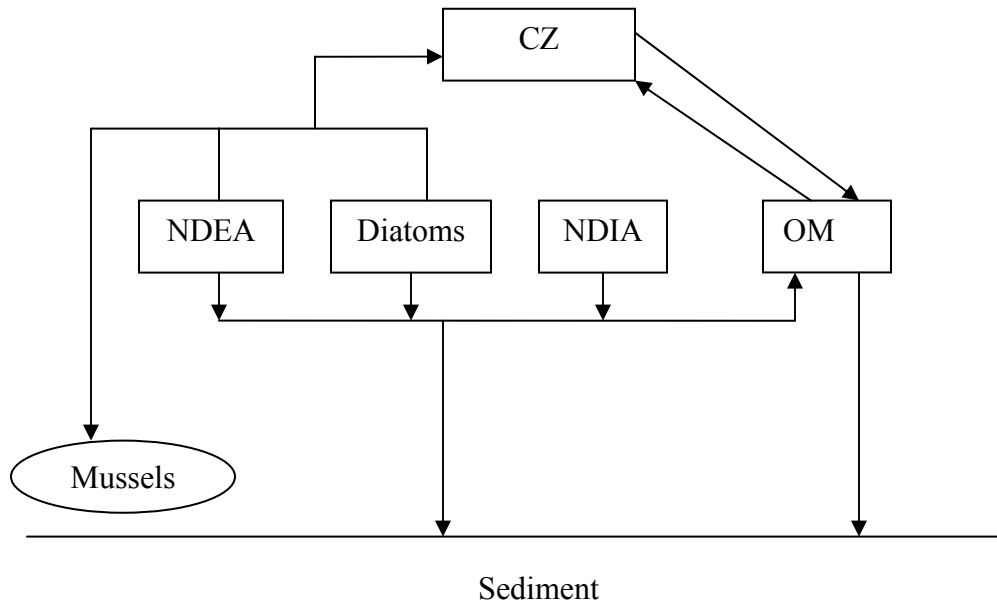


Figure 2.31. Carbon pools (in boxes) and carbon flows (arrows) in the model. CZ: crustacean zooplankton; NDEA: non-diatom edible algae; NDIA: non-diatom inedible algae; OM: organic matter; Mussels: zebra and quagga mussels. Pool sizes and transfer rates are shown in the subsequent figures.

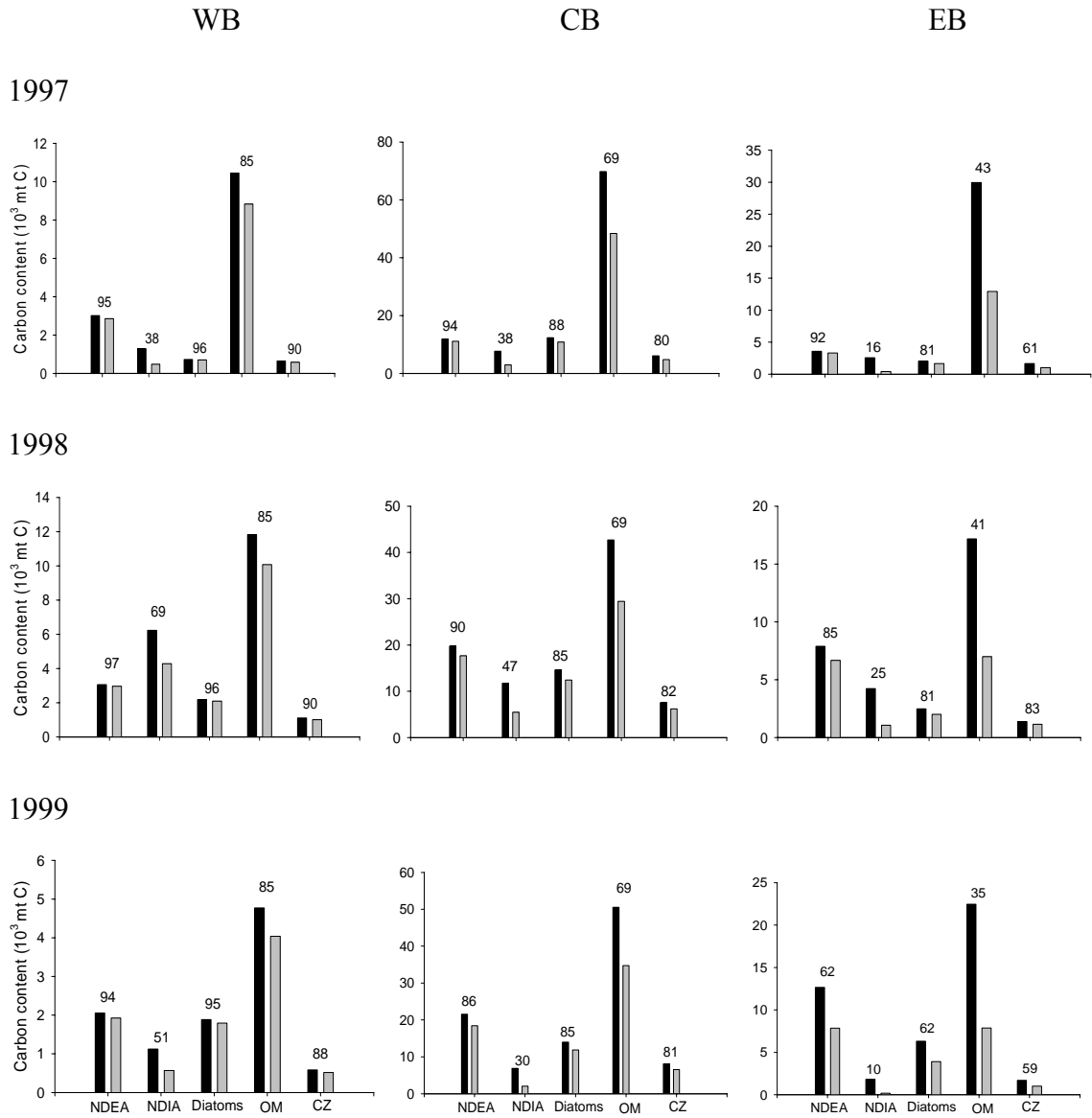
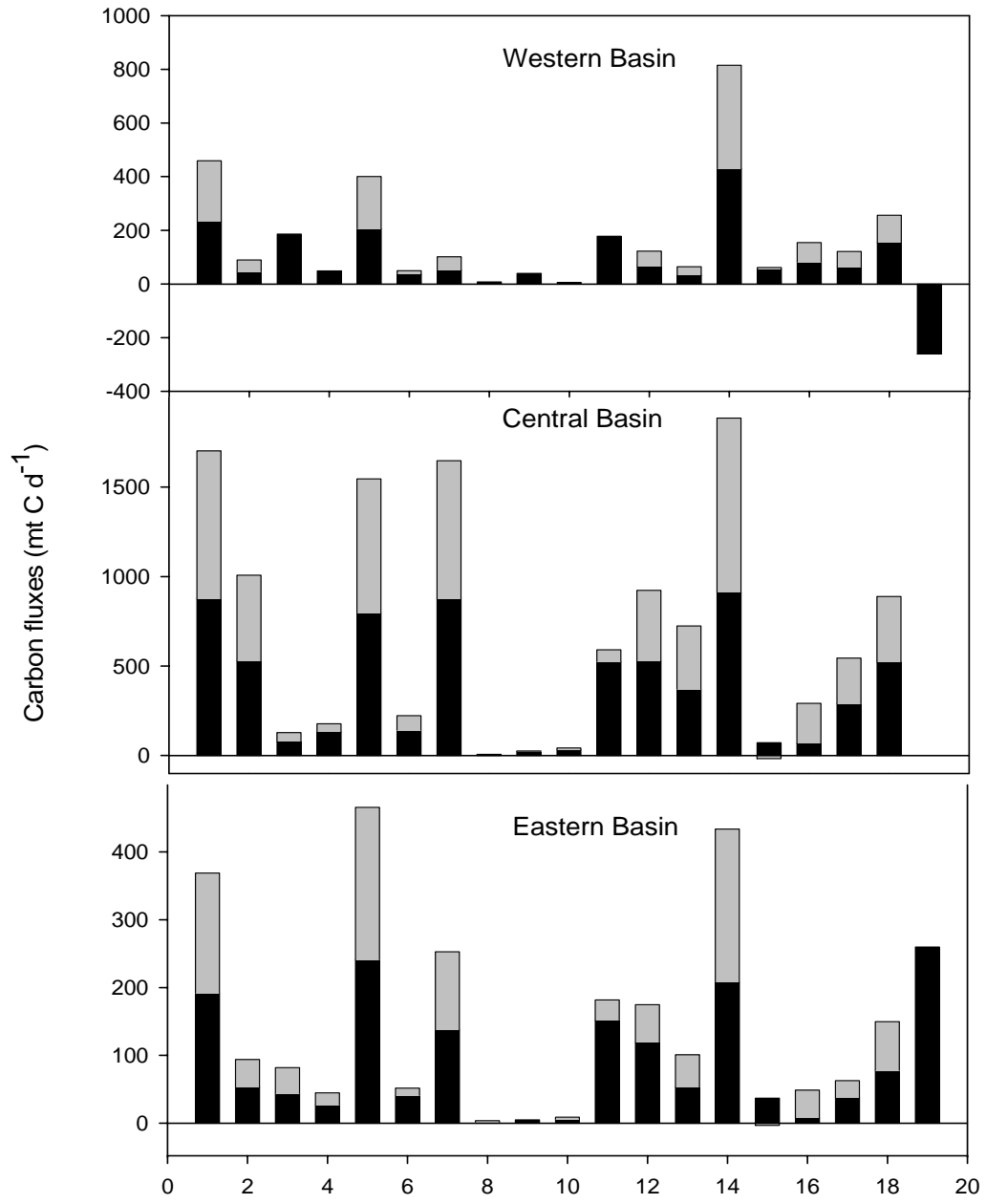


Figure 2.32 Relative sizes of the carbon pools (10^3 mt C) in the model. Values are the averages over simulation period of each year. Dark bars are basin-wide carbon mass. Light bars are carbon mass in the top 12m water column or non-bottom layer water column if water is less than 12m deep. Numbers on the bars indicate the percentage of light bar values to the corresponding dark bar values. NDEA stands for non-diatom edible algae; NDIA stands for non-diatom inedible algae; OM stands for organic matter; and CZ stands for crustacean zooplankton.

Figure 2.33. The 1997 simulation's averaged carbon flows (mt C d^{-1}) over simulation period. Note the flows were calculated every 30 minutes and the averaged values have been converted from g C s^{-1} to mt C d^{-1} . Dark bars are basin-wide carbon flows; light bars are carbon flows in the water column above 12m. Negative numbers refer to losses from the basin. Bar 1 is carbon flow from NDEA to CZ (NDEA→CZ); 2 is Diatoms→CZ; 3 is NDEA→Mussels; 4 is Diatoms→Mussels; 5 is NDEA→OM; 6 is NDIA→OM; 7 is Diatoms→OM; 8 is NDEA→SED; 9 is NDIA→SED; 10 is Diatoms→SED; 11 is OM→SED; 12 is OM→CZ; 13 is CZ→OM; 14 is NDEA production; 15 is NDIA production; 16 is Diatom production; 17 is CZ production; 18 is SED decomposition; 19 is Exchanges between basins. Note the different scales on the y-axis.



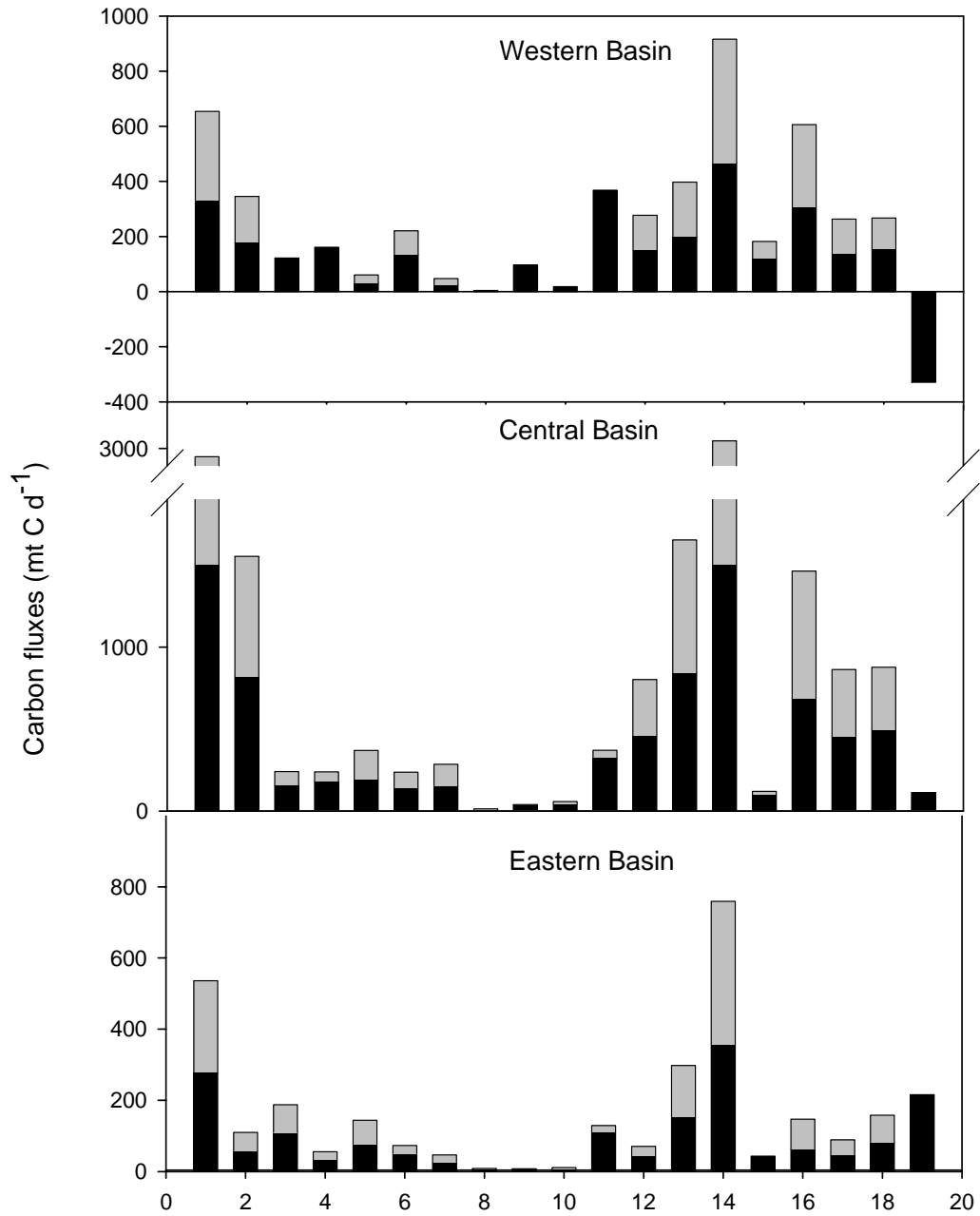


Figure 2.34. As Figure 2.33, but for 1998. Note the different scales on the y-axis.

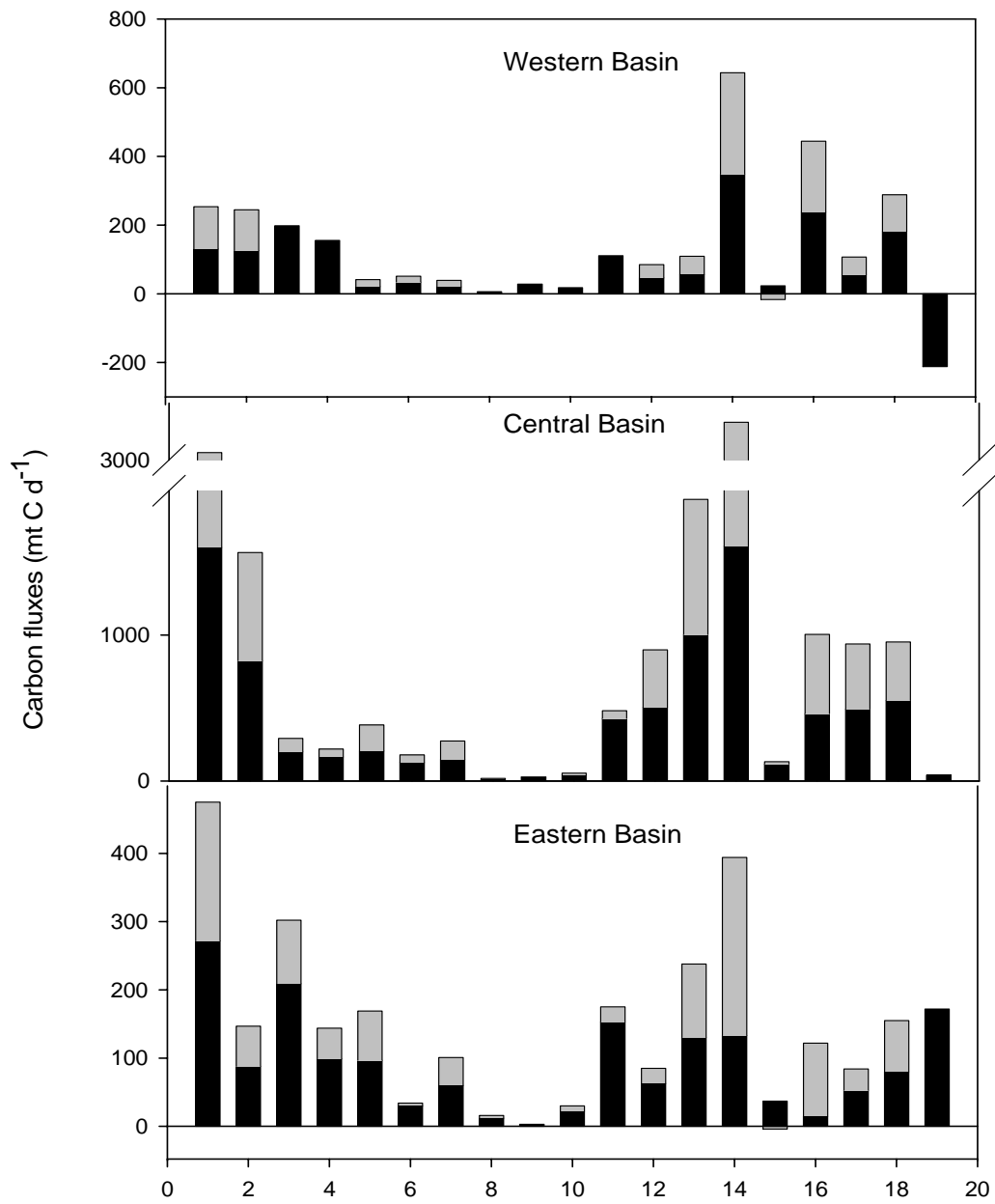


Figure 2.35. As Figure 2.33, but for 1999. Note the different scales on the y-axis.

CHAPTER 3

APPLICATION OF A TWO-DIMENSIONAL ECOLOGICAL MODEL TO EVALUATE THE EFFECTS OF EXTERNAL PHOSPHORUS LOADING ON LAKE ERIE'S LOWER TROPHIC LEVELS

ABSTRACT

It has been more than three decades since the implementation of a phosphorus reduction program for Lake Erie, and water quality has improved from the 1970s. Relaxation of phosphorus control has even been proposed to maintain current fishery productivity. However, a clear understanding of the impacts of the external phosphorus loading on the Lake Erie ecosystem is needed before this risky management strategy is adopted. This study uses a two-dimensional ecological model, EcoLE, to evaluate the impacts of external phosphorus loading on the lower trophic levels of Lake Erie. Analysis of lake-wide longitudinal distributions of phosphorus loaded from external sources show that the external loads are mainly concentrated in the western and west-central basins, with only minor inputs in the east central and eastern basins. The model results show that the external phosphorus loading was of the same magnitude as the internal phosphorus loading in the western basin, while the internal loading was more important than the external in the central and the eastern basins. Phosphorus was distributed homogeneously in the water column in the western basin. In the stratified

central and eastern basins, however, phosphorus released by organic matter decomposition and pelagic communities (algae, and crustacean zooplankters) were concentrated in the epilimnion supporting approximately 60% of the daily algal P-demands, while phosphorus excreted by dreissenids and that released by anoxic sediments was distributed primarily in the hypolimnion. Different algal groups, non-diatom edible algae (NDEA), non-diatom inedible algae (NDIA), and diatoms responded differently to changes in the external phosphorus loading among years, which was simulated by turning external phosphorus loading off and on in the model. Simulation results suggest that caution should be used before considering making changes in the current phosphorus loading reduction program.

INTRODUCTION

A clear correlation between the concentration of total phosphorus and phytoplankton biomass in freshwater lakes has been repeatedly documented (Lean 1973, Schindler 1977, Scavia and Chapra 1977, Smith 1982, Knoll *et al.* 2002), because phosphorus is the most commonly limiting macronutrient in freshwater lakes (Schindler 1977, Arnott and Vanni 1996, Wetzel 2001, Wilhelm *et al.* 2003). Excessive phosphorus inputs have dramatically increased water productivity and caused the eutrophication of many lakes (Chapra and Robertson 1977, Beeton 2002, Jin 2003). Lake Erie was diagnosed as eutrophic in the 1970s, resulting from excessive external phosphorus loading (Burns and Ross, 1972).

Since the shoreline of Lake Erie became deforested and urbanized, municipal and industrial wastes and agricultural runoff entering Lake Erie increased dramatically (Kemp

et al. 1976, Ongley 1976). High nutrient inputs led to excessive phytoplankton in the lake (Braidech *et al.* 1972). Consequently, abundant senescent and dead algae caused a high oxygen depletion rate in the hypolimnion of the central basin, which caused severe anoxia in late summer. Anoxic sediment released a large amount of phosphorus (Arnott and Vanni 1996), which further enhanced the high nutrient input and established an undesirable cyclic process in the ecosystem, i.e., high nutrients in the water → high phytoplankton production → high organic matter input to the hypolimnion → high oxygen depletion rate in the hypolimnion → anoxia in the hypolimnion → high nutrients released from sediments to the water (Burns and Ross 1972).

The external phosphorus loading reduction program started to lead to encouraging water quality responses by the Lake Erie ecosystem soon after it was carried out in the early 1970s. Not only did total phosphorus concentrations decrease in the water column (Rosa and Burns 1987, Rockwell *et al.* 1989), but also the total phytoplankton biomass decreased 40% in the western basin by the late 1970s, 65% by the mid-1980s, and the blue-greens and filamentous greens decreased by 80% by the mid-1980s (Makarewicz and Bertram 1991; Gopalan *et al.* 1998). The oxygen conditions improved on the bottom of the western basin (Krieger *et al.* 1996) and the rate of oxygen depletion in the central basin hypolimnion showed a slight downward trend (Bertram 1993).

Decreases in phytoplankton biomass became even more obvious shortly after zebra mussels (*Dreissena polymorpha* Pallas) invaded and established a dense population on the bottom of the western basin in the early 1990s (Holland 1993, Leach 1993). The dreissenid invasion distracted the attention of researchers from the phosphorus reduction program because dreissenids' great filtering capability was assumed to exceed the

magnitude of the effects of the phosphorus reduction (MacIsaac *et al.* 1992). Decreases of phytoplankton biomass raised concerns among some fisheries managers that the system productivity may become too low to support desired rates of sport fish production (Schloesser and Nalepa 2001, Anderson *et al.* 2001, Wilhelm *et al.* 2003). Accordingly, some suggested the phosphorus loading restrictions could be relaxed to advantage, in part because the program was very expensive (McGucken 2000) and because many assumed dreissenids controlled the concentration of phytoplankton biomass. However, recent studies show that impacts of dreissenids on phytoplankton are confined to the shallow areas and bottom boundary layers (Ackerman *et al.* 2001, Edwards *et al.* 2005). Furthermore, phosphorus loads in some tributaries have increased since 1995 (Peter Richards at Heidelberg College, personal communication). Increase in the frequency and magnitude of *Microcystis* blooms in recent years (Vanderploeg *et al.* 2001, Vincent *et al.* 2004, Rinta-Kanto *et al.* 2005, Bierman *et al.* 2005, Conroy and Culver 2005) suggest that there is still a lot more P available than is desirable. Moreover, phytoplankton biomass has increased in recent years (Conroy *et al.* 2005a). A clear evaluation of the phosphorus loading reduction program is therefore needed before making any changes in P management policies.

While external loading reduction can cause oligotrophication, its onset is always delayed by internal phosphorus loading (Phillips *et al.* 2005). This phosphorus excreted by organisms in the water and released from sediments has recently attracted more attention (Pettersson 1998) because phosphorus release from planktonic communities keeps phosphorus recycling within the water column and maintains most primary productivity (Moegenburg and Vanni 1991, Hudson *et al.* 1999, Gulati *et al.* 1995,

Hudson *et al.* 2000). Fish excretion, although much lower than planktonic community excretion, transports nutrients from the hypolimnion to the epilimnion during thermal stratification periods. Sediment-feeding fish can be particularly effective transporters, and all such excretion adds “new” phosphorus to the epilimnion (Brabrand *et al.* 1990, Schaus *et al.* 1997, Vanni 2002, Bunnell *et al.* 2005). Sediment release plays an important role in the nutrient recycling in an ecosystem, especially in eutrophic ecosystems (Søndergaard *et al.* 2005). Another important internal phosphorus source to Lake Erie is the excretion by zebra mussels and quagga mussels (*D. bugensis* Andrusov). They excrete a considerable amount of phosphate (Gardner *et al.* 1995, Heath *et al.* 1995, Holland *et al.* 1995, Arnott and Vanni 1996, James *et al.* 1997, Mellina *et al.* 1995) at a rate as high as $2.8 \text{ mg m}^{-2} \text{ day}^{-1}$ and a turnover time of 10.1 days (Conroy *et al.* 2005b).

Mathematical models have been constructed to better integrate our knowledge obtained from field observations and laboratory experiments, generate a holistic view, and arrive at a deeper understanding (Kreis 2000). From the simple model involving a statistical correlation between chlorophyll and total phosphorus developed by Chapra (1977), to the much more complex models that include many state variables and two or three water layers, plus the effects of sediment on the bottom (Di Toro and Connolly 1980, Lam *et al.* 1983), none of the existing eutrophication models applied to Lake Erie have fine spatial resolution. Each basin (or even the whole lake) has been considered as a compartment that is completely mixed. Although recent models separate the stratified water column into two layers (epilimnion and hypolimnion), it is simply inappropriate to assume that nutrients entering the epilimnion at one location would be instantly equally accessible to all phytoplankton in the epilimnion of a lake the size of Lake Erie. To

better understand the effects of the phosphorus reduction program on Lake Erie and the relative importance of different nutrient sources (internal and external), a model with finer spatial resolution is needed.

In this study, therefore, we used a 2-dimensional ecological model (see Chapter 2) to simulate the spatial distributions of the external and internal phosphorus loading throughout Lake Erie during the 1997, 1998 and 1999 summer growing season. The effects of external phosphorus loading on phytoplankton were evaluated by simulating the biomass and productivity of various phytoplankton groups with and without external P loading. We hypothesize that the internal phosphorus loading is more important to phytoplankton than is external loading, both in terms of distribution and flow, under the lake's current status during the growing season (nominally May-September). A phosphorus flow diagram of the ecosystem was generated from the model, which provides an overview of the phosphorus fate in the Lake Erie ecosystem during the summer growing season.

MODEL DESCRIPTION

A two-dimensional ecological model of Lake Erie, EcoLE, is used (for details see Chapter 2) to simulate the impacts of external and internal phosphorus loading on the Lake Erie ecosystem. This model divides Lake Erie into 222 horizontal segments from west to east and up to 65 vertical layers (1-m intervals) from surface to bottom. Using daily meteorological input data, it calculates variation in the lake's physical conditions (water level, current velocities, temperature, etc.) every 10 minutes. The biological state

variables are non-diatom edible algae (NDEA), non-diatom inedible algae (NDIA), diatoms, cladocerans and copepods, while chemical state variables are ammonium (NH_4), nitrate (NO_3), soluble reactive phosphorus (SRP), dissolved organic matter (DOM), particulate organic matter (POM), silicon (Si), silicon particulate organic matter (POM_s), and dissolved oxygen (DO). The *Dreissena* spp. are external forcers, that is, their grazing and nutrient remineralization activities are calculated with a pre-determined (and invariant) population density distribution.

As we mentioned in Chapter 2, we output all the calculated results of limiting factors from the model for all three years and found no case where nitrogen was a limiting factor. So we will focus on phosphorus resources and their impacts on plankton during this study.

External phosphorus loading is phosphorus (as SRP and organic phosphorus) derived from WasteWater Treatment Plants (WWTP) and non-point sources entering via rivers (Figure 3.1). Internal phosphorus (as SRP) loading includes excretion by dreissenids and crustacean zooplankters, release from organic matter decay and the sediments. The simulation periods are May 10-September 30, 1997, June 10-October 30, 1998, and May 20-September 29, 1999.

External phosphorus loading

External phosphorus considered in EcoLE is the phosphorus loaded from tributaries of Lake Erie (Table 3.1 and Figure 3.1). Phosphorus loaded from unmonitored non-point sources is not included due to data limitations. Phosphorus loaded from rivers is measured as SRP and TP. SRP is input into EcoLE directly, while other phosphorus

(TP minus SRP) is converted into organic matter by a ratio of phosphorus to organic matter of 0.01 (Bowie *et al.* 1985).

The external phosphorus is assumed to be well mixed in its entrance model cells (i.e., specific segments and layers) and reaches other cells by physical or biochemical transport and varied from location to location within the lake. The total external phosphorus loads (L , g P s⁻¹) over the simulation periods are estimated by:

$$L = \sum_i \sum_j u_{ij} C_{ij} (t_{j+1} - t_j)$$

where, u_{ij} is the inflow velocity of the source i at time j , m³ s⁻¹. C_{ij} is the total phosphorus concentration of the source i at the time j or the monthly mean phosphorus concentration of source i , when the instantaneous concentration is not available, in g P m⁻³.

Crustacean zooplankton excretion (f_{CP})

Copepods and cladocerans are the two crustacean zooplankters simulated in our model, using Fennel and Neumann's (2003) stage-structured population model for copepods and a general bioenergetic model for cladocerans (see Chapter 2). The stage-structured population model outputs the average size of each stage (m_i) which allows estimating of the population phosphorus excretion using size-specific nutrient release rates. Since egestion has been simulated explicitly in EcoLE by adding the egestion mass to particulate organic matter, size-specific nutrient release rates are indeed excretion rates and not a combination of excretion and egestion release (Vanni 2002). However, such excretion rates were unavailable for freshwater copepods, so a ratio of phosphorus to dry weight (δ_{P-cop}) was used to convert maintenance cost to phosphorus excretion.

Cladoceran excretion was also calculated by converting their maintenance cost to phosphorus excretion by using a ratio of phosphorus to dry weight (δ_{P-clad}) (Andersen and Hessen 1991). Therefore, the total crustacean P excretion (f_{CP}) is calculated as:

$$f_{CP} = \sum^T (\delta_{P-clad} r_{clad} m_{cladoceran} + \sum_i^{copepod} (\delta_{P-cop} r_{cop} m_i))$$

where, r is respiration rate (s^{-1}). T is the duration of a growing season.

Dreissenid P excretion (f_{zmP} for zebra mussels; f_{qmP} for quagga mussels)

Zebra mussels first invaded Lake Erie in the late 1980s, but have been more or less replaced by quagga mussels recently (Stoeckmann, 2003), such that by 1998, 84.4 % of mussels in the eastern basin were quagga mussels, 99.7% in the central basin, but only 36.9% in the western basin (Jarvis *et al.*, 2000). We assume therefore, for simplicity, that during the 1997-1999 periods mussels in the western basin were 100% zebra mussels, whereas those in the central and the eastern basins were 100% quagga mussels. As their density distribution and size frequency vary greatly in time and space, there has never been a good estimation of the two populations. Nevertheless, the depth-dependent estimations by Jarvis *et al.* are used in EcoLE (Table 3.2). For simplicity, it is assumed that mussels are uniform in size (10 mm). Using size frequency from Jarvis *et al.*'s Figures 7-20, their depth-dependent densities (Table 3.2) and length-mass equations (Table 2.4), we calculated Jarvis *et al.*'s mussel population biomass (g DW m^2). Their population biomass is very close to that of our 10-mm mussel population (Table 3.2). In Chapter 4 mussel densities and lengths were varied during the uncertainty analysis to assess the effects of inaccurate estimations of mussel population density and size

distribution on our simulation of dreissenid impacts on the plankton and nutrients. Zebra mussels and quagga mussels have different weight-specific phosphorus excretion rates, ZMP and QMP ($\mu\text{g P (mg DW d)}^{-1}$) (Conroy *et al.*, 2005b).

$$\log_{10}(ZMP) = 0.506[\log_{10}(W_{zm})] - 1.172$$

$$\log_{10}(QMP) = 0.297[\log_{10}(W_{qm})] - 1.195$$

where, W_{zm} and W_{qm} are dry weight (mg) of 10-mm mussels

Thus, the phosphorus excretion of a mussel population over the growing season is calculated as the sum of the products of individual excretion rate and number of mussels.

$$f_{zmP} = \sum^T (N_{zm} (W_{zm} ZMP))$$

$$f_{qmP} = \sum^T (N_{qm} (W_{qm} QMP))$$

Organic matter release

The organic matter pools (dissolved organic matter (DOM), particulate organic matter (POM), and silicon particulate organic matter (POM_s)) have temperature-related decay rates, which are converted to phosphorus release rates by a ratio of phosphorus to organic matter of 0.01 (Bowie *et al.* 1985).

Sediment phosphorus release

Under oxic conditions, sediments hardly release phosphorus to the overlying water, while sediments release phosphorus dramatically under anoxic conditions (e.g. Mortimer 1941, 1971). Burns and Ross (1972) reported that sediment P release was 11

times faster under anoxic than under oxic conditions in the central basin of Lake Erie. Di Toro and Connolly (1980) assumed that sediment P release was zero under oxic conditions, while sediment P release increased dramatically under anoxic conditions. Chapra and Canale (1991) found that sediment total phosphorus concentration increased dramatically when the dissolved oxygen concentration of the bottom water was below 1.5 mg l⁻¹. Lam *et al.* (1987) assumed that anoxia occurred at 1.5 mg l⁻¹ oxygen in the lower layer of their two-layer model. In our model, we assume that no phosphorus was released when the DO concentrations of the bottom water were above 1.0 mg l⁻¹, while a constant release rate was used, 0.002 mg P m⁻² d⁻¹, when the DO concentrations were below 1.0 mg l⁻¹. We used a lower DO threshold for anoxia than Lam *et al.* (1987), because our deepest water layer was thinner than theirs.

Basin-wide phosphorus cycling

Three phosphorus pools, dissolved phosphorus (DP), particulate phosphorus (PP) and crustacean phosphorus (CP), and six cycling pathways were considered (Figure 3.2). Phosphate was a very active form and its overturn times were as short as several minutes (Lean 1973, Burns 1976, Hudson *et al.* 2000), so we combined phosphate and DOM-P together as DP. PP refers to the phosphorus in particulate organic matter, and algae. CP includes the phosphorus content of cladocerans and copepods. The pathway from DP to PP includes phosphorus uptake by algae, while PP to DP includes phosphorus excretion of algae and phosphorus release by POM decay. Our model has a traditional grazing food web. However, by including organic matter the model implicitly includes the microbial food web (Debruyne *et al.* 2004).

Phosphorus pools (g P, converted to metric tons P later) are calculated by

$$\frac{\sum^t \sum^j \sum^i C_{ijt} V_{ijt}}{N},$$

where C_{ijt} is the concentration of phosphorus content of a state variable in the i^{th} model layer, the j^{th} segment and at time t , in g P m⁻³. V_{ijt} is the water volume of the corresponding model cell (i, j) , m³, at time t . N is the total numbers of outputs of a phosphorus pool during a simulation period.

Daily basin-wide phosphorus flows (F , g P d⁻¹, converted to mt P d⁻¹ later) between state variables and mussels and sediment are calculated by:

$$F = \frac{\sum^t \sum^j \sum^i Q_{ijt} V_{ijt}}{N},$$

where, Q_{ijt} is the phosphorus flow from one state variable to another within a model cell (i, j) at time t , g P m⁻³s⁻¹. For example, Q_{ijt} for phosphorus flow from CZ to DP is the total phosphorus excretion by crustacean zooplankton per m³ in model cell (i, j) at time t .

External phosphorus loaded to each basin and interbasin exchanges were calculated by the model to complete the phosphorus budget. The net phosphorus exchanges between connected basins are the sum of the net phosphorus flows of NDEA-P, NDIA-P, diatom-P, SRP, DOM-P and POM-P. The phosphorus exchanges at the intersection between segment 49 and 50 are considered the exchanges between the western and the central basins, while the phosphorus exchanges at the intersection

between segment 156 and segment 157 are considered the exchanges between the central and the western basins. Both horizontal advection and dispersion are included.

SIMULATION AND RESULTS

External phosphorus loading

The total phosphorus loaded into Lake Erie from tributaries during the simulation periods was primarily from the Maumee and the Detroit Rivers, whereas loads from waste water treatment plants were relatively small (Table 3.1). Phosphorus loads from the Sandusky River decreased significantly from 1997 to 1999, matching a trend of decreasing P in the annual whole-lake loads from 1997 to 1999. However, the loads during the simulation periods were only about 30% of the annual external loads (Table 3.1), so that the largest fraction of the annual loads entered outside the period simulated. For example, our simulation periods were from May to September in 1997 and 1999, from June to October in 1998, which missed the additional high phosphorus loading season from January through April from the Maumee River (Figure 3.3).

To determine the cumulative distribution of TP and SRP input over the season from external sources, all biological and chemical processes (including sedimentation) were turned off, the initial concentrations of phosphorus (SRP, DOM, POM) in Lake Erie were set to zero, and the model (with wind and other mixing forcing in operation) run to the last simulation day, with external phosphorus loads allowed to “accumulate.” Under these conditions, most of the external phosphorus loading was concentrated in the western and west central basins (Figures 3.4-6), and contributed little to the phosphorus concentrations in the east central and eastern basins. Very high TP and SRP

concentrations accumulated in the non-bottom-layer water column of the west western basin in all three years (Figure 3.6), especially in 1998. The high phosphorus concentrations in the west western basin of 1998 reflected the late increases in input of TP and SRP during the growing season (Figure 3.3).

External P loading in the model was next turned off (i.e. set SRP and DOM concentrations in the tributaries to zero) and then back on to investigate its impacts on the growth of the non-diatom edible algae (NDEA), non-diatom inedible algae (NDIA), diatoms and crustaceans (Tables 3.3-5). NDEA and crustaceans responded positively to external P loading, but the magnitudes of the response varied widely with the basin involved. NDIA and diatoms had a mixture of positive and negative responses to external P loading. These responses are discussed in detail below.

NDEA

The 1997 simulation (Table 3.3) showed that the basin-wide total NDEA biomass without P loading was less than 20% of that with P loading in the western basin, while the 1998 and 1999 simulations showed (Tables 3.4, 3.5) 49% and 32% of those with P loading, respectively. In the central and eastern basins, the NDEA biomass percentages remaining when external P loading was turned off were much higher (93-99%) than those in the western basin, for all three years. The effects of external P loading on NDEA productivity rates were similar to those for NDEA biomass (Tables 3.3-3.5).

NDIA

In the western basin, NDIA (dominated by cyanobacteria) responded to the changes of external loading differently from NDEA. The largest decrease in the western

basin in NDIA biomass occurred in 1998 when external loading was turned off, followed by 1997 and then 1999. Moreover, the decrease in 1998 (68%) was much larger than those in 1997 (20%) and 1999 (2%). Since the biomass of NDIA was much higher in 1998 in the western basin than it was in 1997 and 1999, high NDIA biomass thus tends to be more sensitive to phosphorus availability, especially when a large amount of phosphorus input occurred during fall of 1998 (Figure 3.3) when cyanobacteria were abundant in the water column. In contrast, turning on/off external P loading had little influence on NDIA in 1999. Little phosphorus entered in July, August, or September 1999 (Figure 3.3), so turning off external P loading did not affect growth of NDIA in late summer 1999. Similar to NDEA, NDIA biomass remained high in the central (above 80%) and eastern (99%) basins when external loading was turned off. The effects of external P loading on NDIA productivity were similar to those for NDIA biomass (Tables 3.3-3.5).

Diatoms

Modeling extends from May to September or October. If a big P input occurs prior to May, e.g. 1998, shutting off P loading from May to September is probably less important to the diatoms. Basin-wide diatom biomass decreased in 1997 and 1999 in the western basin if no external loading occurred, while it even increased in 1998. The basin-wide biomass of diatoms in the central basin and the eastern basin slightly decreased without the external phosphorus loading, except for a slight biomass increase in the central basin in 1999. The impacts of external phosphorus loading on diatom productivity were similar to those for basin-wide biomass, except that the net production of diatoms without external phosphorus loading was only 46.6% of that with external

phosphorus loading in the central basin in 1997 (Table 3.3). The responses of diatoms to the changes of the external loading were thus more complex than those of other algal groups, perhaps because diatom growth is limited by phosphorus as well as silica, while other groups are limited only by phosphorus. Besides, zooplankton selective grazing affects the algal competition. Some species of diatoms are inedible by zooplankton and the zooplankton grazing selective factor for diatoms is only 0.5 in the EcoLE model (Scavia *et al.* 1988), which means that half of the diatoms are selectively rejected. Nevertheless, the reasons for those responses above are not obvious and need further investigation.

Crustacean zooplankton

When external phosphorus loads were turned off in the simulations, crustacean zooplankton biomass and production decreased largely in the western basin for all three years, while only a small decrease occurred in the central and eastern basin.

Internal phosphorus loading as SRP

Six internal phosphorus sources were considered, cladoceran excretion, copepod excretion, dreissenid mussel excretion, DOM decomposition release, POM decomposition release, and anoxic sediment release. Phosphorus from each internal source is associated with a state variable whose values are updated each modeling time-step as the combined results of inputs from the internal source and water mixing processes. Those values are not affected by chemical-biological processes. Thus, the model output of the final lake-wide distribution of SRP from each internal source was the

total accumulated load over the simulation periods (142 days for 1997, 143 days for 1998 and 131 days for 1999) and distributed over the lake by water mixing processes.

The distributions of internally loaded SRP are similar among the three simulation years. Thus only the results of 1997 are presented here (Figures 3.7-3.10) as the spatial distributions of SRP (upper panels), the water column concentrations of SRP of each segment (middle panels), and the average SRP concentrations of upper water (refers to the top 12 m water or non-bottom water column if the water is less than 12m deep) of each segment (lower panels). SRP excreted by copepods was more than one order of magnitude lower than that of cladocerans. As we are more interested in the total SRP input from zooplankton community rather than each zooplankton group, the excretion of copepods and cladocerans have been combined as the excretion of crustaceans (Figure 3.7). Crustaceans excreted a large amount of SRP in the upper water between segments 60 and 130. The concentrations in the other upper water areas in the central and eastern basins were also high, between 5-10 $\mu\text{g P l}^{-1}$. The phosphorus concentrations excreted by crustaceans in the western basin between segment 12 and 24 were extremely low, which showed the influence of the Detroit River with high flows, low phosphorus content, and no plankton (no plankton loading data are available).

The distributions of SRP released by DOM and POM decomposition were similar, and thus were combined (Figure 3.8). The spatial distribution of phosphorus released by organic matter was similar to that of crustacean excreta but with a higher magnitude.

The simulations show that dreissenids excreted an amount of SRP as high as that released by organic matter (Figure 3.9). However, in the stratified central and eastern basins, most of the phosphorus was concentrated in the lower water with extremely high

concentrations on the bottom cells. Although dreissenids were distributed throughout the water column in the central and eastern basins (Figure 2.5a), the much larger sedimental area in the hypolimnion than that in the epilimnion means that most of the dreissenid mussels are distributed in the hypolimnion cells. Dreissenid excretion contributed a total of as much as $25 \mu\text{g P l}^{-1}$ over the simulation period into the upper water in the western and the west-central basins, while it contributed less than $3 \mu\text{g P l}^{-1}$ into the upper water in the rest of the lake.

Anoxic sediment released an amount of phosphorus as high as 1.5 g P m^{-2} over the simulation period (Figure 3.10), primarily at the bottom of the central basin. Sediment phosphorus release showed little influence on the epilimnion phosphorus concentration during the growing season. As sediment only releases phosphorus when it is under anoxic conditions, the sediment phosphorus release profiles also reflect the simulated oxygen conditions on the lake bottom.

Comparisons between the amounts and spatial distributions of internal phosphorus and external phosphorus (Figures 3.4-3.10) show that internal phosphorus is the major phosphorus source to the central and eastern basins, while the external phosphorus load is concentrated in the western and west central basins.

Basin-wide phosphorus cycling

The amount of basin-wide P in each pool, mt P , and the daily P flows along each pathway, mt P d^{-1} varied among 1997, 1998 and 1999 (Tables 3.6-3.8). Less than 50% of the DP was in the upper water, which indicated the importance of the benthic internal

sources of soluble phosphorus to DP. More than 50% of PP was in the epilimnia of the central and eastern basins. Crustacean phosphorus was a small phosphorus pool.

In the western basin in 1997 (Table 3.6), the most active pathway was from DP to PP, which was the phosphorus uptake by phytoplankton. Phytoplankton uptake could deplete the DP pool within 5 days, while the phosphorus regenerated daily in the water was only 73% of the algal demand with 30% from PP, 16% from crustaceans and 27% from dreissenids. A small amount of sediment SRP was released in the western basin which indicates that anoxic conditions occurred during the simulation period, but sedimentation of P was still much higher than sediment release. The external phosphorus loaded into the western basin was higher than the other inputs. During the simulation period the western basin retained more than 60% (9.6 metric tons) of the daily external phosphorus loads.

In the central basin of 1997, phytoplankton took up 100 metric tons of phosphorus every day with 93% of that occurring in the epilimnion. SRP regenerated in the epilimnion contributed 67% of the daily phosphorus demand by phytoplankton with 46% from PP and 21% from crustaceans. Only 10% of the phosphorus released by dreissenids reached the epilimnion, which was less than 2% of the total SRP regeneration in this water stratum. At the same time, more than 8 metric tons of PP was lost to the sediment daily, relative to 3.1 metric tons of external TP loaded to the central basin each day. Together with the net gain of 0.3 metric tons of TP from the western basin, the central basin gained 3.4 metric tons of TP each day during the simulation period.

In the eastern basin in 1997, 86.8% of the algal phosphorus uptake occurred in the epilimnion. SRP regeneration in the epilimnion contributed 68% of the algal demand.

45% was from PP and crustacean excretion contributed 17%, while dreissenid excretion contributed 6%. There was a net sedimentation of PP of 3.7 metric tons per day. The eastern basin had a net gain of TP of 5.2 metric tons daily during the simulation period.

Similar situations occurred in 1998 and 1999 to the phosphorus recycling in the water column (Tables 3.7-3.8). Phosphorus recycling within the upper water contributed the major portion of the phytoplankton demands, while dreissenid excretion was highly restricted to the hypolimnion in the central and eastern basins. Phosphorus released from the sediment was less than the sedimentation losses. The numbers related to basin-wide TP budget are worth reiterating here. The net sedimentations of PP were 10.5, 4.1 and 3.3 mt P d⁻¹ for the western, central and eastern basins in 1998, respectively, while they were 3.6, 10.1 and 4.3 mt P d⁻¹ in 1999. The western basin retained 2.8 mt P d⁻¹ of external loads in 1998 and the central basin retained 4.3 mt P d⁻¹, and the eastern basin retained 2.5 mt P d⁻¹. The corresponding data for 1999 decreased to 2.1, 2.9 and 0.2 mt P d⁻¹.

DISCUSSION

External phosphorus loading

Excessive anthropogenic phosphorus inputs have been identified as the major cause of eutrophication of most of freshwaters (Burns and Ross 1972). Consequently, reduction of external phosphorus loading (oligotrophication) has been adopted to remedy unsatisfactory water quality conditions in eutrophic waters (Anderson *et al.* 2005).

Although our model does not include all tributaries along the lake shore (Bolsenga and Herdendorf 1993, Dolan 1993), the major tributaries are all included. Furthermore,

considering the overwhelming loads from the Maumee River and the Detroit River, our model catches the main character of the external loading of Lake Erie during each summer growing season. However, it would improve the model performance if the phosphorus loading data from the Grand River, Ontario were available, for this river is the major source of external nutrient loading to the eastern basin.

To our knowledge, our study depicted for the first time, explicitly how far the major external phosphorus loads from western Lake Erie could reach into central and eastern Lake Erie. If the biochemical processes (e.g. phytoplankton uptake) were activated during the simulation, the external phosphorus loads would go even less far to the east. When the external phosphorus loads were set to zero, carbon fixation in the western basin decreases sharply, while the decreases were less than 10% in the central basin and less than 2% in the eastern basin. The 10% decrease in the central basin was due to the loss of phosphorus loads from the western basin, the Sandusky River, and the Cuyahoga River. Thus, our results suggested that external loading into the western basin had little direct effect on the central and eastern basin algal production. In the non-bloom years, 1997 and 1999, NDIA were less sensitive to the change of external loading than NDEA, while in the bloom year (1998), NDIA decreased dramatically if there was no external loads. One distinct characteristic of the temporal variation in loading in 1998 was that there was an external loading peak in August when NDIA became abundant and needed more phosphorus to support the biomass. Thus, we speculate that not only the amounts of loads, but also their temporal schedules are important to the production of blue-green algal blooms. The phosphorus loading reduction program should attract more attention in later summer.

We assume that all phosphorus from external sources is ultimately available to algae. However, De Pinto *et al.* (1981) estimated that only 22% phosphorus from suspended sediment was ultimately available to *Selenastrum capricornutum* loaded from rivers, while Young *et al.* (1982) estimated that 63% of particulate phosphorus from WWTP was ultimately available to algal uptake. According to their studies, our estimations of bioavailability of the external phosphorus are 50-60% overestimates for rivers and 15% overestimates for higher from WWTPs.

However, the overestimated phosphorus was organic phosphorus, which was not instantaneously available to algae but at a maximum decay rate of 0.12 d^{-1} (Cole and Buchak 1995). Moreover, the significant overestimation occurs in the western basin which receives big rivers. Our simulations (Figures 2.14-2.16) showed that the modeled TP-F was lower than the field measurements even with the overestimated phosphorus external loading, which indicates that there are some other big sources missing, for example unmonitored non-point sources. The total amount of unmonitored non-point phosphorus input during the simulation period of 1997 is 1089 mt (see below), which is 50% of the total phosphorus input into the western basin from tributaries of EcoLE. So while I have overestimated the available phosphorus loaded from seven tributaries considered in EcoLE, I might not have overestimated the real available phosphorus loaded from external sources of Lake Erie.

With adjusted availability of external phosphorus (based on De Pinto *et al.* 1981 and Young *et al.* 1982) and higher decay rate 0.154 d^{-1} of organic matter (De Pinto *et al.* 1981), the redone Figures 2.14-16 (Figures 3.11-13) show that even lower TP-F concentrations for a simulation in the western basin. Simulations of algal and

zooplankton biomass are lower, too. The changes in the central and eastern basins are negligible. The paired t-test shows (Table 3.9) that all modeled NDEA, TP-F are significantly lower than field measurements in the western basin. Some cases of cladocerans become significantly lower, too. However, cases in the central and eastern basins are slightly improved. Thus, we speculate that including data of external phosphorus from the unmonitored non-point sources is very important to improving EcoLE's performance in the western basin.

Dolan (1993) suggested that there was not much room for further point source controls, while much work should be done on controlling non-point sources (in both monitored tributaries and unmonitored areas). The land within the Lake Erie drainage basin has either intensive agricultural uses or has become urbanized (Sly 1976). Agriculture is the largest non-point source of phosphorus in the United States, while urban runoff also contributes a significant amount of P to continental water bodies (Carpenter *et al.* 1998). Recent research showed that nutrient loading in rivers is increasing (Peter Richards at Heidelberg College, personal communication). Due to lack of data on non-point P sources in unmonitored areas (e.g., Portage River, Canadian Grand River, Black River, etc.), I did not consider loading from these sources in the model. Nevertheless, these sources contribute a big portion, 26% in 1997, 21% in 1998 and 17% in 1999, of the total external loading to the lake (Dolan, personal communication). However, with some reasonable assumptions, we can use our model to make a rough estimation of the importance of these sources to the lake for 1997. If we assume that these sources have a continuous input to Lake Erie, that the flow was evenly and instantaneously distributed throughout the top 5 m of water, and the phosphorus input

was 100% bioavailable, then the daily accumulation of P in the top 5 m of water can be calculated, which is 26% of total external loading of 1997 divided by the water volume of the top 5m and then divided by 365 days per year. Thus the daily input of P from unmonitored areas was $0.19 \mu\text{g P l}^{-1} \text{d}^{-1}$. Under these assumptions, our simulation results (Table 3.10) showed that non-monitored areas are responsible for an increase of NDEA biomass by 25, 52, and 71% in the western, central and eastern basins, respectively. Diatoms increased by 22% in the western basin, but by less than 5% in the central and the eastern basins. In contrast, NDIA increased by 65-87% in the central and eastern basins but increased less than 10% in the western basin. The role of competition among the algal groups on relative algal abundance and productivity are unclear at present. However, the simulation results do indicate the importance of unmonitored non-point sources to the trophic status of the lake. A small amount of new phosphorus input in the phosphorus-depleted epilimnion in the central and eastern basins during stratification would be efficiently used and might enhance potentially toxic blue-green algal blooms.

Internal phosphorus loading

The ratios of particulate phosphorus to total phosphorus have not changed from those in Burns's (1976) study, which were from 50-70% in the epilimnia of the three basins of Lake Erie. Pelagic communities are recycling a large amount of phosphorus within the water column at a rapid speed. The dominant phosphorus regeneration pathway is from PP to DP which is always the largest in both whole water column and epilimnia.

It is well known that zooplankton excretion is an important phosphorus source in lakes (Hudson *et al.* 1999, Vanni 2002, Conroy *et al.* 2005b). Zooplankton excreta and organic matter release were readily available to phytoplankton and were the major P supply that supported phytoplankton production (Scavia *et al.* 1988). Zooplankton excretion supported as high as 58% of the primary producer phosphorus demand (Garney and Elser 1990, see in Vanni 2002). The results of our model were lower than that. The crustacean excretion was only 6-22% of the algal phosphorus demand. However, in their laboratory experiments, it is hard to separate metabolic excretion of zooplankton from phosphorus regeneration by egestion and sloppy feeding. Our model outputs only the metabolic regeneration while the regeneration due to egestion is integrated into organic matter decay and sloppy feeding is not considered. Considering the maximum ingestion rate of 1.0 d^{-1} and a simulation efficiency of 0.6 in the model, the egestion rate could be as high as 0.4 d^{-1} . The basic metabolic rate is 0.1 d^{-1} in the model. Thus, the crustacean regenerated phosphorus might triple the above values to as high as 66%.

Olsen and Ostgaard (1985) reported that total phosphorus release rates by *Daphnia* were from 0.05 (P-starved phytoplankton) to $1.5 \mu\text{g P mg DW}^{-1} \text{ h}^{-1}$ (P-saturated phytoplankton). Similar release rates were reported by Vadstein *et al.* (1995). Our results, values of CP→DP divided by crustacean biomass (dry wt) (Tables 3.6-8), were close to the lower range from 0.04-0.1 $\mu\text{g P mg DW}^{-1} \text{ h}^{-1}$. Our consistent low estimations of crustacean release rates make it important to discuss more about the release processes: metabolic excretion, egestion release and sloppy feeding release (Vanni 2002). The metabolic release should be proportional to the body content as this process burns body tissue and has little to do with the food nutrient content. Egestion release is the release

from feces which is highly affected by the food nutrient content. P-rich food leads to high egestion release rates as there is more phosphorus, proportional to other nutrients, in the food than crustaceans need to build body, while P-low food leads to low egestion release rates as phosphorus is assimilated proportionally with other nutrient to build body and little is left in the feces (Andersen and Hessen 1991, Elser *et al.* 2000, Andersen *et al.* 2004). Sloppy feeding release is phosphorus released from food cells that are broken due to crustacean feeding. This process is affected by the food nutrient content as high-phosphorus-content food will release high phosphorus when the food cells are broken and low-phosphorus-content food will release low phosphorus when the food cells are broken. If algae are phosphorus-limited and egestion release dominates the release processes, the phosphorus limitation to algal growth will be enhanced (Urabe *et al.* 1995, Elser *et al.* 2000). The release rates measured with P-starved food are closer to metabolic excretion rates. This explains why our results are at the lower range of the laboratory measurements. However, our lower simulation of crustacean biomass in the western and west central basins (Figures 2.14-2.16), due to limited data (e.g., algal loaded from tributaries, spring recruitment from diapause eggs, etc), might be another answer to the low SRP excretion of crustacean zooplankters.

Numerous studies have been focused on dreissenid phosphorus excretion and its ecological impacts (Gardner *et al.* 1995, Heath *et al.* 1995, Holland *et al.* 1995, Arnott and Vanni 1996, James *et al.* 1997, Mellina *et al.* 1995, Conroy *et al.* 2005b). Mellina *et al.* (1995) estimated that the phosphorus excretion rate of the zebra mussel population in western Lake Erie was $6.1 \text{ mg P m}^{-2} \text{ d}^{-1}$ with a density of $2.2 \times 10^5 \text{ m}^{-2}$. Our model showed a zebra mussel population excretion rate of $0.8\text{-}2.1 \text{ mg P m}^{-2} \text{ d}^{-1}$ with a depth-

dependent density of 3000-6000 m⁻². We would have a similar excretion rate to that of Mellina et al.'s if their population density were used.

Arnott and Vanni (1996) made a rough quantitative comparison among the phosphorus sources including zebra mussel excretion, *Daphnia* excretion, zooplankton excretion, macrophyte excretion, sediment release and external loading in the western basin of Lake Erie. While their estimates provide us a comprehensive reference, there were several differences between this study and theirs.

First, their zebra mussel excretion was one or two orders higher than zooplankton excretion and the external loading, while ours has the same order as the other sources. Calculated from their figure 7, zebra mussel excretion rates ranged from 3.1 to 31 $\mu\text{g P l}^{-1} \text{d}^{-1}$, while other sources released phosphorus at rates of 0.31-3.1 $\mu\text{g P l}^{-1} \text{d}^{-1}$. The results of our model showed that zebra mussels excreted 0.26 $\mu\text{g P l}^{-1} \text{d}^{-1}$, while crustaceans excreted 0.11-0.19 $\mu\text{g P l}^{-1} \text{d}^{-1}$ and the external loading rates were 0.3-0.6 $\mu\text{g P l}^{-1} \text{d}^{-1}$. Their higher zebra mussel excretion maybe due to their higher weight specific P excretion rate (0.76 $\mu\text{g P mg DW}^{-1} \text{d}^{-1}$, calculated from their Table 6) compared with ours (0.11 $\mu\text{g P mg DW}^{-1} \text{d}^{-1}$), higher population density (10,500 ind m⁻²) than ours (3000-6000 ind m⁻²) and differences in mussel size frequency, while we used a fixed mussel size, 10 mm. Our external P loading was at the lower range of theirs, but is probably reasonable as our simulation periods are seasons that receive low external P loads (Figure 3.3). As mentioned above, our zooplankton excretion would be higher if the egestion release and sloppy feeding were taken into account. Moreover, our zooplankton estimates were lower than theirs as they tended to “present high estimates or ranges of the magnitudes of other sources”.

Second, their estimates did not include the organic matter decay, while our estimates showed that this pathway dominated the phosphorus recycling processes. However, their estimates included macrophyte contributions, while ours do not because macrophytes were not considered in our model.

Finally, the anoxic sediment phosphorus release was at the same order as phosphorus released by zooplankton and external loading in their estimates, while an order or more lower than other sources in our results. They estimated the sediment P release from a constant value that was either measured in Lake St. Clair or calculated from regressions with a mean water column TP. In fact, sediment P release rates are highly site-specific and are usually determined largely by model calibration of the dissolved nutrients (Bowie *et al.* 1985). Burns and Ross (1972) estimated that the phosphate regeneration rate under oxygenated conditions in the central basin of Lake Erie was $22 \text{ umoles P m}^{-2} \text{ d}^{-1}$ ($0.0007 \text{ g m}^{-2} \text{ d}^{-1}$); while the anoxic regeneration rate was $245 \text{ umoles P m}^{-2} \text{ d}^{-1}$ ($0.0076 \text{ g m}^{-2} \text{ d}^{-1}$). Lam *et al.* (1983) assumed that the release rate was $0.0044 \text{ g m}^{-2} \text{ d}^{-1}$ under anoxic conditions. After more than three decades, we assume the release rate under anoxia has decreased to $0.002 \text{ g P m}^{-2} \text{ d}^{-1}$ as a result of phosphorus reduction. Our estimates take the concentration of dissolved oxygen in the bottom water into account, which makes the sediment anoxic P release site-specific. However, we could not claim that our estimates were more accurate than Arnott and Vanni's, because our dissolved oxygen state variable is not well calibrated yet. Nevertheless, our results showed that anoxia occurred in the western basin during growing seasons, while the sediment P release during the same growing season was not high.

With the advantage of being spatially explicit, our model depicts the spatial distribution of P loaded from internal sources. In the western basin, the P distribution is homogeneous over water column. In the central and the eastern basins, P excreted by crustaceans and released by organic matter decay is concentrated in the upper water, while P excreted by dreissenids and that released by anoxic sediment is concentrated in the hypolimnion. We accept our hypothesis that the internal P loading is more important to phytoplankton growth than the external P loading in terms of availability and quantity in the east central and eastern basins. In the western basin and the west central basin (segments 50-80) the hypothesis is rejected, likely due to the large external loads from the Detroit, Maumee, and Sandusky Rivers.

Phosphorus budget

It has been decades since Burns (1976) calculated the phosphorus budget for 1970 for Lake Erie. The comparisons between his study and ours (Table 3.11) show that the mean total phosphorus concentration decreased by 80% in the western basin and about 50% in the central and the eastern basins. The net P sedimentation rates of our study were less than 10-20% of those of Burns' (1976) in the western basin, and 20-40% in the central basin, and 60-80% in the eastern basin. These large decreases could be attributed to the phosphorus reduction program. In the western basin, the sedimentation processes could deplete the total phosphorus within 25 days in 1970, while 85 days in 1997, 58 days in 1998 and 66 days in 1999. Although sedimentation in our model shows less influence on the total phosphorus in water column, these processes retain more than 30% of the external phosphorus load of 1997, and 100% of that in 1998 and 1999. In the

central basin we had a net P loss to the sediments, because anoxic releases were 50% less than the sedimentation rate. Burns's (1976) results also showed a net sedimentation loss from May to October in 1970. Our model showed that phosphorus releases from anoxic sediment were not a big concern in terms of quantity and availability to the epilimnion during the growing seasons (Figure 3.10 and Tables 3.6-8). Thus, we conclude that phosphorus released from anoxic sediment does not enhance the anoxic conditions in the central basin during growing seasons by stimulating algal growth in the epilimnion and leading to increasing organic matter sedimentation. However, when fall turnover occurs, a phosphorus input to the epilimnion of relatively high quantity occurs over a short time (Wetzel 1983). Burns (1976, their table 7) showed a dramatic increase of phosphorus input during November, 1970, when water column turnover occurred. The net gain of phosphorus in November was 4 times higher than the net loss in October. The increases in the water column included inputs of the accumulated phosphorus released from anoxic sediments, re-suspended sediment particulate phosphorus and increased external phosphorus loads. More studies are needed to investigate the fate of this pulse of phosphorus input during fall turnover.

Implications

The results of our model demonstrated the complexity of the Lake Erie ecosystem. Algae respond to changes in phosphorus loads differently among groups, basins and years. Increases in P loads will not necessarily increase commercial fish production. Instead, increase of P loading may increase cyanobacteria, which are not edible to zooplankton and benthos. Wilhelm *et al.* (2003) suggested that increased TP loading

would selectively favor cyanobacteria, which respond to available phosphorus rapidly. Assisted by zebra mussel's selective proliferation of cyanobacteria in Lake Erie (Bierman *et al.* 2005), relaxation of phosphorus control will degrade lake conditions rapidly. An unintended experiment has been carried out in Lake Erie such that the external phosphorus loading has increased since 1995 (P. Richards at Heidelberg College, personal communication), and this experiment has contributed to the increased frequency and magnitude of blue-green algal blooms in recent years (Vanderploeg *et al.* 2001, Vincent *et al.* 2004, Rinta-Kanto *et al.* 2005, Bierman *et al.* 2005, Conroy and Culver 2005).

In summary, our model for the first time depicts the spatial (longitudinal and vertical) distributions of external and internal phosphorus loads in Lake Erie over three growing seasons. It can easily be applied to other years for which initial condition data are available. The phosphorus loading from external sources is concentrated in the western and the west central basins. Organic matter releases the most phosphorus among the internal phosphorus sources. Crustacean-excreted phosphorus concentrated in the epilimnion while dreissenid-excreted phosphorus and sediment-released phosphorus concentrate in the bottom water. These interactions show that caution should be applied before making any changes in the current phosphorus loading reduction program.

	1997		1998		1999	
	(May 10-Sep.30)		(Jun.10 – Oct. 30)		(May 20-Sep. 29)	
	TP	SRP	TP	SRP	TP	SRP
Maumee River	1221	203	577	143	116	26
Toledo WWTP	29	3	26	3	18	2
Detroit River	1166	207	891	304	776	296
Sandusky River	275	31	168	17	5	1
Cleveland westerly WWTP	15	1	13	1	9	1
Cuyahoga River	93	12	61	15	65	7
Cleveland easterly WWTP	44	4	31	3	22	2
Erie WWTP	26	3	21	2	15	1
Total	2870	464	1788	487	1026	336
Annual TP Loading (mt y ⁻¹)*	10,765	-	8,190	-	3,868	-

Table 3.1. TP and SRP loads (metric tons per season) from tributaries and WasteWater Treatment Plants (WWTP) in 1997, 1998, 1999. The sources are listed by location around the lake basin from the west to the east (see Table 2.5 for data sources). Although the seasonal data are listed here, daily loads are used and interpolated into every-10- min inputs in the model. *data from D. Dolan, personal communication.

Depth (m)	Density (ind m ⁻²)	Biomass (g DW m ⁻²)					
		WB		CB		EB	
		Jarvis <i>et al.</i> 's	10 mm	Jarvis <i>et al.</i> 's	10 mm	Jarvis <i>et al.</i> 's	10 mm
0-5	2927	10.8	9.0	14.8-62.8	9.5	9.9-36.5	10.7
5-10	6419	23.8	19.7	32.4-137.7	20.8	21.7-80.0	23.4
10-20	3233	12.0	9.9	16.3-69.4	10.5	11.0-40.3	11.8
20-30	3431			17.3-73.6	11.1	11.6-42.8	12.5
30+	3172			16.0-68.0	10.3	10.7-39.5	11.6

Table 3.2. Comparisons of mussel biomass (g DW m⁻²) between Jarvis *et al.*'s population with various sizes and EcoLE's 10-mm mussel population.

1997		WB			CB			EB		
		With	Without	%	With	Without	%	With	Without	%
<i>Biomass</i>	mt DW									
NDEA		6,727	1,069	15.9	27,524	25,778	93.7	8,242	8,153	98.9
NDIA		2,892	2,306	79.7	19,281	16,571	85.9	6,065	6,017	99.2
Diatoms		1,631	1,407	86.2	27,446	26,878	97.9	4,582	4,575	99.8
Cladocerans		1,135	330	29.0	7,418	6,923	93.3	2,181	2,174	99.7
Copepods		327	76	23.3	6,825	5,857	85.8	1,688	1,672	99.0
<i>Gross primary production</i>	mt DW d ⁻¹									
NDEA		1,743	251	14.4	5,388	4,907	91.1	1,438	1,419	98.7
NDIA		333	268	80.4	1,153	953	82.7	345	341	98.7
Diatoms		378	337	89.1	3,442	3,280	95.3	539	537	99.7
<i>Net primary production</i>	mt DW d ⁻¹									
NDEA		959	130	13.5	2,224	1,948	87.6	492	483	98.3
NDIA		124	99	79.8	181	166	91.8	85	84	99.3
Diatom		185	170	92.0	174	81	46.6	21	20	96.9
<i>Net secondary production</i>	mt DW d ⁻¹									
Cladocerans		119	37	30.6	449	402	89.4	77	76	99.5
Copepods		23	4	18.8	266	200	75.3	16	15	94.1

Table 3.3. Comparison of the 1997 basin-wide plankton biomass and productivity with or without the external phosphorus loading, averaged over the entire simulation period from May 10 to September 30.

1998		WB			CB			EB		
		With	Without	%	With	Without	%	With	Without	%
<i>Biomass</i>	mt DW									
NDEA		6,831	3,327	48.7	45,900	44,697	97.4	18,026	17,929	99.5
NDIA		14,432	4,663	32.3	31,017	25,901	83.5	9,911	9,860	99.5
Diatoms		4,934	6,104	123.7	33,351	33,337	100.0	5,634	5,617	99.7
Cladocerans		1,466	1,159	79.0	7,549	7,280	96.4	882	873	98.9
Copepods		1,104	361	32.7	10,830	10,093	93.2	2,427	2,405	99.1
<i>Gross primary production</i>	mt DW d ⁻¹									
NDEA		1,451	666	45.9	6,450	6,099	94.6	1,904	1,885	99.0
NDIA		1,089	410	37.7	1,320	1,106	83.8	423	420	99.3
Diatoms		974	1,062	109.0	3,622	3,502	96.7	482	478	99.3
<i>Net primary production</i>	mt DW d ⁻¹									
NDEA		1,049	470	44.8	3,797	3,517	92.6	865	852	98.5
NDIA		294	74	25.2	276	240	87.2	98	98	99.6
Diatom		698	721	103.3	1,690	1,573	93.1	156	154	98.5
<i>Net secondary production</i>	mt DW d ⁻¹									
Cladocerans		174	121	69.7	488	453	92.9	20	19	96.8
Copepods		150	46	30.3	716	625	87.3	100	98	98.0

Table 3.4. As Table 3.3, but for June 10 through October 30, 1998.

1999		WB			CB			EB		
		With	Without	%	With	Without	%	With	Without	%
<i>Biomass</i>	mt DW									
NDEA		3,989	1,273	31.9	50,652	49,252	97.2	28,331	28,281	99.8
NDIA		2,593	2,550	98.3	19,298	18,280	94.7	4,206	4,182	99.4
Diatoms		4,775	3,478	72.8	30,617	32,089	104.8	14,203	14,172	99.8
Cladocerans		818	492	60.2	6,783	6,642	97.9	1,558	1,556	99.8
Copepods		478	241	50.4	12,831	12,376	96.5	2,351	2,339	99.5
<i>Gross primary production</i>	mt DW d ⁻¹									
NDEA		921	293	31.8	7,061	6,724	95.2	1,619	1,610	99.4
NDIA		253	251	99.0	1,336	1,243	93.0	274	272	99.5
Diatoms		869	656	75.5	2,827	2,949	104.3	798	794	99.6
<i>Net primary production</i>	mt DW d ⁻¹									
NDEA		688	219	31.8	4,216	3,961	94.0	324	318	98.0
NDIA		49	50	101.5	312	296	94.8	87	86	99.4
Diatom		600	458	76.3	1,055	1,095	103.8	43	41	96.1
<i>Secondary production</i>	mt DW d ⁻¹									
Cladocerans		85	55	64.8	446	433	97.3	58	58	99.8
Copepods		38	19	49.4	866	812	93.8	68	67	98.4

Table 3.5. As Table 3.3, but for May 20 through September 29, 1999.

Table 3.6. Basin-wide P cycling of 1997, shown as concentrations in major pools, rates of transfer between pools, and the fraction (%) of those located in the top 12 m of the water column. DP: SRP and P in dissolved organic matter; PP: P in phytoplankton and detritus; CP: P in crustaceans; PP→DP: phosphorus excretion by phytoplankton and release due to decomposition of detritus; CP→DP: phosphorus excretion by crustaceans; MP→DP: phosphorus excretion by dreissenids; SED→DP: phosphorus release by sediments under anoxic conditions; PP→SED: phosphorus loss to sediment due to sedimentation of PP; External loading: DP loading from tributaries of Lake Erie; Withdrawals: total phosphorus (DP+PP) loss through the Welland Canal and the Niagara River; Exchange between basins: net total phosphorus transported by horizontal currents between basins. All values are an average over the simulation period from May 10 to September 30, 1997.

1997		WB		CB			EB	
		Basin	Basin	12m	%	Basin	12m	%
<i>P pools</i>	mt P							
DP		199.3	1,707.9	675.6	39.6	956.4	197.7	20.7
PP		176.1	1,533.5	1,139.0	74.3	433.3	244.0	56.3
CP		14.6	142.4	114.0	80.0	38.7	23.8	61.4
<i>P pathways</i>	mt P d ⁻¹							
PP→DP		7.4	52.1	42.6	81.9	12.4	9.1	73.8
CP→DP		3.8	22.1	18.4	83.2	5.0	3.4	68.0
MP→DP		6.6	13.4	1.4	10.7	6.4	1.3	20.0
SED→DP		0.6	5.3	-	-	0.0	-	-
DP→PP		24.6	100.0	93.2	93.2	23.2	20.2	86.8
PP→SED		5.2	13.5	-	-	3.7	-	-
<i>External loading</i>	mt P d ⁻¹	15.6	3.1	-	-	0.2	-	-
<i>Withdrawals</i>	mt P d ⁻¹					-3.4		
<i>Exchange between basins</i>	mt P d ⁻¹	-5.9	0.3			5.6		

1998		WB		CB		EB		
		Basin	Basin	12m	%	Basin	12m	%
<i>P pools</i>	mt P							
DP		200.6	1,885.4	526.3	27.9	1,111.0	134.4	12.1
PP		391.5	1,492.9	1,104.7	74.0	481.4	271.2	56.3
CP		21.0	133.5	106.7	80.0	19.7	15.4	78.3
<i>P pathways</i>	mt P d ⁻¹							
PP→DP		14.5	51.2	42.9	83.8	15.4	11.3	73.5
CP→DP		4.7	19.8	16.2	82.1	2.0	1.5	76.0
MP→DP		6.3	13.0	1.4	11.0	6.4	1.3	20.0
SED→DP		1.2	6.5	-	-	0.0	-	-
DP→PP		33.8	103.3	97.5	94.3	26.1	22.9	87.8
PP→SED		11.7	10.6	-	-	3.3	-	-
<i>External loading</i>	mt P d ⁻¹	10.2	2.1			0.1		
<i>Withdrawals</i>	mt P d ⁻¹					-2.8		
<i>Exchange between basins</i>	mt P d ⁻¹	-7.4	2.2			5.2		

Table 3.7. As Table 3.6, but for June 10 through October 30, 1998.

1999		WB		CB		EB		
		Basin	Basin	12m	%	Basin	12m	%
<i>P pools</i>	mt P							
DP		83.4	1,473.6	499.9	33.9	1,119.1	112.4	10.0
PP		150.4	1,696.6	1,257.5	74.1	689.4	355.7	51.6
CP		13.0	196.2	159.0	81.0	39.1	23.5	60.1
<i>P pathways</i>	mt P d ⁻¹							
PP→DP		6.6	64.0	50.9	79.5	22.3	14.7	66.2
CP→DP		2.7	22.1	18.4	83.0	3.8	2.2	57.1
MP→DP		6.6	13.4	1.4	10.7	6.4	1.3	20.0
SED→DP		0.1	2.2	-	-	0.0	-	-
DP→PP		20.5	112.4	103.4	92.0	26.9	23.5	87.3
PP→SED		3.7	12.3	1.8	14.7	4.3	0.8	18.7
<i>External loading</i>	mt P d ⁻¹	6.9	1.0	-	-	0.1	-	-
<i>Withdrawals</i>	mt P d ⁻¹					-2.8		
<i>Exchange between basins</i>	mt P d ⁻¹	-4.7	1.9			2.9		

Table 3.8. As Table 3.6, but for May 20 through September 29, 1999.

	WB	CB	EB
1997			
NDEA	- (+)	+	+
Diatoms	+	+	+
Cladocceans	- (+)	+	+
Copepods	-	-	+
TP-F	-	+ (-)	+
NH4	-	+	+
1998			
NDEA	- (+)	+ (-)	+
Diatoms	-	+	+
Cladocceans	- (+)	+	-
Copepods	+	+ (-)	-
TP-F	- (+)	+	+
NH4	+ (-)	+ (-)	+
1999			
NDEA	-	+	+
Diatoms	+	+	+
Cladocceans	+	-	+
Copepods	+	+	+
TP-F	-	+ (-)	+
NH4	+	+	+

Table 3.9. Results of paired t-test ($p < 0.05$) of the mean difference between modeled and observed values of six state variables for three years with modified external phosphorus loading. “-” indicates significant difference. “+” indicates no significant difference. Different results between with and without modification of external phosphorus loading are indicated by the parentheses, which hold the t-test results of Table 2.6.

	WB			CB			EB		
	without	with	%	Without	With	%	Without	With	%
NDEA	6726.5	8386.6	124.7	27524.3	41869.4	152.1	8241.8	14114.6	171.3
Diatom	1631.2	1998.8	122.5	27446.3	28182.9	102.7	4582.3	4779.9	104.3
NDIA	2892.3	3153.3	109.0	19280.7	36229.2	187.9	6065.4	10044.2	165.6

Table 3.10. The effects of phosphorus loading from unmonitored non-point sources on basin-wide phytoplankton biomass, under the conditions of 1997.

	WB				CB				EB			
	Burns	1997	1998	1999	Burns	1997	1998	1999	Burns	1997	1998	1999
Net sedimentation rate (mmol P m ⁻³ d ⁻¹)	0.437	0.043	0.104	0.032	0.045	0.014	0.007	0.021	0.028	0.018	0.017	0.022
Mean total phosphorus concn (mmol P m ⁻³)	1.43	0.52	0.82	0.28	0.66	0.35	0.36	0.40	0.57	0.29	0.32	0.36
Mean particulate phosphorus concn (mmol P m ⁻³)	0.94	0.25	0.55	0.19	0.4	0.17	0.17	0.22	0.31	0.10	0.10	0.14
Mean basin depth (m)	7.6	8.2	8.1	7.7	17.8	19.3	19.2	18.9	27.0	28.1	28.0	27.6
Mean elimination coefficient* (% d ⁻¹)	4.02	1.18	1.72	1.52	0.38	0.24	0.12	0.30	0.18	0.26	0.20	0.23
Mean net settling velocity of particulate phosphorus** (m d ⁻¹)	0.46	0.17	0.19	0.17	0.11	0.08	0.04	0.10	0.09	0.19	0.16	0.16

Table 3.11. Comparisons of the net sedimentation rates of phosphorus in the three Lake Erie basins from Burn's (1976) study (their table 8) and ours.

*Mean elimination coefficient = (P sedimentation flux)/(depth)/(mean P concentration).

** Mean net settling velocity = (P sedimentation flux)/(mean particulate P concentration) (after Burn 1976).

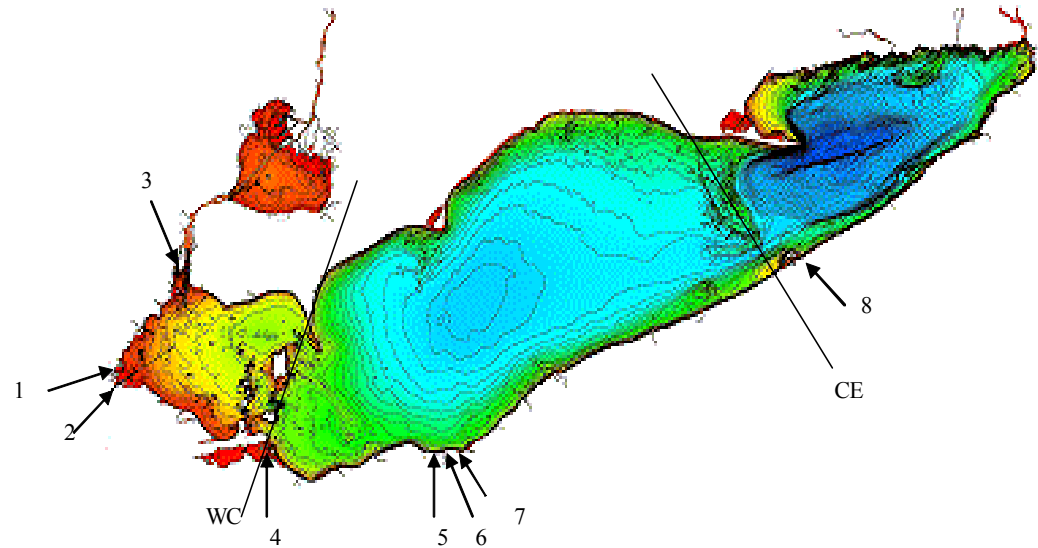


Figure 3.1. Locations of tributaries around Lake Erie. 1. the Maumee River (segment 2); 2.the Toledo WWTP (segment 2); 3. the Detroit River (segments 12-14); 4. the Sandusky River (segment 50); 5. the Cleveland westerly WWTP (segment 82); 6. the Cuyahoga River (segment 83); 7. the Cleveland easterly WWTP (segment 89); 8. the Erie WWTP (segment 158). The line WC is the border between the western basin and the central basin, and the line CE is the border between the central basin and the eastern basin.

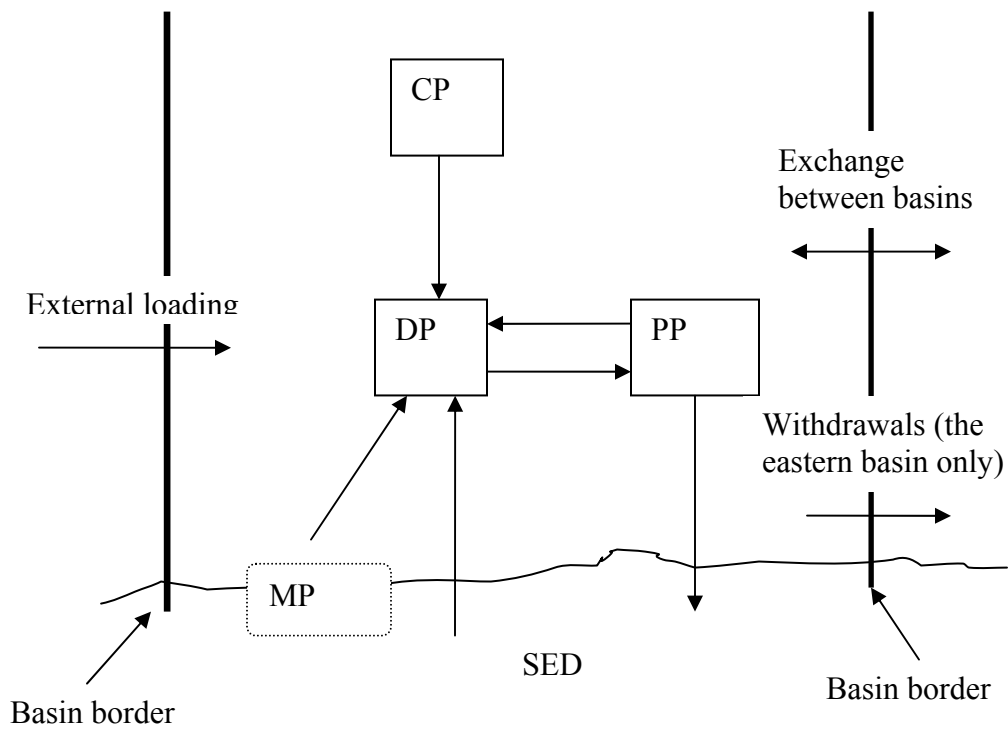
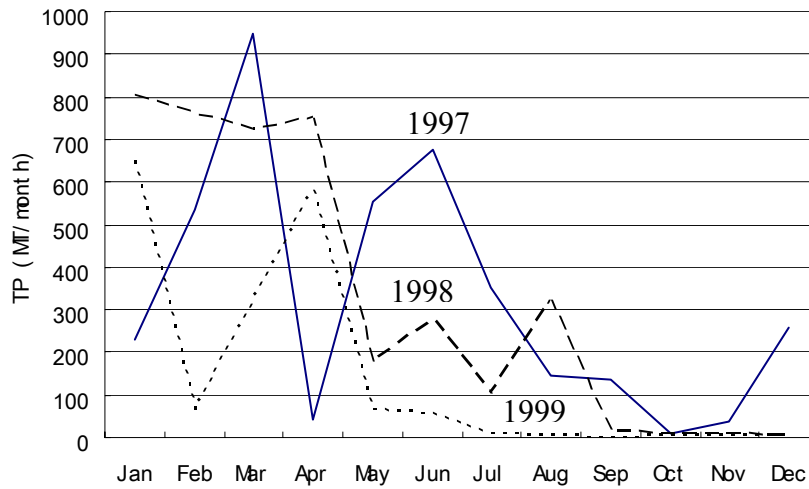


Figure 3.2. P pools and cycling pathways that considered in EcoLE. DP: SRP and P in dissolved organic matter; PP: P in phytoplankton and detritus; CP: crustacean phosphorus content; PP→DP: phosphorus excretion by phytoplankton and release due to decomposition of detritus; CP→DP: phosphorus excretion by crustaceans; MP→DP: phosphorus excretion by dreissenids; SED→DP: phosphorus release by sediments under anoxic conditions; PP→SED: phosphorus loss to sediment due to sedimentation of PP; External loading: TP loading from tributaries of Lake Erie; Withdrawals: total phosphorus (DP+PP) loss through the Welland Cannel and the Niagara River; Exchange between basins: net total phosphorus transported by horizontal currents between basins.

a)



b)

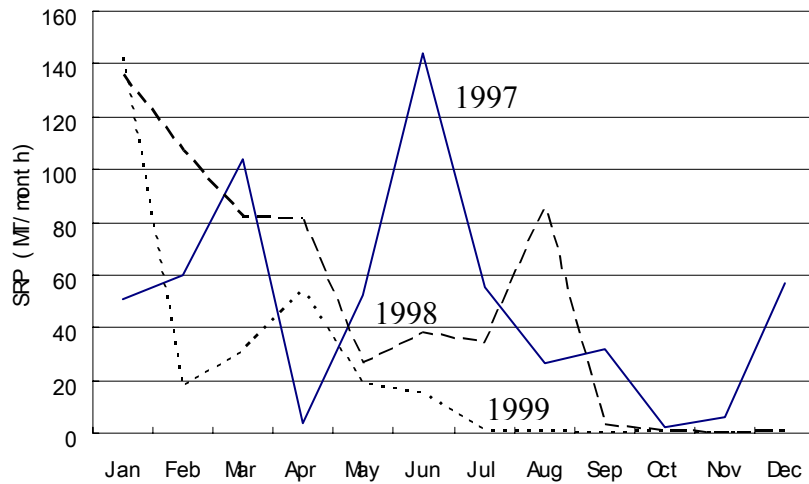


Figure 3.3. Monthly phosphorus inputs into Lake Erie from the Maumee River. a) total phosphorus and b) soluble reactive phosphorus. Solid lines for 1997, dash lines for 1998 and dot lines for 1999. There are four loading peaks: March and June of 1997 and the spring and autumn of 1998. Data are from Richards, R.P., Water Quality Laboratory, Heidelberg College, Ohio.

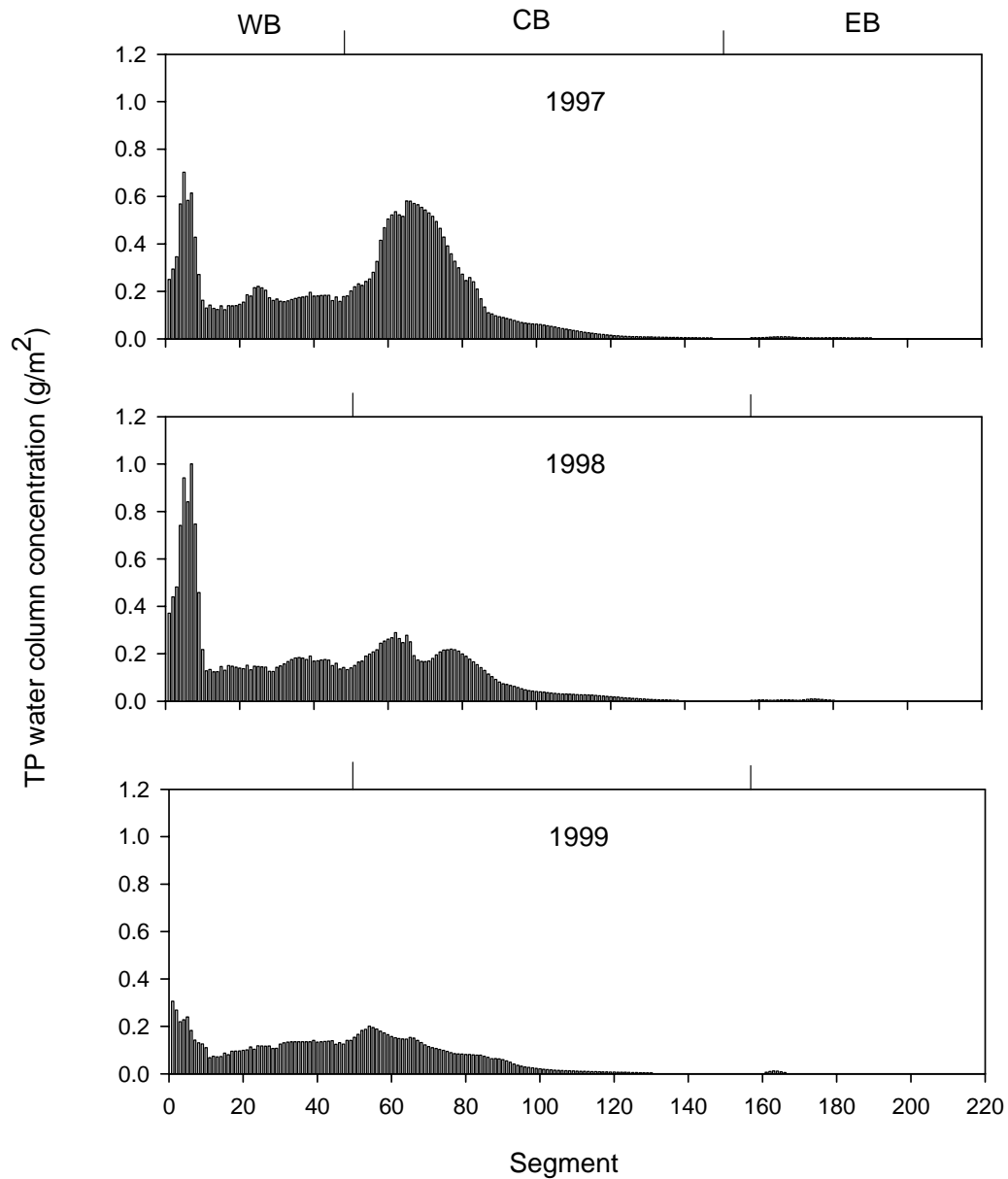


Figure 3.4. The horizontal distribution of the total external P loading in Lake Erie at the end of simulations (September 30, 1997; October 30, 1998; and September 29, 1999). These distributions reflect physical mixing processes, while the chemical and biological processes were inactivated. The phosphorus peaks at the west central basin (segment 50 - 80) were more likely an accumulation of loading in the western basin, rather than the direct external loading into the central basin. The peak was centered at segment 70 in the highest external loading year (1997), at segment 55 in the lowest external loading year (1999). In 1998, the peak was a median one in terms of magnitude and location.

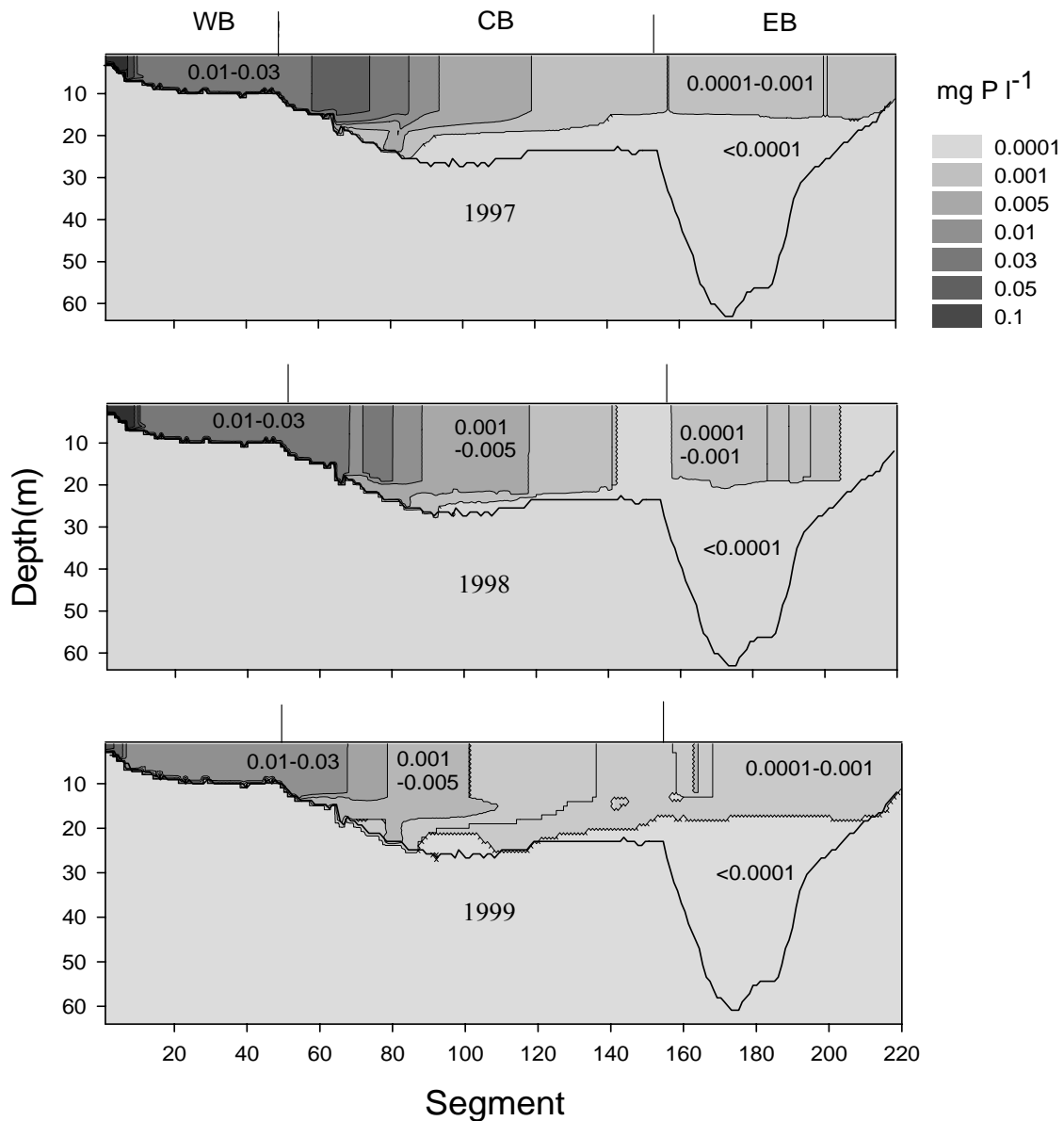


Figure 3.5. The spatial distribution of the external TP loading in Lake Erie at the end of simulation periods (September 30, 1997; October 30, 1998; and September 29, 1999). The distributions were the results of physical mixing processes, while the chemical and biological processes were inactivated.

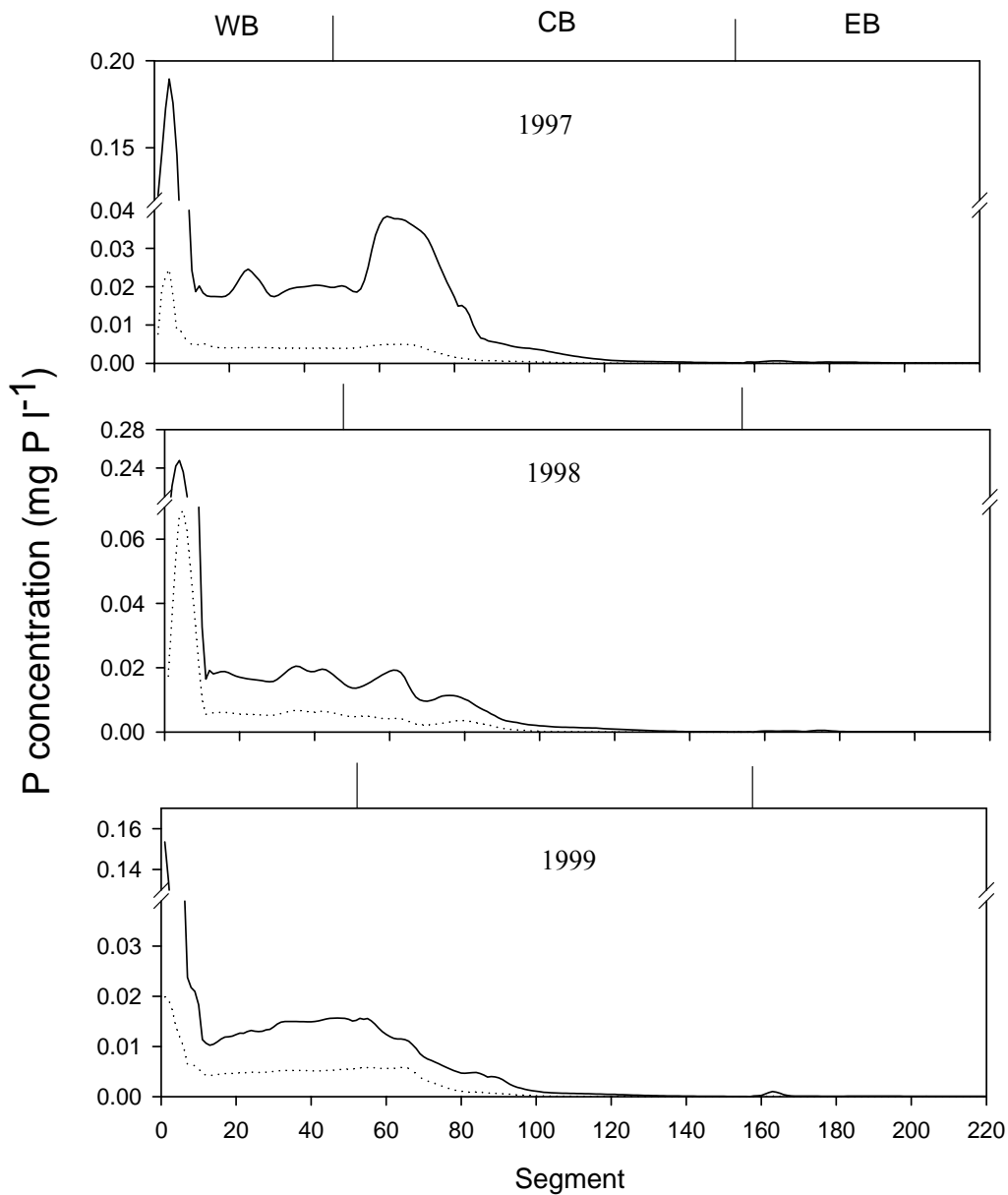


Figure 3.6. The concentrations of TP (solid lines) and SRP (dot lines) loaded in Lake Erie accumulated over simulation periods (May 10-September 30, 1997; June 10 – October 30, 1998; May 20 – September 29, 1999). These concentrations are averages over the upper water above 12m of each segment. There was a much higher cumulative peak of TP and SRP input in the west western basin in 1998 than in 1997 and 1999.

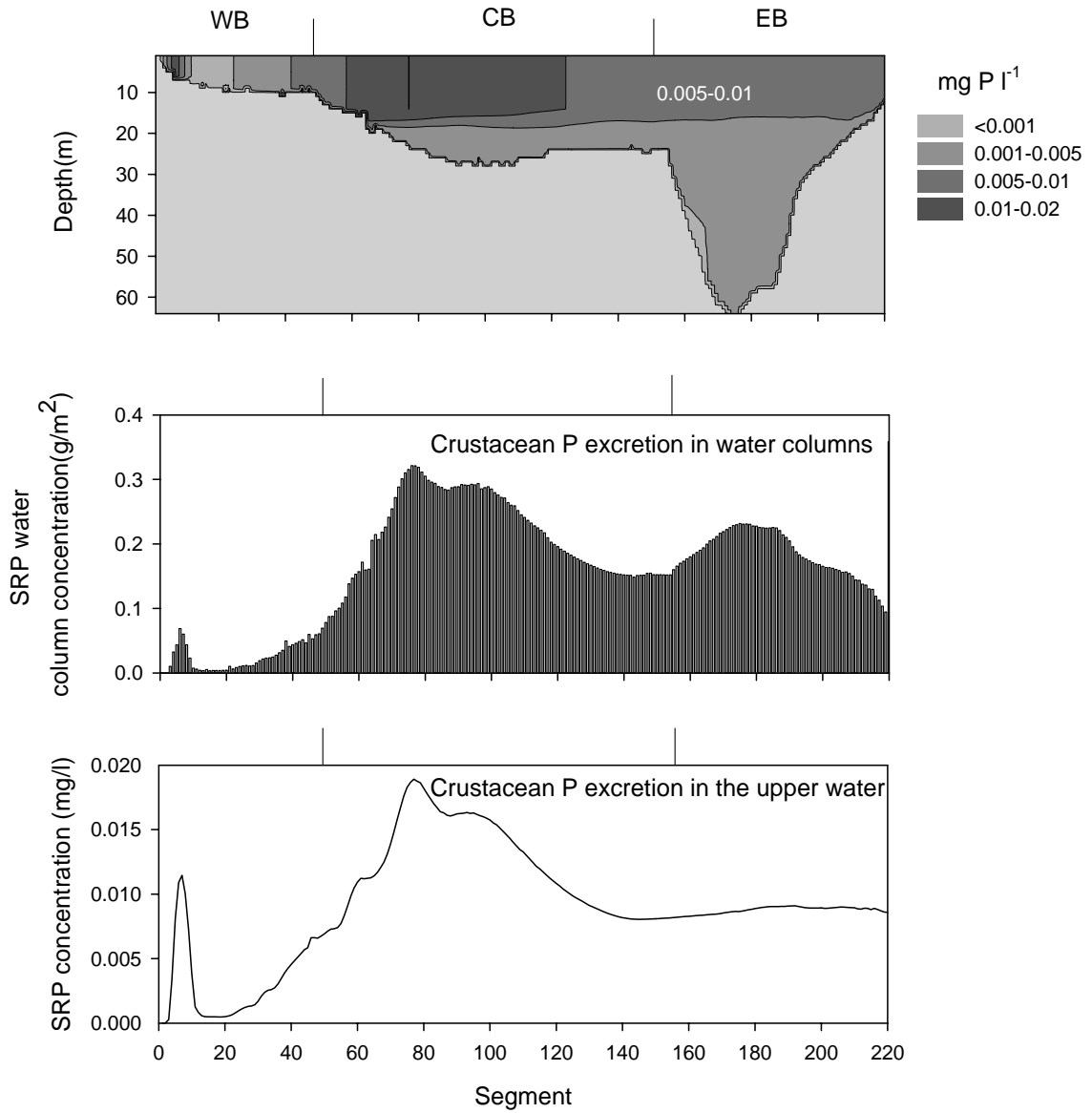


Figure 3.7. SRP excreted by crustaceans over the simulation period of 1997: the spatial distributions of SRP (upper panels), the water column concentrations of SRP of each segment (middle panels) and the average SRP concentrations of the non-bottom top 12 m water of each segment (lower panels).

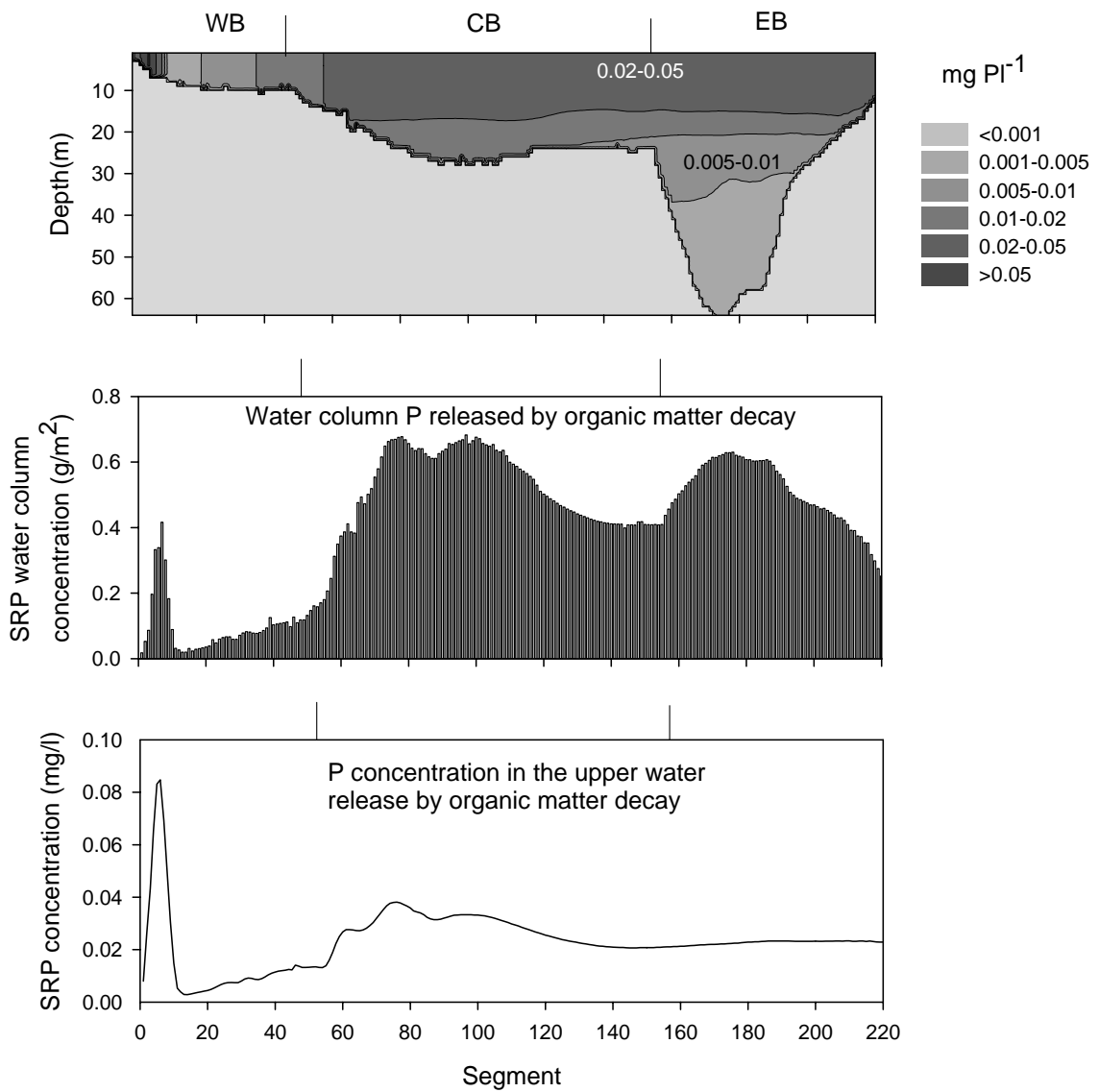


Figure 3.8. SRP released by organic matter decay over the simulation period of 1997: the spatial distributions of SRP (upper panels), the water column concentrations of SRP of each segment (middle panels) and the average SRP concentrations of the non-bottom top 12 m water of each segment (lower panels).

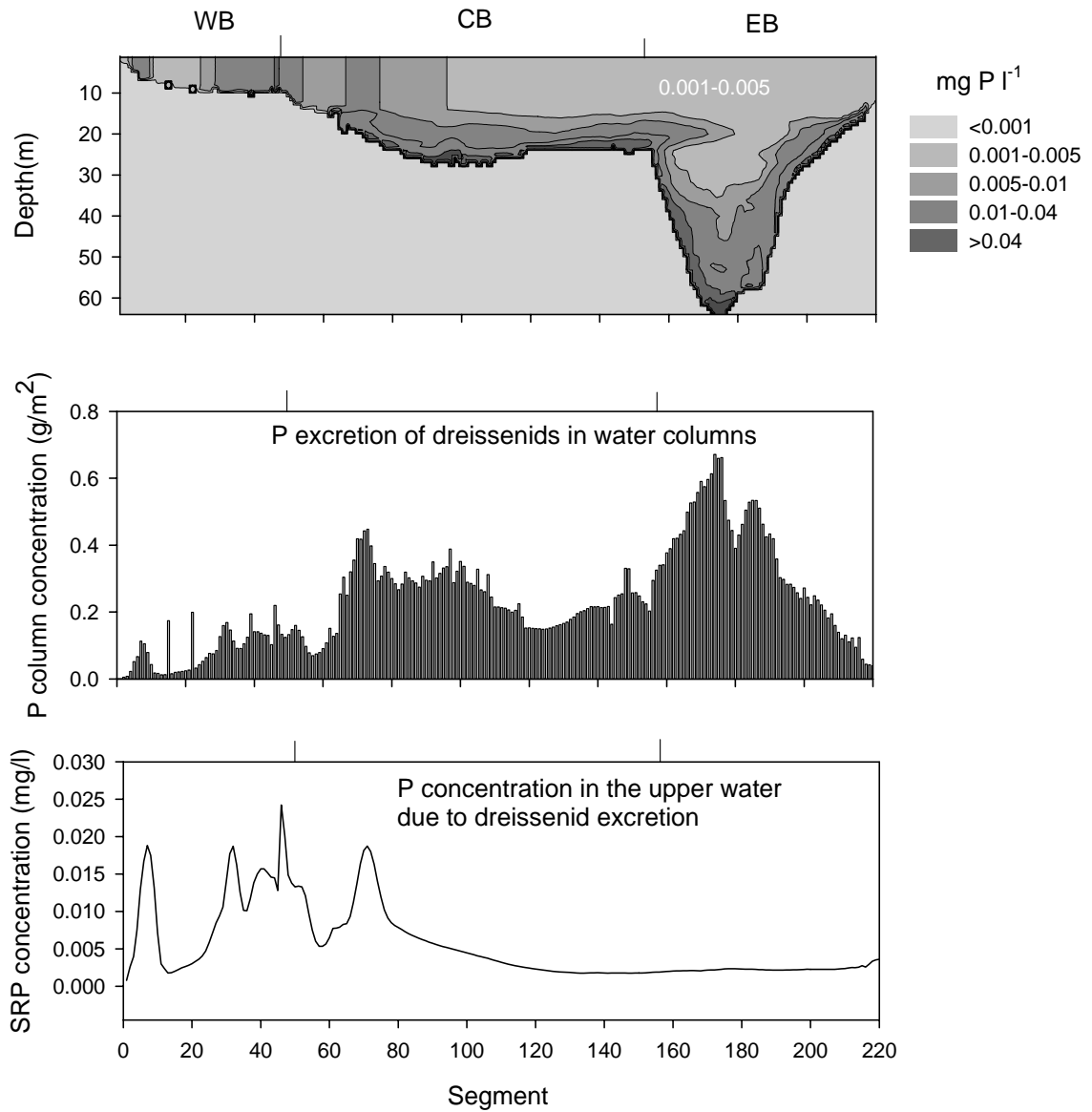


Figure 3.9. SRP excreted by dreissenid mussels over the simulation period of 1997: the spatial distributions of SRP (upper panels), the water column concentrations of SRP of each segment (middle panels) and the average SRP concentrations of the non-bottom top 12 m water of each segment (lower panels).

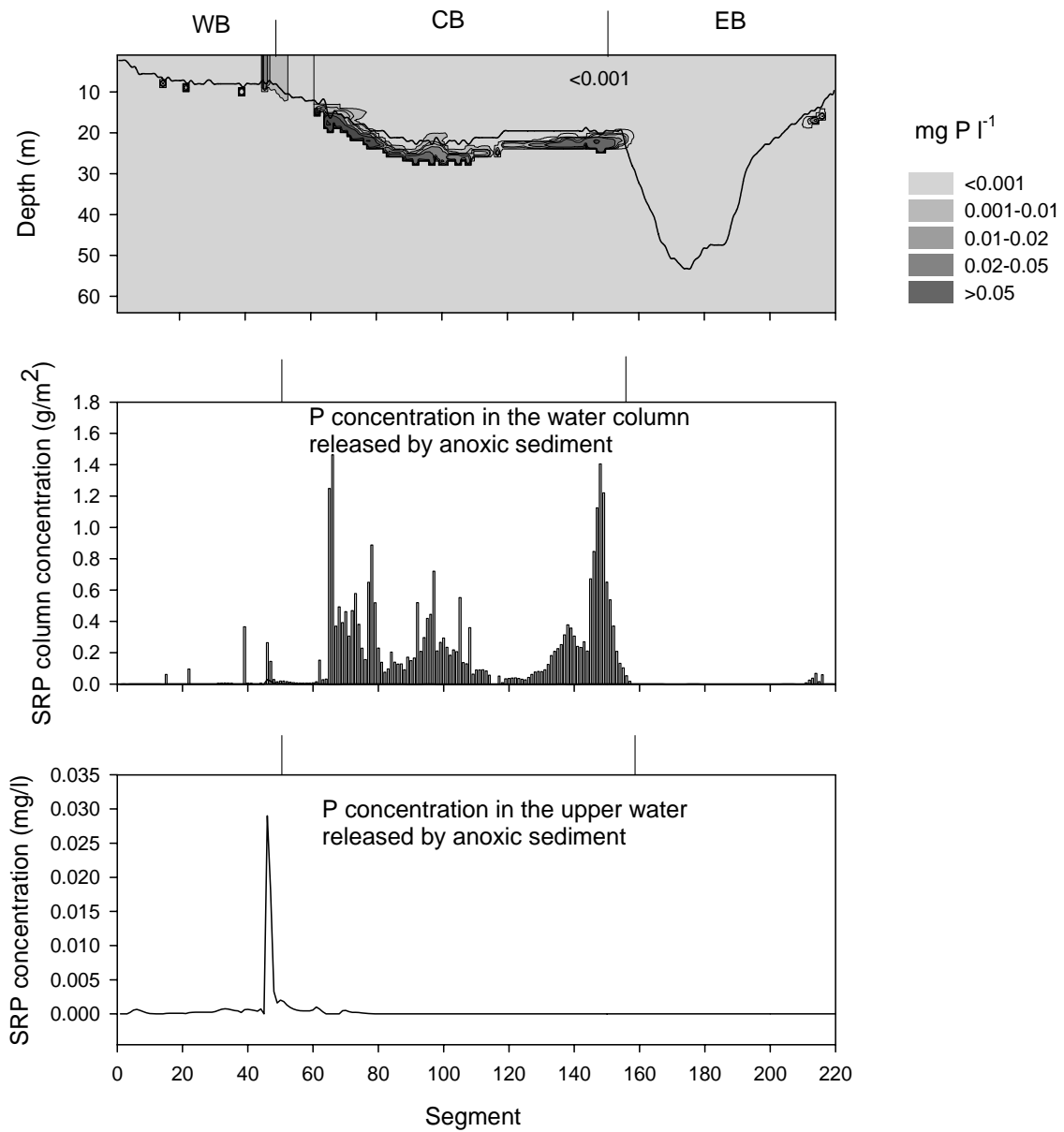


Figure 3.10. SRP released by anoxic sediment over the simulation period of 1997: the spatial distributions of SRP (upper panels), the water column concentrations of SRP of each segment (middle panels) and the average SRP concentrations of the non-bottom top 12 m water of each segment (lower panels).

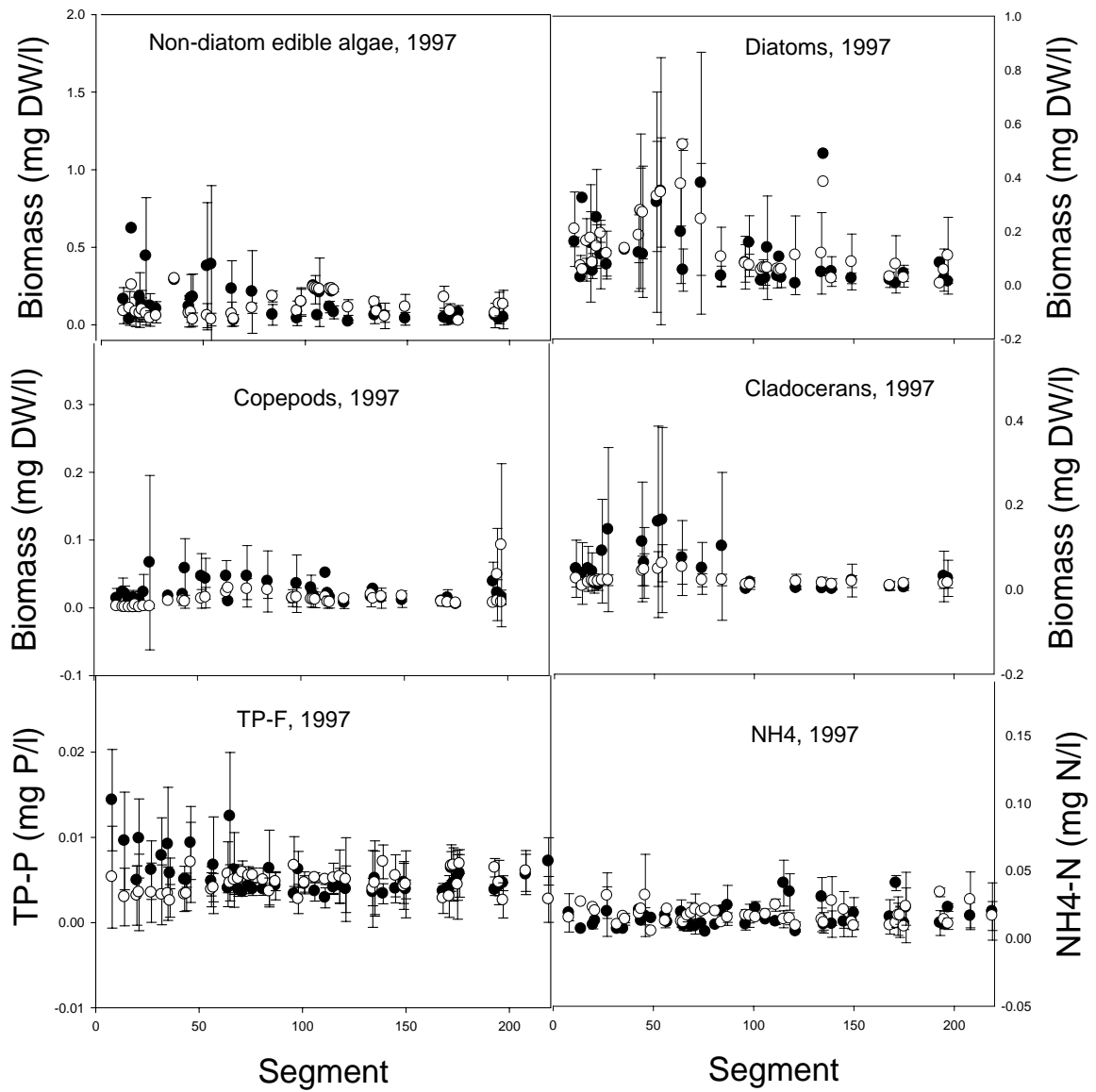


Figure 3.11. 1997's comparisons between the simulations and field observations of state variables with bioavailable phosphorus from external sources being adjusted according to De Pinto *et al.* (1981) and Young *et al.* (1982).

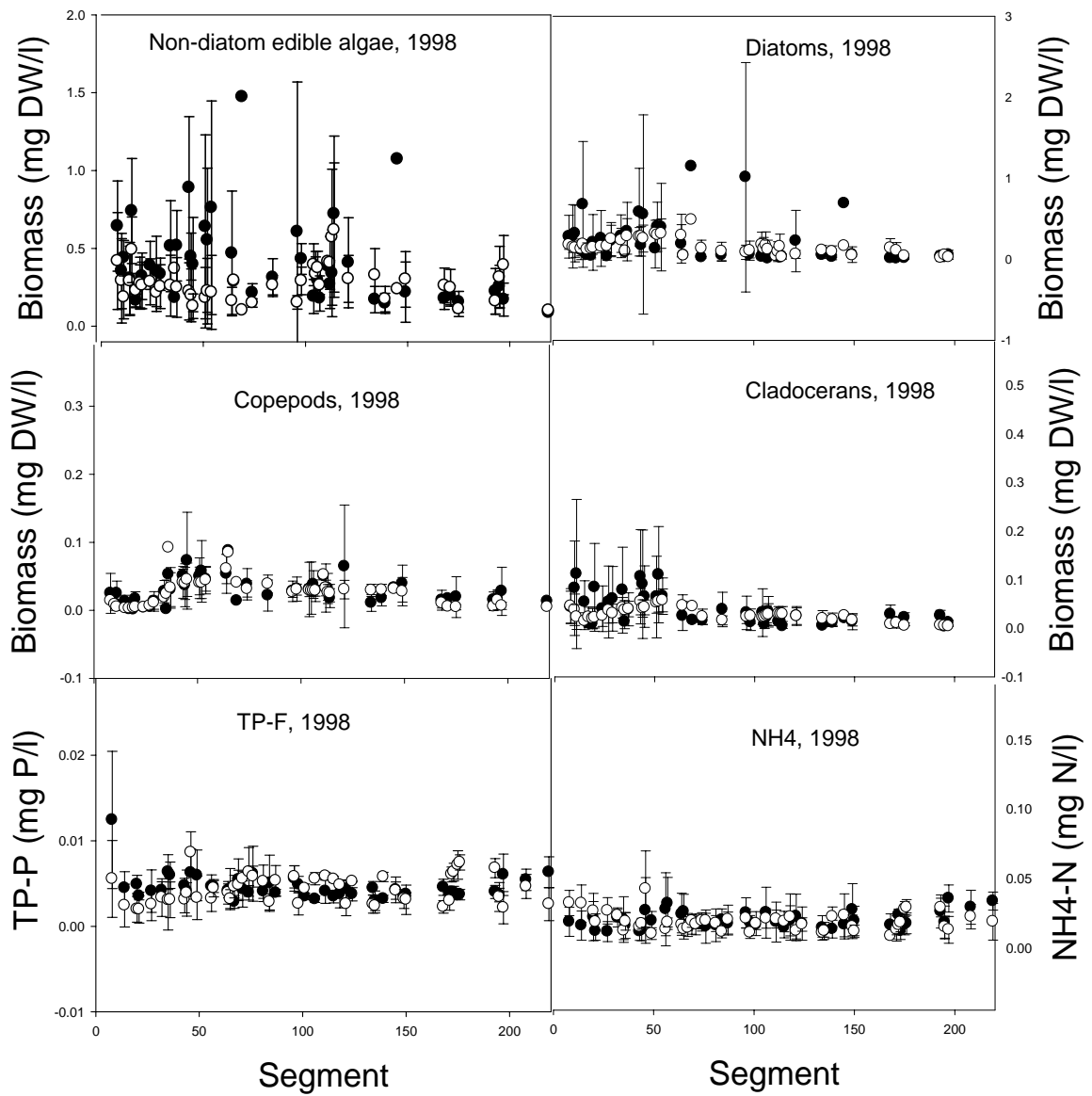


Figure 3.12. 1998's comparisons between the simulations and field observations of state variables with bioavailable phosphorus from external sources being adjusted according to De Pinto *et al.* (1981) and Young *et al.* (1982).

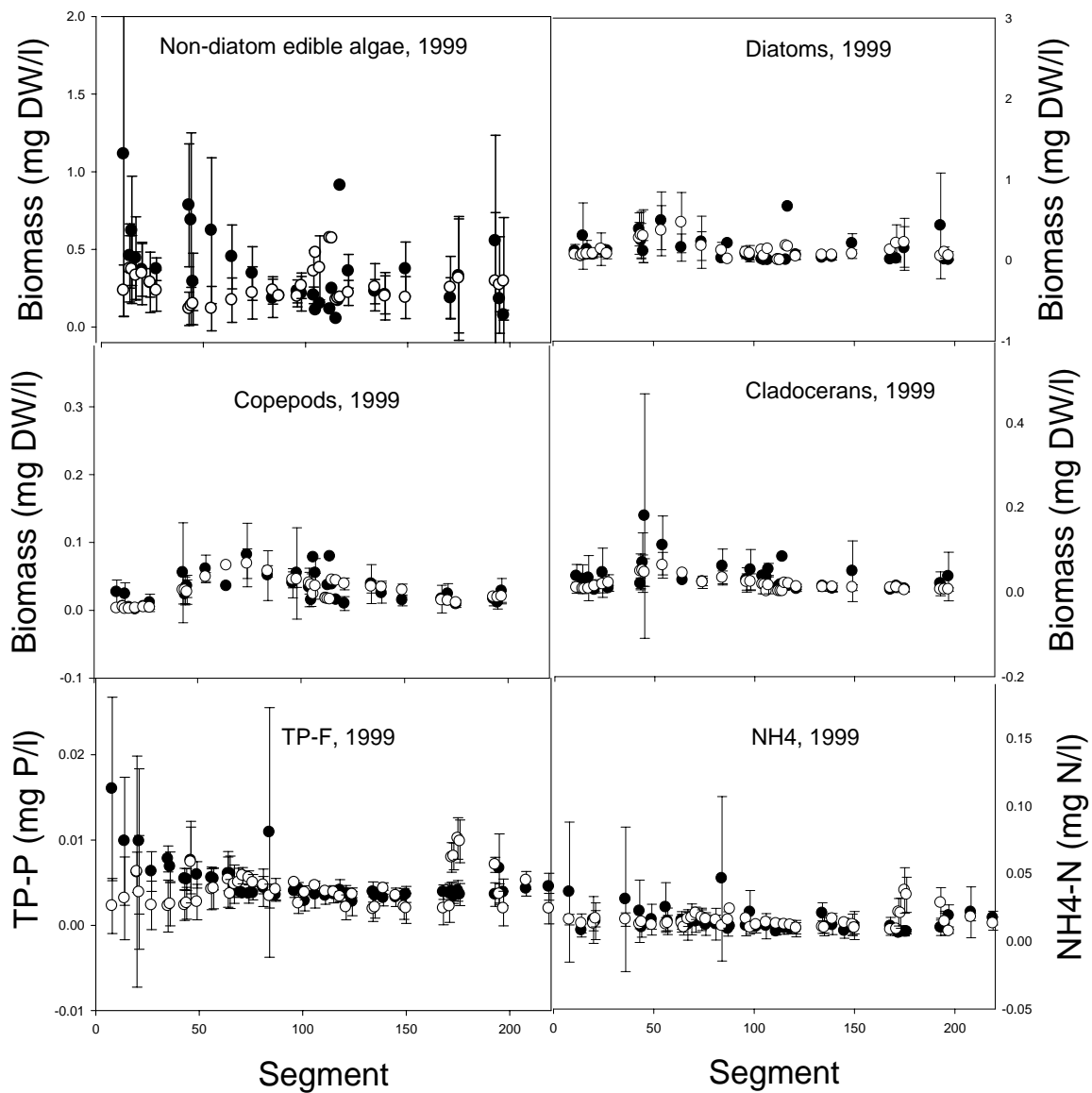


Figure 3.13. 1999's comparisons between the simulations and field observations of state variables with bioavailable phosphorus from external sources being adjusted according to De Pinto *et al.* (1981) and Young *et al.* (1982).

CHAPTER 4

APPLICATION OF A TWO-DIMENSIONAL ECOLOGICAL MODEL TO EVALUATE THE IMPACTS OF EXOTIC MUSSELS ON THE LAKE ERIE ECOSYSTEM

ABSTRACT

A two-dimensional ecological model, EcoLE, is used to investigate the impacts of *Dreissena* spp., zebra mussels (*D. polymorpha*) and quagga mussels (*D. bugensis*), on water quality of Lake Erie for the years 1997, 1998 and 1999. Compared with that of zooplankton, dreissenids' grazing impact on non-diatom edible algae (NDEA) varies among years in the western basin. For the dry year, 1999, the model results show that their impact on NDEA exceeds those of crustacean zooplankton, while it is less than those of crustaceans for the other two years. Dreissenids have equal grazing impacts on diatoms as crustacean zooplankton in the western basin, but mussel daily grazing impact in the western basin was less than 10% of NDEA and diatom biomass. Dreissenids graze only 1-2% of the NDEA and diatoms in the central and eastern basins. When we simulate an increase in mussel population density or body size, their grazing impacts on NDEA decrease in the western basin, while grazing on diatoms continues to increase. Dreissenid mussels cause increases in non-diatom inedible algae (NDIA) rapidly with increasing population size. Dreissenid mussels affect crustacean zooplankton mainly

through their impacts on NDEA. The dreissenid population can excrete a large amount of ammonia and phosphate. These amounts increased rapidly with increasing mussel population size, whereas nitrification of ammonia might speed oxygen depletion in the hypolimnion of the central basin. Our results indicate that dreissenid mussels have weak direct grazing impacts on algal biomass, while their nutrient excretion causes a lot more impacts on the system.

INTRODUCTION

Lake Erie is a very dynamic system in terms of changes in water quality, fish populations and invasions of exotic species. With the growth of the human population along its shoreline, especially along its southern shoreline, Lake Erie underwent eutrophication into the 1970s, when the system was thoroughly studied and diagnosed to be overloaded with phosphorus. With the reduction of point-source phosphorus, Lake Erie became clearer. However, the invasion of *Dreissena* spp. into Lake Erie from Europe complicates evaluation of the effectiveness of efforts to reduce external P loading.

Zebra mussels (*Dreissena polymorpha*) invaded Lake Erie in the late 1980s, followed by another exotic species, quagga mussels (*D. bugensis*), which invaded in the early 1990s and are replacing zebra mussels and have become dominant in the central and eastern basins (May and Marsden 1992, Mills *et al.* 1999, Jarvis *et al.* 2002). Zebra mussels are well known successful invaders. Within several years after they were first seen in Lake St. Clair in 1988, zebra mussels were found in all of the Great Lakes and the waterways that connect with the Great Lakes. They originated in the Ponto-Caspian Sea

and dispersed through ships' ballast water. They can tolerate low dissolved oxygen and extensive periods of desiccation. They have high fecundity, with a million oocytes produced each year by 24-mm females (Neumann *et al.* 1993) and they spawn at temperatures as low as 12 °C (Sprung 1989). Their larvae are briefly planktonic and settlers reach sexual maturity within 1 year (Garton and Haag 1993). These traits help zebra mussels rapidly colonize an empty niche and develop dense populations. Quagga mussels have attracted increasing attention because they are competitively replacing zebra mussels in many waters. Compared with zebra mussels, quagga mussels have a lower respiration rate and devote a greater proportion of their energy input to body mass growth and less to reproduction (Stoeckmann 2003). Quagga mussels also have a lower egg maturation temperature, 4.8 °C (Roe and MacIsaac 1997), and a higher tolerance of starvation (Baldwin *et al.* 2002). All these traits make quagga mussels competitive even in an established mussel bed.

Although zebra mussels and quagga mussels are different species, they have similar ecological impacts on Lake Erie. Although intensive studies have been carried out to investigate the structures and functions of ecosystems invaded by dreissenids, dreissenids' impacts on the water column are still unclear because they are bottom dwellers. Early studies based on laboratory experiments tended to overestimate mussels' impacts. For example, MacIsaac *et al.* (1992) linearly extrapolated from laboratory measurements and reported that the zebra mussel population in the western basin of Lake Erie could theoretically filter a 7 m water column between 3.5 and 18.8 times per day. Recent field experiments by Ackerman *et al.* (2001) and Edwards *et al.* (2005) took hydrodynamics into account and showed that zebra mussels created a 1-m thick

concentration boundary layer, which had a low phytoplankton biomass compared with the upper waters. Because hydrodynamics and boundary layers are so important to the delivery of algae to dreissenids, mathematical simulation models of the ecological functions of dreissenids must explicitly include chemical, biological, and hydrologic components.

Di Toro *et al.*'s (1973) eutrophication model is one of the best-documented, comprehensive ecological models among the successful ecological models that have been constructed for Lake Erie. Their phytoplankton-zooplankton-nutrient model of western Lake Erie had seven vertically integrated segments and a steady-state circulation pattern. Most of their calculated water quality variables (chlorophyll *a*, inorganic phosphorus, NH₃-N and NO₃-N) showed reasonable agreement with the observed data in the magnitude and temporal variation of the state variables. Based on this eutrophication model, Di Toro and Connolly (1980) developed a more sophisticated ecological model, which divided Lake Erie into 10 segments and had 15 state variables plus sediment oxygen demand (SOD) and sediment nutrient flux modules. It produced a good simulation of the seasonal and spatial dynamics of chlorophyll *a*, carbon, total phosphorus, orthophosphorus, nitrogen and reactive silica. Lam *et al.* (1983) constructed a series of ecological models of increasing morphometric detail (three-box, six-box and nine-box models) of Lake Erie to investigate the causes of anoxia in the central basin hypolimnion. The outstanding feature of Lam *et al.*'s models is their use of a one-dimensional model to adjust the position and thickness of the metalimnion each day. The three-box model divided the lake into three segments based on the western, central, and eastern basins. The six-box model divided each segment in the three-box model into two

vertical layers, namely the epilimnion and the hypolimnion. The nine-box model added a metalimnion layer, with its position and thickness determined daily. The food web was not a focus in this series of models, but was used only to model dissolved oxygen, total phosphorus and soluble reactive phosphorus. Lam *et al.* found that meteorological conditions played an important role in the formation of anoxia in the central basin hypolimnion, so over twelve-years of data, they could not get a significant correlation between the occurrence of hypolimnetic anoxia and phosphorus loading.

However, these models were developed and applied before dreissenids invaded into Lake Erie, so they included neither dreissenid nor a hydrologic component. Accordingly, our study uses an ecological model, EcoLE (chapter 2), and data collected in 1997, 1998 and 1999 to assess the impacts of dreissenids on the Lake Erie ecosystem. Besides a dreissenid component, the model simulates a dynamic physical environment driven by daily meteorological data. This model also has much higher spatial and temporal resolutions than did Lam *et al.*'s (1983) model and the impacts of dreissenid mussels on phytoplankton, nutrient and macrozooplankton are explicitly simulated. We hypothesize that dreissenids can depress the phytoplankton community in Lake Erie and mask the influence of zooplankton grazing. Therefore, the impacts of dreissenid grazing are more important than the impacts of dreissenid nutrient remineralization and there is a severe food competition between dreissenids and zooplankton. We also hypothesize dreissenids affect the formation of “dead zone” in the hypolimnion of the central basin of Lake Erie.

Methods

A two-dimensional ecological model of Lake Erie, EcoLE, is used (for details see Chapter 2) to simulate the impacts of *Dreissena* spp. on the Lake Erie ecosystem. This model divides Lake Erie into 222 horizontal segments from west to east and up to 65 vertical layers from the surface to the bottom. Using daily meteorological input data, it calculates physical conditions (water level, current velocities and temperature) every 10 minutes. The biological state variables are diatoms, non-diatom edible algae (NDEA), non-diatom inedible algae (NDIA), cladocerans and copepods, while chemical state variables are ammonium, nitrate+nitrite, soluble reactive phosphorus, labile organic matter, particulate organic matter, silicon, silicon particulate organic matter, and oxygen. However, *Dreissena* biomass is not a state variable in the model. Although intensive studies have been carried out since zebra mussels were first found in the Great Lakes, there is not yet enough knowledge to simulate dreissenids as a state variable (as growth, reproduction, mortality, etc.), in part because dreissenids have a complicated life history. For example, the dispersal and settlement of their planktonic veligers are especially hard to simulate, so predicting the population dynamics of dreissenids is not a goal of this study. Instead, dreissenids are treated as external forces of the model, and mussel abundances and size distribution are assumed to remain constant over time. That is, their grazing impacts and nutrient remineralization impacts were calculated with a pre-determined population density. Since zebra mussels and quagga mussels have different physiology, they were modeled as two separate groups.

For simplicity, we assume that for 1997, 1998, and 1999, all western basin dreissenids are zebra mussels, while all are quagga mussels in the central and eastern

basins. In the shallow and flat western basin, each modeling water column (segment) is adjusted to a cube by setting the surface area of the segment constant and adjusting the depth (1-m resolution) until the volume of the cube is closest to the real volume of the segment measured from the bathymetry (Figure 2.5). Mussels are located only in the bottom cell, which has a sedimental area that equals the surface area of the segment, while other cells have no sedimental area. In the deep central and eastern basins, mussels are located in each cell, which has a sedimental area equal to the sum of both south and north sediment areas of the cell. Zebra mussels prefer hard surfaces, while quagga mussels can attach to soft surfaces as well as hard surfaces. Their distribution is also affected by oxygen conditions, food conditions, and their predators, etc. As their distributions vary greatly in time and space, there has never been a good estimation of the two populations. Nevertheless, the depth-dependent estimations by Jarvis *et al.* (2000) are used in this model (Table 3.2). Thus, dreissenid population size in each model cell is the product of depth-dependent density (ind. m⁻²) and the sedimental area (m²) of each model cells. For simplicity, it is assumed that mussels are uniform in size (10 mm), but mussel densities and lengths were then varied during the uncertainty analysis part of the study to assess the effect of inaccurate estimations of mussel population density and size distribution on our simulation of dreissenid impacts on the plankton and nutrients.

Study site

Lake Erie is the smallest Laurentian Great Lake and is centered at 42°15' north latitude and 81° 15' west longitudes, with its long axis orientated at about N 70° E. The lake is approximately 386 kilometers (240 miles) long and more than 80 kilometers (50

miles) wide near the midpoint of its long axis, so wind stress has an ample opportunity to affect the distribution of heat, solutes, and suspended matter in the lake. Lake Erie has three distinct geographic basins, the western, central and eastern basins. The western basin is shallowest, with an average depth of 8 m; the central basin is relatively flat with an average depth of 18 m; and the eastern basin is the deepest with an average depth of 25 m (Bolsenga and Herdendorf 1993). During late May or the beginning of June, water starts to stratify in the central and eastern basins. By mid July, the stratification is firmly established. By early October, the stratification disappears quickly with the fall turnover event (Schertzer *et al.* 1987). The stratification thus lasts throughout the growing season. The metalimnion in the stratified basins blocks or slows down the exchange of nutrients between the epilimnion and the hypolimnion, and traps particles settling from the epilimnion. Thus, seasonal stratification in the central and eastern basins cannot be ignored when evaluating the effects of *Dreissena* on the ecosystem. Even in the western basin, diurnal stratification can restrict mussels' effects within a bottom boundary layer (Edwards *et al.* 2005).

SIMULATION AND RESULTS

Dreissenid impacts on phytoplankton

Filtering rate is the volume of water that an individual organism filters per day ($\text{ml ind}^{-1} \text{d}^{-1}$) and clearance rate is the volume of water that an individual organism clears of particles per day ($\text{ml ind}^{-1} \text{d}^{-1}$) (Wu and Culver 1991). Generally, filtering rates were higher than clearance rates. Only if the organism can clear all food particles in the water as it filters (100% removal) and avoids refiltering water it has already processed, are the

filtering rates equal to the clearance rates. In dreissenids, these rates are a function of body mass (Table 2.4). The grazing rate of a population (mg d^{-1}) is a product of the clearance rate and the food particle concentration in the water (mg l^{-1}) and number of individuals in the population. One tends to overestimate the grazing rate if one uses filtering rates instead of clearance rates.

We estimate the dreissenids' grazing impacts, defined as the percentage of algal biomass of the whole basin or lake that is grazed by dreissenid populations in a given period of time. Thus, the daily grazing impacts of dreissenids (I) on algae are computed as the percentage of algal biomass (B) that is grazed by dreissenids (G) during one day in the basins. The grazing rates (g_j) of mussels in model cell j are the product of mussel clearance rates (c_j) and the algal concentration (b_j) and the number (n_j) of mussels in the model cell. That is, we assume only algae in the same model cell with dreissenids are instantaneously available to the mussels. Algae in other model cells will be available to dreissenids only when they are transported or sink into the model cell where dreissenids were located.

$$G = \sum_j g_j, \text{ where } g_j = c_j b_j n_j$$

$$I = \frac{G \times 100}{B} \%$$

We then compare the grazing impacts of mussels with the grazing impacts of crustacean zooplankton, which are calculated using the same equations for dreissenids, except that the grazing rates, g_j , for crustacean zooplankton are calculated differently. They are a function of ingestion rate, algal concentrations, and population size (see Table 2.1). Crustacean zooplankters are evenly distributed in the water column at the beginning

of simulations. Their vertical and horizontal distributions are, then, determined by physical mixing and biological processes (such as growth, death, maintenance cost, etc). Their active mobility, such as diel vertical migration, is not considered in the model.

Model results suggest that in the western basin dreissenids processed 20% of the water daily, while the grazing impacts on NDEA were only 6, 4 and 10% for 1997, 1998 and 1999, respectively, and on diatoms were 7-8% for all three years (Table 4.1). In the central and the eastern basins dreissenids processed 3% of the water daily, while the grazing impacts on NDEA and diatoms were around 1% in the central basin and 1-2% in the eastern basin.

The comparisons of the grazing impact of crustaceans and dreissenids on NDEA and diatoms show that their relative importance varies among basins and years (Table 4.1). Crustacean zooplankters have higher impact than dreissenids on NDEA in all three basins for 1997 and 1998, while they have a lower impact in the western basin in the dry year, 1999. However, the real situation of mussels in that dry year is unknown. Our assumption of constant mussel population among model years might not reflect the real situation of 1999. The impact of zooplankton grazing on diatoms was slightly higher than that of dreissenids in the western basin in 1998, while it was slightly lower in 1997 and 1999. Zooplankton had a consistently higher grazing impact on diatoms in the central basin than did dreissenids in all three years. In the eastern basin, the impact on diatoms of zooplankton grazing was one to two times higher than that of dreissenids in 1997 and 1998, while slightly lower in 1999. NDIA are selectively rejected by dreissenids and zooplankton. Therefore, there is no direct grazing impact by dreissenids or zooplankton on NDIA.

Besides direct grazing impacts on algal groups by dreissenids and crustacean zooplankters, there are indirect impacts on algae, such as selective grazing and nutrient excretion. To illustrate these impacts, we set up 7 treatments of the model, the full model, no dreissenids, no dreissenid grazing, no dreissenid P excretion, no zooplankton, no zooplankton grazing, and no zooplankton P excretion. The impacts of the treatments on algal groups have similar patterns among years (Figures 4.1-4.3).

Impacts on NDEA

The treatment without zooplankton grazing results in the most abundant NDEA among all treatments (Figure 4.1). Without zooplankton-grazing loss, NDEA maintains a high biomass. This high biomass, then, supports a larger zooplankton population. Large zooplankton population excretes a larger amount of phosphorus which, in turn, relieves NDEA from phosphorus limitation and NDEA grow even faster. This positive feedback does not occur in the treatment without dreissenid grazing, because dreissenid populations do not grow over time in the model. However, the dreissenid populations continuously excrete SRP into water. Treatments without dreissenids or without zooplankton have substantially higher NDEA biomass than the full model, which indicates that grazing loss of NDEA by dreissenids or zooplankton are greater than the gain of NDEA from phosphorus excreted by dreissenids or zooplankton. Compared to NDEA biomass in the full model, treatments without dreissenid P excretion or without zooplankton P excretion decrease NDEA biomass consistently for all three basins and all three years, while treatment without zooplankton P excretion result in lower NDEA biomass than the treatment without dreissenid P excretion in most of the cases.

Impacts on Diatoms

Compared to the full model, the treatments without dreissenids or without dreissenid grazing increase diatom biomass in all three basins and all three years, while the treatment without zooplankton or without zooplankton grazing decrease diatom biomass in most of the cases (Figure 4.2). The results suggest that dreissenids impact diatoms by direct grazing, while zooplankters affect diatoms by indirectly affecting competition between algal groups. For example, diatoms lost competition to NDEA in the treatment without zooplankton, because NDEA gained more without zooplankton and became a strong nutrient competitor to diatoms. However, as mentioned in Chapter 3, the responses of diatoms to changes in the system are not easily explained because more factors being are involved, such as silica limitation.

Impacts on NDIA

Compared to the full model, the treatment without dreissenids decreased NDIA biomass in the western basin, while it generates similar, if not lower, NDIA biomass in the central and eastern basins (Figure 4.3). Treatment without dreissenid grazing increases NDIA biomass in all basins and all three years, except in the western basin of 1998 when phosphorus concentration decreased (Table 4.3). Treatments without dreissenid P excretion, or without zooplankton, or without zooplankton P excretion decrease NDIA biomass consistently in all cases, while the treatment without zooplankton grazing increases NDIA biomass in all cases. NDIA's changes reflect the changes in availability of phosphorus to them, i.e., NDIA increase as more phosphorus is made available to them, and vice versa. For example, compared with the full model, the

treatment without zooplankton has higher NDEA, which implies lower phosphorus availability to NDIA as NDEA is a strong competitor (Table 4.3). Accordingly, treatment without zooplankton has lower NDIA than the full model. For another example, compared with the full model, the treatment without zooplankton grazing has much higher NDEA. However, instead of having lower NDIA (as NDIA is a weak phosphorus competitor) the treatment also has much higher NDIA than the full model. The reason is the positive feedback mentioned above still resulting in higher phosphorus availability to NDIA given abundant NDEA (Table 4.3).

Dreissenid impacts on nutrients

Nutrient excretion by dreissenids in each model cell is estimated as the product of lab-measured individual nutrient remineralization rates of phosphorus or nitrogen (Table 2.4) and the number of mussels of the model cell.

On basin-wide phosphorus Dreissenid mussels excreted each day an amount of SRP equivalent to a high proportion of the water column SRP in the western basin: 23% in 1997, 19% in 1998 and 56% in 1999, while the proportions decreased to about 1% in the central and the eastern basins (Table 4.2) due to the large water volume of the basins and the lower mass-specific phosphorus excretion rates of quagga mussels.

On basin-wide nitrogen Dreissenid mussel nitrogen excreta contributed 13% of the water column concentration in 1997, 12% in 1998 and 15% in 1999 in the western basin (Table 4.2). These numbers were also high in the central basin, 4%. More attention should be given as this increase in ammonia originated in the hypolimnion,

which can lead to an early anoxia in the hypolimnion in the central basin by nitrification (see discussion section).

Dreissenid impacts on crustacean zooplankton

The impacts of mussels on crustacean zooplankton (cladocerans and copepods) were investigated by turning on/off the mussel processes and calculating the means and standard deviations of modeled daily outputs of basin-wide total crustacean zooplankton biomass, production and grazing rates over the simulation period for each of three years. We tested four treatments: full model, no mussels, no mussel grazing and no mussel excretion. The results showed that these four treatments had similar impact patterns on the zooplankton biomass in all three basins and all three model years (Figure 4.4).

Compared to that in the full model, basin-wide zooplankton biomass increased in the treatments without mussels or without mussel grazing, and decreased in the treatment without mussel P excretion. The treatment without mussel grazing resulted in higher zooplankton abundance than did the treatment without mussels. These impact patterns also persisted on zooplankton production (the difference between assimilation gain and respiration loss) and grazing rates (Figures 4.5 and 4.6), which are consistent with the impact patterns of mussels on NDEA (Figure 4.1).

Model sensitivity analysis: Dreissenid population estimates

Because no direct measurements of dreissenid population structure (density and size frequency) were available for all three years, densities and shell lengths of mussels were varied under the model conditions of year 1997 to investigate the sensitivity of the

model to mussel density and mussel size. Specifically, we repeat simulations with dreissenid densities at 0.1, 1.0, 10, and 20 times of density estimates from Table 3.2, and repeated the simulations for mussel at four sizes (body length = 5, 10, 15, and 20 mm) for each population density option.

Dreissenid population density effects on NDEA

NDEA biomass Model results show that increases in mussel populations (density or mussel size) decrease NDEA biomass when mussel populations are small, but increase NDEA biomass when mussel populations are large. For example, the smallest sized mussels (5 mm) decrease NDEA biomass with increasing densities (Figure 4.7) in the western basin. For another example, in the western basin 10-mm mussels decrease NDEA biomass with increasing density at first, then turn to increase the NDEA biomass when density continue to increase and become very high (density factor of 20). In the central and eastern basin, depression of NDEA by dreissenids becomes less obvious.

NDEA net production Increases in mussel length or density both result in increases in NDEA net production (Figure 4.8). It indicates that increases of production attributed to mussel nutrient excretion are much larger than decreases attributed to mussel grazing.

Dreissenid grazing on NDEA In the western basin, a small dreissenid population size (small mussels with low density) tends to increase its grazing impact with increases in its population size, while a large mussel population tends to decrease its grazing impact with increases in its population size (Figure 4.9). For example, the 5-mm mussel population increases grazing impacts with an increase in its density, while the 15- and 20-mm mussel populations' grazing impacts decrease with increasing density. For another

example, at lower population densities (density factors of 0.1 or 1) increasing mussel sizes increased the population grazing impacts at first, then the population grazing impacts stabilize, while at high population densities (density factors of 10 or 20) increasing mussel sizes increase the population grazing impacts at first, then the population grazing impacts decrease. Interestingly, the larger mussel population sizes (high densities and large body size), that result in the highest NDEA biomass and production in the water column, have smaller population grazing impacts. This indicates a strong algal concentration boundary layer above the mussel bed.

In the central and eastern basins, grazing impacts increase consistently and dramatically with increasing mussel population density or mussel body size or both, likely because mussels are located in each model cell throughout the water column in these two basins. The lack of a third dimension in the model allows mussels situate on the south shore to consume algae at both the south and north shore, which is not true in the field. Thus, the mussel grazing estimates from the EcoLE model for the central and the eastern basins are more like estimations from previous study, Edwards *et al.*'s (2005) fully mixing model, while the case in the western basin is more realistic.

Dreissenid population density effects on Diatoms

Diatom biomass Model results show that mussel impacts on diatoms are more complicated than those on NDEA. On NDEA biomass, the impacts have only one turning point as mussel population increases: from decreasing to increasing NDEA biomass. On diatom biomass, the impacts have two turning points: decreasing-increasing-decreasing. That is, unlike the mussels' increasing NDEA biomass at high

population size (high density and large mussels) large mussel populations decrease diatom biomass. For example, in the western basin, 10-mm mussels, first, depress diatom biomass with increasing density, and then turn to increase the diatom biomass when density continues to increase (Figure 4.10), while the other larger two size groups (15- and 20-mm) show the opposite impacts on diatom biomass compared with the 10-mm mussels. They increase diatom biomass dramatically with increased density from 0.1- to 1-fold, and then decrease diatom biomass with continuing increases in density. In the central and eastern basin, mussels decrease diatom biomass consistently with increasing density or mussel size.

Diatom production In the western basin, the diatom productivity has similar distribution patterns with diatom biomass along mussel population size (density and body size) (Figure 4.11), which indicates that the growth of diatoms determines their biomass in this basin. However, in the central and eastern basins, this is not the case. The productivity increases rapidly with increasing mussel density or body size at first, then stabilizes or even decreases (in the central basin with 20-mm mussel population increasing density from 10- to 20-fold). The unrealistically high grazing rates (Figure 4.12) of large mussel population determine the diatom biomass in these two basins.

Dreissenid grazing on diatoms In the western basin, dreissenid grazing impact show a non-linear response to dreissenid population sizes (Figure 4.12). For example, the increase in grazing impacts is much larger when we increase the population density factor from 0.1 to 1 for 10-mm mussels than when we increase the population density factor from 1 to 10, while the grazing impact even decreases slightly with further increasing of the density factor from 10 to 20. However, the boundary layer shows less effective to

dreissenid grazing on diatoms than on NDEA, which might due to high sinking rates of diatoms.

Dreissenid density effects on NDIA

Mussels increase NDIA biomass and productivity consistently with increasing density or body size for all three basins (Figures 4.13-14). High biomass and productivity occurs with large mussel populations. Noticeably, with the largest mussel population (20-mm and 20-fold) NDIA productivity exceeds NDEA productivity in the western and eastern basins.

Dreissenid density effects on nutrients

With increases in mussel density and body size, the mussel population P and NH_4^+ excretion rates increase consistently and rapidly (Figures 4.15 and 4.16, Table 2.4). This main because the excretion rates are an exponential function of individual body mass, while the body mass is an exponential function of body length (or size as we mentioned here) The 5-mm mussel population with density of 600 m^{-2} (density factor of 0.1) excrete $0.01 \text{ mg P m}^{-2} \text{ d}^{-1}$ (or $0.002 \text{ } \mu\text{g P l}^{-1} \text{ d}^{-1}$) and $0.2 \text{ mg N m}^{-2} \text{ d}^{-1}$ (or $0.03 \text{ } \mu\text{g N l}^{-1} \text{ d}^{-1}$) in the western basin, while the 20 mm mussel population with density of 120,000 m^{-2} (density factor of 20) excreted more than $240 \text{ mg P m}^{-2} \text{ d}^{-1}$ (or $30 \text{ } \mu\text{g P l}^{-1} \text{ d}^{-1}$) and $2500 \text{ mg N m}^{-2} \text{ d}^{-1}$ (or $320 \text{ } \mu\text{g N l}^{-1} \text{ d}^{-1}$).

Dreissenid density effects on Crustacean zooplankton

The changes in crustacean zooplankton biomass along with increasing mussel population size (Figure 4.17) were similar to the changes in NDEA biomass (Figure 4.7), except the decreases in zooplankton biomass were less obvious than those in NDEA biomass.

Zooplankton population grazing rates (g_{clad}) are products of population biomass and individual ingestion rates, while the latter are a function of food concentrations (Table 2.1). Hence, zooplankton population grazing impacts (Figure 4.18) are highly correlated to the combined changes in both NDEA and diatom biomass with different mussel population sizes (Figures 4.7 and 4.10). Diatom biomass shows a strong influence on zooplankton grazing in the western basin, while it only shows influences with high mussel population sizes in the central and eastern basins. Changes in the zooplankton production (Figure 4.19) were similar to those in zooplankton biomass (Figure 4.17).

DISCUSSION

Dreissenid impacts on phytoplankton

MacIsaac *et al.* (1992) estimated zebra mussel filtering rates by combining lab-measured clearance rates with field population densities at Hen Island Reef in the western basin. Their extremely high filtering rate estimate, $132 \text{ m}^3 \text{ m}^{-2} \text{ d}^{-1}$, brought zebra mussels to the attention of many ecologists and the public. Other early studies also showed a high grazing impact on phytoplankton in Lake Erie (Bunt *et al.* 1993). The observations that water became clearer (Holland 1993; Leach 1993) and phytoplankton biomass decreased

(Leach 1993, MacIsaac *et al.* 1992; Holland 1993) in water bodies with invasion of zebra mussels supported these estimates.

Knowing the dreissenid field population density is important in estimating the grazing impacts. Our mussel densities, 2927 or 6419 m⁻² (depth-dependent) in the western basin, are 40-90 times lower than those used by MacIsaac *et al.* (1992), 2.6×10^5 m⁻² from Hen Island Reef. Using the different filtering rates from Kryger and Riisgard (1988), Krondratev (1963), and Micheev (1966), MacIsaac *et al.* calculated three filtering rates, 132 m³ m⁻² d⁻¹, 115 m³ m⁻² d⁻¹, and 25 m³ m⁻² d⁻¹. If the population density is updated for their study by using our field density data (Table 3.2), then their filtering rates would be 1.5-3.3 m³ m⁻² d⁻¹, 1.3-2.9 m³ m⁻² d⁻¹, and 0.3-0.6 m³ m⁻² d⁻¹. For a water column of 7 m, the updated population would process a volume equivalent to 4%-47% of the water column per day. Our result of 20% per day (Table 4.1) is well within this range. The filtering capability of mussel populations is now far less striking than it was predicted during the first several years when they first successfully colonized western Lake Erie. Moreover, Jarvis *et al.*'s (2000) basin-wide estimate of 418 m⁻² is much lower than the ones we used in our simulations. Jarvis *et al.*'s abundance data imply an even lower filtering rate (Barbiero and Tuchman 2004).

MacIsaac *et al.*'s estimation of the filtering impacts on phytoplankton was made under the assumption of a shallow and well-mixed freshwater ecosystem without refiltration of the water. The western Lake Erie is shallow and has no seasonal stratification. However, it certainly is not a well-mixed reactor (Figures 2.8-10). Ackerman *et al.* (2001) studied an isolated reef in western Lake Erie and found that 60% of the time, the water column was stratified during the day due to solar heating (diel

thermocline) and intrusions of cold central basin water. This calm water would delay the transport of upper water algae to the mussel bed. MacIsaac *et al.* (1999) found a chlorophyll *a* boundary layer of 1.85 m above the lakebed at 6 locations in the western basin of Lake Erie. Their location-parameterized two-dimensional hydrodynamic model predicted that mussel grazing caused as high as 90% of the reduction in chlorophyll *a* near the lake bottom. Their model also predicted much lower reductions in surface chlorophyll *a* concentration. Edwards *et al.* (2005) also reported a zone of depletion in algal biomass near the mussel bed, but they found little evidence of algal depletion in the upper water column. All studies mentioned above were carried out at one or several stations. No study has previously estimated the grazing impacts on the algae in the whole basin or lake as was done in our simulation model. We found that mussels consumed few algae basin-wide from June to September. Even in the western basin, where there was no seasonal stratification and mussels had the highest impact among the three basins, the daily grazing impacts were <10% of the NDEA and diatoms, which indicates a refiltering rate of more than 50%. That is, >50% of the water being taken in by a feeding mussel has already been cleared of algae.

Our sensitivity analysis shows that a bigger dreissenid population (high density and large mussel sizes) will increase instead of decrease basin-wide NDEA biomass due to increased phosphorus excretion. Mellina *et al.* (1995) demonstrated this increase by measuring chlorophyll *a* in mesocosm (tank) experiments. NDEA are mainly small, rapidly growing species and have low sinking rates. Vanderploeg *et al.* (2001) speculated that with increased nutrients excreted by mussels, NDEA should increase in

growth faster than the mortality imposed by mussel clearance. Hence, these results suggest that dreissenid mussels play a more important role by recycling nutrients than they do by depressing algal biomass as population increases, especially in the nutrient-limited, less productive water bodies.

It has been reported that dreissenid mussels depress diatoms in lakes (Nicholls *et al.* 2002). Our simulation results indicate that the depression of diatoms may be attributed to their high sinking rates as well as their competition with NDEA for nutrients.

NDIA is dominated by *Microcystis* in our model, so we will discuss *Microcystis* instead of NDIA below. *Microcystis* blooms have occurred with increased frequency and magnitude in Lake Erie since dreissenid mussels established large populations on the lake bottom. Vanderploeg *et al.* (2001) showed that zebra mussels selectively rejected toxic *Microcystis aeruginosa* in pseudofeces. Bierman *et al.* (2005) demonstrated the selective promotion of *Microcystis* by mussels in Saginaw Bay using a well-mixed-water-column model. The rising time and mechanism of *Microcystis* transport from the bottom to the water column are still unclear. In late May or early June, there are few *Microcystis* colonies in the water column, which makes it difficult to initialize these dynamics in our model, because many model segments have no *Microcystis* present. However, by adding an arbitrarily small amount of *Microcystis* as “seeds” on the lake bottom to replace zeros, we investigated the influence of dreissenids on *Microcystis* dynamics. Our simulations show that *Microcystis* is not a strong nutrient competitor with other algal groups. When phosphorus concentration is low, *Microcystis* biomass decreases due to competition with other algae (e.g. Figures 4.1 and 4.3). However, unlike NDEA and diatoms that relied on phosphorus in the upper water, *Microcystis* is less affected by the vertical distribution of

P, but was more affected by the total amount of available P in the water column (Chapter 2). Thus, a high mussel population that excretes a large amount of phosphorus on the bottom, benefits *Microcystis* more than other algae, consistent with our finding that *Microcystis* has a higher net productivity than do NDEA in the western and eastern basins when the mussel population size is large (Figures 4.8 and 4.14). Nevertheless, our simulation results differ from those of Bierman *et al.* (2005) in several ways. First, their model consists of just one well-mixed layer, while ours has 2 to 65 layers depending on the depth of water in a given segment. The assumption of well-mixed water column may be appropriate for shallow Saginaw Bay, Lake Huron, but not for Lake Erie, even the shallow western basin. As we have discussed earlier, their assumptions led to an overestimate of the dreissenid grazing impacts on algae other than *Microcystis*, which, in turn, enhanced the development of *Microcystis*. This is unlikely because *Microcystis* is not a strong competitor. Our results show that selective grazing by dreissenids showed little impact on the development of *Microcystis* (e.g., Figure 4.3), except in the western basin of 1998 when a *Microcystis* bloom occurred. Second, Bierman *et al.* did not separate the effects of dreissenid grazing on *Microcystis* from those of nutrient excretion when they tested the sensitivities of their model to variations in mussel densities. Our results clearly show that mussels have much stronger impacts on *Microcystis* by P excretion than by grazing in Lake Erie.

Dreissenid impacts on nutrient cycling

Dreissenid mussels are an important internal nutrient source. They excrete phosphorus and nitrogen in the forms of SRP and NH_3 (Arnott and Vanni 1996; Gardner

et al. 1995; Heath *et al.* 1995), which are directly taken up by phytoplankton.

Makarewicz *et al.* (2000) found that SRP increased by 180% in western Lake Erie from the pre-*Dreissena* period to the post-*Dreissena* period. They attributed this directly to input from dreissenid mussel excretion and lower uptake by phytoplankton due to their grazing loss to dreissenid mussels. Our model predicts that mussels excrete 20-56% of the SRP and graze <10% of NDEA and diatoms in the western basin and about 1% SRP and 1-2 % NDEA and diatoms in the other basins.

The dreissenid populations in our model were much smaller (in density and mussel size) than populations studied by others on rocky reef locations. When we increased dreissenid body size from our modeled 10 mm to 15 mm or even 20 mm, or increasing density by 10 fold, the population excretion increased dramatically. These population densities and size distribution are quite realistic for those found on many hard substrates on the lake bottom. A high phosphorus concentration gradient from the concentration boundary layer to the rest of the water column will enable phosphorus molecular movements to overcome the thermal stratification barrier and to reach the upper water layers. Dreissenid internal loading thus counters the effects of the Lake Erie external phosphorus reduction program.

Published studies have recorded an increase in ammonium concentration in the water after the *Dreissena* invasion (Johengen *et al.* 1995; Effler *et al.* 1997; Makarewicz *et al.* 2000). Our results show that mussel excretion has more impact on nitrogen than on phosphorus in the central basin. Conroy *et al.* (2005b) also speculated that dreissenid mussels might be more important in increasing the recycling of nitrogen than of phosphorus. However, no research has ever related ammonia regeneration to oxygen

depletion in the central basin. Dobson and Gilbertson (1972) reported a critical oxygen depletion rate of $3.0 \text{ mg l}^{-1} \text{ month}^{-1}$ in a hypolimnion with a thickness of 4 m. That is, the depletion rate is $12 \text{ g O}_2 \text{ m}^{-2} \text{ month}^{-1}$. Our model shows that nitrification of ammonia excreted by dreissenid mussels consumed $4 \text{ g O}_2 \text{ m}^{-2} \text{ month}^{-1}$, which is one fourth of the above-mentioned depletion rate. With increasing mussel body sizes or mussel population densities, this excretion rate increased dramatically and consumed $350 \text{ g O}_2 \text{ m}^{-2} \text{ month}^{-1}$ (20 mm and $120,000 \text{ m}^{-2}$) (Figure 4.16). Nitrification will speed up the oxygen depletion during summer stratification and lead to early anoxia in the hypolimnion of the central basin.

Dreissenid impacts on zooplankton

The impacts of dreissenid mussels on zooplankton have been less well studied. Field observations indicated that rotifer abundance declined by 74% between before and after the establishment of *Dreissena* populations in the western Lake Erie (Leach 1993; MacIsaac and Rocha 1995). Evidence was provided that showed that rotifers could be ingested directly by mussels (MacIsaac *et al.* 1991; Pace *et al.* 1998). There were far fewer studies on the impacts of dreissenid mussels on macrozooplankton. Pace *et al.* (1998) found lower abundances of copepods and cladocerans post-*Dreissena* than pre-*Dreissena*, but the differences were not statistically significant. Idrisi *et al.* (2001) found no significant impacts of zebra mussels on cladoceran biomass in Oneida Lake, New York. Our simulations suggest that zooplankton biomass, production and grazing rates on NDEA are depressed substantially by zebra mussels or mussel grazing (Figures 4.4-6), which indicates food competition between zooplankters and mussels.

However, the competition should not be strong, since mussel grazing is limited by boundary layers and both mussels and zooplankters only grazed about 10% of algal biomass over the growing season. However, a clear-water phase occurs during early July, when food is sparse for zooplankton, and competition among zooplankters might be more severe than between zooplankton and mussels during this period. Treatments with no zooplankton or no zooplankton grazing caused substantial changes in algal biomass (increased or decreased) compared to the full model. We reject our hypothesis that dreissenids can depress the phytoplankton community in Lake Erie and mask the influence of zooplankton grazing.

Sensitivity analysis suggests that increases in density or body size of a small mussel population (low density and small mussels) decreases zooplankton biomass and production. However, high mussel population densities or large mussels increased zooplankton biomass and production with zooplankton biomass being less affected than zooplankton production. Therefore, a very large mussel population will increase NDEA biomass dramatically, which slows down the decreasing trend in zooplankton production or even turns it into the increasing direction. In the real world, however, the basin bottom habitat is heterogeneous in character, with mussels at various densities from place to place, which will mask the basin-wide average effects of mussels on macro-zooplankton, and may show no effects at all.

In summary, dreissenids decrease NDEA and diatom biomass by grazing while they increase NDEA and diatom biomass even more by nutrient excretion. Dreissenids cause NDIA to proliferate mainly by nutrient excretion instead of by selective rejection.

Dreissenid mussels excrete large amounts of SRP and NH_3 to the nutrient pool. With increases in mussel biomass or densities, impacts on the lake change non-linearly. Nutrient excretion rates increase rapidly with increases in mussel biomass or densities. NDEA and NDIA production increase with the resulting reduction in phosphorus limitation. Mussel grazing impacts are depressed by stronger boundary layers, while nutrient excretion impacts become dominant with increasing mussel populations. As a result, NDEA and NDIA biomass increase with increasing mussel population to a high level. Diatom biomass decreases with large mussel population due to high sinking rates. The zooplankton community shows clear and strong impacts on algal biomass, and their impacts are not masked by those of mussel populations. Zooplankton shows a mixed response to the variation of mussel populations, with biomass being less sensitive to mussel abundance than production.

	unit	1997			1998			1999		
		WB	CB	EB	WB	CB	EB	WB	CB	EB
Basin Volume	km ³	24	316	161	24	316	161	23	309	159
Water processed	km ³ d ⁻¹	5	10	5	5	10	5	5	10	5
	%	21	3	3	21	3	3	22	3	3
Basin-wide NDEA	mt DW	6,712	26,320	7,982	6,903	43,849	17,561	4,595	47,862	28,119
NDEA grazed by mussels	mt DW d ⁻¹	414	173	99	282	346	245	443	445	465
	%	6	1	1	4	1	1	10	1	2
NDEA grazed by crustacean zooplankton	mt DW d ⁻¹	521	1,944	426	746	3,340	618	291	3,557	604
	%	8	7	5	11	8	4	6	7	2
Basin-wide diatoms	mt DW	1,625	27,429	4,576	4,766	32,416	5,522	4,175	31,162	14,006
Diatom grazed by mussels	mt DW d ⁻¹	108	294	60	345	405	73	344	367	219
	%	7	1	1	7	1	1	8	1	2
Diatom grazed by crustacean zooplankton	mt DW d ⁻¹	101	1,172	118	385	1,816	128	278	1,834	196
	%	6	4	3	8	6	2	7	6	1

Table 4.1. Basin-wide impacts of dreissenids on NDEA (non-diatom edible algae) and diatoms, compared with those of crustacean zooplankton.

		1997			1998			1999		
	unit	WB	CB	EB	WB	CB	EB	WB	CB	EB
Basin-wide SRP-P	mt P	28.6	837.0	515.4	34.2	1203.4	824.8	11.9	809.6	825.1
P excretion by dreissenids	mt P d ⁻¹	6.6	13.6	6.4	6.6	13.6	6.4	6.6	13.6	6.4
	%	23.2	1.6	1.2	19.4	1.1	0.8	55.5	1.7	0.8
Basin-wide NH ₄ -N	mt N	715.9	6357.8	4218.1	760.7	6625.3	3450.8	613.0	5729.3	4614.1
N excretion by dreissenids	mt N d ⁻¹	89.6	244.0	116.7	89.6	244.0	116.7	89.6	244.0	116.7
	%	12.5	3.8	2.8	11.8	3.7	3.4	14.6	4.3	2.5

182 Table 4.2. The relative importance of nutrients excreted by dreissenid mussels to the basin-wide nutrient mass.

	WB		CB		EB	
	Means	Fractions	Means	Fractions	Means	Fractions
1997						
Full model	62	1.00	904	1.00	201	1.00
No mussels	42	0.68	902	1.00	185	0.92
No mussel grazing	64	1.03	995	1.10	209	1.04
No mussel P excretion	46	0.74	816	0.90	177	0.88
No zooplankton	45	0.73	551	0.61	145	0.72
No zooplankton grazing	82	1.32	7947	8.79	1855	9.23
No zooplankton P excretion	56	0.90	592	0.65	160	0.80
1998						
Full model	91	1.00	734	1.00	162	1.00
No mussels	50	0.55	710	0.97	161	0.99
No mussel grazing	77	0.85	847	1.15	195	1.20
No mussel P excretion	64	0.70	632	0.86	132	0.81
No zooplankton	52	0.57	366	0.50	113	0.70
No zooplankton grazing	200	2.20	25941	35.34	7179	44.31
No zooplankton P excretion	75	0.82	370	0.50	119	0.73
1999						
Full model	32	1.00	754	1.00	158	1.00
No mussels	23	0.72	821	1.09	188	1.19
No mussel grazing	35	1.09	934	1.24	223	1.41
No mussel P excretion	25	0.78	649	0.86	133	0.84
No zooplankton	22	0.69	317	0.42	123	0.78
No zooplankton grazing	115	3.59	19775	26.23	5495	34.78
No zooplankton P excretion	29	0.91	344	0.46	130	0.82

Table 4.3. Comparisons of effects of different treatments on SRP (metric tons) in the upper water. Means are the averages of daily model outputs of basin-wide SRP over the simulation periods. Fractions are the means of treatments to that of the full model.

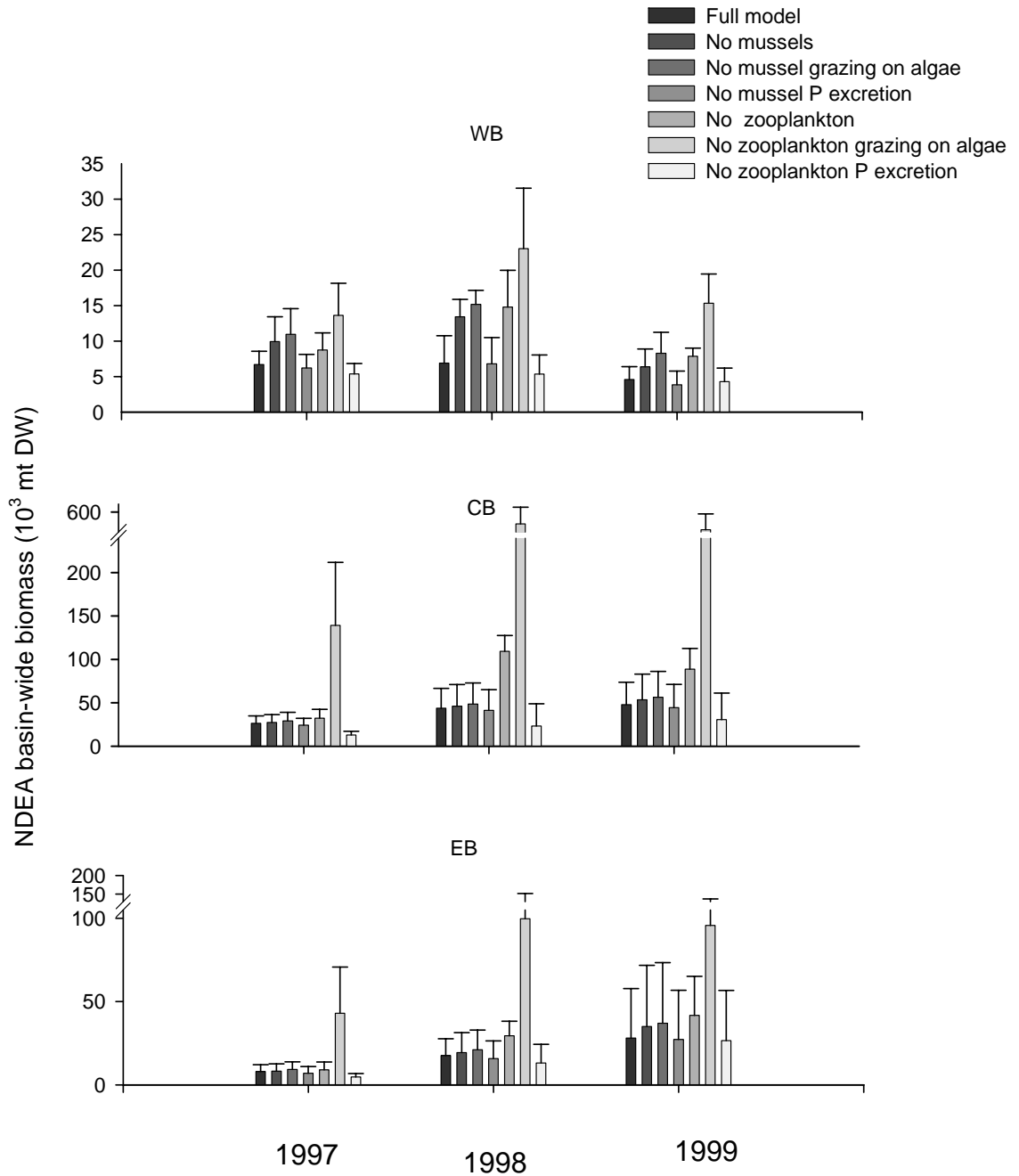


Figure 4.1. Comparisons of seasonal means of basin-wide NDEA biomass of seven model treatments. The error bar represents one standard deviation of the mean. Note the different scales on the y-axis.

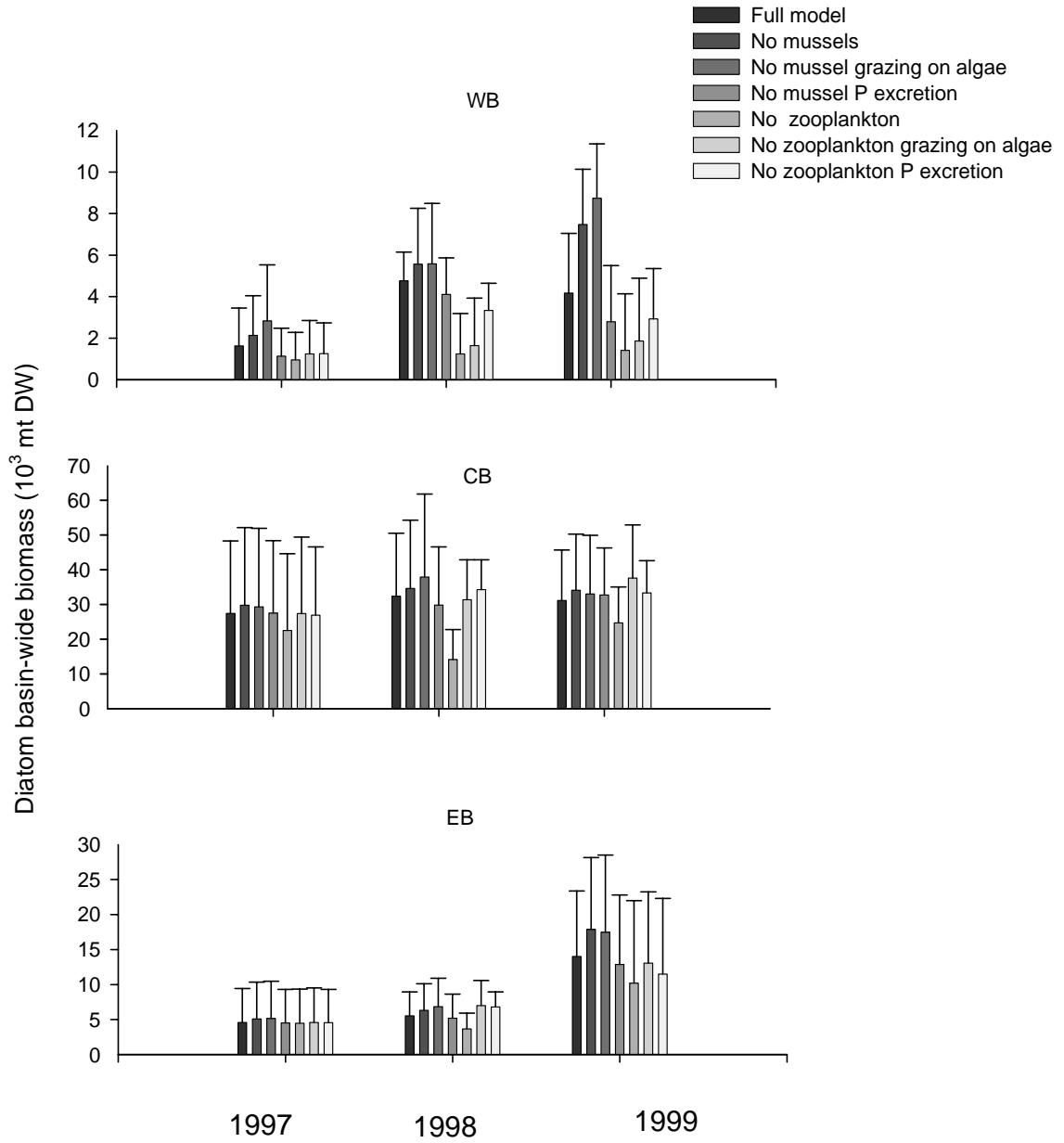


Figure 4.2. As Figure 4.1, but for basin-wide diatom biomass.

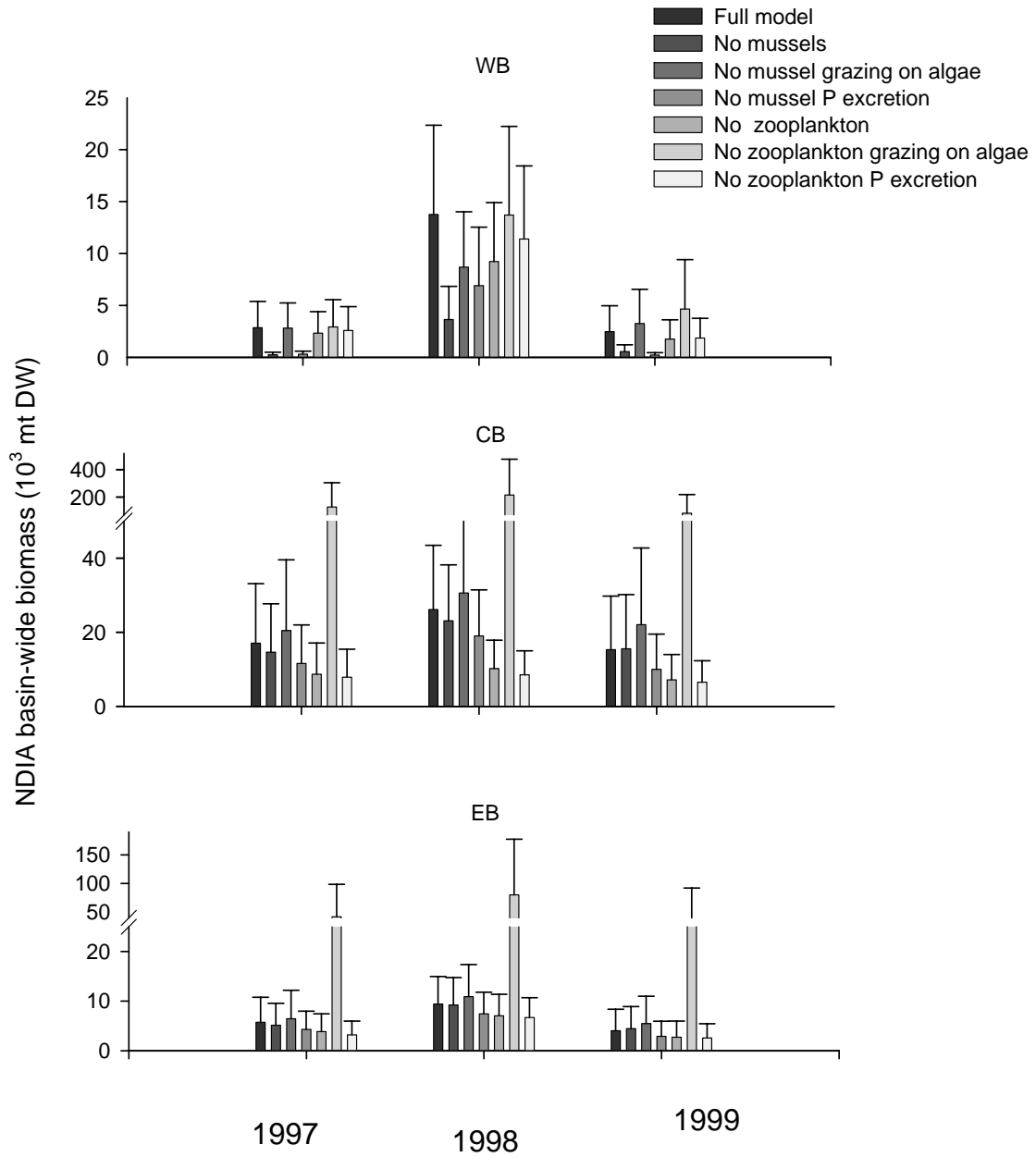


Figure 4.3. As Figure 4.1, but for basin-wide NDIA biomass

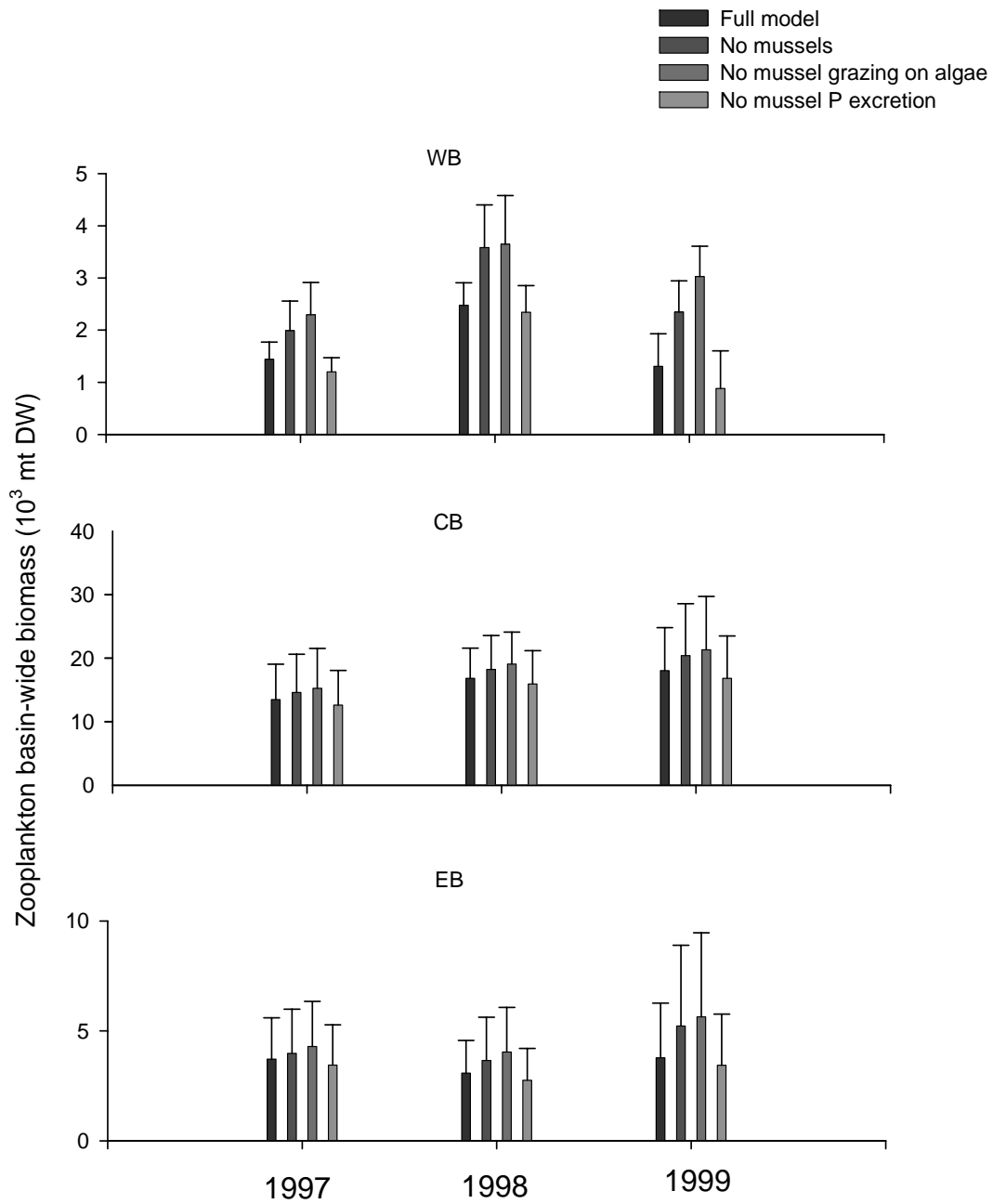


Figure 4.4. Comparisons of seasonal means of basin-wide zooplankton biomass of different model treatments of mussels. The error bar represents one standard deviation of the mean. Note the different scales on the y-axis.

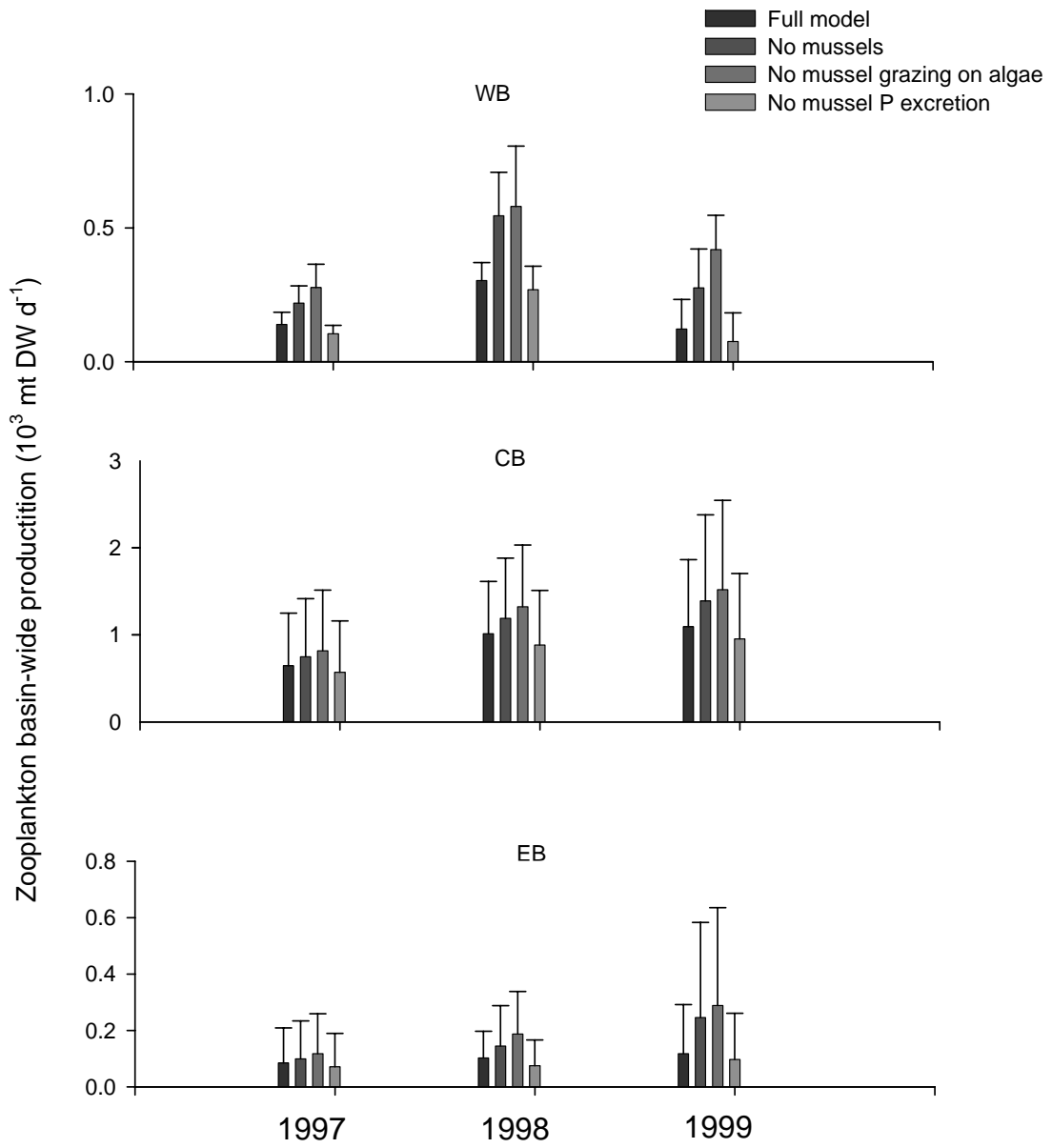


Figure 4.5. As Figure 4.4, but on crustacean zooplankton production.

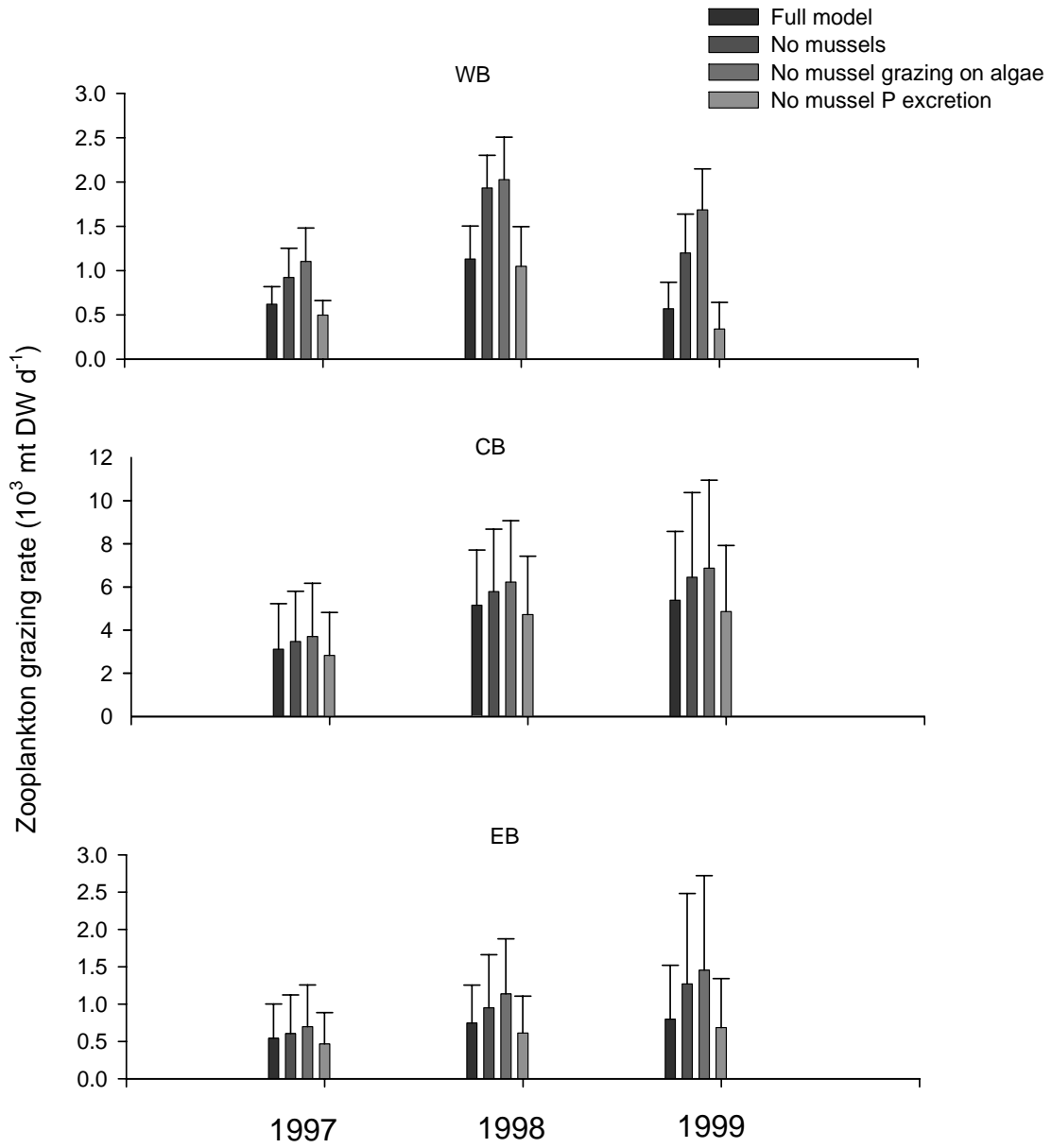


Figure 4.6. As Figure 4.4, but on grazing rates of crustacean zooplankton.

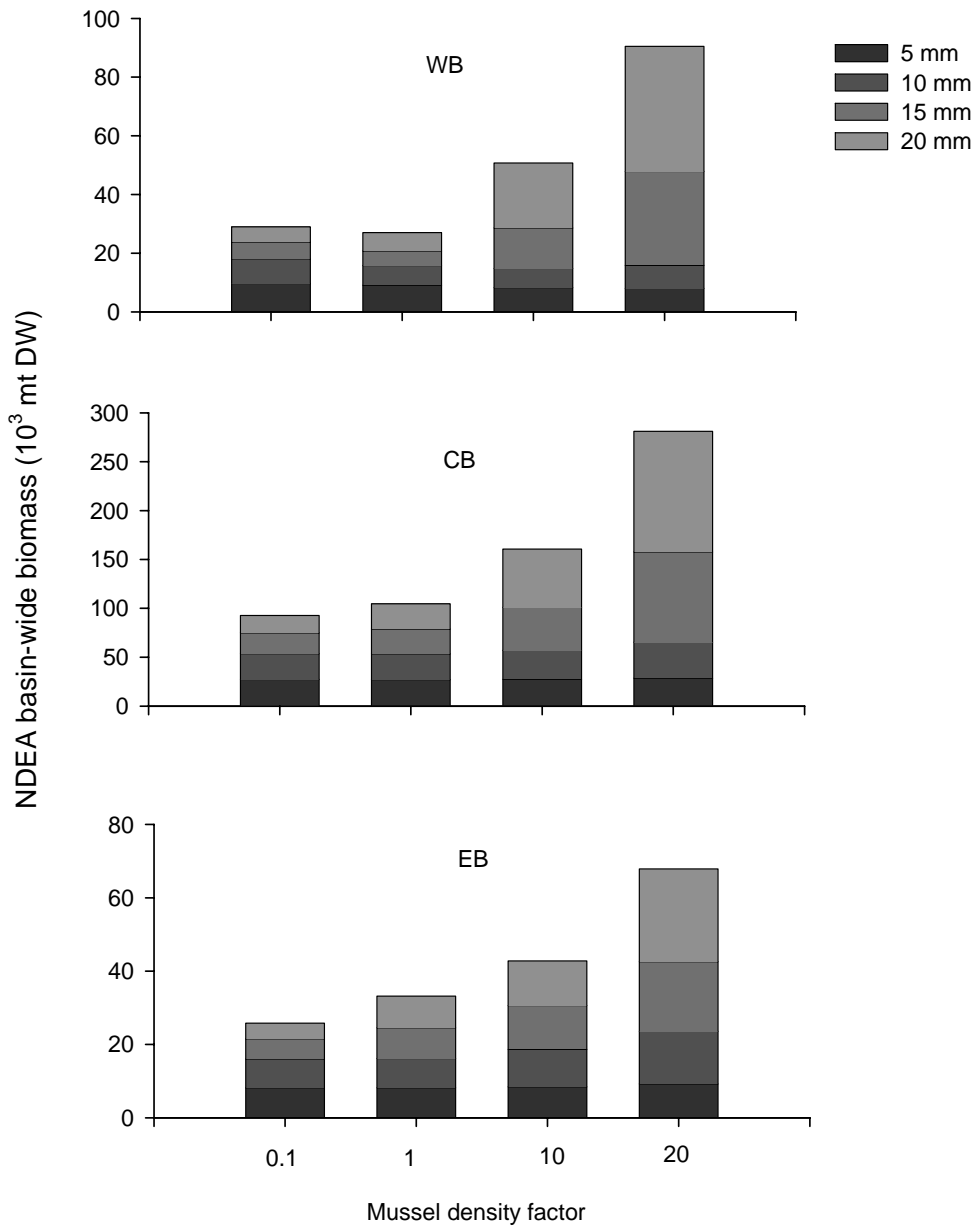


Figure 4.7. Uncertainty analysis of different combinations of density and body size of dreissenid mussel populations on basin-wide NDEA biomass. The values are averaged over the simulation period. Note the different scales on the y-axis.

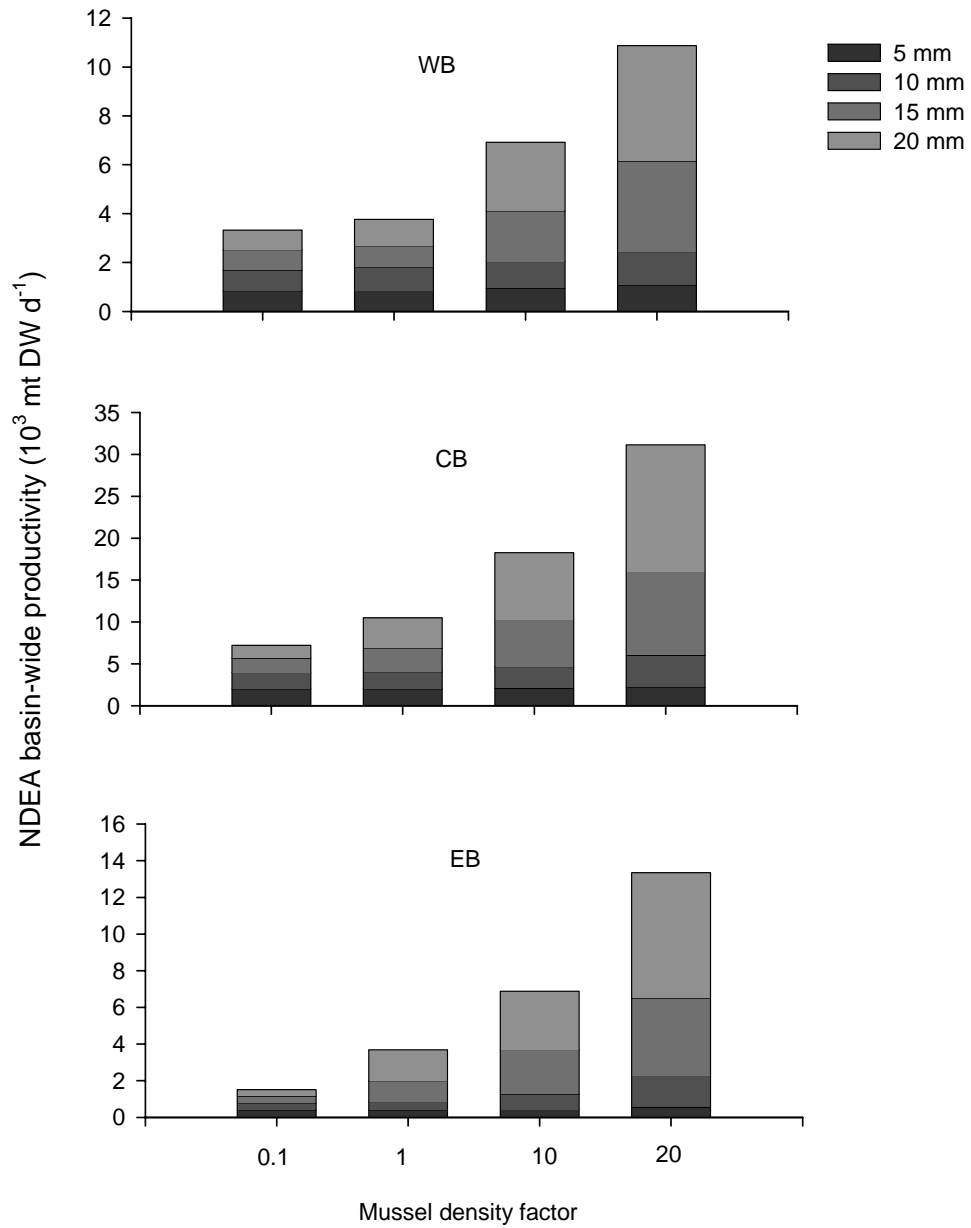


Figure 4.8. Uncertainty analysis of different combinations of density and body size of dreissenid mussel populations on basin-wide NDEA net productivity. The values are averaged over the simulation period. Note the different scales on the y-axis.

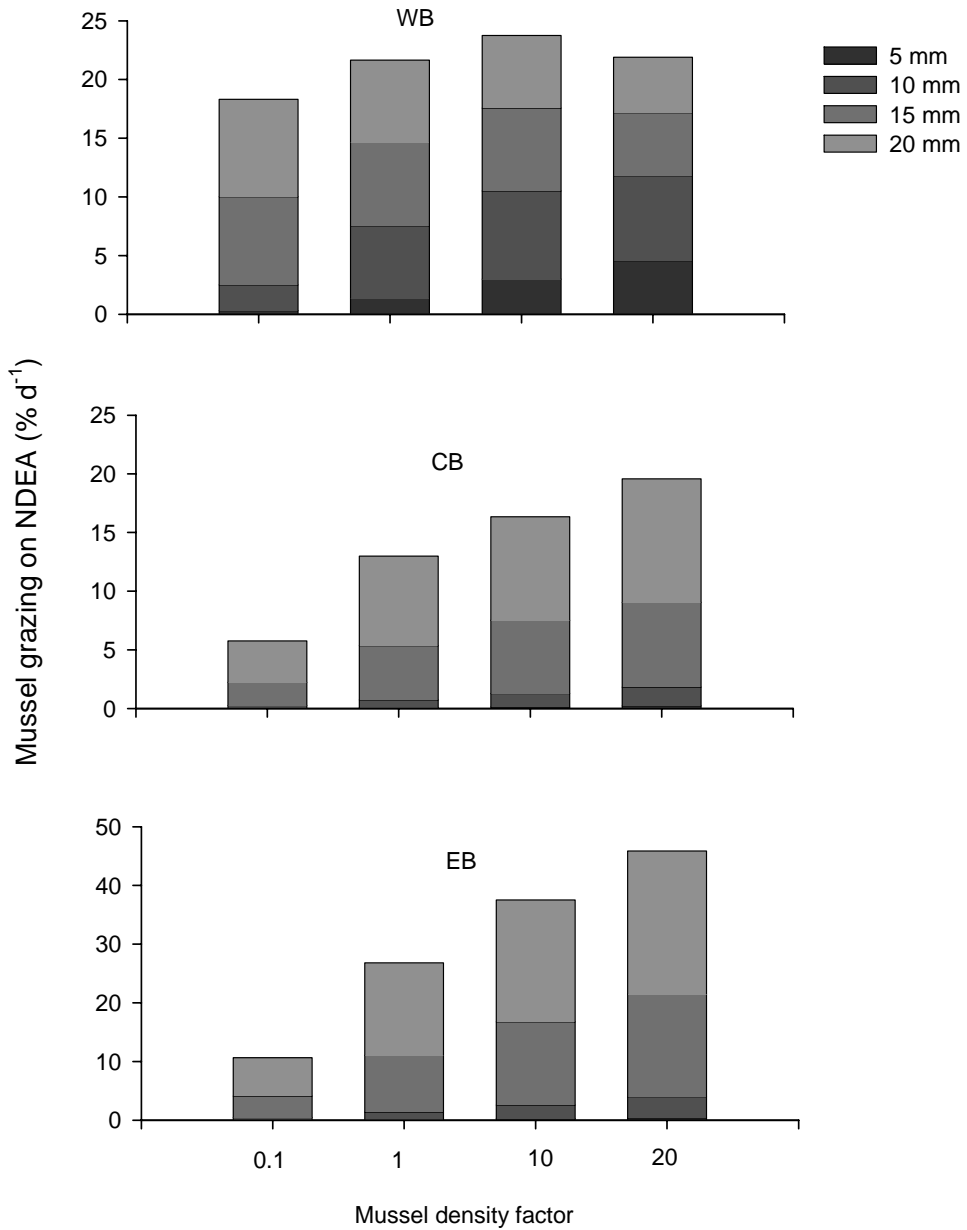


Figure 4.9. Uncertainty analysis of different combinations of density and body size of dreissenid mussel populations on basin-wide mussels' grazing impacts on NDEA. The values are averaged over the simulation period. Note the different scales on the y-axis.

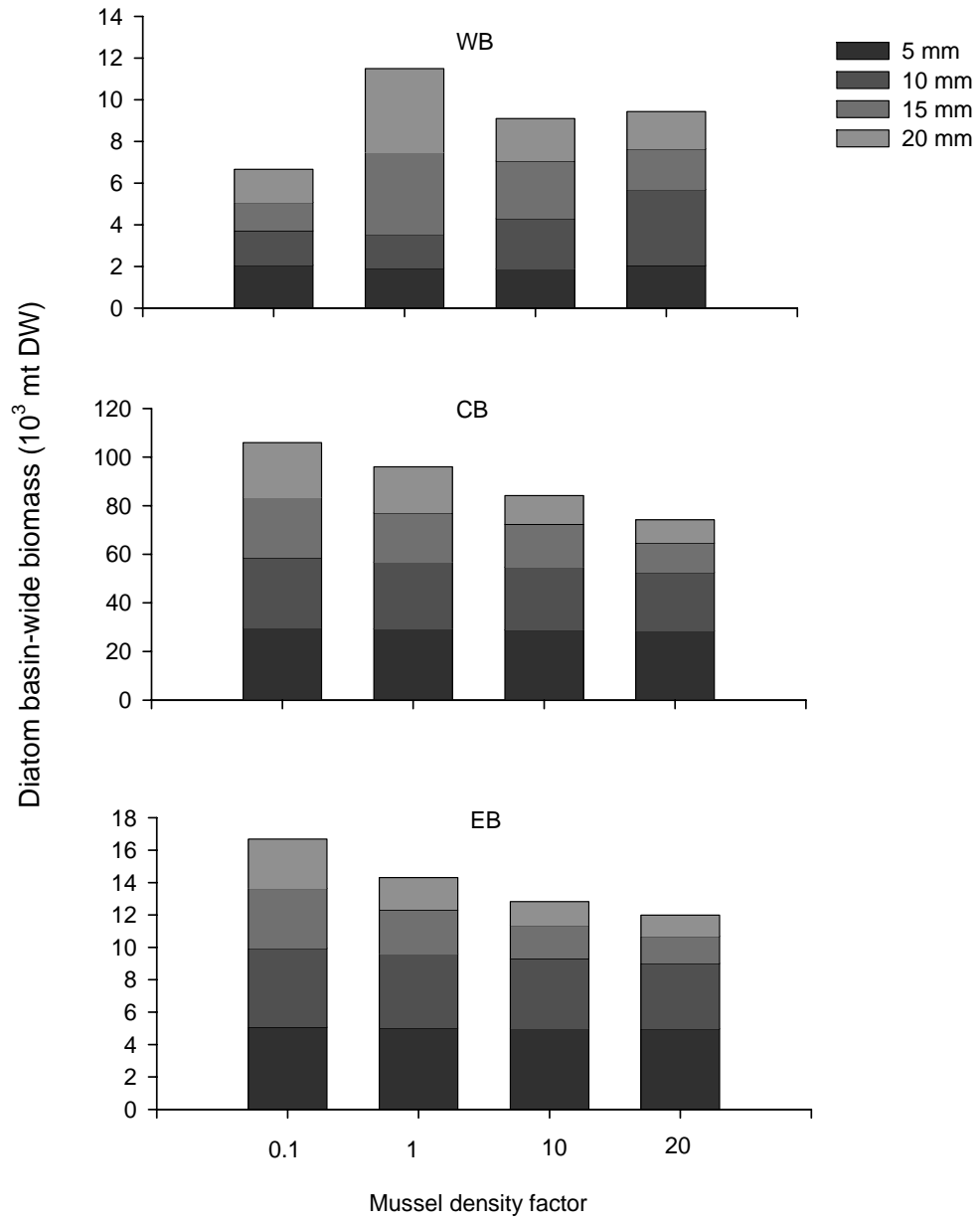


Figure 4.10. As Figure 4.7, but on basin-wide diatom biomass.

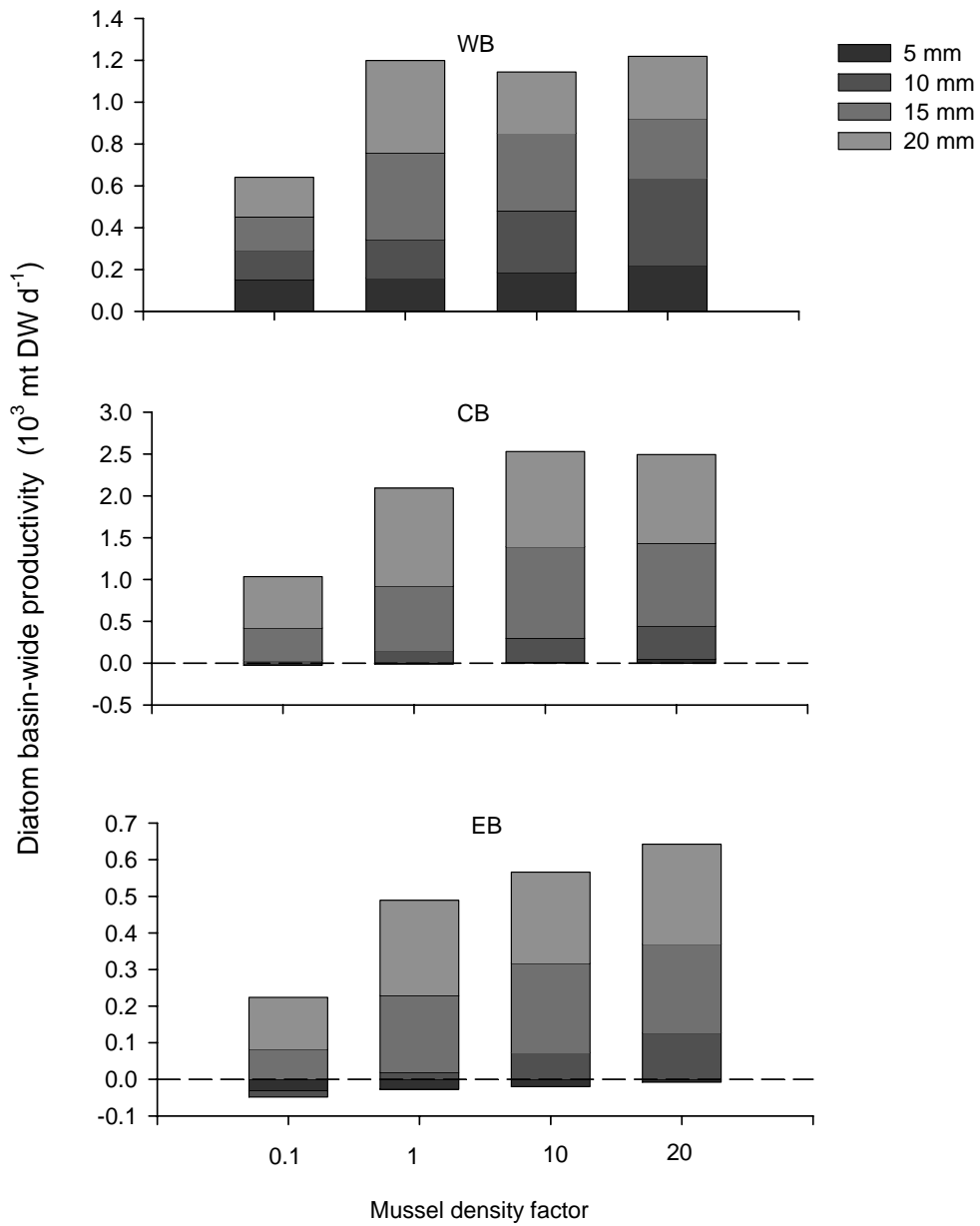


Figure 4.11. As Figure 4.8, but on diatom net productivity. The negative values indicate that the respiration loss is greater than the photosynthesis in the whole basin.

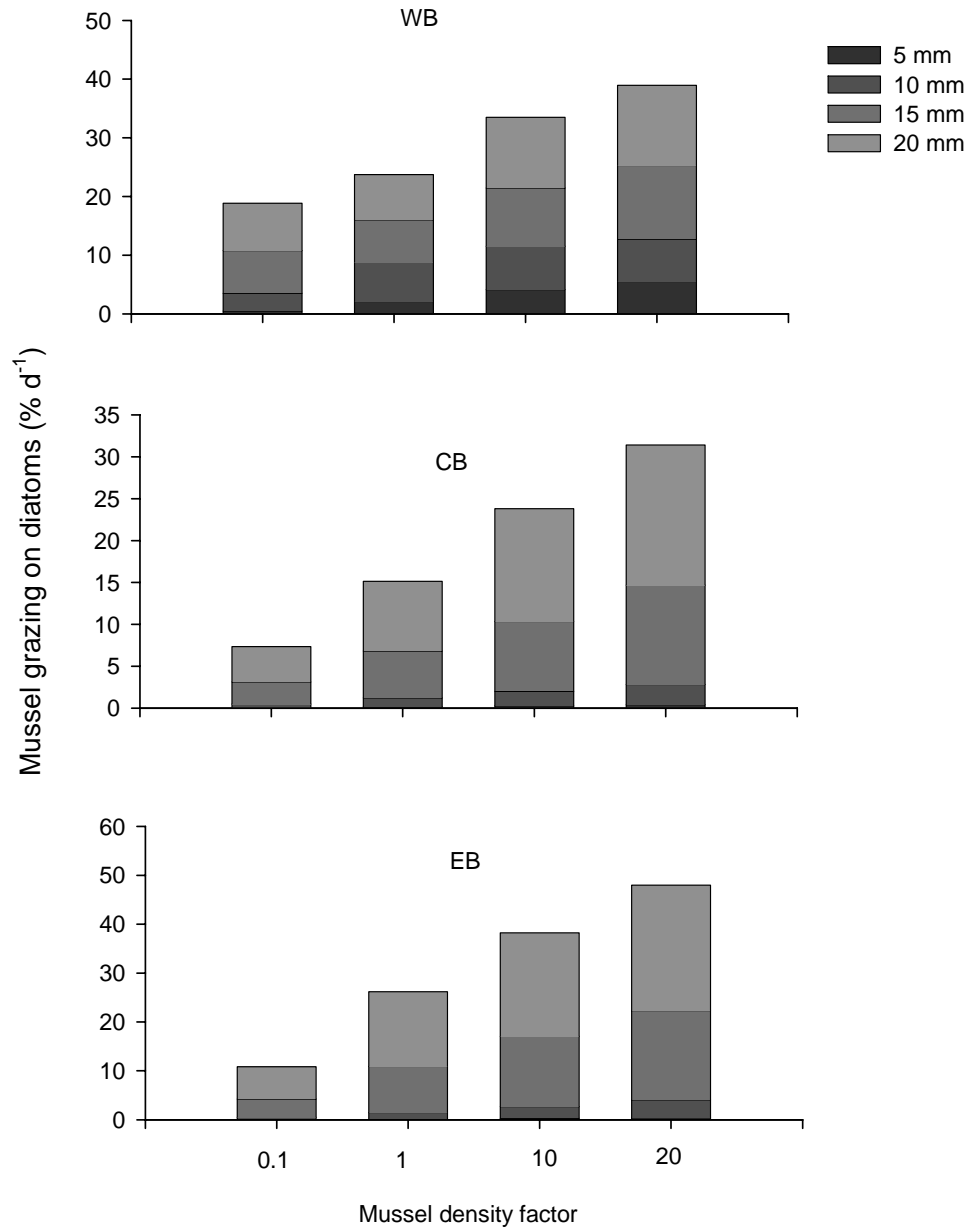


Figure 4.12. As Figure 4.9, but on mussels' grazing impacts on diatoms

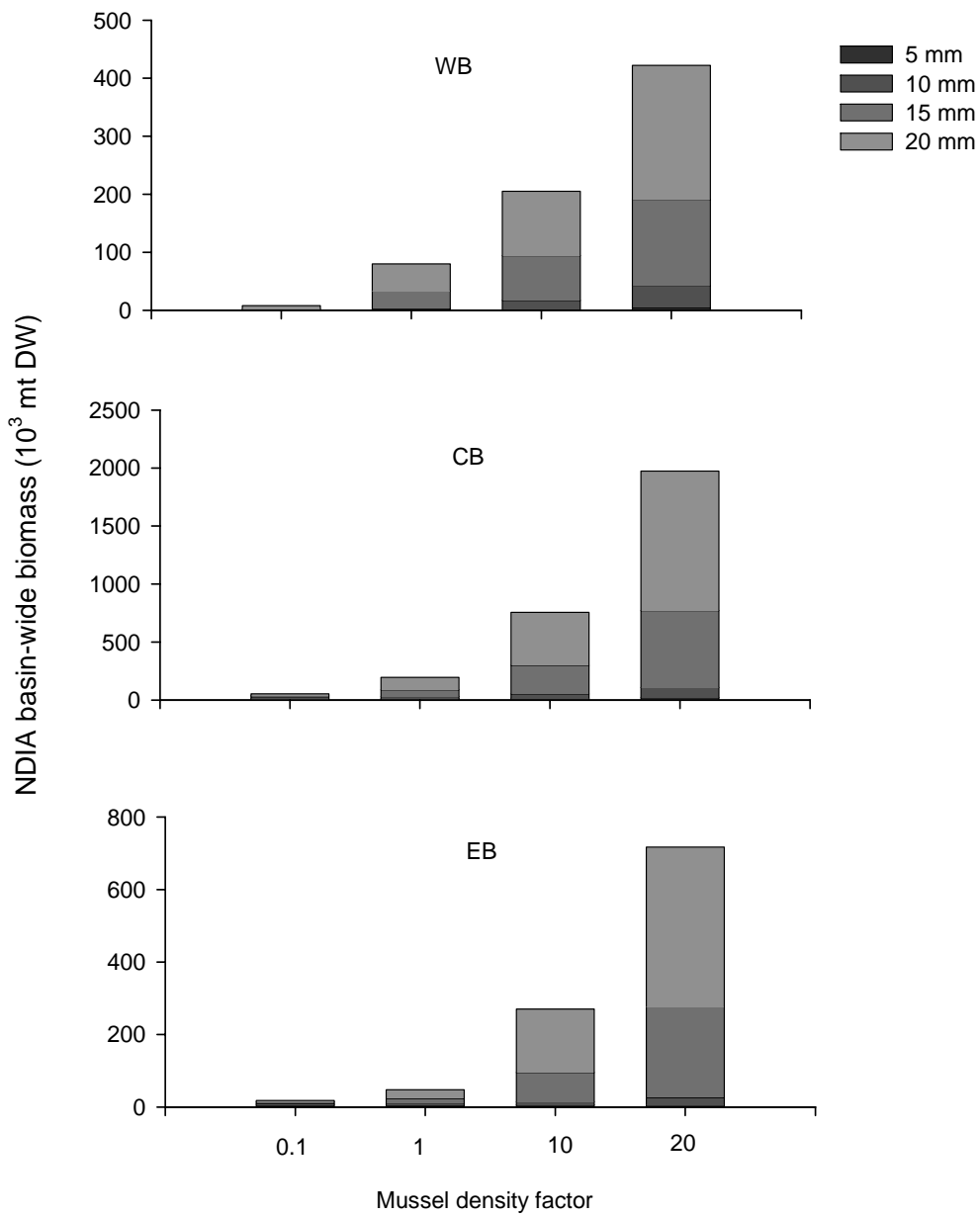


Figure 4.13. As Figure 4.7, but on basin-wide NDIA biomass

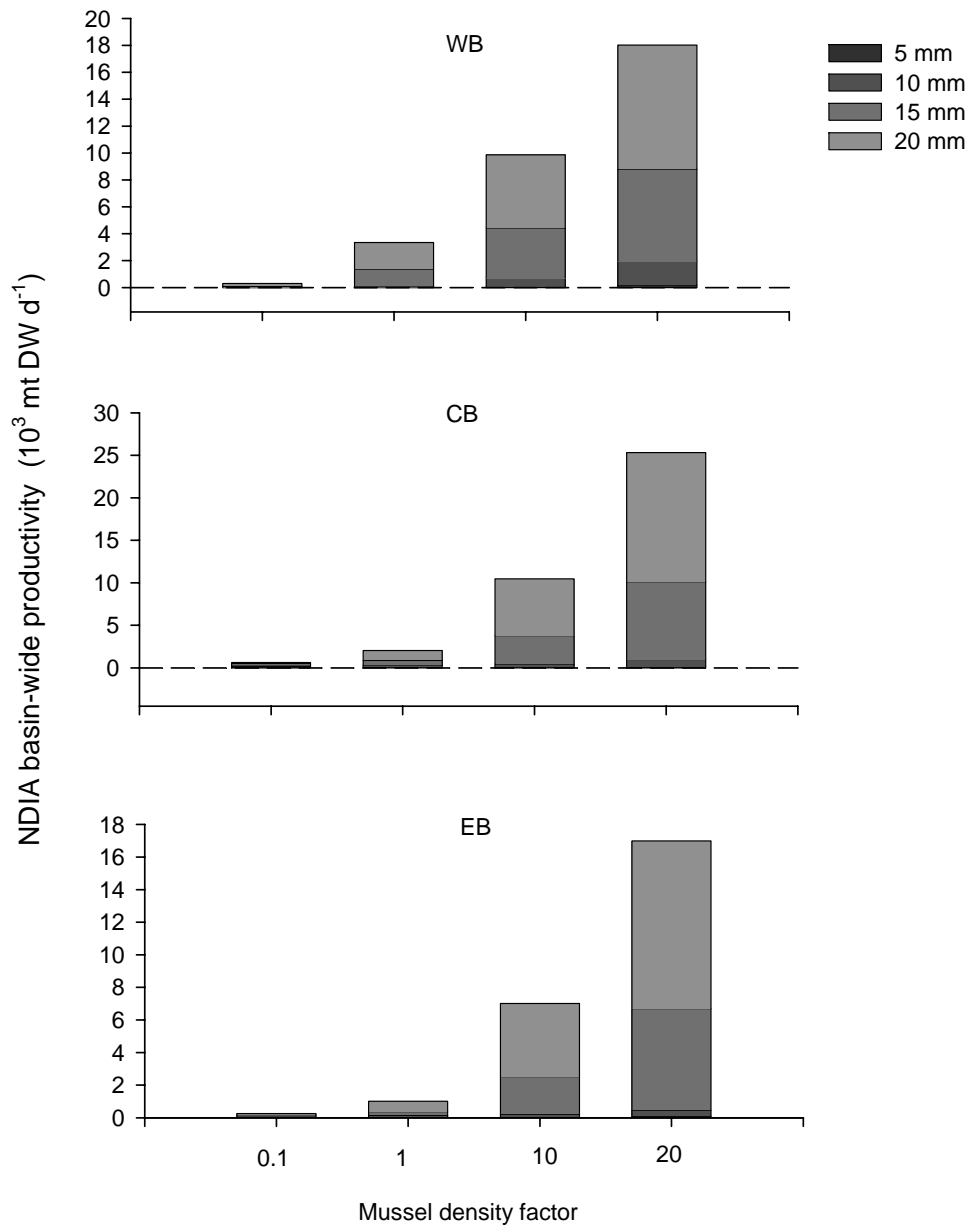


Figure 4.14. As Figure 4.8, but on NDIA net productivity. The negative values indicate that the respiration loss is greater than the photosynthesis in the whole basin.

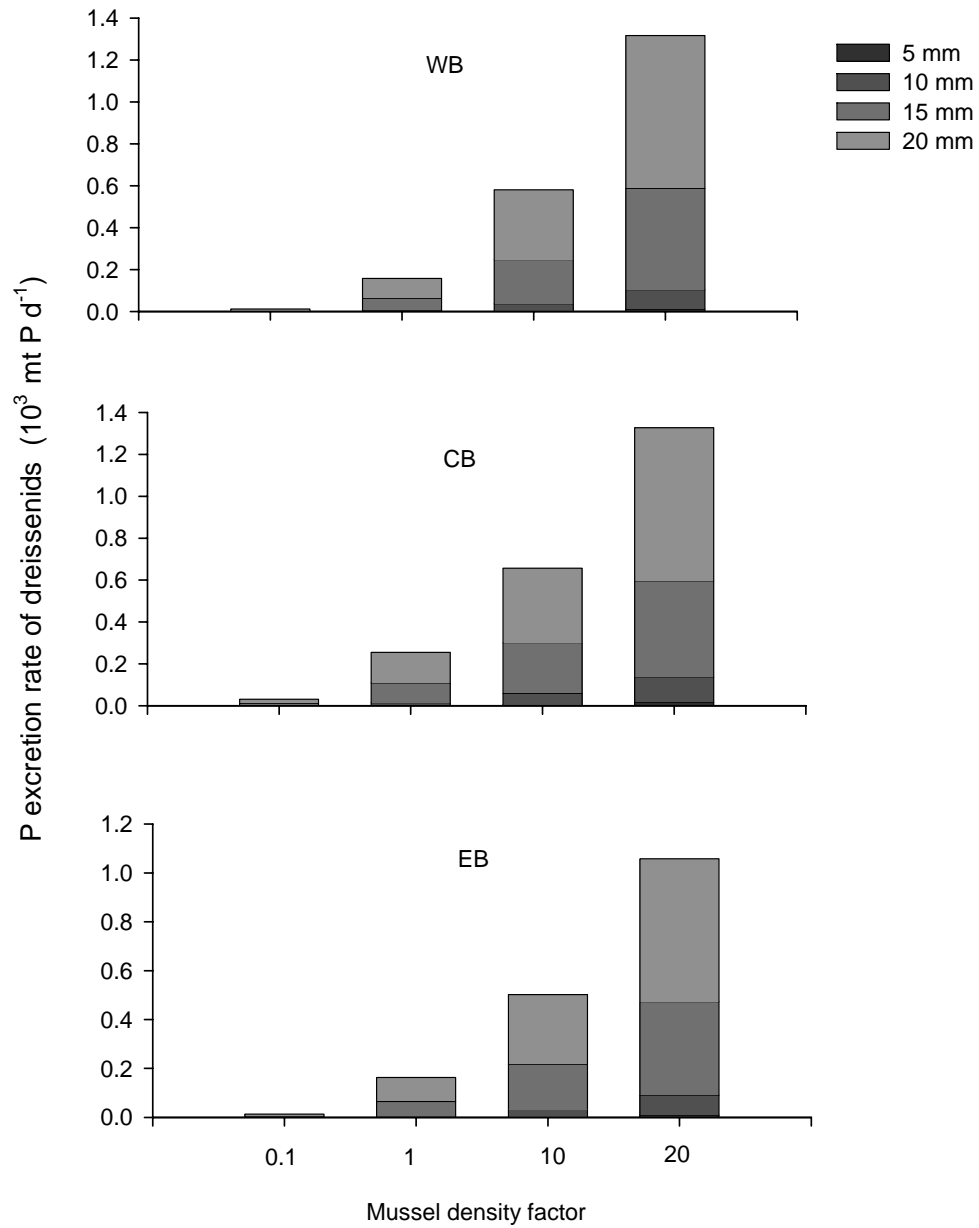


Figure 4.15. Uncertainty analysis of different combinations of density and body size of dreissenid mussel populations on basin-wide P excretion rates of dreissenid mussel populations. The values are averaged over the simulation period. Note the different scales on the y-axis.

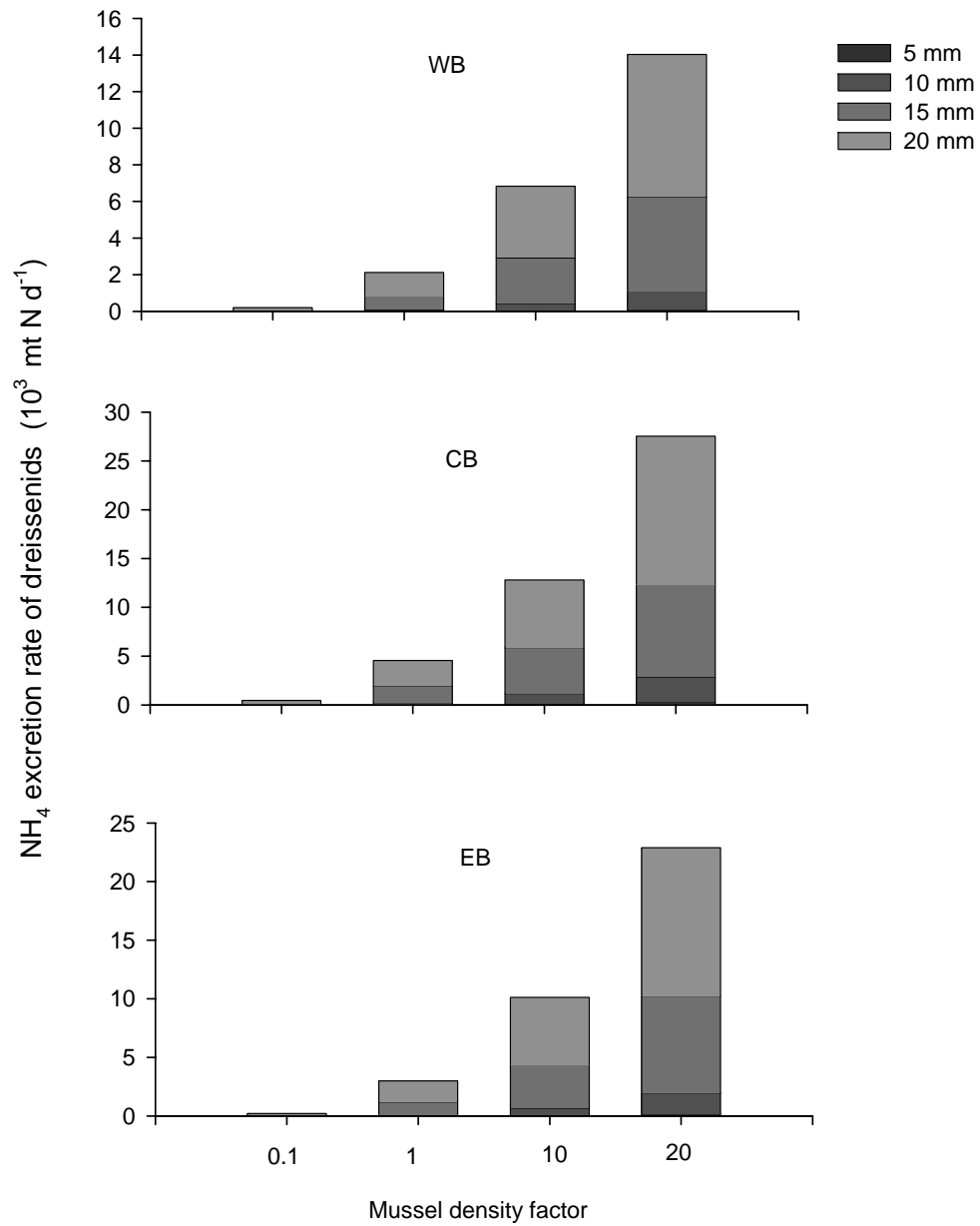


Figure 4.16. As Figure 4.15, but on ammonia excretion rates of dreissenid mussel populations.

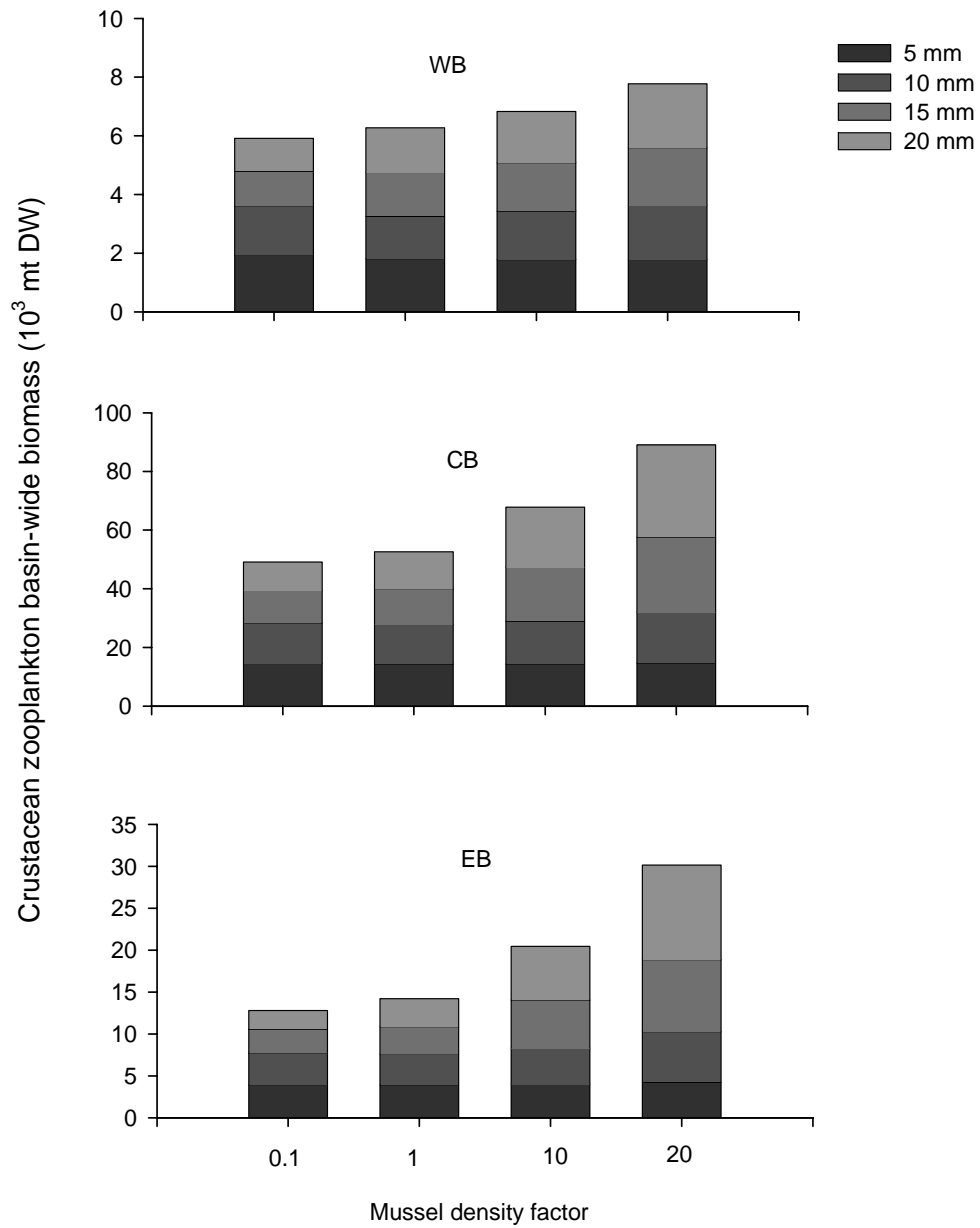


Figure 4.17. Uncertainty analysis of different combinations of density and body size of dreissenid mussel populations on basin-wide crustacean zooplankton biomass. The values are averaged over the simulation period. Note the different scales on the y-axis.

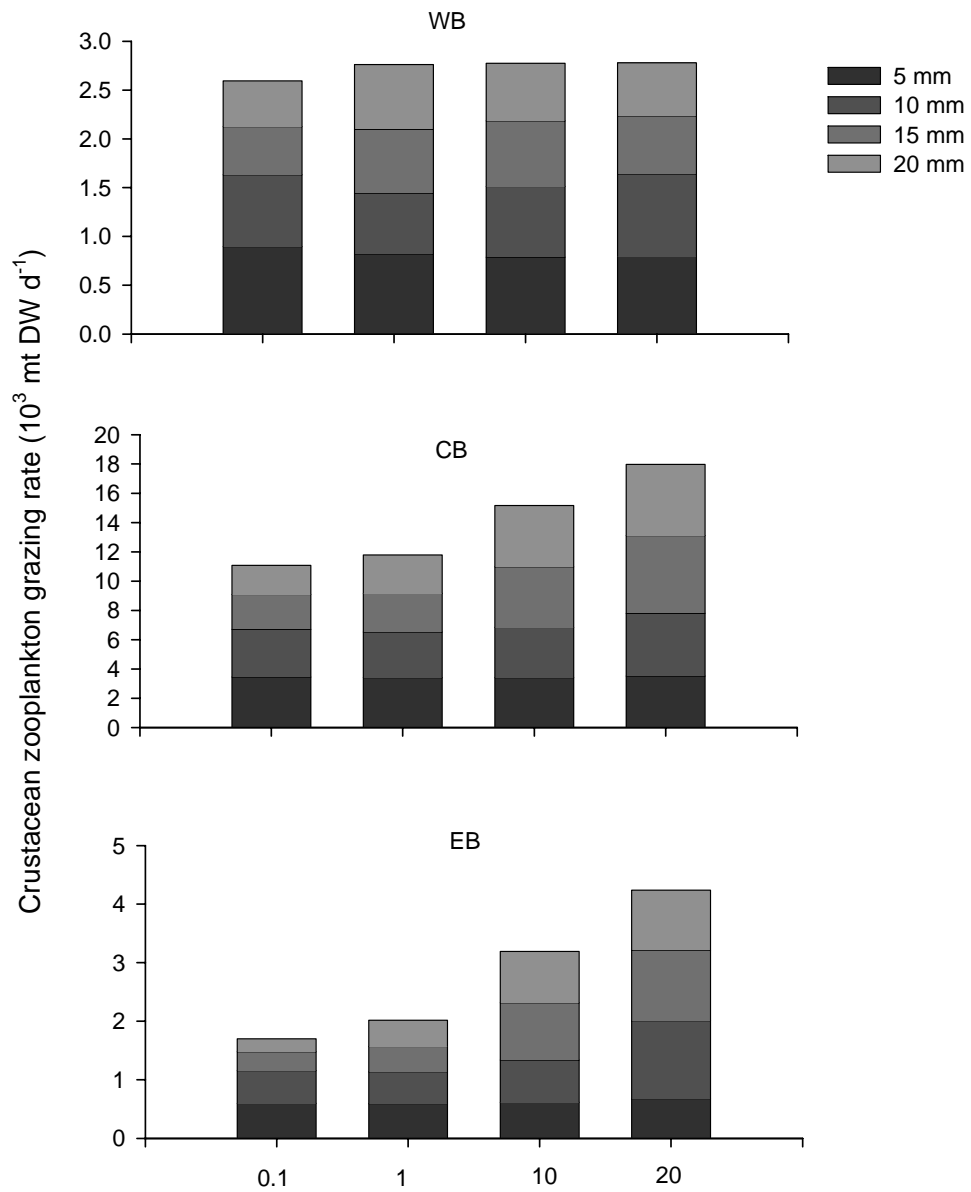


Figure 4.18. Uncertainty analysis of different combinations of density and body size of dreissenid mussel populations on basin-wide crustacean zooplankton grazing on NDEA and diatoms. The values are averaged over the simulation period. Note the different scales on the y-axis.

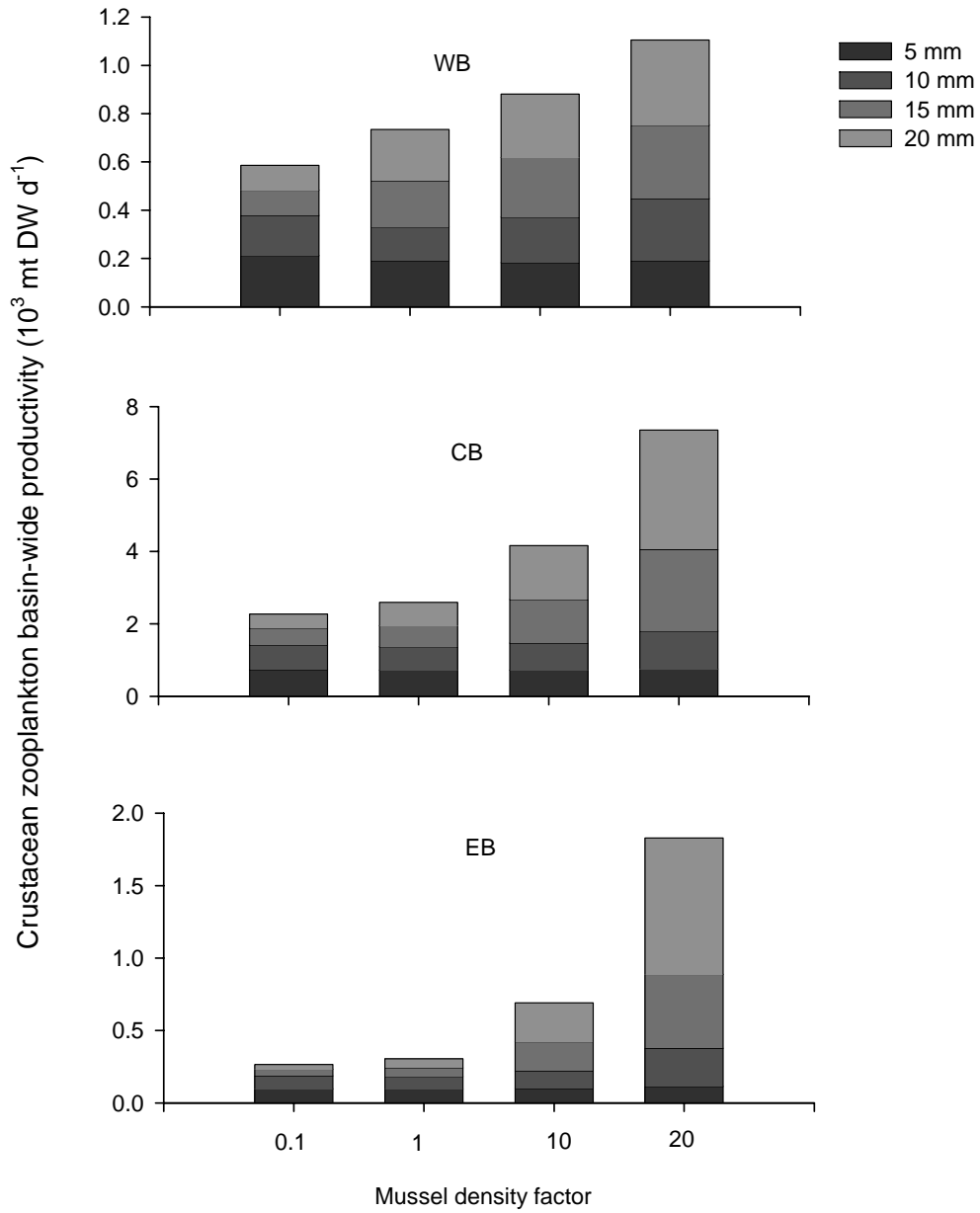


Figure 4.19. As Figure 4.17, but on basin-wide crustacean production.

CHAPTER 5

CONCLUSIONS AND DISCUSSION

Conclusions

In this study, a complex ecological model of Lake Erie, EcoLE, has been built that has physical, chemical and biological components on fine temporal and spatial scales. Data from 1997 are used to calibrate the model, while data from 1998 and 1999 are used to verify the model. We consider our model as an analytical tool rather than as a predictive tool at this point in its development.

Using this model, we have tested 4 hypotheses. I accept hypothesis 1 that hydrodynamics plays an important role in the availability of nutrients to phytoplankton and the availability of phytoplankton to dreissenids. In chapter 2, by turning physical mixing processes on and off, I use the model to explicitly demonstrate that with mixing processes operative, phosphorus, NDEA and diatoms are more abundant in the upper water, and less total dissolved phosphorus (TP-F) accumulated in the whole water column than without; furthermore, the model demonstrate that dreissenids graze fewer algae without mixing processes operative than they do with them. In chapter 4, dreissenids process 20% of western basin water daily, while they graze less than 10% of NDEA and diatoms, because dreissenid grazing impacts are restricted by a bottom boundary layer which weakened mixing processes. However, the phrase of

‘phytoplankton’ in the hypothesis should be changed to ‘non-diatom edible algae (NDEA) and diatoms’. Although the other algal group, non-diatom inedible algae (NDIA, dominated by *Microcystis*) show different spatial distributions depending upon the presence/absence of mixing processes, its biomass in the whole water column changes little. Dreissenids’ direct grazing impacts on NDIA are not investigated because dreissenids selectively reject *Microcystis*.

We reject hypothesis 2 for the western basin that internal phosphorus loading is more important to phytoplankton growth than external loading in terms of availability and quantity, but accept it for the central and eastern basins. In chapter 3, turning off all chemical and biological processes and modifying the model to accumulate the external phosphorus loading over the growing season, the external phosphorus loads reach only as far as the west central basin. By turning on and off external phosphorus loading, the model also showed that external phosphorus loading affects algal biomass and production substantially in the western basin while it has much smaller effects in the central and eastern basins. External phosphorus loads have the same magnitudes of internal phosphorus loads in the western basin but are much smaller than the internal loads in the central and eastern basins.

I reject hypothesis 3 that dreissenids can depress the phytoplankton community in Lake Erie and mask the influence of zooplankton grazing. The basin-wide grazing impacts of dreissenid mussels on NDEA and diatoms are less than 10% of algal biomass in the western basin, and only 1-2% in the central and eastern basins. Furthermore, sensitivity analysis showed that increasing the mussel population would increase NDEA biomass instead of depressing edible algal biomass. However, dreissenids continuously

decrease diatom biomass with increasing population size. Dreissenid grazing cannot mask the influence of zooplankton grazing, because NDEA biomass increases substantially without zooplankton, while diatom biomass decreases considerably due to loss of competition with NDEA.

I accept hypothesis 4 that dreissenids affect the formation of oxygen depletion in the hypolimnion of Lake Erie. It has been discussed that dreissenid mussels increase the oxygen depletion rates in the water by respiration and enforce this increase with their highly rich organic deposit (Effler *et al.* 1998, 2004, Gelda *et al.* 2001). Our simulations suggest that ammonia excreted by dreissenids also could consume a large amount of oxygen in the hypolimnion of the central basin, which has not yet been mentioned by other studies.

Discussion and future studies

Anoxia in the hypolimnion

Our model results show that ammonia excreted by dreissenids can play an important role in the formation of anoxia in the hypolimnion of the central basin. Nitrogen has not received the attention in studies of Lake Erie that it deserves. One reason is that some early models (Vollenweider *et al.* 1980, Chapra 1980) showed that phosphorus was the ultimate cause of anoxia in the hypolimnion, while other models (e.g., Di Toro and Connolly 1980) showed that nitrogen had a negligible effect on formation of anoxia in the hypolimnion of the central basin. Another reason is that control of nitrogen might result in blue-green algal blooms (Schindler 1977). However, things have been

changed. Our model shows that ammonia excretion of dreissenids concentrated in the lower water can consume a large amount of oxygen near the bottom, potentially contributing to early anoxia in the hypolimnion as reported by USEPA in recent years.

Keeping high N:P ratios in dissolved inorganic nutrients in the lake to prevent blue-green algal blooms works for some blue-green algae, like *Aphanizomenon flos-aquae* but seems not to do so for *Microcystis*, which is not a nitrogen-fixer. It might be time to call attention for nitrogen control. However, will reduction in nitrogen external loading mitigate nitrification of mussels' ammonium excreta? We are not sure because the mussels' excretion activities are concentrated in the hypolimnion, while external nitrogen loading likely enters the upper waters of the central basin. Furthermore, decreases of N:P ratios in the upper water might induce other nitrogen-fixing cyanobacteria blooms.

Microcystis

Our model does not have a good simulation of blue-green algae. However, under our model parameter settings, competition patterns among algal groups are interesting. *Microcystis* is not a strong nutrient competitor at all with a lower maximum growth rate and higher phosphorus demands than other groups. As they can grow under low light intensity (Watanabe *et al.* 1996), they developed a big population in the lower water body where nutrients are high. Edwards *et al.* (2005) reported high concentrations of *Microcystis* in the bottom water of the western basin. I postulate that it is not when conditions in the upper water favor *Microcystis* that *Microcystis* is raised to the upper water bodies, but when conditions are adverse or when strong physical mixing occurs.

Pettersson (1998) found that the cyanobacteria *Gloeotrichia echinulata* fertilizes the upper water in Lake Erken, Sweden instead of competing for nutrient with other algae during the summer

Can the effects of dreissenid mussels on Lake Erie phytoplankton be offset by manipulation of external phosphorus loading?

This study showed that the grazing impacts of dreissenids are much less striking than their impacts on nutrient remineralization. At small population sizes, mussels graze NDEA down more than they stimulate the growth of NDEA by nutrient excretion. However, at higher population sizes, mussels' stimulation of NDEA growth by nutrient excretion increases dramatically, and the loss of NDEA due to grazing becomes less noticeable. The exact turning point of mussel population size at which the two processes are identical has not been determined. It is more important to get insights from complex ecological models than the exact numbers. Mussels increase NDIA biomass by selective rejection and, more importantly, by nutrient excretion which is more accessible to NDIA than to other algal groups. Can the effects of mussel nutrient excretion on algae be offset by reduced external phosphorus loading? In the less stratified western basin, which receives the most tributary phosphorus, the external phosphorus loading has a similar magnitude as mussel phosphorus excretion (note the mussel population size). However, in the central and eastern basins, which receive little tributary phosphorus, the external phosphorus loading is much smaller than mussel excretion loading. Reduction in external phosphorus loading might offset mussel nutrient impacts in the western basin, but not in the central and eastern basin. However, here, external phosphorus loading

refers to the phosphorus loaded from monitored tributaries and wastewater treatment plants. Phosphorus from non-monitored non-point sources is not included. As Dolan (1993) pointed out that there was now little room for further reduction of phosphorus loads from point sources, so non-point sources should attract more attention and monitoring.

Spatially, dreissenid mussels' phosphorus excretion is concentrated in lower water strata, whereas external phosphorus enters the upper water. A whole-year or even long-term simulation is needed to investigate this aspect, which should include spring and fall water turnover periods.

Model calibration

Although there are thousands of observation data (input data, initial values of state variables, and observations for calibration and verification) available for our model, they are still sparse for a model with such high temporal and spatial resolutions. Moreover, there are rare measurements about mechanic rates of the biological processes, such as algal growth rates, in complex ecosystems like Lake Erie. There are numerous parameters to calibrate. Usually such models are over-parameterized (Yang 1996, Arthonditsis and Brett 2005). All these makes model calibration and verification difficult, just as Cole and Buchak (1995) suggest:

“Calibration is an iterative process whereby model coefficients are adjusted until an adequate fit of observed versus predicted data is obtained. . . . Unfortunately, there are no hard and fast guidelines for determining when an adequate fit is obtained. There is no good way to evaluate the performance of such models.”

Complex ecological models are simplified ecosystems and are ‘process-oriented’ (Arthonditsis and Brett 2005), which are combinations of many small statistical or empirical models. All these introduce a variety of errors and resulting weak statistical understandability. There were three statistical methods for evaluating the “fit” of a model documented in the 1980s (Di Toro 1983), however, they have seldom used since then. The most commonly used method is to observe the agreement of the model predictions and direct field measurements. The adoption of this poor evaluation approach is rooted in poor calibration methods, given the absence of a mathematical or statistical way to calibrate such complex models. All modelers can do is to keep trying different values of parameters within empirical ranges until a reasonably good agreement is obtained between observed and modeled data. For a model with 50 parameters and 3 test values of each parameter, the full combination would be 3^{50} possible parameterizations, which might not include the best value set of the parameters. Moreover, it is also unknown how to find the best one among the testing sets. Frequently, one state variable obtains a good match, while others might obtain worse ones. Modelers try to find a balanced performance among variables (no one variable gets the best and no one gets the worst). Recent studies tried to increase the mathematics and statistical contributions in calibration. For example, Yang (1996) and Yang *et al.* (2000) used the least squares method to calibrate two biological parameters, maximum growth rates and respiration rates of phytoplankton of a water quality model. Although they only calibrated two parameters for one state variable between two sampling times, they made a nice connection between statistics and calibration of water quality model, i.e., to simplify and break down complex models to small submodels and then to calibrate the most sensitive

parameters. Questions might rise when bringing those broken-down pieces back together. However, this is definitely an area worthy of more efforts. As computing capability increases rapidly, numerical experiments of more complex food web models can be carried out by running the model hundreds of times. For instance, Arhonditsis and Brett (2005) generated 10^5 parameter sets and ran their two-compartment eutrophication model 754 times. The importance of parameters was indicated by the squared semi-partial coefficients of the parameters in the regression models between parameters and state variables. However, they did not mention how their final parameter value set was determined. They argued that because there might be many equally fit sets of parameters due to over-parameterization, there is no use trying to find the single best fit value set of parameter for this class of models. It is more important to use the model to do sensitivity and scenario analysis, unravel model behavior and gain insights of ecosystem processes (Brun *et al.* 2001).

BIBLIOGRAPHY

- Ackerman, J.D., Loewen, M.R., and Hamblin, P.F. 2001. Benthic-Pelagic coupling over a zebra mussel reef in western Lake Erie. *Limnol. Oceanogr.*, 46(4): 892-904.
- Andersen, T., Elser, J.J., and Hessen, D.O. 2004. Stoichiometry and population dynamics. *Ecol. Lett.*, 7: 884-900.
- Andersen, T. and Hessen, D.O. 1991. Carbon, Nitrogen, and phosphorus content of freshwater zooplankton. *Limnol. Oceanogr.*, 36(4): 807-814.
- Anderson, N. J., Jeppesen, E., and Søndergaard, M. 2005. Ecological effects of reduced nutrient loading (oligotrophication) on lakes: an introduction. *Freshwater Biol.*, 1589-1593.
- Arhonditsis, G.B. and Brett, M.T. 2005. Eutrophication model for Lake Washington (USA) Part I. Model description and sensitivity analysis. *Ecol. Model.*, 197: 140-178.
- Arnott, D.L., and Vanni, M.J. 1996. Nitrogen and phosphorus recycling by the zebra mussel (*Dreissena polymorpha*) in the western basin of Lake Erie. *Can. J. Fish. Aquat. Sci.*, 53 (3): 646-659.
- Asaeda, E., and Acharya, K. 2000. Application of individual growth and population models of *Daphnia pulex* to *Daphnia magna*, *Daphnia galeata* and *Bosmina longirostris*. *Hydrobiologia*, 421: 141-155.
- Babcock-Jackson, L. 2000. Toxic *Microcystis* in western Lake Erie: ecotoxicological relationships with three non-indigenous species increase risks to the aquatic community. PhD. Thesis, Department of Evolution, Ecology, and Organismal Biology, The Ohio State University, Columbus, OH.
- Baldwin, B.S., Mayer, M.S., Dayton, J., Pau, N., Mendilla, J., Sullivan, M., Moore, A., Ma, A., and Mills, E.L. 2002. Comparative growth and feeding in zebra and quagga mussels (*Dreissena polymorpha* and *Dreissena bugensis*): implications for North American lakes. *Can. J. Fish. Aquat. Sci.*, 59: 680-694.
- Barbiero, R.P., and Tuchman, M.L. 2004. Long-term dreissenid impacts on water clarity in Lake Erie. *J. Great Lakes Res.*, 30(4): 557-565.
- Beeton, A.M. 2002. Large freshwater lakes: present state, trends, and future. *Environ. Conserv.*, 29: 21-38.

- Bertram, P.E. 1993. Total phosphorus and dissolved oxygen trends in the central basin of Lake Erie, 1970-1991. *J. Great Lakes Res.*, 19(2):224-236.
- Bierman, V.J., Dolan, D.M., Kasprzyk, R., and Clark, J.I. 1984. Retrospective analysis of the response of Saginaw Bay, Lake Huron, to reduction in phosphorus loadings. *Environ. Sci. Technol.*, 18(1):23-31.
- Bierman, V.J., Kaur, J., DePinto, J.V., Feist, T.J., and Dilks, D.W. 2005. Modeling the role of zebra mussels in the proliferation of blue-green algae in Saginaw Bay, Lake Huron. *J. Great Lakes Res.*, 31: 32-55.
- Blanton, J.O. and Winklhofer, R.A. 1972. Physical processes affecting the hypolimnion of the central basin of Lake Erie. *Project Hypo: an intensive study of the Lake Erie central basin hypolimnion and related surface water phenomena*. Canada Centre for Inland Waters, Paper No. 6. United States Environmental Protection Agency, Technical Report, TS-05-71-208-24. February 1972.
- Boegman, L. 1999. Application on a two-dimensional hydrodynamic and water quality model to Lake Erie. M.A.Sc. thesis, Department of Mechanical and Industrial Engineering, University of Toronto, Toronto, Canada.
- Boegman, L., Loewen, M.R., Hamblin, P.F. and Culver, D.A. 2001. Application of a two-dimensional hydrodynamic reservoir model to Lake Erie. *Can. J. Fish. Aquat. Sci.*, 58: 858-869.
- Boegman, L., Loewen, M.R., Culver, D.A., Hamblin, P.F., and Charlton, M.N. 2006. Spatial-dynamic modelling of lower trophic levels in Lake Erie: relative impacts of zebra mussels and nutrient loading. Submitted
- Bolsenga, S.J. and Herdendorf, C.E (Editors), 1993. *Lake Erie and Lake St. Clair Handbook*. Wayne State University Press, Detroit.
- Bonnet, M.P., and Poulin, M. 2002. Numerical modeling of the planktonic succession in a nutrient-rich reservoir: environmental and physiological factors leading to *Microcystis aeruginosa* dominance. *Ecol. Model.*, 156: 93-112.
- Bowie, G.L., Mills, W.B., Porcella, D.B. *et al.* 1985. Rates, constants, and kinetics formulations in surface water quality modeling (2nd ed). U.S. Environmental Protection Agency, Environmental Research Laboratory, Athens, Georgia. EPA/600/3-85/040.
- Brabrand, A., Faafeng, B.A., and Nilssen, J.P.M. 1990. Relative importance of phosphorus supply to phytoplankton production – fish excretion versus external loading. *Can. J. Fish. Aquat. Sci.*, 47(2): 364-372.

- Braidech, T., Gehring, P. and Kleveno, C. 1972. Biological studies related to oxygen depletion and nutrient regeneration processes in the Lake Erie central basin. *Project Hypo: an intensive study of the Lake Erie central basin hypolimnion and related surface water phenomena*. Canada Centre for Inland Waters, Paper No. 6. United States Environmental Protection Agency, Technical Report, TS-05-71-208-24. February 1972.
- Breckling, B., and Dong, Q. 2000. Uncertainty in ecology and ecological modelling. *In Handbook of Ecosystem Theories and Management*. Eds: S.E. Jorgensen and F. Muller. CRC Press LLC, Boca Raton, Florida.
- Brookes, J.D., and Ganf, G.G. 2001. Variations in the buoyancy response of *Microcystis aeruginosa* to nitrogen, phosphorus and light. *J. Plank. Res.*, 23: 1399-1411.
- Brookes, J.D., Ganf, G.G., and Burch, M.D. 1998. Buoyancy regulation of *Microcystis aeruginosa*. *Verh. Internat. Verein. Limnol.*, 26: 1670-1673.
- Brun, R., Reichert, P., and Künsch, HR. 2001. Practical identifiability analysis of large environmental simulation models. *Water Resource Res.*, 37: 1015-1030.
- Bunnell, D.B., Johnson, T.B., and Knight, C.T. 2005. The impact of introduced round gobies (*Neogobius melanostomus*) on phosphorus cycling in central Lake Erie. *Can. J. Fish. Aquat. Sci.*, 62(1): 15-29.
- Bunt, C.M., MacIsaac, H.J., and Sprules, W.G. 1993. Pumping rates and projected filtering impacts of juvenile zebra mussels (*Dreissena polymorpha*) in the western Lake Erie. *Can. J. Fish. Aquat. Sci.*, 50(5): 1017-1022
- Burns, N.M. 1976. Temperature, oxygen, and nutrient distribution patterns in Lake Erie, 1970. *J. Fish. Res. Board Can.*, 33: 485-511.
- Burns, N.M., and Ross, C. 1971. Nutrient relationships in a stratified eutrophic lake. *Proc. Conf. Great Lakes Res., Int. Assoc. Great Lakes Res.*, 14: 749-760.
- Burns, N.M., and Ross, C. 1972. Project hypo-an introduction. *Project Hypo: an intensive study of the Lake Erie central basin hypolimnion and related surface water phenomena*. Canada Centre for Inland Waters, Paper No. 6. United States Environmental Protection Agency, Technical Report, TS-05-71-208-24. February 1972.
- Carlotti, F., and Sciandra, A. 1989. Population dynamics model of *Euterpina acutifrons* (copepoda: Harpacticoida) coupling individual growth and larval development. *Mar. Ecol.-Prog. Ser.*, 56: 225-242
- Carlotti, F., and Wolf, K.U. 1998. A Lagrangian ensemble model of *Calanus finmarchicus* coupled with a 1-D ecosystem model. *Fish. Oceanogr.*, 7:191-204.

- Carlotti, F., Giske, J., and Werner, F. 2000 . Modeling zooplankton dynamics. *In ICES Zooplankton Methodology Manual*. Edited by R. Harris, P. Lenz, H.R., Skjoldal, and M. Huntley. Academic Press, San Diego. 684PP.
- Chapra, S.C. 1979. Application of the phosphorus loading concept to the Great Lakes. Proceedings of the 1979 Conference on Phosphorus Management Strategies for Lakes, New York, pp. 135-152.
- Chapra, S.C. and Robertson, A. 1977. Great Lakes eutrophication: the effect of point source control of total phosphorus. *Science*, 196: 1448-1450.
- Chen, C., Ji, R., Schwab, D.J., Beletsky, D. *et al.* 2002. A model study of the coupled biological and physical dynamics in Lake Michigan. *Ecol. Model.*, 152: 145-168.
- Cole, T.M. and Buchak, E.M. 1995. *CE-QUAL-W2: A two-dimensional, laterally averaged, hydrodynamic and water quality model, version 2.0: User manual*. Instruction Report EL-95-1, US Army Corps of Engineers, Washington, DC 20314-1000.
- Cole, T.M., and Wells, S.A. 2003. *CE-QUAL-W2: A two-dimensional, laterally averaged, hydrodynamic and water quality model, version 3.1: User manual*. Instruction Report EL-03-1, US Army Corps of Engineers, Washington, DC 20314-1000.
- Conroy, J.D. and Culver, D.A. 2005. Do dreissenids affect Lake Erie ecosystem stability processes? *Am. Midl. Nat.*, 153: 20-32.
- Conroy, J.D., Kane, D.D., Dolan, D.M., Edwards, W.J., Charlton, M.N., and Culver. D.A. 2005a. Temporal trends in Lake Erie plankton biomass: roles of external phosphorus loading and dreissenid mussels. *J. Great Lakes Res.*, 31(Suppl. 2): 89-110.
- Conroy, J.D., Edwards, W.J., Pontius, R.A., Kane, D.D., Zhang, H., Shea, J.F., Richey, J.N., and Culver, D.A. 2005b. Soluble nitrogen and phosphorus excretion of exotic freshwater mussels (*Dreissena* spp.): potential impacts for nutrient remineralization in western Lake Erie. *Freshwater Biol.*, 50: 1146-1162.
- Cox, P.M, Betts, R.A., Jones, C.D., Spall, S.A., and Totterdell, I.J. 2000. Acceleration of global warming due to carbon-cycle feedbacks in a coupled climate model. *Nature*, 408: 184-187.
- Culver, D.A. 2000. Ecological modeling of Lake Erie trophic dynamics – 1999. *In Great Lakes Modeling Focus on Lake Erie*. Council of Great Lakes Research Managers. 2000. Edited by L.A. Tulen and J.V. DePinto. International Joint Commission, Windsor, Ontario.

- Davis, C.C. 1964. Evidence for the eutrophication of Lake Erie from phytoplankton records. *Limnol. Oceanogr.*, 9 (3): 275-283.
- Deneke, R, and Nixdorf, B. 1999. On the occurrence of clear-water phases in relation to shallowness and trophic state: a comparative study. *Hydrobiologia*, 409: 251-262.
- DePinto, J.V., Young, T.C., and Martin, S.C. 1981. Algal-available phosphorus in suspended sediments from Lower Great Lakes tributaries. *J. Great Lakes Res.*, 7(3): 311-325.
- DePinto, J.V., Bierman, V.J, Feist, T.J, and Kaur, J. 2000. Conceptualization of an aquatic ecosystem model for integrated management of Lake Erie. Great Lakes Modeling Summit: Focus on Lake Erie. Council of Great Lakes Research Managers. 2000. International Joint Commission, Windsor, Ontario.
- Di Toro, D.M. 1983. Documentation for water quality analysis simulation program (WASP) and model verification program (MVP). For USEPA, Duluth, MN, 68-01-3872.
- Di Toro, D.M., O'Connor, D.J., Mancini, J.L., and Thomann, R.V. 1973. A preliminary phytoplankton-zooplankton-nutrient models of western Lake Erie. IN: *Systems Analysis and Simulation in Ecology*, Vol 3, Academic Press.
- Di Toro, D.M., and Connolly, J.P. 1980. Mathematical models of water quality in large lakes. Part 2: Lake Erie. USEPA, Office of Research and Development, ERL-Duluth, LLRS, Grosse Ile, MI. EPA Ecological Research Series EPA-600/3-80-065.
- Dobson, H.H. and Gilbertson, M. 1972. Oxygen depletion in the hypolimnion of the central basin Lake Erie, 1929 to 1970. In N.M. Burns and C. Ross (Editors), *Project Hypo: an intensive study of the Lake Erie central basin hypolimnion and related surface water phenomena*. Canada Centre for Inland Waters, Paper No. 6. United States Environmental Protection Agency, Technical Report, TS-05-71-208-24. February 1972. pp. 3-8.
- Dolan, D.M. 1993. Point source loadings of phosphorus to Lake Erie: 1986-1990. *J. Great Lakes Res.*, 19:212-223
- Edwards, W.J. 2002. Impacts of the zebra mussel (*Dreissena polymorpha*) on large lakes: influence of vertical turbulent mixing. PhD. Thesis, Department of Evolution, Ecology, and Organismal Biology, The Ohio State University, Columbus, OH.
- Edwards, W.J., Rehmann, C.R., McDonald, E., and Culver, D.A. 2005. The impact of a benthic filter feeder: limitations imposed by physical transport of algae to the benthos. *Can. J. Fish. Aquat. Sci.*, 62:205-214.

- Effler, S.W., Boons, S.R., Siegfried, C.A., Walrath, L. and Ashby, S.L. 1997. Mobilization of ammonia and phosphorus by zebra mussels (*Dreissena polymorpha*) in the Seneca River, New York. In: F.M. D'Itri (Editor), *Zebra Mussels and Aquatic Nuisance Species*. Ann Arbor Press Inc., Chelsea, MI, pp. 187-207.
- Effler, S.W., Boone, S.R., Siegfried, C.A., and Ashby, S.L. 1998. Dynamics of zebra mussel oxygen demand in Seneca River, New York. *Environ. Sci. Technol.*, 32(6): 807-812.
- Effler, S.W., Matthews, D.A., Brooks-Matthews, C.M., Perkins, M.G., Siegfried, C.A., and Hassett, J.M. 2004. Water quality impacts and indicators of metabolic activity of the zebra mussel invasion of the Seneca River. *J. Am. Water Resour. As.*, 40(3): 737-754.
- Elser, J.J., Sterner, R.W., Galford, A.E., Chrzanowski, T.H, Findlay, D.L., Mills, K.H., Paterson, M.J., Stainton, M.P., and Schindler, D.W. 2000. Pelagic C:N:P stoichiometry in eutrophied lake: responses to a whole-lake food-web manipulation. *Ecosystems*, 3: 293-307.
- Fanslow, D.L., Nalepa, T.F, and Lang, G.A. 1995. Filtration rates of the zebra mussel (*Dreissena polymorpha*) on natural seston from Saginaw Bay, Lake Huron. *J. Great Lakes Res.*, 21(4):489-500.
- Fennel, W. 2001. Modeling of copepods with links to circulation models. *J. Plankton Res.*, 23:1217-1232.
- Fennel, W and Neumann, T. 2003. Variability of copepods as seen in a coupled physical-biological model of the Baltic Sea. *ICES Mar. Sci. Symosia*, 216:1-12.
- Gardner, W.S., Cavaletto, J.F., Johengen, T.H., Johnson, J.R., Heath, R.T., and Cotne, Jr., J.B. 1995. Effects of the zebra mussel, *Dreissena polymorpha*, on community nitrogen dynamics in Saginaw Bay, Lake Huron. *J. Great Lakes Res.*, 21(4): 529-544
- Garton, D.W., and Haag, W.R. 1993. Seasonal reproductive cycles and settlement patterns of *Dreissena polymorpha* in western Lake Erie. In T.F. Nalepa and D.W. Schloesser (Editors), *Zebra Mussels: biology, impacts, and control*. Lewis Publishers, Ann Arbor, MI, pp. 111-128
- Garnier, J., Billen, G., and Palfner, L. 2000. Understanding the oxygen budget and related ecological processes in the river Mosel: the RIVERSTRAHLER approach. *Hydrobiologia*, 410: 151-166.
- Gelda, R.K., Effler, S.W., and Owens, E.M. 2001. River dissolved oxygen model with zebra mussel oxygen demand (ZOD). *J. Environ. Eng. –ASCE*, 127(9): 790-801.

- Gilbertson, M., Dobson, H.H., and Lee, T.R. 1972. Appendix III - Phosphorus and hypolimnial dissolved oxygen in Lake Erie. *Project Hypo: an intensive study of the Lake Erie central basin hypolimnion and related surface water phenomena*. Canada Centre for Inland Waters, Paper No. 6. United States Environmental Protection Agency, Technical Report, TS-05-71-208-24. February 1972.
- Goma, R.H., Aizaki, M., Fukushima, T., and Otsuki, A. 1996. Significance of zooplankton grazing activity as a source of dissolved organic nitrogen, urea and dissolved free amino acids in a eutrophic shallow lake : experiments using outdoor continuous flow pond systems. *Jpn. J. Limnol.*, 57: 1-13.
- Gopalan, G., Culver, D.A., Wu, L., and Trauben, B.K. 1998. Effects of recent ecosystem changes on the recruitment of young-of-the-year fish in western Lake Erie. *Can. J. Fish. Aquat. Sci.*, 55: (12) 2572-2579
- Gregor, D.J., and Johnson, M.G. 1979. Nonpoint source phosphorus inputs to the Great Lakes. *Proceedings of the 1979 Conference on Phosphorus Management Strategies for Lakes*, New York, pp. 33-59.
- Griffiths, R.W., Schloesser, D.W., Leach, J.H., and Kovalak, W.P. 1991. Distribution and dispersal of the zebra mussel (*Dreissena polymorpha*) in the Great Lakes region. *Can. J. Fish. Aquat. Sci.*, 48: 1381-1388.
- Gulati, R.D., C.P.Martinez, and K. Siewertsen. 1995. Zooplankton as a compound mineralizing and synthesizing system: phosphorus excretions. *Hydrobiologia.*, 315:25-37.
- Gurney, W.S., McCauley, E., Nisbet, R.M., and Murdoch, W.W. 1990. The physiological ecology of *Daphnia*: a dynamic model of growth and reproduction. *Ecology*, 71(2):716-732.
- Haltuch, M.A., Berkman, P.A., Garton, D.W. 2000. Geographic information system (GIS) analysis of ecosystem invasion: Exotic mussels in Lake Erie. *Limnol. Oceanogr.*, 45(8): 1778-1787.
- Hamblin, P.F. 1987. Meteorological forcing and water level fluctuations on Lake Erie. *J. Great Lakes Res.*, 13: 436-453.
- Hantke, B., Fleischer, P., Domany, I., Koch, M., Pless, P., Wiendl, M., and Melzer, A. 1996. P-release from DOP by phosphatase activity in comparison to P excretion by zooplankton: studies in hard water lakes of different trophic levels. *Hydrobiologia*, 317: 151-162.
- Hartley, R.P. and Potos, C.P. 1971. Algal-temperature-nutrient relationships and distribution in Lake Erie. Environment Protection Agency, Water Quality Office Region V, Lake Erie Basin. February.

- Heath, R.T., Fahnenstiel, G.L., Gardner, W.S., Cavaletto, J.F., and Hwang, S.J. 1995. Ecosystem-level effects of zebra mussels (*Dreissena polymorpha*): An enclosure experiment in Saginaw Bay, Lake Huron. *J. Great Lakes Res.*, 21: 501-516.
- Hebert, P.D.N., Muncaster, B.W., and Mackie, G.L. 1989. Ecological and genetic studies on *Dreissena polymorpha* (Pallas): a new mollusk in the Great Lakes. *Can. J. Fish. Aquat. Sci.*, 46: 1587-1591.
- Hesse, K. and Kohl, J. 2001. Effect of light and nutrient supply on growth and microcystin content of different strains of *Microcystis aeruginosa*. *In* Cyanotoxins – occurrence, causes, consequences. *Edited* by I. Chorus. Springer-Verlag Berlin Heidelberg, Germany.
- Holland, R.E. 1993. Changes in planktonic diatoms and water transparency in Hatchery Bay, Bass Island area, western Lake Erie since the establishment of the zebra mussel. *J. Great Lakes Res.*, 19: 717-724.
- Holland, R.E., Johengen, T.H., and Beeton, A.M. 1995. Trends in nutrient concentrations in Hatchery Bay, western Lake Erie, before and after *Dreissena polymorpha*. *Can. J. Fish. Aquat. Sci.*, 52: 1202-1209.
- Horgan, M.J., and Mills, E.L. 1997. Clearance rates and filtering activity of zebra mussel (*Dreissena polymorpha*): implications for freshwater lakes. *Can. J. Fish. Aquat. Sci.*, 54: 249-255.
- Houghton, J.T. 1997. *Global Warming: the complete briefing*. Cambridge University Press, Cambridge, N.Y.
- Howard, A. 2001. Modeling movement patterns of the cyanobacterium, *Microcystis*. *Ecol. Appl.*, 11: 304-310.
- Hudson, J.J., Taylor, W.D., and Schindler, D.W. 2000. Phosphate concentrations in lakes. *Nature*, 406(6) 54-56.
- Hudson, J.J., Taylor, W.D., and Schindler, D.W. 1999. Planktonic nutrient regeneration and cycling efficiency in temperate lakes. *Nature*, 400: 659-661.
- Hwang, S.-J. 1995. Carbon dynamics of plankton communities in nearshore and offshore Lake Erie: The significance of the microbial loop for higher trophic levels. PhD Dissertation, Kent State University, Kent, OH.
- Hwang, S.-J., and Heath, R.T. 1999. Zooplankton bacterivory at coastal and offshore sites of Lake Erie. *J. Plankton Res.*, 21(4): 699-719.
- Idrisi, N., Mills, E.L., Rudstam, L.G., and Stewart, D.J. 2001. Impact of zebra mussels (*Dreissena polymorpha*) on the pelagic lower trophic levels of Oneida Lake, New York. *Can. J. Fish. Aquat. Sci.*, 58: 1430-1441.

- Imberger, J. 1998. Flux paths in a stratified lake: a review. *In physical process in lakes and oceans. Edited by J. Imberger. Coast. Estuar. Stud.*, 54: 1-18.
- James, W.F., Barko, J.W., Eakin, H.L. 1997. Nutrient regeneration by the zebra mussel (*Dreissena polymorpha*). *J. Freshwater Ecol.*, 12(2): 209-216.
- Jarvis, P., Dow, J., Dermott, R. and Bonnell, R. 2000. Zebra (*Dreissena polymorpha*) and quagga mussel (*Dreissena bugensis*) distribution and density in Lake Erie, 1992-1998. *Can. Tech. Rep. Fish. Aquat. Sci.*, 2304: 46P.
- Jin, X. 2003. Analysis of eutrophication state and trend for lakes in China. *J. Limnol.*, 62(2): 60-66.
- Jorgensen, S.E., Nielsen, S.N., and Jorgensen L.A. 1991. *Handbook Of Ecological Parameters And Ecotoxicology*. Elsevier publish.
- Johannsson, O.E., Dermott, R., Graham, D.M., Dahl, J.A., Millard, E.S., Myles, D.D., and LeBlanc, J. 2000. Benthic and pelagic secondary production in Lake Erie after the invasion of *Dreissena* spp. with implications for fish production. *J. Great Lakes Res.*, 26(1):31-54.
- Johengen, T.H., Nalepa, T.F., Fahnenstiel, G.L., and Goudy, G. 1995 Nutrient changes in Saginaw Bay, Lake Huron, after the establishment of the zebra mussel (*Dreissena polymorpha*). *J. Great Lakes Res.*, 21: 449-464.
- Jørgensen, S.E., and Müller, F. 2000. *Handbook of Ecosystem theories and management*. CRC Press, Boca Raton, FL.
- Jørgensen, S.E., Nielsen, S.N., and Jørgensen L.A. 1991. *Handbook of Ecological Parameters and Ecotoxicology*. Elsevier publish.
- Kemp, A.L.W., Thomas, R.L., Dell, C.I., and Jaquet, J-M. 1976. Cultural impact on the geochemistry of sediments in Lake Erie. *J. Fish. Res. Board Can.*, 33: 440-462.
- Knoll, L.B., Vanni, M.J., Renwick, W.H. 2003. Phytoplankton primary production and photosynthetic parameters in reservoirs along a gradient of watershed land use. *Limnol. Oceanogr.*, 48(2): 608-617.
- Kronratev, G.P. 1963. O nekotoryh osobennostjah filtracii u presnovodnyh molljuskov. *Nauncnye doklady vysszej skoly Biol Nauki (Moskow)*, 1: 13-16.
- Kreis, J.R.G. 2000. Integrated ecosystem response models for Lake Erie. *In Great Lakes Modeling Focus on Lake Erie. Council of Great Lakes Research Managers. 2000. Edited by L.A. Tulen and J.V. DePinto. International Joint Commission, Windsor, Ontario.*
- Krieger, K.A., Schloesser, D.W., Manny, B.A., Trisler, C.E., Heady, S.E., Ciborowski, J.J.H., and Muth, K.M. 1996. Recovery of burrowing mayflies (Ephemeroptera:

- Ephemerae: *Hexagenia*) in western Lake Erie. J. Great Lakes Res., 22(2): 254-263.
- Kryger, J., and Riisgard, H.U. 1988. Filtration rate capacities in 6 species of European freshwater bivalves. Oecologia, 77: 34-38.
- Lam, D.C., Schertzer, W.M., and Fraser, A.S. 1987. Oxygen depletion in Lake Erie: modeling the physical, chemical, and biological interactions, 1972 and 1979. J. Great Lakes Res., 13(4):770-781.
- Lam, D.C.L., Schertzer, W.M., and Fraser, A.S. 1983. Simulation of Lake Erie water quality responses to loading and weather variations. Scientific series No. 134. National Water Research Institute, Inland Waters Directorate, Canada Center for Inland Waters, Burlington, Ontario.
- Lashof, D.A., and Ahuja, D.R. 1990. Relative contributions of greenhouse gas emissions to global warming. Nature, 344: 529-531.
- Lathrop, R.C. 1999. Summer water clarity responses to phosphorus, *Daphnia* grazing, and internal mixing in Lake Mendota. Limnol. Oceanogr., 44(1): 137-146.
- Leach, J. H. 1993. Impacts of the zebra mussel (*Dreissena polymorpha*) on water quality and fish spawning reefs in western Lake Erie. In Zebra Mussels: Biology, Impacts, and Control. Edited by T.F. Nalepa and D.W. Schloesser, Lewis Publishers/CRC press, Boca Raton, FL.: pp381-397.
- Lean, D.R. 1973. Phosphorus dynamics in lake water. Science, 179: 678-680.
- Lucas, A.M., and Thomas, N.A. 1972. Sediment Oxygen Demand in Lake Erie's Central basin, 1970. In Project Hypo—an intensive study of the Lake Erie central basin hypolimnion and related surface water phenomena. Edited by N.M. Burns and C.Ross. p45.
- Ludsin, S.A., Kershner, M.W., Blocksom, K.A., Knight, R.L., and Stein, R.A. 2001. Life after death in Lake Erie: nutrient controls drive fish species richness, rehabilitation. Ecol. Appl., 11(3): 731-746.
- MacIsaac, H.J. and Rocha, R. 1995. Effects of suspended clay on zebra mussel (*Dreissena polymorpha*) faeces and pseudofaeces production. Arch. Hydrobiol., 135: 53-64.
- MacIsaac, H.J., Sprules, W.G., and Leach, J.H. 1991. Ingestion of small-bodied zooplankton by zebra mussels (*Dreissena polymorpha*): can cannibalism on larvae influence population dynamics? Can. J. Fish. Aquat. Sci., 48: 2051-2060.
- MacIsaac, H.J., Johannsson, O.E., Ye, J., Sprules, W.G., Leach, J.H., McCorquodale, J.A. and Grigorovich, I.A. 1999. Filtering impacts of an introduced biovalve

- (*Dreissena polymorpha*) in a shallow lake: application of hydrodynamic model. *Ecosystems*, 2: 338-350.
- MacIsaac, H.J., Sprules, W.G., Johannsson, O.E., and Leach, J.H. 1992. Filtering impacts of larval and sessile zebra mussels (*Dreissena polymorpha*) in western Lake Erie. *Oecologia*, 92(1): 30-39.
- Makarewicz, J.C. 1993. Phytoplankton biomass and species composition in Lake Erie, 1970 to 1987. *J. Great Lakes Res.*, 19: 285-274.
- Makarewicz, J. C., and Bertram, P. 1991. Evidence for the restoration of the Lake Erie North America ecosystem: water quality oxygen levels and pelagic function appear to be improving. *Bioscience*, 41:216-223.
- Makarewicz, J.C., Bertram, P., and Lewis, T.W. 2000. Chemistry of the offshore surface waters of Lake Erie: Pre- and post-Dreissena introduction (1983-1993). *J. Great Lakes Res.*, 26: (1) 82-93.
- Mathias, J.A., and Barica, J. 1980. Factors controlling oxygen depletion in ice-covered lakes. *Can. J. Fish. Aquat. Sci.*, 37:185-194.
- May, B., and Marsden, J.E. 1992. Genetic identification and implications of another invasive species of dreissenid mussel in the Great Lakes. *Can. J. Fish. Aquat. Sci.*, 49: 1501-1506.
- McCauley, E.W., Murdoch, W.W., Nisbet, R.M. and Gurney, W.S. 1990. The physiological ecology of *Daphnia*: development of a model of growth and reproduction. *Ecology*, 71:703-715.
- McCauley, E.W., Nisbet, R.M., de Roos, A.M., Murdoch, W.W., and Gurney, W.S. 1996. Structured population models of herbivorous zooplankton. *Ecol. Monogr.*, 66(4):479-501.
- McCune, K.C. 1998. Temperature gradient microprofiling in the central basin of Lake Erie: a study of vertical turbulent processes. Thesis. The Ohio State University.
- McGucken, W. 2000. Lake Erie rehabilitated: controlling cultural eutrophication, 1960s-1990s. Akron, Ohio. The University of Akron Press.
- Mellina, E., Rasmussen, J.B., and Mills, E.L. 1995. Impact of zebra mussel (*Dreissena polymorpha*) on phosphorus cycling and chlorophyll in lakes. *Can. J. Fish. Aquat. Sci.*, 52:2553-2573.
- Micheev, V.P. 1966. O skorosti fil tracii vody Drejessenoj. *Tr. Inst. Biol. Vodokhran Akad Nauk SSSR*, 12: 134-138.
- Mills, E.L., Chrisman, J.R., Baldwin, B.S., Howell, T., Owens, R.W., O’Gorman, R. Roseman, E.F., and Raths, M.K. 1999. Changes in the dreissenid community

- and a shift toward dominance of the quagga mussel (*Dreissena bugensis*) in the lower Great Lakes. *J. Great. Lakes Res.*, 25: 187-197.
- Moegenburg, S.M., and Vanni, M.J. 1991. Nutrient regeneration by zooplankton: effects on nutrient limitation of phytoplankton in a eutrophic lake. *J. Plankton Res.*, 13: 573-588.
- Mortimer, C.H. 1941. The exchange of dissolved substances between mud and water in Lakes (Parts I and II). *J. Ecol.*, 29: 280-329.
- Mortimer, C.H. 1971. Chemical exchanges between sediments and water in the Great Lakes – speculations on probable regulatory mechanisms. *Limnol. Oceanogr.*, 16: 387-404.
- Neumann, D., Borcharding, J., and Jantz, B. 1993. Growth and seasonal reproduction of *Dreissena polymorpha* in the Rhine River and adjacent waters. In: T.F. Nalepa and D.W. Schloesser (Editors), *Zebra mussels: biology, impacts, and control*. Lewis Publishers, Boca Raton, FL, pp. 95-110.
- Nicholls, K.H. 1997. Planktonic green algae in western Lake Erie: the importance of temporal scale in the interpretation of change. *Freshwater Biol.*, 38: 419-425.
- Nicholls K.H., Heintsch, L., and Carney, E. 2002. Univariate step-trend and multivariate assessments of the apparent effects of P loading reductions and zebra mussels on the phytoplankton of the Bay of Quinte, Lake Ontario. *J. Great Lakes Res.*, 28(1): 15-31.
- Nicholls, K.H., and Hopkins, G.J. 1993. Recent changes in Lake Erie (north shore) phytoplankton: cumulative impacts of phosphorus loading reduction and the zebra mussel introduction. *J. Great Lakes Res.*, 19: 637-647.
- Nicholls, K.H., Hopkins, G.J., and Standke, S.J. 1999. Reduced chlorophyll to phosphorus ratios in nearshore Great Lakes waters coincide with the establishment of dreissenid mussels. *Can. J. Fish. Aquat. Sci.*, 52: 153-161.
- Nicholls K.H., Hopkins, G.J., Standke, S.J., and Nakamoto, L. 2001. Trends in total phosphorus in Canadian near-shore waters of the Laurentian Great Lakes: 1976-1999. *J. Great Lakes Res.*, 27(4): 402-422.
- Olsen, Y. and Ostgaard, K. 1985. Estimating release rates of phosphorus from zooplankton: model and experimental verification. *Limnol. Oceanogr.*, 30(4):844-852.
- Pace, M.L., Findlay, S.G., and Fischer, D. 1998. Effects of an invasive bivalve on the zooplankton community of the Hudson River. *Freshwater Biol.*, 39: 103-116.

- Padilla, D.K., Adolph, S.C., Cottingham, K. L., and Schneider, D.W. 1996. Predicting the consequences of dreissenid mussels on a pelagic food web. *Ecol. Model.*, 85: 129-144.
- Pearl, H.W. 1988. Nuisance phytoplankton blooms in coastal, estuarine, and inland waters. *Limnol. Oceanogr.*, 33: 823-847.
- Peters, R.H. 1981. Phosphorus availability in Lake Memphremagog and its tributaries. *Limnol. Oceanogr.*, 26(6): 1150-1161.
- Pettersson, K. 1998. Mechanisms for internal loading of phosphorus in lakes. *Hydrobiologia*, 373/374: 21-25.
- Phillips, G., Kelly, A., Pitt, J., Sanderson, R., and Taylor, E. 2005. The recovery of a very shallow eutrophic lake, 20 years after the control of effluent derived phosphorus. *Freshwater Biol.*, 50: 1628-1638.
- Pontius, R. A. 2000. The impact of zebra mussels (*Dreissena polymorpha*) on pelagic food webs. PhD. Thesis, Department of Evolution, Ecology, and Organismal Biology, The Ohio State University, Columbus, OH.
- Richards, R.P. and Baker, D.B. 1993. Trends in nutrient and suspended sediment concentrations in Lake Erie tributaries, 1975-1990. *J. Great Lakes. Res.*, 19:200-211.
- Rinta-Kanto, I.M., Ouellette, A.J.A., Boyer, G.L., Twiss, M.R., Bridgeman, T.B., and Wilhelm, S.W. 2005. Quantification of toxic *Microcystis* spp. during the 2003 and 2004 blooms in western Lake Erie using quantitative real-time PCR. *Environ. Sci. Technol.*, 39(11): 4198-4205.
- Rockwell, D.C., Salisbury, D.K., and Lesht, B.M. 1989. Water quality in the middle Great Lakes: results of the 1985 USEPA survey of lakes Erie, Huron and Michigan. Rep. No. EPA 605/6-89-001. U.S. Environmental Protection Agency, Great Lakes National Program Office. 230 South Dearborn, Chicago, IL 60604.
- Rodgers, P.W. And Salisbury, D. 1981. Water quality modeling of Lake Michigan and consideration of the anomalous ice cover of 1976-1977. *J. Great Lakes Res.*, 7(4):467-480.
- Rodhe, H. 1990. A comparison of the contribution of various gases to the greenhouse effect. *Science*, 248 (4960): 1217-1219.
- Roe, S.L., and MacIsaac, H.J. 1997 Deepwater population structure and reproductive state of quagga mussels (*Dreissena bugensis*) in Lake Erie. *Can. J. Fish. Aquat. Sci.*, 54: 2428-2433.
- Romare P, Bergman E., and Hansson LA. 1999. The impact of larval and juvenile fish on zooplankton and algal dynamics. *Limnol. Oceanogr.*, 44(7):1655-1666.

- Scavia, D. 1980. An ecological model of Lake Ontario. *Ecol. Model.*, 8: 49-78.
- Scavia, D., Lang, G.A. and Kitchell, J.F. 1988. Dynamics of Lake Michigan plankton: a model evaluation of nutrient loading, competition, and predation. *Can. J. Fish Aquat. Sci.*, 45: 165-177.
- Scavia, D. and Chapra, S.C. 1977. Comparison of an ecological model of Lake Ontario and phosphorus loading models. *J. Fish. Res. Board Can.*, 34: 286-290.
- Schaus, M.H., Vanni, M.J., Wissing, T.E., Bremigan, M.T., Garvey, J.E., and Stein, R.A. 1997. Nitrogen and phosphorus excretion by detritivorous gizzard shad in a reservoir ecosystem. *Limnol. Oceanogr.*, 42(6): 1386-1397.
- Schertzer, W.M., Saylor, J.H., Boyce, F.M., Robertson, D.G., and Rosa, F. 1987. Seasonal thermal cycle of Lake Erie. *J. Great Lakes Res.*, 13: 468-486.
- Schindler, D.W. 1977. Evolution of phosphorus limitation in lakes. *Science*, 195: 260-262.
- Schloesser, D.W., and Nalepa, T.F. 2001. Changing abundance of *Hexagenia* mayfly nymphs in western Lake Erie of the Laurentian Great Lakes: impediments to assessment of Lake recovery? *Int. Rev. Hydrobiol.*, 86: 87-103.
- Seo, D. and Canale, R.P. 1996. Performance, reliability and uncertainty of total phosphorus models for lakes –I. Deterministic analysis. *Water. Res.*, 30(1): 83-94.
- Sly, P.G. 1976. Lake Erie and its basin. *J. Fish. Res. Board Can.*, 33: 355-370.
- Smith, V.H. 1982. The nitrogen and phosphorus dependence of algal biomass in lakes: An empirical and theoretical analysis. *Limnol. Oceanogr.*, 27(6):1101-1112.
- Sonzogni, W.C., Uttormark, P.D., and Lee, G.F. 1976. The phosphorus residence time model. *Water Res.*, 10:429-435.
- Sprules, W.G., Johannsson, O.E., Millard, E.S., Munawar, M., Stewart, D.S., Tyler, J., Dermontt, R., Whipple, S.J., Legner, M., Morris, T.J., Ghar, D., and Jech, J.M. 2000. Trophic transfer in Lake Erie: a whole food web modeling perspective. Great Lakes Modeling Summit: Focus on Lake Erie. Council of Great Lakes Research Managers. 2000. International Joint Commission, Windsor, Ontario.
- Sprung, M. 1989. Field and laboratory observations of *Dreissena polymorpha* larvae: abundance, growth, mortality and food demands. *Arch. Hydrobiol.*, 115:537-561.
- Steele, J.H. 1962. Environmental control of photosynthesis in the sea. *Limnol. Oceanogr.*, 7: 137-150.

- Stepien , C.A., Taylor, C.D., and Dabrowsky, K.A. 2002. Genetic variability and phylogeographical patterns of a nonindigenous species invasion: a comparison of exotic vs. native zebra and quagga mussel populations. *J. Evol. Biol.*, 15(2002) 314-328.
- Stoeckmann, A. 2003. Physiological energetics of Lake Erie dreissenid mussels: a basis for the displacement of *Dreissena polymorpha* by *Dreissena bugensis*. *Can. J. Fish. Aquat. Sci.*, 60: 126-134.
- Søndergaard, M., Jensen, J.P., and Jeppesen, E. 1999. Internal phosphorus loading in shallow Danish lakes. *Hydrobiologia*, 408/409: 145-152.
- Søndergaard, M, Jensen, J.P., and Jeppesen, E. 2005. Seasonal response of nutrients to reduced phosphorus loading in 12 Danish lakes. *Freshwater Biol.*, 50: 1605-1615.
- Talling, J.F. 2003. Phytoplankton-zooplankton seasonal timing and the 'clear-water phase' in some English lakes. *Freshwater Biol.*, 48(1):39-52.
- Thornton, K.W. and Lessem, A.S. 1978. A temperature algorithm for modifying biological rates. *T. Am. Fish. Soc.*, 107(2): 284-287.
- Tyson, J.T. and Knight, R.L. 2001. Response of yellow perch to changes in the benthic invertebrate community of western Lake Erie. *T. Am. Fish. Soc.*, 130: 766-782.
- Urabe, J., Nakanishi, M., Kavabata, K. 1995. Contribution of metazoan plankton to the cycling of nitrogen and phosphorus in Lake Biwa. *Limnol. Oceanogr.*, 40(2): 232-241.
- Vadstein, O., Brekke, O., Andersen, T., and Olsen, Y. 1995. Estimation of phosphorus release rates from natural zooplankton communities feeding on planktonic algae and bacteria. *Limnol. and Oceanogr.*, 40(2): 250-262.
- Vanderploeg, H.A., Liebig, J.R., Carmichael, W.W., Age, M.A., Johengen, T.H., Fahnenstiel, G.L., Nalepa, T.F. 2001. Zebra mussel (*Dreissena polymorpha*) selective filtration promoted toxic *Microcystis* blooms in Saginaw Bay (Lake Huron) and Lake Erie. *Can. J. Fish. Aquat. Sci.*, 58: 1208-1221.
- Vanni, M.J. 2002. Nutrient cycling by animals in freshwater ecosystems. *Annu. Rev. Ecol. Syst.*, 33: 341-370.
- Vanni, M.J., Bowling, A.M., Dickman, E.M., Hale, R.S., Higgins, K.A, Horgan, M.J., Knoll, L.B., Renwick, W.H., and Stein, R.A. 2006. Nutrient cycling by fish supports relatively more primary production as lake productivity increases. *Ecology*, 87(7): 1696-1709.

- Vollenweider, R.A., Rast, W. and Kerekes, J. 1979. The phosphorus loading concept and Great Lakes eutrophication. Proceedings of the 1979 Conference on Phosphorus Management Strategies for Lakes, New York, pp. 207-234.
- Watanabe, M.F., Oishi, S. 1985. Effects of environmental factors on toxicity of cyanobacterium (*Microcystis aeruginosa*) under culture conditions. Appl. Environ. Microb., 49: 13-42.
- Watanabe, M.F. 1996. Toxic Microcystis. CRC press, Boca Raton, FL.
- Wen, Y.H. and Peters, R.H. 1994. Empirical models of phosphorus and nitrogen excretion rates by zooplankton. Limnol. Oceanogr., 39(7): 1669-1679.
- Wetzel, R.G. 1983. Limnology. Saunders College Publishing.
- Wetzel, R.G. 2001. Limnology. 3rd Edition. Academic Press, San Diego, CA
- Wilhelm, S.W., DeBruyn, J.M., Gillor, O., Twiss, M.R., Livingston, K., Bourbonniere, R.A., Pickell, L.D., Trick, C.G., Dean, A.L., McKay, R.M.L. 2003. Effect of phosphorus amendments on present day plankton communities in pelagic Lake Erie. Aquat. Microb. Ecol., 32(3): 275-285.
- Williams, J.D.H., Joquet, J-M, and Thomas, R.L. 1976. Rorms of phosphorus in the surficial sediments of Lake Erie. J. Fish. Res. Board Can., 33: 413-429.
- Winkel, Ten E.H., and Davids, C. 1982. Food selection by *Dreissena polymorpha* Pallas (Mollusca: Bivalvia). Freshwater Biol., 12: 553-558.
- Wu, L. and Culver, D.A. 1991. Zooplankton grazing and phytoplankton abundance an assessment before and after invasion of *Dreissena polymorpha*. J. Great Lakes Res., 17(4): 425-436.
- Wu, L. and Culver, D.A. 1994. *Daphnia* population-dynamics in western Lake Erie - regulation by food limitation and yellow perch predation. J. Great Lakes Res., 20(3): 537-545
- Yang, M.D. 1996. Adaptive short-term water quality forecasts using remote sensing and GIS. Ph. D. dissertation, Department of Civil and Environmental Engineering and Geodetic Science, The Ohio State University, Columbus, OH.
- Yang, M.D., Sykes, R.M. and Merry, C.J. 2000. Estimation of algal biological parameters using water quality modeling and SPOT satellite data. Ecol. Model., 125:1-13.
- Young, T.C., DePinto, J.V., Flint, S.E., Switzenbaum, M.S., and Edzwald, J.K. 1982. Algal availability of phosphorus in municipal wastewater. Journal of Water Pollution Control Federation, 54(11): 1505-1516.